Federal University of Ceará

Ph.D. in Chemistry

MANGIFERIN: MICROENCAPSULATION IN PECTIN/CHITOSAN SYSTEMS, *IN VITRO* INTESTINAL METABOLISM AND ANTICANCER ACTIVITY

In Cooperation with:

DKFZ – German Cancer Research Center

JOSÉ ROBERTO RODRIGUES DE SOUZA

FORTALEZA

2012

JOSÉ ROBERTO RODRIGUES DE SOUZA

MANGIFERIN: MICROENCAPSULATION IN PECTIN/CHITOSAN SYSTEMS, *IN VITRO* INTESTINAL METABOLISM AND ANTICANCER ACTIVITY

Thesis submitted to the coordination of the graduate program in chemistry at the Federal University of Ceará, as a partial requirement for obtaining a doctoral degree in chemistry.

Supervisors:

Federal University of Ceara:

Supervisor: Prof. Ph.D. Judith Pessoa de Andrade Feitosa

Co-supervisor: Prof. Ph.D. Nágila Maria Pontes Silva Ricardo

German Cancer Research Center:

Supervisor: Prof. Ph.D. Robert Wyn Owen

JOINT PROGRAM OF DOCTORAL SCHOLARSHIPS
in the Federal Republic of Germany 2010/2011
DAAD - CAPES - CNPq

FORTALEZA
2012

Dados Internacionais de Catalogação na Publicação
Universidade Federal do Ceará
Biblioteca de Ciências e Tecnologia

S713m Souza, José Roberto Rodrigues de.
Mangiferin: microencapsulation in pectin/chitosan Systems, in vitro intestinal metabolism and anticancer activity / José Roberto Rodrigues de Souza – 2012.
242 f. : il. color., enc. ; 30 cm.

Tese (doutorado) – Universidade Federal do Ceará, Centro de Ciências, Departamento de Química Orgânica e Inorgânica, Programa de Pós-Graduação em Química, Fortaleza, 2012.
Área de Concentração: Química.
Orientação: Profa. Dra. Dra. Judith Pessoa de Andrade Feitosa.
Coorientação: Nágila Maria Pontes Silva Ricardo.

1. Pectin. 2. Encapsulation. 3. Mangiferin. 4. Câncer. I. Título.

CDD 547

Esta Tese foi apresentada como parte dos requisitos necessários à obtenção do Grau de Doutor em Química, área de concentração Química, outorgado pela Universidade Federal do Ceará, e em cuja Biblioteca Central encontra-se à disposição dos interessados.

José Roberto Rodrigues de Souza

Tese aprovada em: **28/08/2012**

Dra. Judith Pessoa de Andrade Feitosa
(Orientadora-UFC)

Dra. Nágila Maria Pontes Silva Ricardo
(Coorientadora-UFC)

Dra. Maria Teresa Salles Trevisan
(UFC)

Dr. Robert Wyn Owen
(Univ. de Heidelberg Alemanha)

Dra. Thais Mauad
(USP)

Thanks to God, The Creator, whose laws we are trying to understand

Thanks to my family for the support, especially during the first years of my life and to my friends for the encouragement

ACKNOWLEDGEMENTS

I would like firstly to thank all professors of the Polymers group, especially Professors Judith and Nágila who helped to develop the feelings of being a scientist during these research years as well as their friendship and teachings as well as Professors Sandra and Regina for their teachings.

I would like to thank Professor Teresa for the collaboration opportunity, friendship and teachings.

I thank all the Professors and their teachings during my graduation studies.

I would like to thank Professor Bob for the teachings and patience during my stay at DKFZ, in Germany.

I would like to thank Gerd Würtele for his special patience in the lab at DKFZ and to Roswitha for the explanations.

I would like to thank Eva Frei and Andrea Breuer for the practice and explanations with cell culturing.

I would like to thank Professor Neli for the opportunity to have worked in the preventive oncology research group at the DKFZ and all group colleagues for the acquaintanceship.

I would like to thank my colleague Helder for the early years work in the lab as well as Pablyana for her early motivation and enthusiasm.

I would like to thank all lab colleagues of the polymers group in Brazil for the acquaintanceship along these years.

I would like to thank Samuel for his work contribution with pectin isolations.

I would like to thank all colleagues and Professors of the graduation program for the acquaintanceship.

I would like to thank staff Teresa for thermal analysis, Orlando for the bureaucratic help and CENAUREM (Jeanny and Elenir) for NMR analysis.

I would like to thank some friends and colleagues during my stay in Germany for the time together.

I woud like to thank Prof Berger for the nice conversations and his group for some support. Thank you Michael for the help with flow cytometry.

I would like to thank Felix for the help with fluorescence microscopy.

All colleagues from Goethe Institute for the nice time learning german with so much fun and pleasure.

I would like to thank the financial support from CNPq, Daad and Capes during research and stay in Germany.

ABSTRACT

MANGIFERIN: MICROENCAPSULATION IN PECTIN/CHITOSAN SYSTEMS, *IN VITRO* INTESTINAL METABOLISM AND ANTICANCER ACTIVITY

This work was performed in four parts:

The first part was the isolation of pectin from a regional pumpkin in order to be used as matrix for drug encapsulation: Pumpkin (*Cucurbita moschata*) is an excellent and low cost source of carotenoids, precursors of vitamin A. Moreover, it is also a great source of natural and low-cost pectin. Pectin is a heterogeneous complex polysaccharide found in the primary cell wall of most cells and its effect on health is receiving growing interest for applications such as an ingredient in food products and in pharmaceutical formulations for drug encapsulation. In the first part of this work, high-methoxyl pectin was isolated from a regional pumpkin by the method of acid hydrolysis. The isolated pectin was characterized by FTIR, ^{1}H ^{13}C NMR, GPC, elemental analysis and rheology.

In the second part, pectin with chitosan samples were used for encapsulation procedure: Microencapsulation processes, such as spray-drying is an alternative to enhance solubility of bioactive materials and a good way to preserve, protect and control the release rate of a substance until it reaches its target in the body. Mangiferin is an active phytochemical present in various plants including *Mangifera indica L*. This substance is reported to have anti-cancer, antioxidant and other activities, but has a low solubility in aqueous medium. In the second part of this work we encapsulated mangiferin within four different natural polymers compositions by using spray-drying techniques. The products were characterized by FTIR, SEM and HPLC-ESI-MS. The efficiency of mangiferin incorporation into each encapsulate was calculated by HPLC. The highest encapsulation efficiency was determined to be for pectins using Polysorbate 80 (Tween 80) as emulsifier.

In the third part of this work, a gut metabolic study with mangiferin was performed: Mangiferin has low bioavailability, already reported in many scientific publications, and is more available in the gut, where it will be metabolized into other compounds. The aim of the third part was to produce and identify mangiferin metabolites simulating intestinal conditions as well as their isolation and characterization using different techniques such as HPLC-ESI-MS, Semipreparative HPLC, Nano-ESI-MS, and ^{1}H / ^{13}C NMR.

The fourth part was the investigation of the cytotoxicic effects of mangiferin and its metabolites in human cancer cell lines: The aim of the fourth study was to investigate the cytotoxic effects of mangiferin and its main metabolites in human cancer cell lines such as intestinal cancer cell line Caco-2 in order to observe the potential anticancer activity of these compounds *in vitro.*

Keywords: pectin, encapsulation, mangiferin, metabolism, cancer.

RESUMO

MANGIFERINA: MICROENCAPSULAMENTO EM SISTEMAS PECTINA/QUITOSANA, METABOLISMO INTESTINAL *IN VITRO* E ATIVIDADE ANTICANCER

Este trabalho foi realizado em quatro partes:

A primeira parte trata do isolamento de pectina a partir de uma abóbora regional a fim de ser utilizado como matriz para encapsulamento de fármaco: a abóbora (*Cucurbita moschata*) é uma excelente fonte de baixo custo de carotenóides, precursores da vitamina A. Além disso, é também uma grande fonte de pectina natural e de baixo custo. A pectina é um polissacarídeo complexo e heterogêneo encontrado na parede celular primária da maioria das células vegetais e o seu efeito sobre a saúde está a receber um interesse crescente para aplicações tais como ingrediente em produtos alimentares e em formulações farmacêuticas para o encapsulamento de fármacos. Na primeira parte deste trabalho, pectina de alto grau de metoxilação foi isolada a partir de uma abóbora regional pelo método de hidrólise ácida. A pectina isolada foi caracterizada por FTIR, ^{1}H ^{13}C RMN, GPC, análise elementar e reologia.

Na segunda parte, pectinas e quitosana foram utilizadas para o procedimento de encapsulação: processos de microencapsulação, como atomização por spray-drying é uma alternativa para aumentar a solubilidade de materiais bioativos e uma boa forma de preservar, proteger e controlar a taxa de liberação de uma substância até atingir o seu alvo no corpo. Mangiferina é um fitoquímico ativo presente em várias plantas, incluindo *Mangifera indica L*. Essa substância é relatada por ter potencial anti-câncer, antioxidante e outras atividades, mas tem uma baixa solubilidade em meio aquoso. Na segunda parte deste trabalho, mangiferina foi encapsulada em quatro diferentes composições usando polímeros naturais através da técnica de spray-drying. Os produtos foram caracterizados por FTIR, MEV e HPLC-ESI-MS. A eficiência da incorporação de mangiferina em cada formulação foi calculada por HPLC. A maior eficiência de encapsulação foi determinada como sendo de pectinas utilizando Polissorbato 80 (Tween 80) como emulsionante.

Na terceira parte deste trabalho, um estudo simulando o metabolismo intestinal foi realizado com a mangiferina: mangiferina possui baixa biodisponibilidade, já relatado em muitas publicações científicas, e é mais disponível no intestino, onde irá ser metabolizada em outros compostos. O objetivo da terceira parte foi produzir e identificar metabólitos da mangiferina simulando as condições intestinais, bem como o seu isolamento e caracterização utilizando diferentes técnicas, tais como: HPLC-ESI-MS, HPLC semipreparativa, Nano-ESI-MS, ^{1}H / ^{13}C RMN.

A quarta parte trata da investigação dos efeitos de citotóxicos da mangiferina e seus metabólitos em linhagens tumorais humanas: O objetivo do quarto estudo foi investigar os efeitos citotóxicos da mangiferina e seus metabólitos principais, em linhas de células tumorais humanas, tais como a linhagem tumoral de células intestinais Caco-2, a fim de observar a atividade anticâncer destes compostos *in vitro*.

Palavras-chave: pectina, encapsulamento, mangiferina, metabolismo, câncer.

LIST OF TABLES

CHAPTER 1

CHAPTER 2

CHAPTER 3

CHAPTER 4

LIST OF FIGURES

CHAPTER 1

CHAPTER 2

CHAPTER 3

CHAPTER 4

LIST OF ABBREVIATIONS

A240286S: non-small bronchial carcinoma cells
AFM: anaerobic fermentation of mangiferin
BHI: brain heart infusion
C1, 2, 3: compound 1, 2, 3.
Caco-2: human epithelial colorectal adenocarcinoma cells
CP: citric pectin
Ch: chitosan
DDW: double-distilled water
DM: degree of methoxylation
F: fraction
FBS: Fetal Bovine Serum
FTIR: Fourier transform infrared
GPC: gel permeation chromatography
HG: homogalacturonan
HM: high-methoxyl
HPLC-ESI-MS: chromatography-electrospray-ionization-mass spectrometry
IC_{50}: concentration of compound that causes 50 % reduction in viable cell count
LM: low-methoxyl
Ma: mangiferin
Mang: mangiferin
Mpk: molar mass peak

MS: mass spectrometry
M-1: metabolite 1, homomangiferin
M-2: metabolite 2, norathyriol
M-3: metabolite 3, norathyriol monodehydroxyl
McCT: Multiplex cell Contamination Test
NMR: nuclear magnetic resonance
NEAA: non-essential amino acids
NSCLC: non-small cell lung carcinoma
Pec: pectin
pH: potential hydrogen
PP: pumpkin pectin
RGI: ramnogalacturonan I
RGII: ramnogalacturonan II
SD: spray-drying
SEM: Scanning Electronic Microscopy
SF: subfraction
SPE: solid phase extraction
Suc: sucrose
Tris:Tris (hydroxymethyl) aminomethan
UV: ultraviolet
V-1, 2, 3: volunteer 1, 2, 3.

CONTENTS

CHAPTER 1

ISOLATION AND CHARACTERIZATION OF REGIONAL PUMPKIN PECTIN FOR DRUG ENCAPSULATION

CHAPTER 2

SPRAY-DRYING ENCAPSULATION OF MANGIFERIN USING NATURAL POLYMERS

CHAPTER 3

PRODUCTION AND CHARACTERIZATION OF MANGIFERIN METABOLITES BY INTESTINAL ENVIRONMENT SIMULATION

CHAPTER 4

CYTOTOXIC SCREEN OF MANGIFERIN AND METABOLITES IN TWO HUMAN TUMOR CELL LINES

CHAPTER 1

Isolation and Characterization of Regional Pumpkin Pectin for Drug Encapsulation

Souza, J. R. R[1], Brito, E. S.[2], Ricardo, N. M. P. S[1], Feitosa, J. P. A.[1]

[1]*Departament of Organic and Inorganic Chemistry, Federal University of Ceará P. O. Box: 6.021, ZIP-Code: 60455-760, Fortaleza, Ceará, Brazil*

[2]*Embrapa Tropical Agroindustry, R. Dra. Sara Mesquita, 2270, Pici, 60511-110, Fortaleza, CE, Brazil*

Pumpkin (*Cucurbita moschata*) is an excellent and low cost resource of carotenoids, precursors of vitamin A. Moreover, it is also a great source of natural and low-cost pectin. Pectin is a heterogeneous complex polysaccharide found in the primary cell wall of most cells and its effect on health is receiving growing interest and for applications such as an ingredient in food products and in pharmaceutical formulations for drug encapsulation. In this work, high-methoxyl pectin was isolated from a regional pumpkin by the method of acid hydrolysis. The isolated pectin was characterized by FTIR, ^{1}H and ^{13}C NMR, GPC, elemental analysis and rheology.

Keywords: pectin, pumpkin, infrared, NMR, rheology.

1. Introduction

1.1. Pumpkin

Pumpkin, a member of the plant family *Cucurbitaceae*, is an excelent resource of carotenoids, precursors of vitamin A and has been regarded as a functional food. Several other phytochemicals have been isolated from pumpkin: polysaccharides, phenolic glycosides, 13-hydroxy-9Z, 11E-octadecatrienoic acid from the leaves of pumpkin and proteins from germinated seeds (Arima & Rodriguez-Amaya, 1990; Adams *et al.,* 2012). The Figure 1 shows pictures of pumpkin species *Cucurbita moschata.*

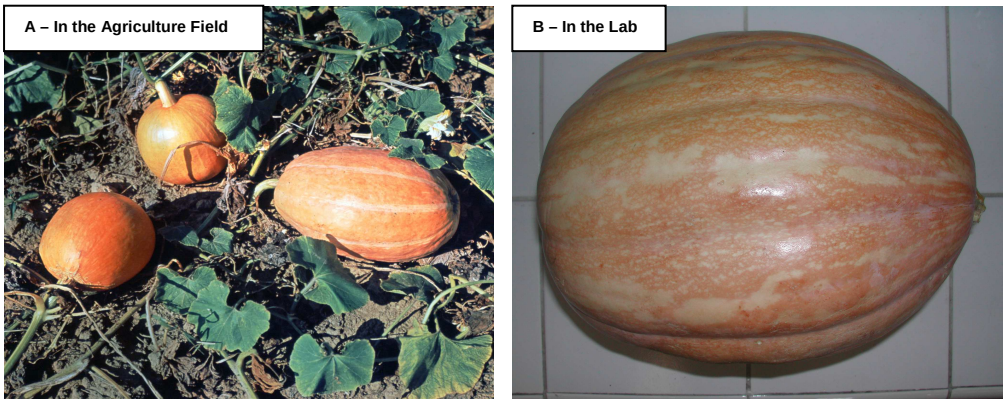

Figure 1 – Pumpkin *Cucurbita moschata.* Family: Cucurbitaceae; genus: Cucurbita; species: moschata. (A) Pumpkin crop photograph from *Encyclopædia Britannica Online, (pumpkin,* 2012). (B) Picture of pumpkin "jerimum de leite", taken in the polymers laboratory at the Federal University of Ceará.

Under the dried form, pumpkin can be stored longer and used in various culinary preparations, contributing with one more food option to combat hypovitaminosis A, which affects thousands of children in Brazil and in other countries of the world. Vitamin A (retinol) is also reported to have an essential role in embryogenesis: during pregnancy, it is transported by retinol binding protein from the maternal blood supply to the embryo through receptor-facilitated transport (Gilchrist *et al.,* 2010). Pumpkin is also reported to be a low cost source of pectin (Murkovic *et al.,* 2002).

1.2. Pectins and its isolation from plant cell wall

Pectin is a multifunctional complex polysaccharide and abundant component from cell walls of all plants (Ngouémazong *et al.,* 2012; Willats *et al.,* 2006). Pectic polysaccharides consist mostly of polymers rich in galacturonic acid, containing significant amounts of rhamnose, arabinose and galactose as well as 13 other different monosaccharides (Vincken *et al.,* 2003a). The three major polysaccharides are currently defined: homogalacturonan (HG), ramnogalacturonan I (RGI) and ramnogalacturonan II (RGII) as shown in Figure 2 (Vincken *et al.,* 2003a; Waldron *et al.,* 2003). Willats *et al.,* (2006) proposed a new pectin structure which may have homogalacturonan as side chains.

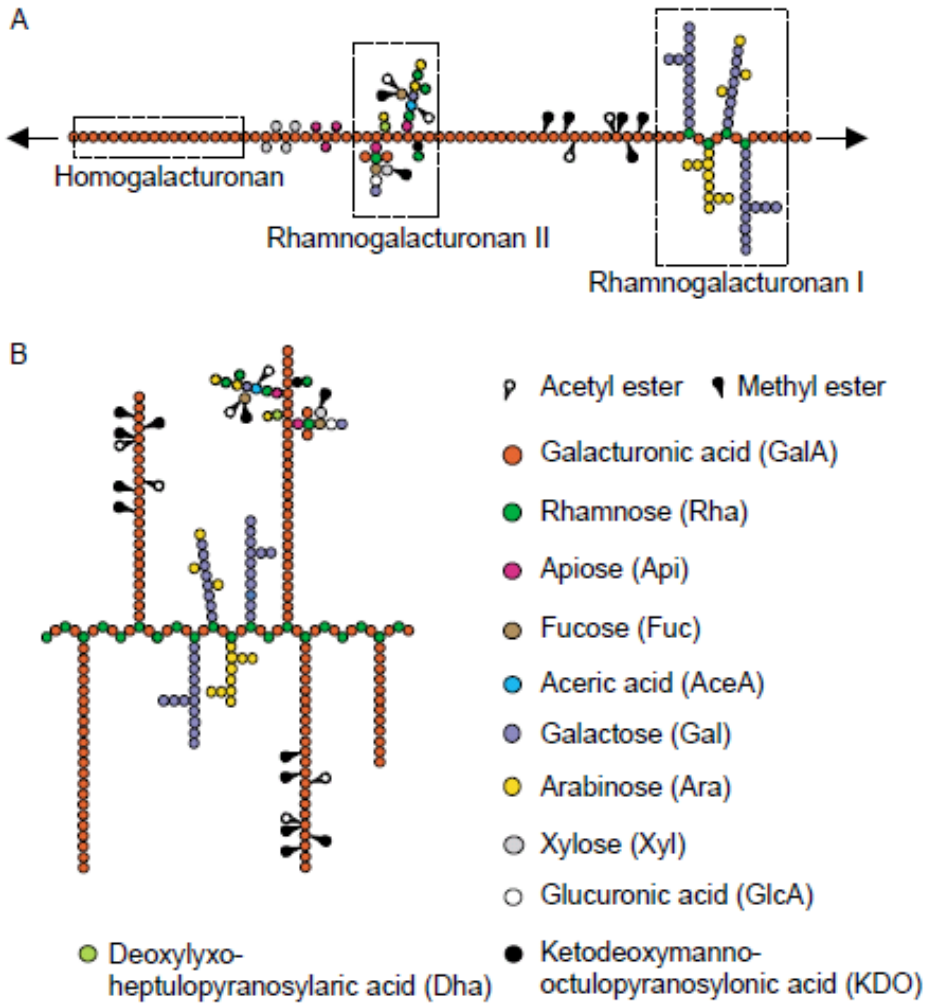

Figure 2 – Conventional (A) and alternative (B) pectin structures proposed by Willats *et al.,* 2006.

HG is a linear polymer consisting of 1,4-linked α-D-GalA, whilst RGI consists of the repeating disaccharide [→4)-α-D-GalA-(1→2)-α-L-Rha-(1→] to which a variety of different glycan chains (principally arabinan and galactan) are attached to the Rha residues. RGII has a backbone of HG rather than RG, with complex side chains attached to the GalA residues (Willats *et al*., 2006). The structures of RGI and RGII are shown in Figure 3.

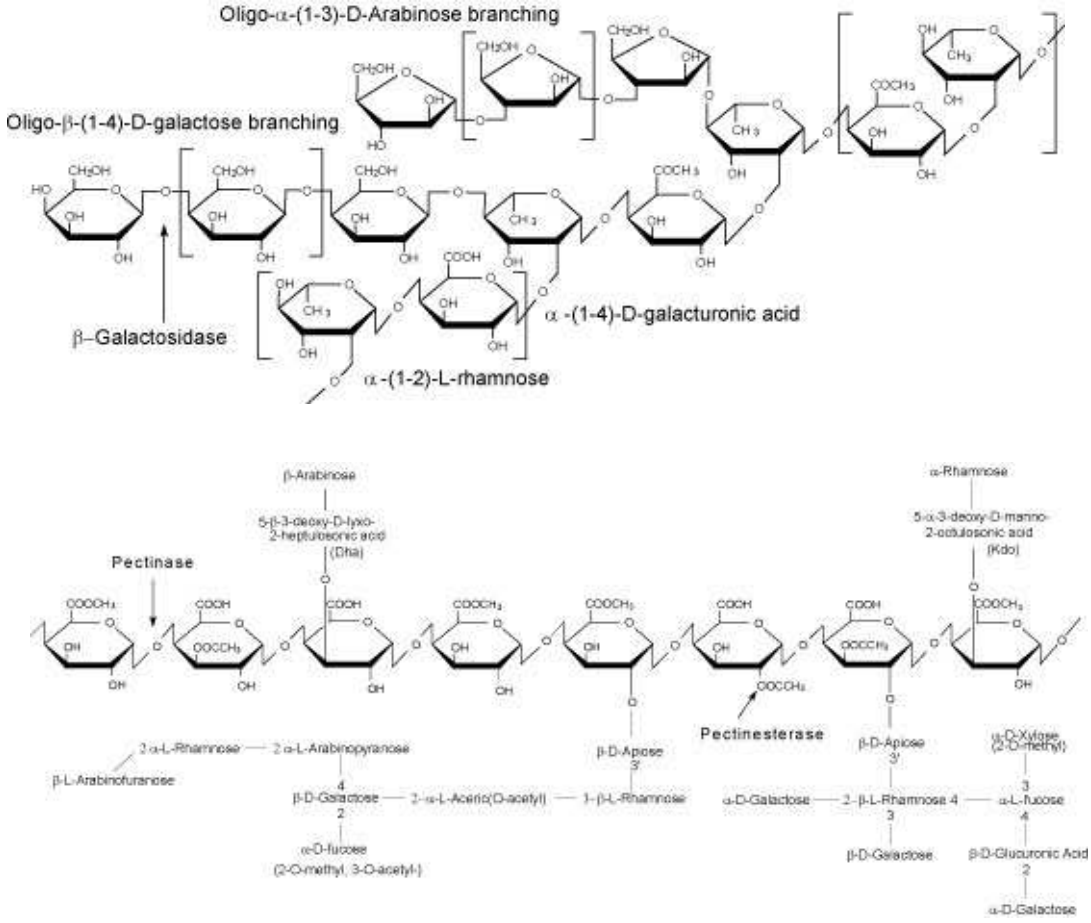

Figure 3 – RGI (A) and RGII (B) structures. Figure from Sigmaaldrich website, 2012.

The primary wall contains 80–90% polysaccharide and 10–20% protein. Cellulose, hemicellulose and pectin are the main polysaccharide components in the primary wall (Etzler & Mohnen, 2009). The main role of pectin is to give physical strength to the plant together with the other polymers. Especially HG and RGII are well known to be involved in strengthening the wall (Harholt *et al.,* 2010). We can see in Figure 4 a general view of a plant cell wall structure showing pectin chains interlaced with other cell wall polysaccharides.

The composition, structure, and physiological properties of pectins can be influenced by extraction conditions as well as source, location and many other environmental factors. The network of pectin must be broken to occur extraction. This may involve extraction with calcium chelating agents, dilute bases or dilute acids. Alternatively, fragments of pectic polysaccharides can be released through the use of enzymatic degradation.

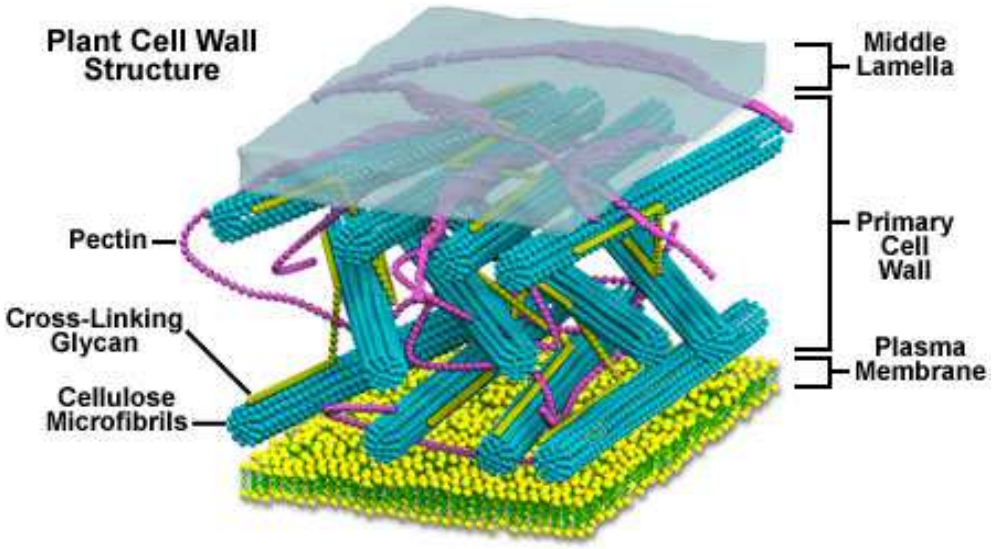

Figure 4 – Plant cell wall. Pectic substances are shown in purple. Figure from Molecular expressions website, 2012.

Pectins are typically extracted from citrus fruits and apple pomace (Waldron *et al.,* 2003). Firmness losses during the heating of fruit and vegetables are related to acid hydrolysis of glycosidic bonds in cell wall polysaccharides. Pectic substances are obtained from cell walls when plant tissues are heated at low pH when protopectin, the natural pectin form found in

plant cell wall, is hydrolyzed into pectin (Krall & McFeeters, 1998; Pagán *et al.*, 2001).

1.3. Pectins and its applications

Pectin is traditionally used as a gelling agent for jellies and marmalades. A pectin gel is formed when portions of HG are crosslinked to form a three dimensional crystalline network in which water and solutes are trapped. Various factors determine gelling properties such as temperature, pectin type, degree of methoxylation (DM), degree of acetylation, pH, sugar and other solutes like calcium ions, for example. Pectins have been categorized as high-methoxyl (HM) or low-methoxyl (LM) with DMs of >50% and <50% respectively. In high-ester pectins, the junction zones are formed by the cross-linking of HG by hydrogen bridges and hydrophobic forces between methoxyl groups, both promoted by high sugar concentration and low pH, whereas in low-ester pectins, junction zones are formed by calcium (or some other divalent metals) crosslinking between free carboxyl groups (Bottger, 1990; Willats *et al.*, 2006) as can be seen in Figure 5.

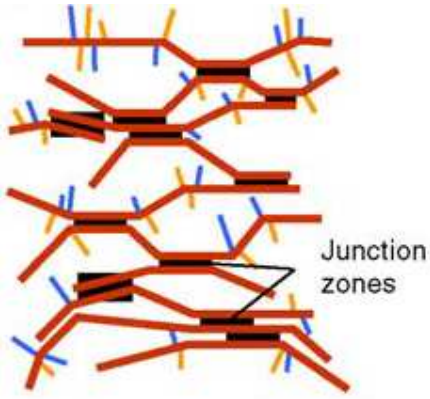

Figure 5 – Junction zones of chemical interactions in pectic HG chains. Adapted from Willats *et al*., 2006.

Pectin is listed among the ingredients of many food products (U.S. code, E440). The global annual consumption is estimated to be around 45,000 metric tonnes (Willats *et al.,* 2006). The many technological interests makes pectin a especially valuable biopolymer for medicine, food production as well as for applications in drug encapsulation (Benjamin *et al*., 2012; Souza *et al*., 2009;

Ptichkina *et al*., 2008). Pectins also offer health benefits to consumers. For example, they are being increasingly recognized as important precursors of substrates for gastrointestinal functions and structures. Foods rich in fiber are usually recommended for diabetics, because they are able to reduce the glycemic response to food and thus reduce the need for insulin (Guillon & Champ, 2000). Pectin is also effective on lowering the cholesterol level in blood, removing heavy metal ions from the body, stabilizing blood pressure, and restoring intestinal functions (Voragen *et al.,* 1995). Pectin and pectic oligosaccharides have been reported to induce apoptosis in human colonic adenocarenoma cells, what suggests it could be applied in oncology prevention formulations (Olano-Martin *et al.,* 2003).

Although the potential stock of these raw materials enables the main pectin producers (USA, Germany, Denmark) to plan an annual increase of pectin production of approximately 3.8% (Phillips, 2000), searching for new pectin-containing raw materials is an important task of science and industry (May, 1990).

In this work pectin was extracted from a pumpkin (*Cucurbita moschata*) regionally known as regional “jerimum de leite” and characterized in order to be used as matrix for future encapsulation studies.

2. Experimental

2.1. Extraction of pectin

For extraction of pectin, mass of about 5 kg of pumpkin mesocarp was pressed in an expeller press. Two types of residues were obtained: and a thinner one which was obtained by filtration of the juice (approx. 209g). The thinner dough was dried in an oven at 60 °C for 12 hours forming a paste that was used for the extraction procedure. For extraction by acid hydrolysis, 2 L of 0.1 mol/L HCl solution was stabilized at 65 °C and after that, approx. 200 g pumpkin pulp was added to the stirring solution and let extracting for 2 hours. After precipitation and washing with ethanol PA (1:10 - solution: ethanol), filtration and freeze-drying, 4.7 g of pectin was obtained which after purification by dialysis membranes remained 2.5 g of pure pectin which was used for further analysis (yield calculated from pumpkin dry fiber of approx. 6.9 %).

2.2. Infrared Spectroscopy (IR)

The Fourier Transform IR spectrum (FT-IR) of pectin was recorded with a Shimadzu IR spectrophotometer (model 8300) in the range of 400 and 4000 cm^{-1} as KBr pellet.

2.3. ^{1}H, ^{13}C NMR Nuclear Magnetic Resonance

Spectra of 0.1% (w/v) solutions in D_2O were recorded at 70 °C on a Fourier Transform Bruker Avance DRX 500 spectrometer with an inverse multinuclear gradient probe-head equipped with z-shielded gradient coils, and with Silicon Graphics. Sodium 2,2-dimethylsilapentane-5-sulphonate (DSS) was used as the internal standard (0.00 ppm for ^{1}H).

2.4. Gel Permeation Chromatography (GPC)

The molar mass peak (Mpk) of pectin was determined by gel permeation chromatography (GPC) using a Shimadzu instrument (Ultrahydrogel linear column, 7.8 x 300 mm), at room temperature, flow rate of 0.5 mL/min, polysaccharide concentration of 0.1% (w/v) and 0.1 mol/L $NaNO_3$ as the solvent. A differential refractometer was used as detector. The elution volume was corrected by the use of the internal marker ethylene glycol at 11.25 mL. Pullulan samples (Shodex Denko) of molar mass 5.9×10^3, 1.18×10^4, 4.73×10^4, 2.12×10^5, and 7.88×10^5 g/mol were used as standards.

2.5. Elemental analysis – protein content

The elemental analysis of carbon, hydrogen and nitrogen of pumpkin pectin was performed using a microanalyzer Carlo ERBA EA 1108.

2.6. Rheological Measurements

All rheological measurements were performed using an Advanced Rheometer AR550 (DP Union). Geometry cone-and-plate (40 mm diameter and angle of 0° 59'' 1') was used for measurements of continuous flow. The viscosity of continuous flow for the aqueous solutions was determined at 25 ° C in the shear range of 1-100 s^{-1}.

3. Results and Discussion

3.1. Infrared Spectroscopy (FTIR)

An overview of the IR spectrum of pectin is shown in Figure 6. The "fingerprint" region of the spectrum (up to approx. 2000 cm^{-1}) includes the region of 1200-1800 cm^{-1} as shown.

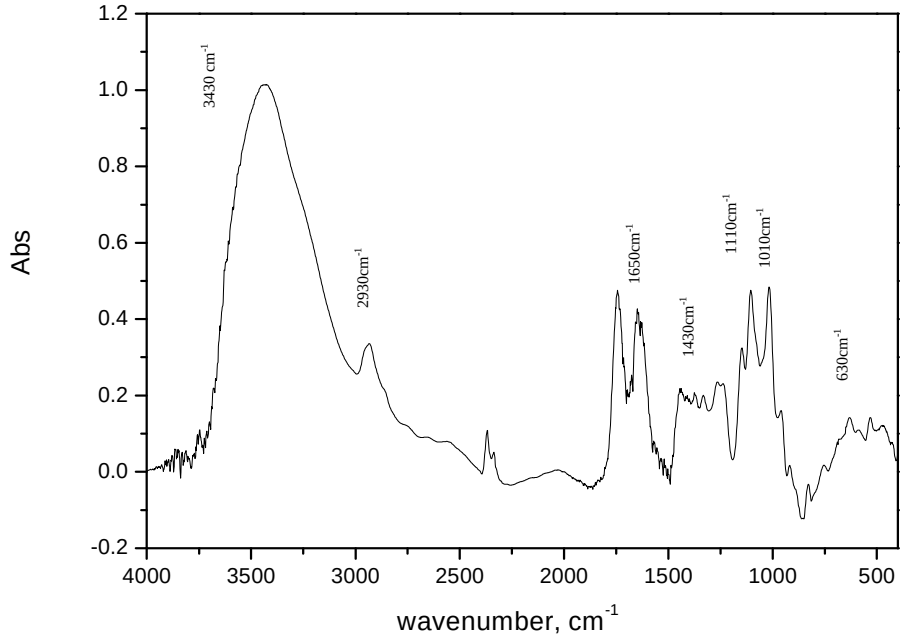

Figure 6 - FTIR spectrum of pectin from pumpkin.

We observe the region that characterizes the state of carboxylic groups (approx. 1750-1350 cm^{-1}) (Filipov, 1992). The band at approx. 1743 cm^{-1} is indicative of the stretching group C=O of non-ionized carboxylic acid (methylated or protonated). Its ionization (formation of salt) leads to their disappearance, and the appearance of stretch modes of COO^- in approx. 1600-1650 and 1400-1450cm^{-1}, respectively (Filipov, 1992). The degree of methylation (DM) is defined as the amount of ester groups compared to the total amount of acid groups and carboxylic ester and it is observed that the high intensity of the band at 1743 cm^{-1} show that the pectin obtained is of high degree of methylation.

3.2. NMR analysis: Determination of methylation (DM) by ^{1}H

For the determination of DM, the integrals of H-5 (see Figure 7) adjacent to ester (I_{COOMe}) are compared with the sum of integrals of H-5 adjacent to the ester (I_{COOMe}) and H-5 adjacent to the carboxylate (I_{COO-}).

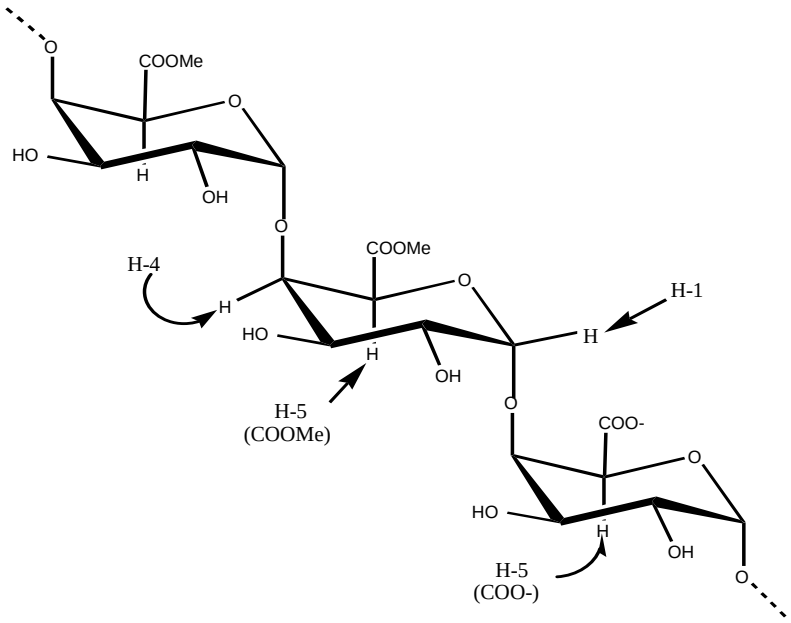

Figure 7 - Structure of a fragment of pectin.

Due to close proximity (or overlap) of the signals for H-1 and H-5_{COOMe}, it is only possible to determine the full combined to H-1 and H-5_{COOMe} (I_{H1} + I_{COOMe}). The value of DM was calculated at 58% (Figure 8, Appendix 1).

We can also observe in the spectrum of the polysaccharide, a very large signal at 3.81 ppm related to methyl groups binding to carboxyl groups of galacturonic acid. Signals at around 2.1 ppm are related to acetyl groups and were not observed for the pectin. There are other signals related to D-galacturonic acid: H-1, 5.09 ppm; H-2, 3.76 ppm; H-3, 3.97 ppm; H-4, 4.41 ppm; H-5, 4.68 ppm (Tamaki *et al.,* 2008).

Grasdalen (Oakenfull, 1991) pioneered the determination of DM by ^{1}H NMR. He performed detailed analysis of the sequence of free galacturonic acid and pectin fragments of groups tri-and tetrameter. By using this simple method, it is possible to characterize pectins having a specific DM, and therefore, with

specific gelling properties that are dependent on DM (Oakenfull, 1991; Axelos & Thibault, 1991).

3.3. Characterization of pectin by ^{13}C NMR

The spectrum of ^{13}C nuclear magnetic resonance for the sample of pectin is shown in Figure 9 (Appendix 2). In the spectrum of the polysaccharide, a signal at about 53.5 ppm was assigned to methyl groups attached to carboxylic groups of galacturonic acid (Keenan *et al.,* 1985) and a signal at 173 ppm was attributed to carboxylic groups linked to methyl groups (Catoire *et al.,* 1998).

In the spectrum of polysaccharides, major and smaller signals can be observed between the region of about 60.0 and 110.0 ppm. The major signals are assigned to D-galacturonic acid while the smaller signals are assigned to D-galactose, as shown in Table 1. These chemical shifts are in good agreement with those related to the pattern of pectin studied by Tamaki *et al*. There are also less intense signal assignments made by Ha *et al*. related to arabinan but those signals are not very intense compared to the noise signals of the spectrum and therefore not all signals will be shown in the table below. There are other signals also reported by Ha *et al.* (2005) related to other galactan carbon that are in the same situation.

Table 1 - Assignments to the peaks of the ^{13}C spectrum of pectic polysaccharides (Tamaki *et al.,* 2008, Ha *et al.,* 2005).

Polymer	Carbon	Shift (ppm)	Shift (ppm) from literature
Galacturonan	C-6 free	176	175.4 (Ha et al., 2005)
Galacturonan	C-6 esther	171	171.4 (Ha et al., 2005)
Arabinan	C-1	106	107.8 (Ha et al., 2005)
Galacturonan	C-1	101	100.8 (Ha et al., 2005)
Arabinan	C-4	84	84.7 (Ha et al., 2005)
Arabinan	C-4	83	83.0 (Ha et al., 2005)
Arabinan	C-2	81	81.6 (Ha et al., 2005)
Galacturonan	C-4	79	81.1 (Tamaki et al., 2008)
Galactan	C-4	78	78.4 (Ha et al., 2005)
Arabinan	C-3	77	77.4 (Ha et al., 2005)
Galacturonan	C-3	71	72.0 (Tamaki et al., 2008)
Galacturonan	C-5	73	74.2 (Tamaki et al., 2008)
Galacturonan	C-2	68	71.3 (Tamaki et al., 2008)
Arabinan	C-5	67	67.7 (Ha et al., 2005)
Galactan	C-6	62	61.5 (Ha et al., 2005)
Arabinan	C-5	61	62.0 (Ha et al., 2005)
Galacturonan	OCH_3	53.5	53.6 (Ha et al., 2005)
Rhamnose	CH_3	17.5	17.7 (Ha et al., 2005)

3.4. Gel permeation chromatography (GPC)

A wide peak (7.0 mL) with a little shoulder (7.6 mL) is present in the chromatogram of pectin sample (Figure 10). The peak molar mass (M_{pk}) of the polysaccharide was estimated using pullulan (a neutral polysaccharide) standard plot. Taking into account that the pectin is a polyelectrolyte, it is expected that it elutes at a lower volume than a neutral macromolecule with the same molar mass. This is due to chain stiffening and extent, as a consequence of electrostatic repulsion of carboxylate groups.

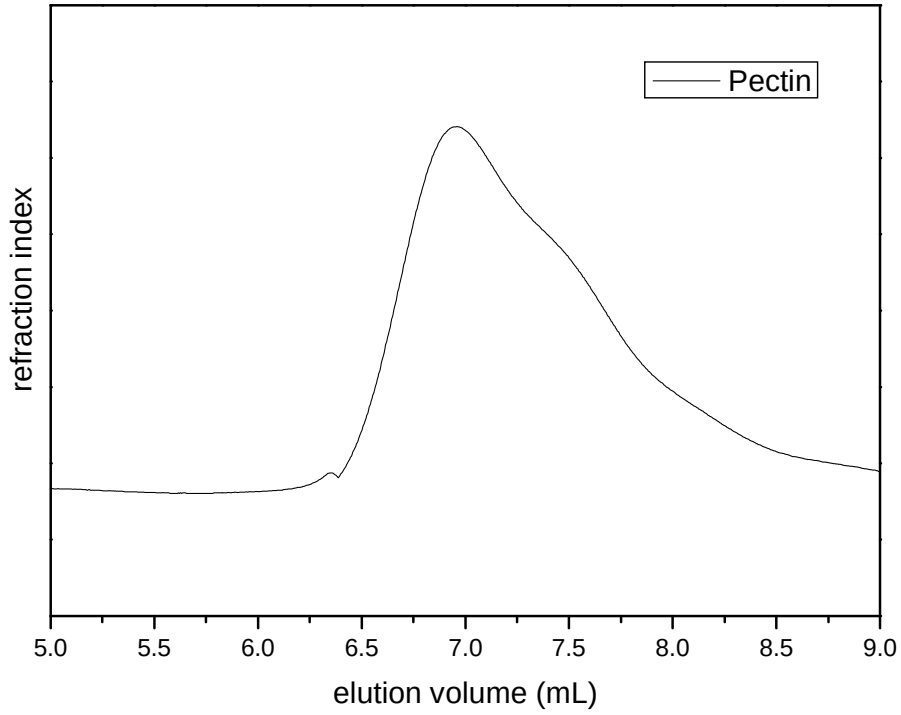

Figure 10 - GPC of pectin sample.

The estimated M_{pk} is 9.5 x 10^5 g/mol. The molar mass of pectin is equal or lower than that value. The molar mass of pectins ranges from 1.4 x 10^5 to 2.3 10^5 g/mol (Yoo *et al.,* 2006; Morris *et al.,* 2008).

3.5. Elemental analysis – protein content

The data of microanalysis of pectin are shown in Table 2. The amount of protein obtained was 2.7%. The calculation was performed using a conversion factor equal to 5.85 (Azero & Andrade, 2002).

Table 2 - Microanalysis data for pumpkin pectin.

% C	34,24
% N	0,46
% H	6,38

The instrument automatically determines C, H, N by combustion of the sample, separation of the combustion gases and measurement by thermal conductivity detector.

3.6. Rheological properties – flow and oscillatory behavior

The flow curves of pectin solutions in the presence and absence of calcium ions are shown in Figure 11. The solution of pectin in the presence of calcium ions exhibited pseudoplastic flow behavior. For the flow curve of the pectin solution in the absence of calcium ions, significantly lower values were observed in a Newtonian flow behavior. The behavior was similar to concentrations of 1 and 3%.

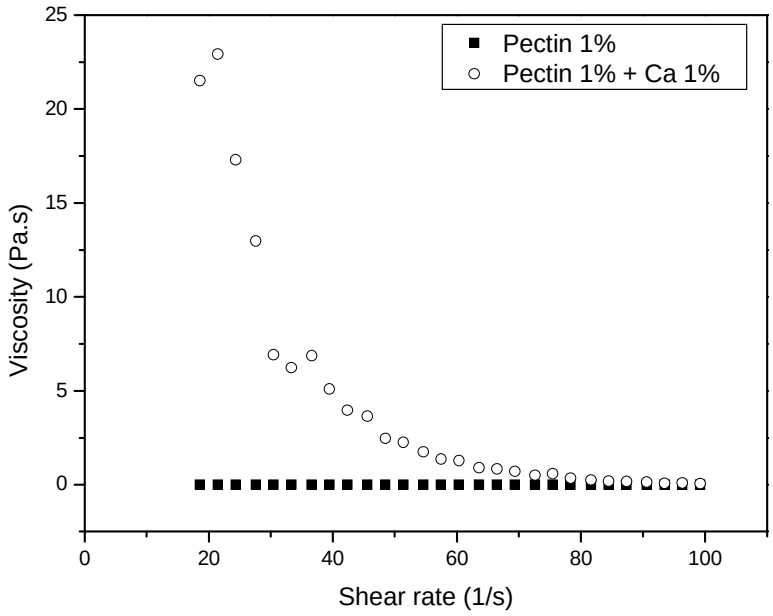

Figure 11 - Flow curves of continuous shear of 1% pectin in presence (○) and absence (■) of 1% calcium ions at 25 °C.

This increase in viscosity values is due to the gelling of the solution. Cross-links are formed between Ca^{2+} and the negatively charged carboxyl groups of HG, leading to the formation of structures known as “Egg-boxes”. Figure 12 shows ‘‘Egg-boxes’’ junction zones in which non-methoxylated galacturonic acid residues blocks interact strongly with calcium ions which have specific positions in well-adapted cavities (Braccini & Pérez, 2001).

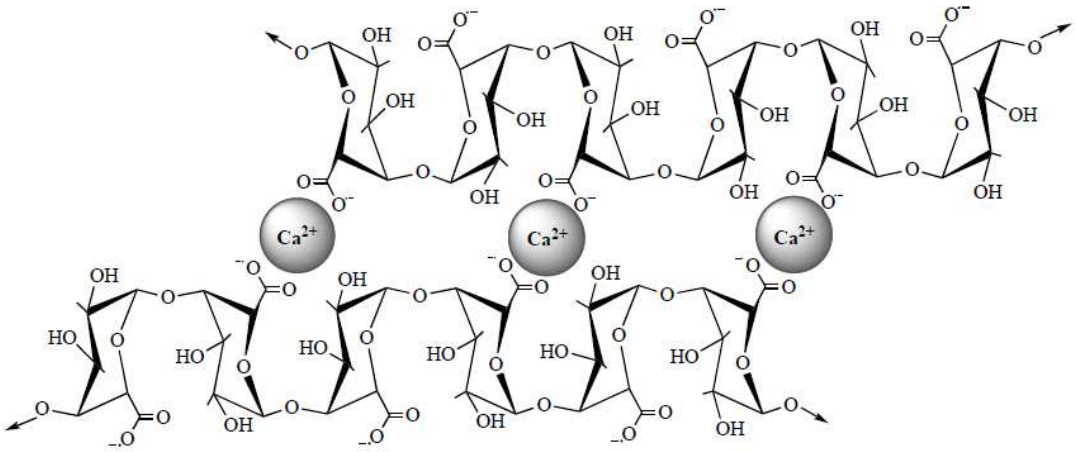

Figure 12 - Interaction between Ca^{2+} ions and unesterified carboxyl groups of galacturonic acid residues of HG chains. Adapted from Vincken *et al.* (2003b).

The flow curves of the 3% pectin solution in the presence and absence of calcium ions are shown in Figure 13. It is observed that the pectin solution in the presence of calcium ions exhibited pseudoplastic flow behavior. For the flow curve of the pectin solution in the absence of calcium ions, significantly lower values were observed in a Newtonian flow behavior as in 1 % pectin solution.

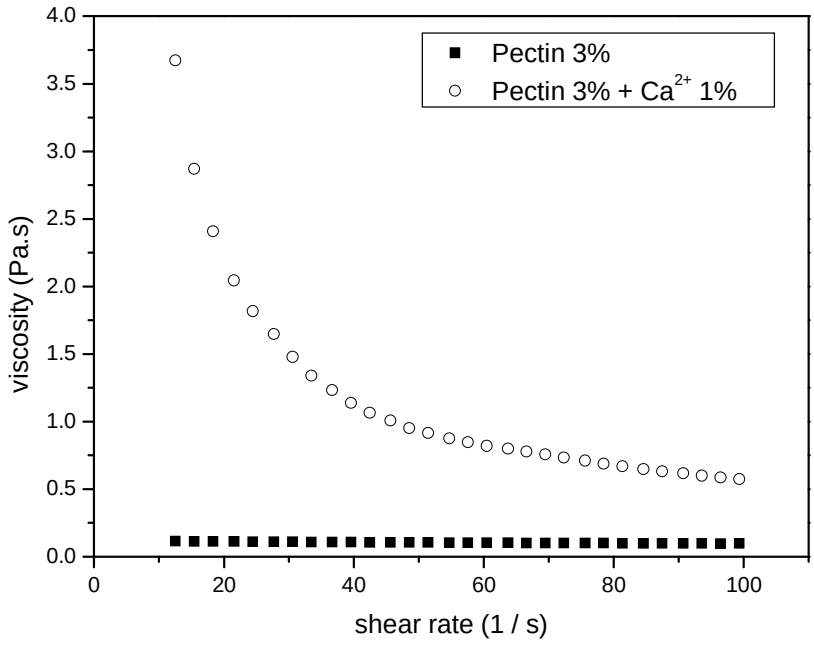

Figure 13 – Shear Flow curves for pectin solution (3%) in presence (○) and absence (■) of calcium ions (1%) at 25 °C.

This increase in viscosity values is due to the gelling of the solution. Cross-links are formed between the Ca^{2+} ions and the negatively charged carboxyl groups of pectin molecules, leading to the formation of “egg-box” structures.

At higher concentration of pectin in aqueous solution (5%), a pseudoplastic behavior was observed to the solution even in the absence of calcium ions (Figure 14). In presence of calcium ions the solution became a firm gel and did not flow. Similar results were determined in the study by Singthong *et al.* (2005) with LM pectin extracted from the leaves of *Cissampelos pareira*, a species of plant used in Chinese herbology.

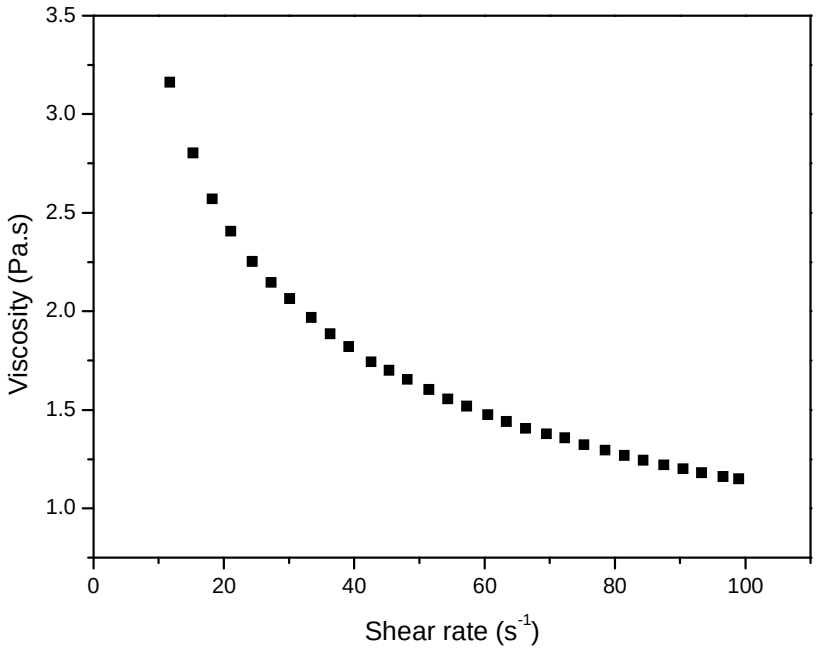

Figure 14 – Shear flow curve plot for an aqueous solution of 5% pumpkin pectin (■) at 25 °C.

It was then carried out an oscillating experiment in a frequency range of 1-10 Hz to compare the values of the modules G 'and G'' of the two solutions to 5% in the presence and absence of calcium ions (Figure 15).

In Figure 14A we can observe an increasing of modulus values over the frequency range and dominance of the G'' modulus values along the route with small oscillations around 5 and 9 Hz. This system was characterized as a fluid material. In the presence of calcium ions the behavior has been somewhat different as can be seen in Figure 14B. High values of G' was observed and this system was characterized as a very tight system, i.e., a strong gel. It was observed with the naked eye that a hardened layer of gel was formed soon after the experiment. The low values of G''/ G' also confirmed the formation of a firm gel. Fraeye *et al.* (2009) studied pectins from plants and fungal origins. They observed the pectin and calcium concentration influence on the formation of gels and noted that at lower pectin concentrations, it behaved as a fluid and at higher concentration, gel properties were observed as in agreement with results obtained in this work.

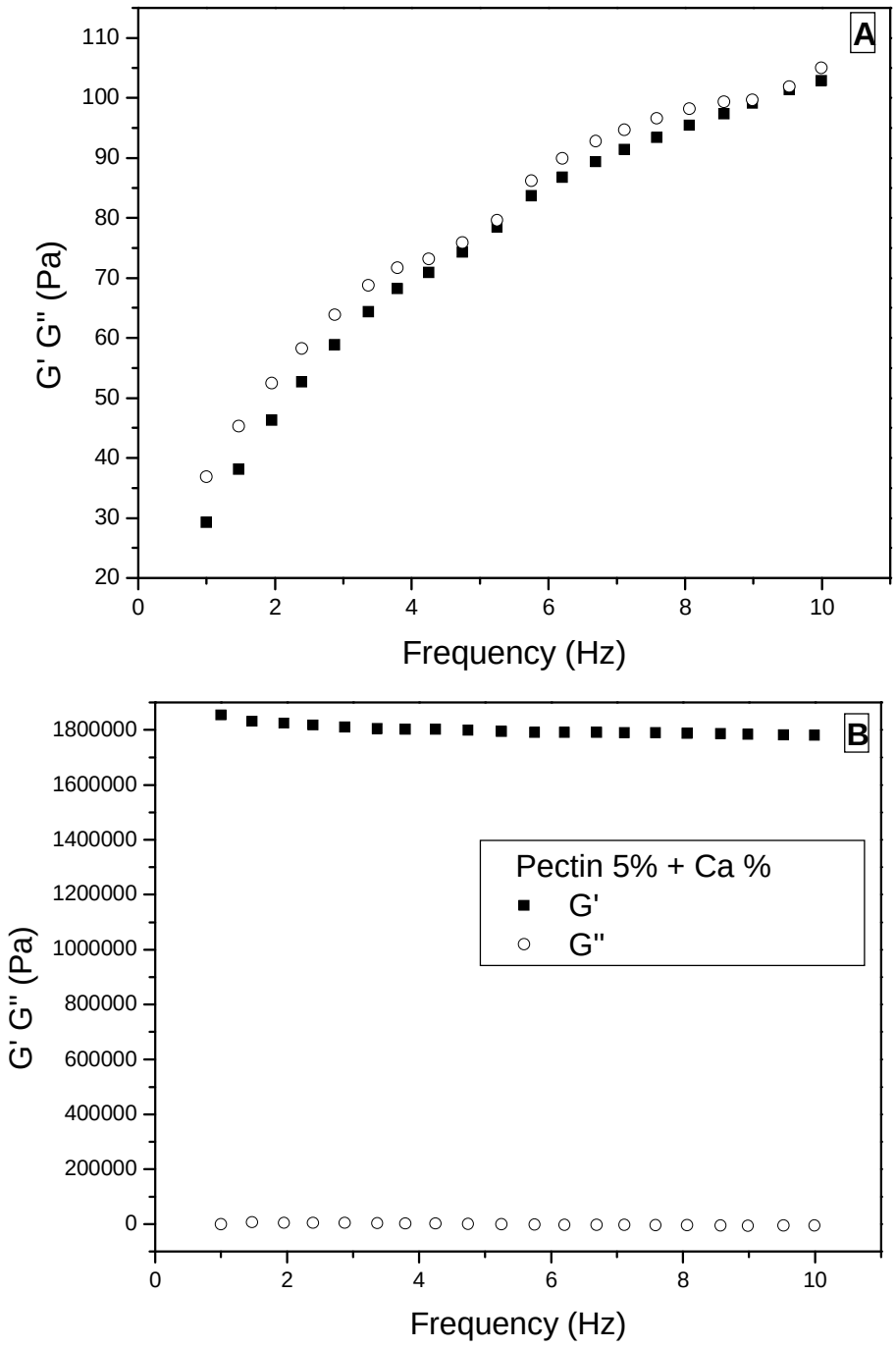

Figure 15 - Elastic (G', ■) and loss modulus (G'', ○) for the solution of pectin 5% in the presence (B) and absence (A) of Ca^{2+} (1%) in frequency range of 1-10 Hz at 25 ° C.

3.7. Rheological experiments – Effect of temperature and sucrose

Sample preparation of pectin and pectin/sucrose was performed in phosphate buffer pH = 3 and after that the solutions were stored overnight at 10 °C. It was observed visually the formation of a gelatinous solution under these conditions. The rheological study was carried out preparing a shear ramp for each sample. The test was performed at different temperatures as shown in Figure 16.

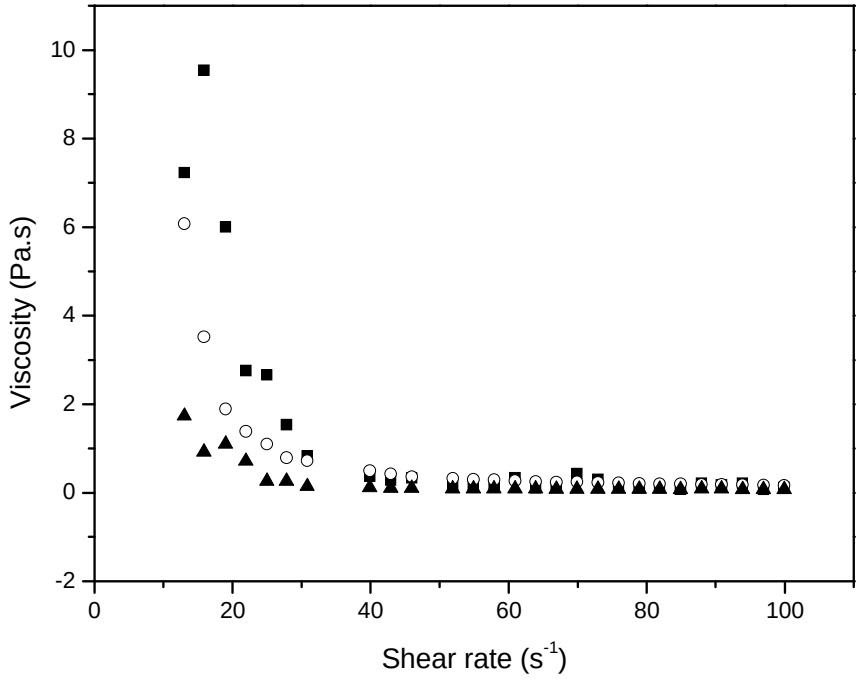

Figure 16 – Shear ramp plot for aqueous 3% pectin at pH = 3 and at different temperatures (20, ■ ; 40, ○ ; 60 °C, ▲).

It was observed in Figure 16 shows a pseudoplastic behavior for all systems, where there is a sudden decrease of the viscosity values increasing shear rate. It can also be observed in Figure 15 the effect of temperature on viscosity. Increasing on the temperature we can observe a decrease of viscosity values and being initially more pronounced as increases shear rate values. There is a tendency to constant values after 50 s^{-1}.

In Figure 17 we can observe a somewhat different behavior on viscosity values for the pectin and sucrose solutions in the same conditions.

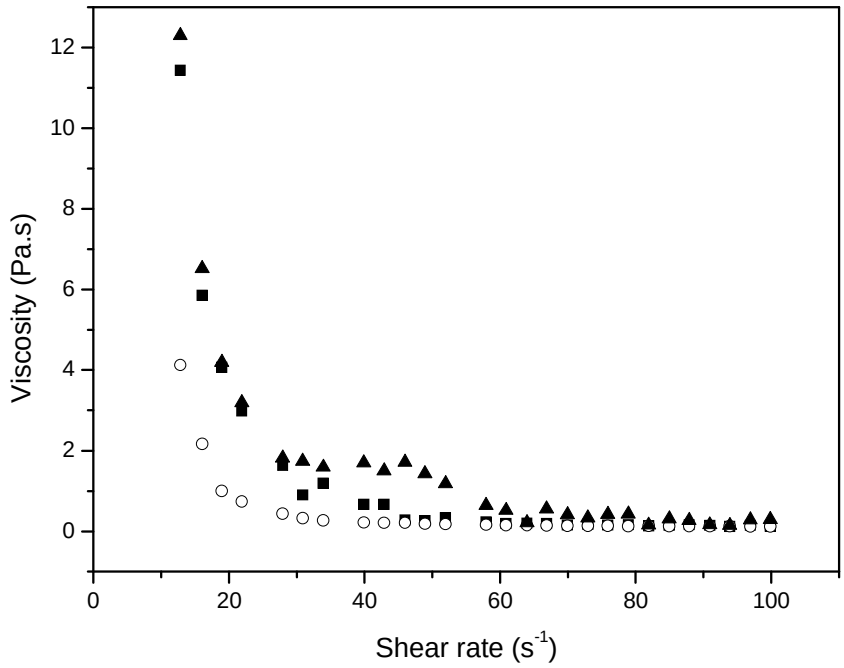

Figure 17 – Shear ramp for 3% pectin + 10% sucrose solution of at pH = 3 and at different temperatures (20, ■ ; 40, ○ ; 60 °C, ▲).

It was observed in Figure 17 the same shear thinning behavior shown in Figure 16, as the viscosity values decrease sharply increasing shear rate. The difference lies in the effect of temperature on the sample. It is observed that with increasing temperature from 20 to 40 º C there is a decrease in viscosity values, while a temperature increase from 40 to 60 ºC causes an increase in viscosity values. This can be explained by interactions between the pectin chains and sucrose that at high temperatures and low pH favors the formation of gel. Studies reported before explains that sucrose may provide more hydroxyl groups to stabilize the structure of junction zones and promote hydrogen bonds to immobilize free water (Fu & Rao, 2001).

In order to study the inversion in viscosity seen in Figure 17, where the values at 60 ºC were above that at 40 ºC, we performed a temperature test between 20 and 60 °C for the same samples and the same inversion in pectin/sucrose could be observed as can be seen in Figure 18.

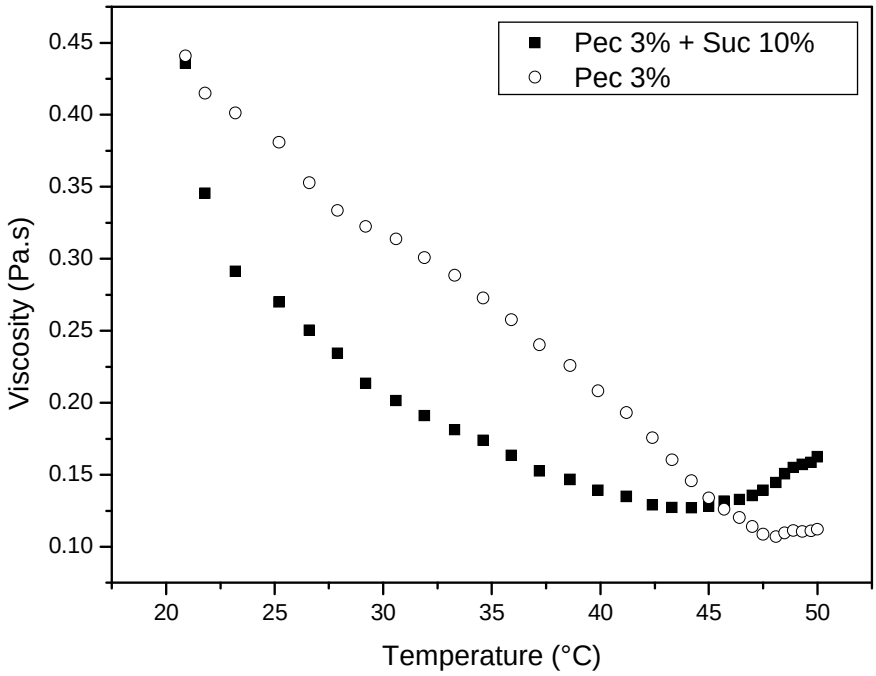

Figure 18 – Temperature ramp plot for an aqueous pectin solution (3%) in presence (■) and absence (○) of sucrose (10%) and at pH = 3.

Between 20 and 40 °C a sharp decrease in viscosity values due to the temperature effect. But around 44 °C it was observed a process of reversing with a rise in viscosity values. Evageliou *et al.* (2000) studied the effect of adding sucrose to pectin (DM 70%) at low pH and observed a reversal of values with increasing temperature, giving evidence for the formation of additional intermolecular associations.

It was also carried out a study of the system pectin / sucrose by oscillatory rheology at 10 rad / s, 2% strain, the angular velocity of 1 °C / min and temperature ranging from 20 to 55 º C, as shown in Figures 19.

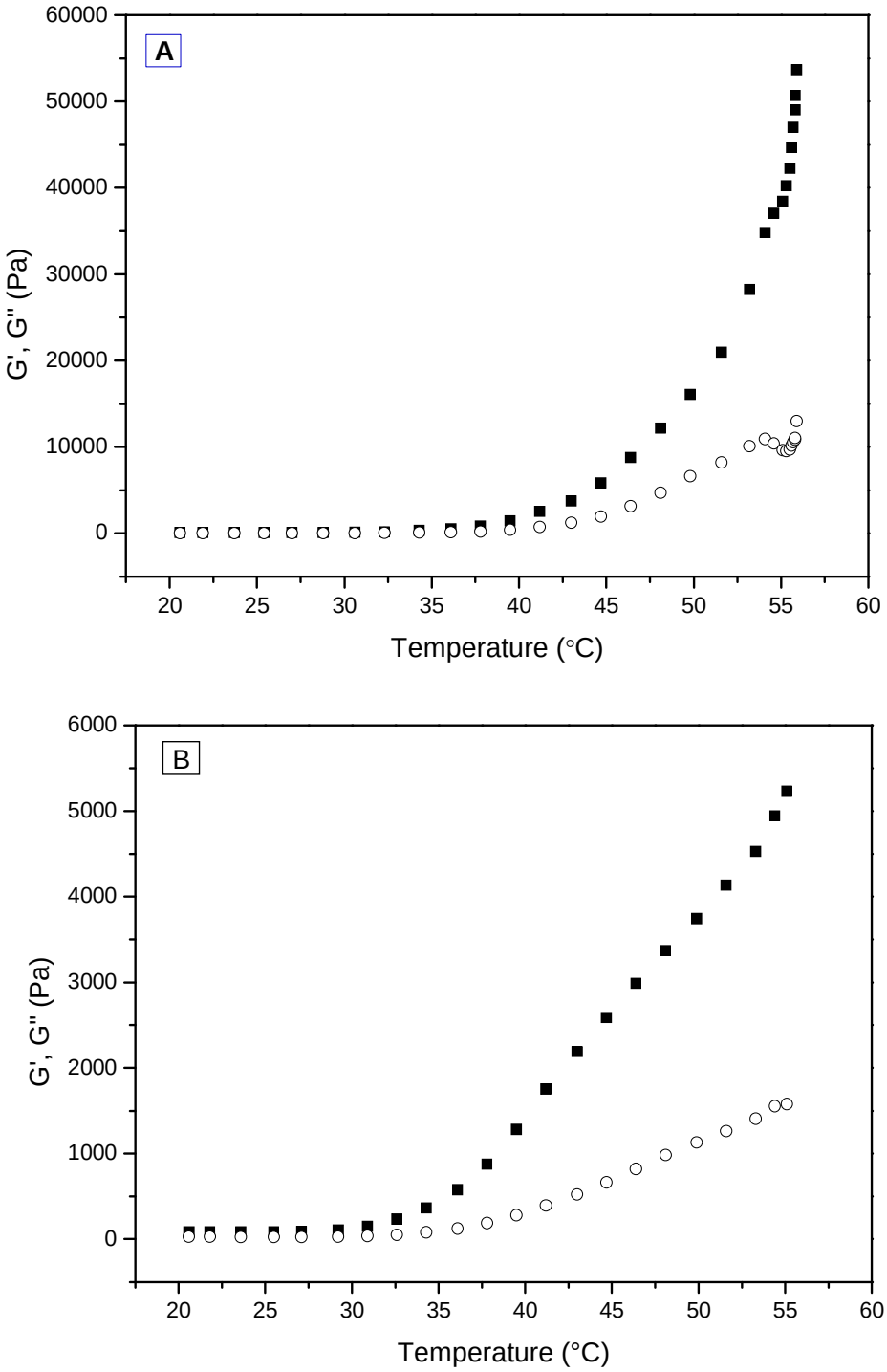

Figure 19 - Parameters G ' (■) and G " (○) *versus* temperature for pectin (3%) (A) and pectin/sucrose (10%) (B) systems.

Observing the graphs in Figure 19 we see that the parameters G 'and G " of the 3% pectin (w / w) solution at pH = 3, with and without 10% sucrose (w / w) increase with temperature. In Figure 19A, G' and G" remain close until approx. 40 °C, and then we can observe a G' predominance along temperature values. In Figure 19B that characteristic observed in graph A is larger; this means that the gel behavior of the sample outweighs the viscous since the beginning of the experiment and increases with more intensity from 30 °C.

Fu & Rao (2001) conducted rheological studies of pectin gels and sucrose in this same conditions and observed similar behavior. But at higher pectin and sucrose concentrations, it was observed a contrary behavior, i.e, where G 'decreases with increasing temperature.

4. Conclusions

IR spectroscopy and ^{1}H NMR were effective to qualify the DM of the pectin sample. DM was 58% for the sample by ^{1}H, and was characterized as high-methoxyl pectin. By ^{13}C NMR spectroscopy, different groups of known polymers were identified in the chains of pectic polysaccharides obtained.

The molecular peak was determined by GPC as a value of 9.5×10^{5} g / mol. Shear measurements, with temperature variations for the pectin solution and pectin with sugar showed the possible formation of stronger interactions between the molecular pectin chains and sucrose around 45 °C. The rheological study of continuous shear of pectin solution showed Newtonian behavior. When in the presence of calcium ions, their behavior was pseudoplastic, showing the formation of electrostatic interactions between pectic chains and calcium ions. We could also observe interactions between pectin and sucrose at low pH = 3, observing an increasing in viscosity values along temperature increasing.

5. Acknowledgments

The authors would like to express their thanks to CNPq for financial support, to CENAUREMN at the Federal University of Ceará for performing the NMR analysis and to INOMAT.

6. References

Adams, G. G., Imran, S., Wang, S., Mohammad, A., Kok, M. S., Gray, D. A., Channell, G. A., Harding, S. E. (2012). Extraction, isolation and characterisation of oil bodies from pumpkin seeds for therapeutic use. *Food Chemistry*, in Press.

Anthon, G. E., Barrett, D. M. (2008). Combined enzymatic and colorimetric method for determining the uronic acid and methylester content of pectin: Application to tomato products. *Food Chemistry*, 10, 239-247.

Arima, H. K., Rodriguez-Amaya, D. B. (1990). Carotenoid composition and vitamin A value of a squash and a pumpkin from northeastern Brazil. *Archivos Latinoamericanos de Nutrición*, 40, 284-292.

Axelos, M. A. V., Thibault. J. F. (1991). The chemistry of low-methoxyl pectin gelation, p. 109–118. In R. H. Walter (ed.), The chemistry and technologyof pectin. Academic Press, San Diego, Calif.

Azero, E. G., Andrade, C. T. (2002). Testing procedures for galactomannan purification. *Polymer Testing*, 21, 551 - 556.

Benjamin, O., Silcock, P., Leus, M., Everett, D. W. (2012). Multilayer emulsions as delivery systems for controlled release of volatile compounds using pH and salt triggers. *Food Hydrocolloids,* 27, 109–118.

Blumenkrantz, N., Asboe-Hansen, G. (1973). New methods for quantitative determination of uronic acid. *Analytical Biochemistry,* 54, 484-489.

Bottger, I. (1990). Pectin application—Some practical problems. In G. O. Phillips, D. J. Wedlock, & P. A. Williams (Eds.), Gums and stabilisers for the food industry, vol. 5 (pp. 247–256). Oxford, UK: IRL Press.

Braccini, I., & Pérez, S. (2001). Molecular basis of Ca^{2+}-induced gelation in alginates and pectins: the egg-box model revisited. *Biomacromolecules*, 2, 1089–1096.

Catoire, L., Goldberg, R., Pierron, M., Morvan, C., Penhoat, C. H. (1998). An efficient procedure for studying pectin structure which combines limited depolymerization and ^{13}C NMR. *European Biophysics Journal*, 27 127–136.

Etzler, M. E., Mohnen, D. (2009). Viridiplantae. In: Varki A, Cummings RD, Esko JD, et al., editors. Essentials of Glycobiology. 2nd edition. Cold Spring Harbor (NY): Cold Spring Harbor Laboratory Press.

Evageliou, V., Richardson, R. K., Morris, E. R. (2000). Effect of pH, sugar type and thermal annealing on high-methoxy pectin gels. *Carbohydrate Polymers*, 42, 245-259.

Filipov, M. P., (1992). Practical infrared spectroscopy of pectic substances, *Food Hydrocolloids*, 6, 115-118.

Fraeye, I., Doungla, E., Duvetter, T., Moldenaers, P., Loey, A. V., Hendrickx, M. (2009) Influence of intrinsic and extrinsic factors on rheology of pectin–calcium gels. *Food Hydrocolloids,* 23, 2069–2077.

Fu, J-T., Rao, M. A., (2001). Rheology and structure development during gelation of low-methoxyl pectin gels: the effect of sucrose. *Food Hydrocolloids*, 15, 93-100.

Gilchrist, H., Taranath, D. A., Gole, G. A. (2010). Ocular malformation in a newborn secondary to maternal hypovitaminosis A. *Journal of AAPOS*. 14, 274-276

Guillon, F., Champ, M. (2000). Structural and physical properties of dietary fibres, and consequences of processing on human physiology. *Food Research International*, 33, 233-235.

Ha, M., Viëtor, R. J., Jardine, G. D., Apperley, D. C. Jarvis, M. C. (2005). Conformation and mobility of the arabinan and galactan side-chains of pectin. *Phytochemistry,* 66, 1817–1824.

Harholt, J., Suttangkakul, A., Scheller, H. V. (2010). Biosynthesis of Pectin. *Plant Physiology*, 153, 384–395.

Keenan, M. H. J., Belton, P. S., Matthew, J. A., Howson, S. J. (1985). A ^{13}C-N.M.R. study of sugar-beet pectin. *Carbohydrate Research*, 138, 168–170.

Krall, S. M., McFeeters, R. F. (1998). Pectin Hydrolysis: Effect of temperature, degree of methylation, pH, and calcium on hydrolysis rates. *Journal of agricultural and food chemistry*, 46, 1311-1315.

May, C. D. (1990). Industrial pectins: Sources, production and applications. *Carbohydrate Polymers*, 12, 79–99.

Molecular Expression Website. Plant Cell Wall. (2012). Retrieved on May 8th from http://micro.magnet.fsu.edu/cells/plants/cellwall.html

Morris, G. A., Garcial de al Torre, J., Ortega, A., Castile, J., Smith, A. & Harding, S. E. (2008). Molecular flexibility of citrus pectins by combined sedimentation and viscosity analysis. *Food Hydrocolloids, 22*, 1435-1442.

Murkovic, M., Mülleder, U., Neunteu, H. (2002). Carotenoid Content in Different Varieties of Pumpkins. *Journal of Food Composition and Analysis*, 15, 633-638.

Ngouémazong, D. E., Tengweh, F. F., Fraeye, I., Duvetter, T., Cardinaels, R., Loey, A. V., Moldenaers, P., Hendrickx, M. (2012). Effect of de-methylesterification on network development and nature of Ca^{2+}-pectin gels: Towards understanding structure-function relations of pectin. *Food Hydrocolloids*, 26, 89-98.

Oakenfull, D. G. (1991). The chemistry of high-methoxyl pectins. In: R. H. WALTER, Editor, The Chemistry and Technology of Pectins, Academic Press Inc., San Diego, 87–106.

Olano-Martin, E., Rimbach, G. H., Gibson, G. R., Rastall, R. A. (2003). Pectin and pectic-oligosaccharides induce apoptosis in *in vitro* human colonic adenocarcinoma cells. *Anticancer Research*, 23, 341–346.

Pagán, J., Ibarz, A., Llorca, M., Pagán, A., Barbosa-Cánovas, G. V. (2001). Extraction and characterization of pectin from stored peach pomace. *Food Research International*, 34, 605–612.

Phillips, G. O. (2000). Colloids: A partnership with nature. In K. Nishinari (Ed.), Hydrocolloids. Part 2. Fundamentals and applications in food, biology and medicine (pp. 3–15). Amsterdam: Elsevier.

Ptichkina, N. M., Markina O. A., Rumyantseva, G. N. (2008). Pectin extraction from pumpkin with the aid of microbial enzymes. *Food Hydrocolloids,* 22, (2008) 192–195.

Pumpkin. Photograph. Encyclopædia Britannica Online. Web. (2012). Retrieved on May 17th from http://www.britannica.com/EBchecked/media/30871/Pumpkin.

Sigmaaldrich website. Pectinases and pectins. (2012). Retrieved on May 17th from http://www.sigmaaldrich.com/life-science/metabolomics/enzyme-explorer/learning-center/carbohydrate-analysis/carbohydrate-analysis-iii.html#Pectin

Singthong, J., Ningsanond, S., Cui, S. W., Goff, H. D. (2005). Extraction and physicochemical characterization of Krueo Ma Noy pectin. *Food Hydrocolloids*, 19, 793-801.

Souza, J. R. R., Carvalho, J. I. X., Trevisan, M. T. S., Paula, R. C. M., Ricardo, N. M. P. S., Feitosa, J. P. A. (2009). Chitosan-coated pectin beads: characterization and in vitro release of mangiferin. *Food Hydrocolloids, 23*, 2278-2286.

Tamaki, Y., Konishi, T., Fukuta, M., Tako, M. (2008). Isolation and structural characterization of pectin from endocarp of Citrus depressa. *Food Chemistry*, 107, 352–361.

Vincken, J. P., Schols, H. A., Oomen, R. J. F. J., Beldman, G., Visser, R. G. F. Voragen, A. G. J. (2003a). Pectin – the hairy thing. In: Voragen, A. G. J., Schols, H. and Visser, R., Editors, Advances in Pectin and Pectinase Research, Kluwer Academic Publishers, Boston, Dordrecht, 47–59.

Vincken, J.-P., Schols, H. A., Oomen, R. J. F. J., McCann, M. C., Ulvskov, P., Voragen, A. G. J., Visser, R. G. F. (2003b). If homogalacturonan were a side chain of rhamnogalacturonan I. Implications for cell wall architecture. *Plant Physiology, 132*, 1781–1789.

Voragen, A. G. J., Pilnik, W., Thibault, J.-F., Axelos, M. A. V., & Renart, C. M. G. C. (1995). Pectins. In A. M. Stephen (Ed.), Food polysaccharides and their applications (pp. 287–369). New York: Marcel Dekker.

Waldron, K. W., Parker, M. L., Smith, A. C. (2003). Plant cell walls and food quality*. Comprehensive Reviews in Food Science and Food Safety*, 2, 101-119.

Willats, W. G. T., Knox, J. P., Mikkelsen D. J. (2006). Pectin: new insights into an old polymer are starting to gel. *Trends in Food Science & Technology,* 17, 97-104.

Yoo, S.-H, Fishman, M. L., Hotchkiss Jr, A. T. Lee, H. G. (2006). Viscometric behavior of high-methoxy and low-methoxy pectin solutions. *Food Hydrocolloids, 20*, 62-67.

CHAPTER 2

Spray-drying Encapsulation of Mangiferin using Natural Polymers

Souza, J. R. R.[1,3], Feitosa, J. P. A.[1], Paula, H. C. B.[2], Ricardo, N. M. P. S[1], Trevisan, T. S.[1], Ulrich C. M.[3], Owen, R. W.[3]

[1]Departament of Organic and Inorganic Chemistry, Federal University of Ceará P. O. Box: 6.021, ZIP-Code: 60455-760, Fortaleza, Ceará, Brazil

[2]Departament of Analytical and Physical Chemistry, Federal University of Ceará – P. O. Box: 6.021, ZIP-Code: 60451-970, Fortaleza, Ceará, Brazil

[3]Division of Preventive Oncology, National Center for Tumor Diseases, Im Neuenheimer Feld 460/German Cancer Research Center, Im Neuenheimer Feld 581, Heidelberg, Germany

Microencapsulation processes, such as spray-drying is an alternative to enhance solubility of bioactive materials and a good way to preserve, protect and control the release rate of a substance until it reaches its target in the body. Mangiferin is an active phytochemical present in various plants including *Mangifera indica L*. This substance is reported to have anti-cancer, antioxidant and other activities, but has a low solubility in aqueous medium. In this work we encapsulated mangiferin within four different natural polymers compositions by using spray-drying techniques. The products were characterized by FTIR, SEM and HPLC-ESI-MS. A calibration curve was constructed by HPLC to determine the efficiency of mangiferin incorporation into each encapsulate. The highest encapsulation efficiency was determined to be for pectins using Polysorbate 80 (Tween 80) as emulsifier.

Keywords: mangiferin, encapsulation, pectin, chitosan, spray-drying.

1. Introduction

1.1. Microencapsulation techniques

Microencapsulation processes have gained considerable attention as a convenient way of preparing drug delivery vehicles for several applications. Encapsulation process is being largely used in the food and pharmaceutical industry. Encapsulation is generally defined as the entrapment of active substances within another wall material where the active substance is present in the core or spread around the network of a coating matrix. The encapsulating substance is also quite often called coating, membrane, shell, capsule or carrier (Nedovik *et al*., 2011; Fang & Bhandari, 2010)

Controlled drug release systems prepared from polymeric materials have been shown to improve pharmacokinetic and pharmacodynamic properties of encapsulated drugs (Beck-Broichsitter *et al.,* 2011). Polymeric particles with desirable properties such as biocompatibility and degradability are generally preferred for controlled drug delivery in order to prolong the release of the drug at the target site (Kurmi *et al.,* 2010; Lebhardt *et al.,* 2010; Roy & Viji, 2010) The Figure 1 show encapsulation systems for the delivery of bioactive molecules to the intestine.

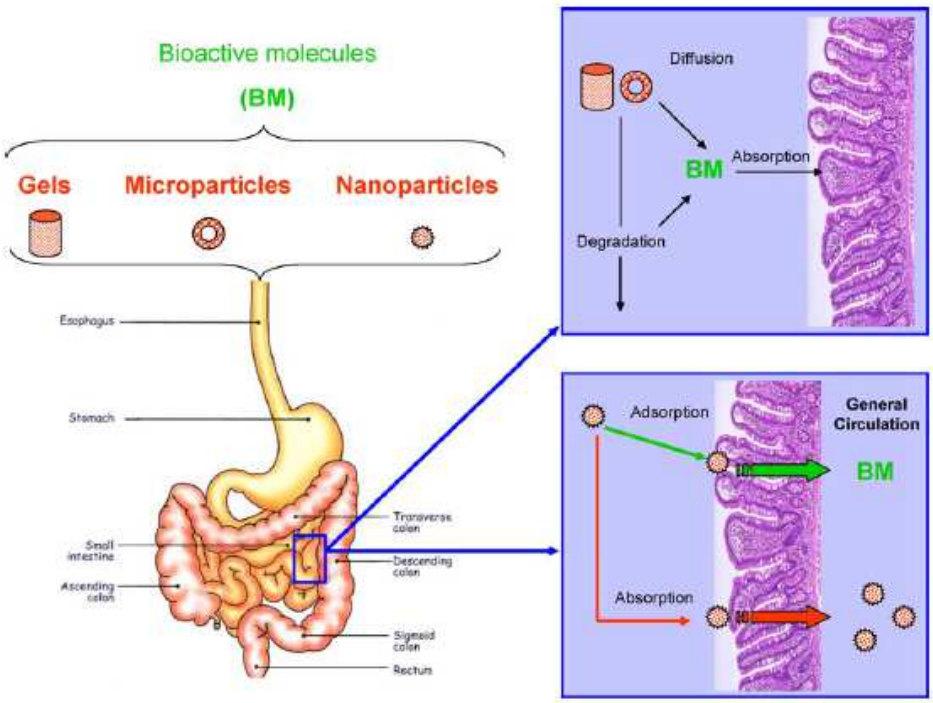

Figure 1 – Different absorbance mechanisms of bioactive molecules released from encapsulation systems to the intestine. Adapted from Chen *et al.,* 2006.

In hydrogel and microparticles systems, bioactive compounds have to be released from the matrix to allow absorbance while nanoparticles may improve absorbance of the bioactive either by adsorbing to the intestinal wall to prolong residence time or by direct uptake by the intestinal epithelium (Chen *et al.,* 2006). Encapsulation matrices provide maximal physical stability, protect ingredients against chemical degradation, and allow precise control over the release of encapsulated components to maximize absorbance (Weiss *et al.,* 2008).

1.2. Spray-drying technique

Different techniques are reported for the preparation of drug-loading systems such as solvent displacement and emulsification solvent evaporation, for example (Kumari *et al.,* 2010; Rao *et al.,* 2011). Spray-drying methods have been widely described for the preparation of microparticles containing bioactives in aqueous media (Gharsallaoui *et al.,* 2007; Gharsallaoui *et al.,* 2010). The Figure 2 shows a picture of benchtop spray dryer equipment Büchi used for preparing microcapsules.

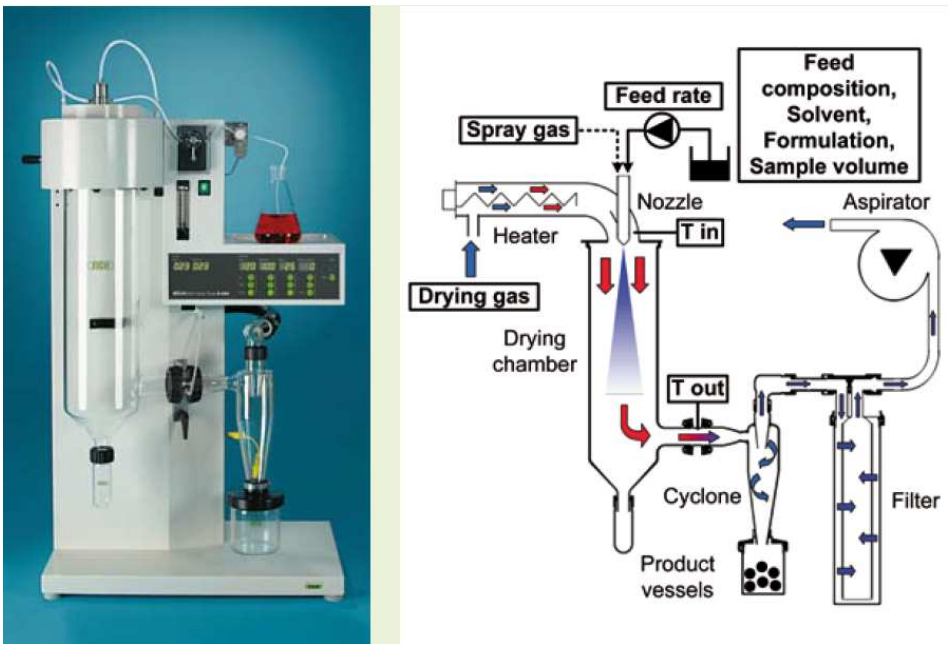

Figure 2 - Spray-dryer equipment Büchi, model B-290, Switzerland. Picture from Büchi website, 2012.

The method consists of liquid atomization into small droplets, a drying step carried out using a warmed gas and collection of the solid particles (Beck-Broichsitter *et al.,* 2011).

The Mini Spray Dryer B-290 from Büchi Labortechnik AG is a laboratory scale instrument to perform spray drying processes. Fine particles are produced because of the short residence time in such a compact spray dryer. The powder collection is provided by a glass-made cyclone separator, which is internally coated with a thin nanosize antistatic film to reduce powder adhesion to the glass wall. The separation works by centrifugal forces by virtue of inertia of the solid particles (Büchi website, 2012).

1.3. Mangiferin – a xanthone glucoside

Mangiferin (1, 3, 6, 7 - tetrahydroxyxanthone-C2-beta-D-glucoside), a xanthone *C*-glucoside, is an active phytochemical present in various plants including *Mangifera indica L.* (Barreto *et al.,* 2008). The substance is reported to have strong antioxidant activities (Dar *et al.,* 2005), anti-allergic properties (Rivera *et al.,* 2006), anthelminthic property (Garcia *et al.,* 2003), gastro-protective effects (Carvalho *et al.,* 2007), antitumor activity (Guha *et al.,* 1996), and antiviral properties (Yoosook *et al.,* 2000). Mangiferin has also been used as foodstuffs for treating diabetes (Wada, 2007) and treating and preventing neurodegenerative diseases and aging symptoms (Matute *et al.,* 2007). Mangiferin can be considered as non-toxic as its reported oral LD_{50} value in mice was 400 mg/kg (Jagetia & Baiga, 2005). Mangiferin structure is shown in Figure 3

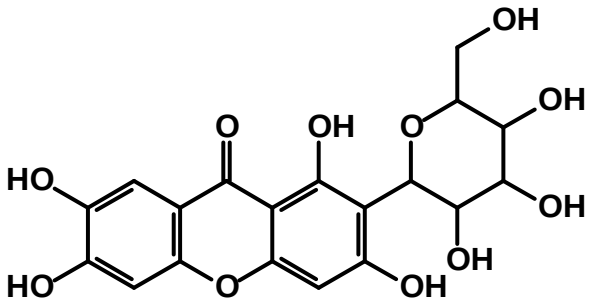

Figure 3 – Structure of mangiferin drew using chemwin software.

Mangiferin is reported to have a very low solubility in aqueous media: 0.111 mg/mL (Wang, 2007) and also a very low bioavailability: Tmax (time point of maximum plasma concentration) of mangiferin was found to be 38.64 $ng.mL^{-1}$ after administration of 0.9 g in a human trial (Hou *et al.,* 2012).

Encapsulation processes are a good way to preserve the chemical integrity and increase bioavailability for poorly water soluble food substrates as well as prolonging the residence time at the target site (Duchateau *et al*., 2008).

1.4. Polymers & Encapsulation of Bioactive Substances

Polymer wall materials can be selected from a wide variety of natural and synthetic polymers. Many biopolymers have been described in microencapsulation applications by spray-drying. The microencapsulation is often achieved with biopolymers of various sources, such as natural polysaccharides (gum arabic, alginates, pectins, carragenans, etc.), proteins (milk or whey proteins, gelatin, etc.), maltodextrins with different dextrose equivalence, waxes and their blends (Gharsallaoui *et al.,* 2007). Polymers have been also used as disintegrating agents, which swell in contact with water, in pharmaceutical solid dosage forms such as tablets, coated tablets and capsules (Lüllmann *et al.,* 2000) as shown in Figure 4.

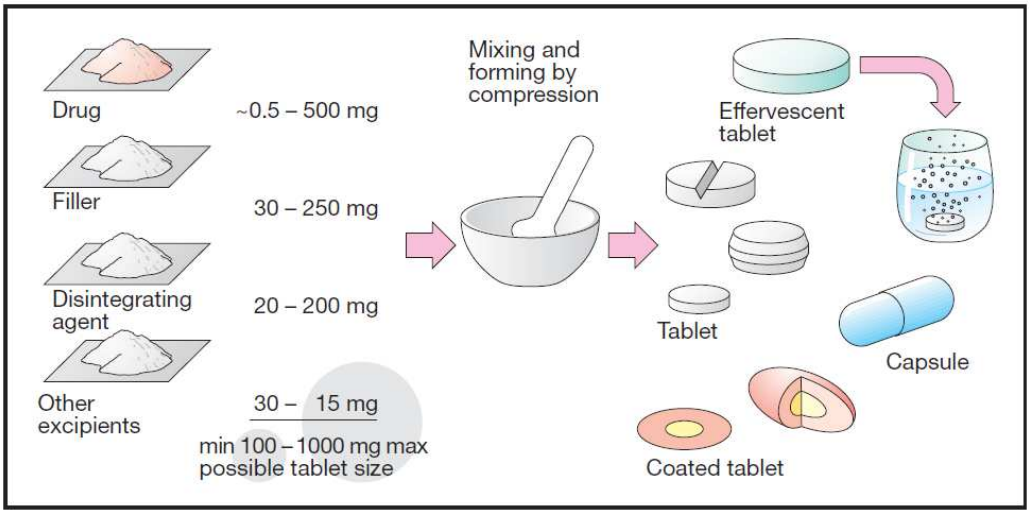

Figure 4 - Preparations of solid formulations for oral application. Figure adapted from Lüllmann *et al.* (2000).

The choice of a polymer wall material for spray-drying microencapsulation is very important for encapsulation efficiency and microcapsule stability. Polymer wall materials should possess good properties of emulsification, film forming, drying of the wall and concentrated solutions should have low viscosity. The wall system is designed to protect the core material from factors that may cause its deterioration, to prevent a premature interaction between the core material and other ingredients, to limit volatile losses, and also to allow controlled or sustained release under desired conditions. The costs should be also considered, naturally (Gharsallaoui *et al.,* 2007).

Pectin capsules have been used as a food carrier for the delivery of folic acid (Madziva, Kailasapathy, & Phillips, 2006). Pectin-based systems have been developed also for colon-specific protein and polypeptide drug delivery via the oral route (Liu *et al.,* 2003). This polysaccharide is non-toxic, not digested by gastric or intestinal enzymes and almost totally degraded by pectinolytic enzymes produced by the colonic microflora (Bourgeois *et al.,* 2006).

Chitosan (copolymer of β - (1→ 4)-D-glucosamine and β - (1→ 4)-N-acetyl-D-glucosamine), is abundant in nature, mainly in the carapace of crustaceans. The cationic polyelectrolyte nature of chitosan can provide a strong electrostatic interaction with the mucus or a negatively charged mucosal surface. This mucoadhesive property may extend the time of residence of the sphere containing the bioactive in the gastri-intestinal tract (Kim *et al.,* 2003).

Many surfactants are commonly used in pharmaceutical formulations as stabilizing excipients. Polyoxyethylene-20-sorbitan monooleate (Polysorbate 80; Tween 80) is an oleate ester of sorbitol and its anhydrides copolymerized with 20 moles of ethylene oxide for each mole of sorbitol and sorbitol anhydride (Adamo *et al.,* 2010). This nonionic surfactant is used to minimize surface tension and increase the drug solubility and stability (Adamo *et al.,* 2010; Khossravi *et al.,* 2002).

In the present work, pectin and chitosan formulations containing mangiferin were prepared by spray-drying technique and characterized by different techniques: FTIR, SEM, and HPLC-ESI-MS. The amount of mangiferin was also determined in each powder material using a calibration curve performed by HPLC.

2. Experimental

2.1. Materials

Citric pectin (CP) samples were obtained from Vetec – Chemicals. Pumpkin pectin (PP) was obtained and characterized in a previous work (Souza *et al.,* 2012). Chitosan (Ch) with a molar mass 7.82 x 10^4 g/mol and degree of deacetylation of 81± 1% was obtained from Quitoquímica –Chemicals and characterized by Magalhães *et al*. (2009). Mangiferin (Ma) was purified and characterized by Barreto *et al.,* (2008). Commercial mangiferin obtained from EXTRASYNTHÈSE Lot: 06113004 (Genay, France) was used as standard. All other chemicals used were of analytical grade.

2.2. Spray-drying encapsulation of mangiferin

The preparation of encapsulated mangiferin materials was performed in a spray-dryer equipment Büchi, Switzerland, model B-290. The inlet and outlet air temperatures were maintained at 160 °C and 80 °C, respectively, with a feed flow of 6 mL/min, an aspirator volume flow of 35 m^3/h, and an air volume flow of 84 L/h. The operational yield for all samples was 65%. In this encapsulation procedure, four different polysaccharide formulations were used as coating to the bioactive mangiferin, as shown in Table 1.

Table 1 – Formulations used as polymer coating for mangiferin.

Polymer Coating Formulations	
Spray drying 1 (SD1)	Citric pectin/mangiferin
Spray drying 2 (SD2)	Citric pectin/mangiferin/Tween
Spray drying 3 (SD3)	Pumpkin pectin/mangiferin/Tween
Spray drying 4 (SD4)	Chitosan/mangiferin/Tween

The first spray-drying formulation (SD1) was performed using commercial citrus pectin. For that, a mass of polysaccharide (2.0 g) was dissolved in 200 mL distilled water and gently stirred for 4 hours at room temperature. Afterwards, 200 mg of mangiferin was added to the solution which was stirred

overnight. The procedure for the other formulations (SD2-SD4) was the same as for SD1 except for the addition of the surfactant polysorbate 80 as emulsifier at a concentration of 0.1% per bioactive immediately before the addition of mangiferin to the solution.

2.3. Methods of characterization

2.3.1. Infrared spectroscopy

The Fourier transform IR spectra (FT-IR) of samples were recorded with a Shimadzu IR spectrophotometer (model 8300) in the range of 400 and 4000 cm^{-1} as KBr pellets.

2.3.2. Digital images of the encapsulated materials

Digital photographs of the encapsulated materials were taken using a 14.1 MP Digital Sony Cyber-shot, Model Carl Zeiss DSC-W350 14.

2.3.3. Scanning electron microscopy (SEM)

The surface of the polymer encapsulated formulations were observed using Phillips X-L 30 Scanning Electron Microscope (at low energy from 13 to 15 kV). The samples were deposited on copper and coated with carbon, using vapor deposition techniques. The surface was scanned using a magnification of 100 and 500.

2.3.4. Analytical HPLC-ESI-MS

High performance liquid chromatography-electrospray-ionization-mass spectrometry (HPLC-ESI-MS) analysis was conducted on a Hewlett-Packard (HP) 1090 liquid chromatograph (Agilent Technologies, Waldbronn, Germany) using a reverse-phase C18 Phenomenex column 250 mm × 4 mm (i.d.), 5 µm, (Latek, Eppelheim, Germany). The mobile phase consisted of 2% acetic acid in water (solvent A) and methanol (solvent B) with the following gradient profile: 95% A for 2 min; reduced to 75% A over 10 min; to 60% A over 20 min; to 50% A over 30 min; to 0% A over 5 min; continuing at 0% A until completion of the run. The flow rate of the mobile phase was 1.0 mL/min. Phenolic compounds in

the eluant were detected at 257, 278, and 340 nm with a diode-array UV detector (HP 1040M).

2.3.5. Electrospray Ionization Mass Spectrometry (ESI-MS)

HPLC-ESI-MS was conducted on an Agilent 1100 HPLC, coupled to an Agilent single-quadrupole, mass-selective detector (HP 1101; Agilent Technologies, Waldbronn, Germany). Chromatographic separation of methanolic extracts was conducted using a column of the same type and dimensions as for analytical HPLC (Phenomenex, Latek, Eppelheim, Germany). The mobile phase consisted of 2% acetic acid in water (solvent A) and acetonitrile (solvent B) with the following gradient profile: initially 95% A for 10 min; to 90% A over 1 min; to 60% A over 9 min; to 80% A over 10 min; to 60% A over 10 min; to 0% A over 5 min and continuing at 0% A until completion of the run. Phenolic compounds were detected by their UV absorbance (A) at 257, 278 and 340 nm at room temperature. Mass spectra in the negative-ion mode were generated under the following conditions: fragmenter voltage = 100 V, capillary voltage = 2500 V, nebulizer pressure = 30 psi, drying gas temperature = 350 °C, mass range = 100 - 1500 D. Instrument control and data handling were performed with the same software as for analytical HPLC.

2.3.6. Detection and Loading efficiency of mangiferin in encapsulated samples by HPLC-ESI-MS

The encapsulated samples were suspended in methanol at a concentration of 3.0 mg/mL for mangiferin extraction, vortexed for 1 minute (VORTEX-2 GENIE Model G-560E, Scientific Industries Inc., Bohemia, N.Y., USA) placed in an ultrasound bath (Transsonic T450, Hans schidbauer KG., Singen-HTW) for 5 minutes and then shaken gently in an Eppendorf mixer (Thermomixer comfort 22331 – Netheler – Hinz GmbH, Hamburg, germany) for 2 hours. Following that the samples were centrifuged (Termoelectron Industries SAS, Chateau, Gontier, France) for 5 min at 14,000 r.p.m. and supernatants (20 µL) samples were then analyzed by HPLC-ESI-MS.

3. Results and Discussion

3.1 Infrared Spectroscopy (IR) of the encapsulated materials

The main assignment of bands and "fingerprint" regions from the IR spectra (Figure 5) of the polysaccharide coatings are shown in Table 2.

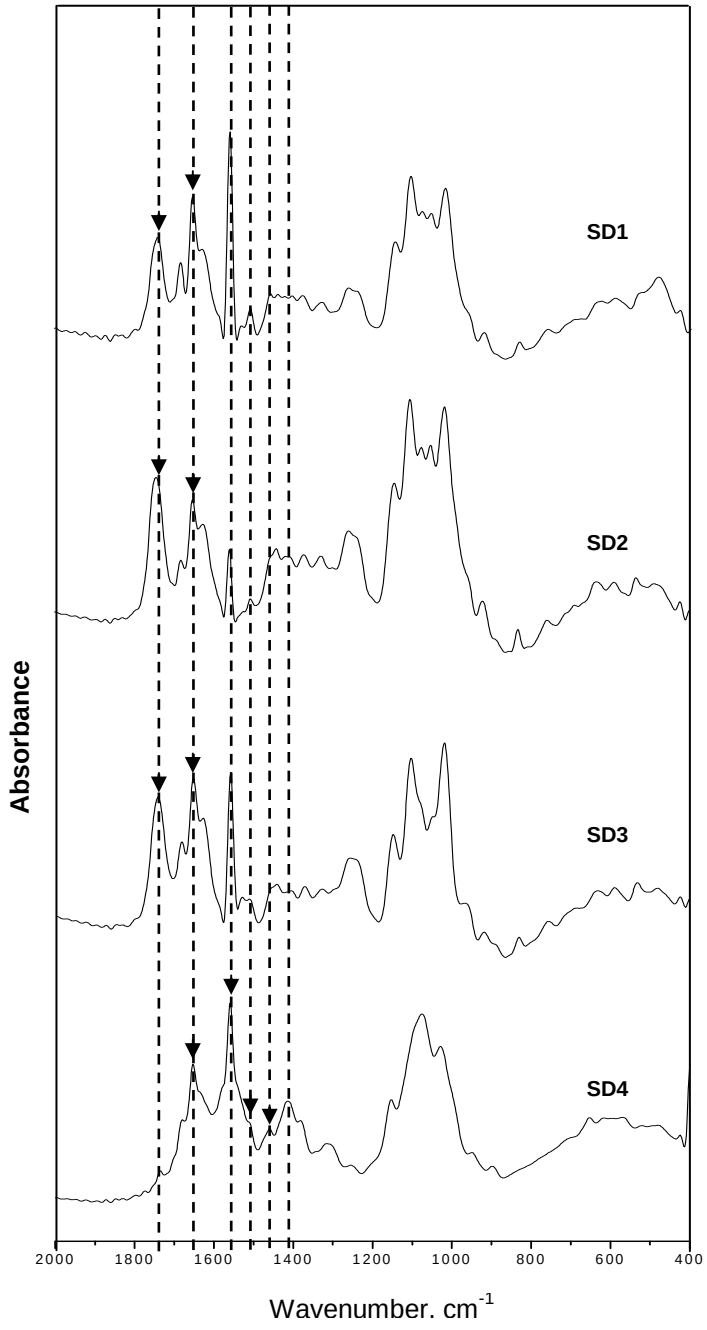

Figure 5 - FTIR of encapsulated mangiferin samples with different polymer coatings.

Table 2 - Assignment of bands in FTIR for encapsulated mangiferin systems (Kamnev *et al*., 1998; Lawrie *et al*., 2007; Rashidova *et al*., 2004)

Systems					Assignment
Chitosan	SD1	SD2	SD3	SD4	
-	1735	1735	1735	-	νC=O of COOH and ester of pectin
1652	1653	1653	1649	1653	νC=O (amide I) of chitosan, $\nu_{as}COO^-$ of pectin and OH from trace or bound water
1560	-	-	-	1560	δNH_2 from amine and δNH (amide II) of chitosan
1520	-	-	-	1516	$\delta_s NH_3^+$ of chitosan
1425	1400	1410	1405	1420	$\delta_s CH_2$ of chitosan and $\nu_s COO^-$ of pectin
1380	1382	1383	1375	1378	$\delta_s CH_3$ of chitosan and pectin
1155	1148	1148	1151	1151	νC-O-C of chitosan and pectin
1077	1102	1100	1103	1102	νC-O-C of chitosan and pectin
1033	1010	1015	1021	1019	Skeletal vibration involving νC-O of chitosan and pectin
920-580	920-580	920-580	920-580	920-580	Pulsation and some types of pyranose ring deformation

Figure 5 shows overviews of the FTIR spectra of the encapsulated materials. The regions between 1750 - 1350 cm^{-1} are characteristic for carboxylic groups. In the pectin samples spectra SD1, SD2 and SD3 an intense band at 1735 cm^{-1}, attributed to C=O group from non-ionized acid and from ester as in agreement with Kamnev *et al.,* (1998) is observed. The region between 1600 - 1650 and 1400 - 1450 cm^{-1} is characteristic of ionized carboxylic acid. In sample SD1 a higher intensity at 1650 than at 1735 cm^{-1} is observed. This is in agreement with the fact that the commercial pectin used for SD1 has a low degree of methoxylation (Souza *et al.,* 2012). On the for SD2, the band at 1735 cm^{-1} was slightly more intense and this effect may be due to the effect of the addition of the surfactant polysorbate 80 to the formulation promoting intermolecular interactions. The pumpkin pectin formulation SD3 exhibited a higher intensity band at 1650 than at 1735 cm^{-1} which is probably due to the addition of both surfactant and mangiferin because the contrary was observed in the spectrum of pumpkin pectin alone. That band can be also related to the presence of water in the sample. (Souza *et al.,* 2012).

The assignments of the chitosan sample SD4 is characterized by the appearance of a band at 1560 cm^{-1}, attributed to the NH_2 and NH functional groups of chitosan, also noted in the spectrum of this polysaccharide alone as shown by Souza *et al.,* (2009). The weak absorbances in the range of 1510-1530 cm^{-1} and near 1630 cm^{-1} (Lawrie *et al.,* 2007) indicate the presence of a protonated amine group from chitosan in SD4.

The FTIR spectra for mangiferin in the same range as that studied for the encapsulated samples namely 400-2000 cm^{-1} is shown in Figure 6. The spectrum showed main absorbances bands at 1650, 1622, 1495, 1256, 1196, 1094 cm^{-1} characteristic of mangiferin. Due to its very low concentration in the samples, polysorbate 80 was not be detected by FTIR.

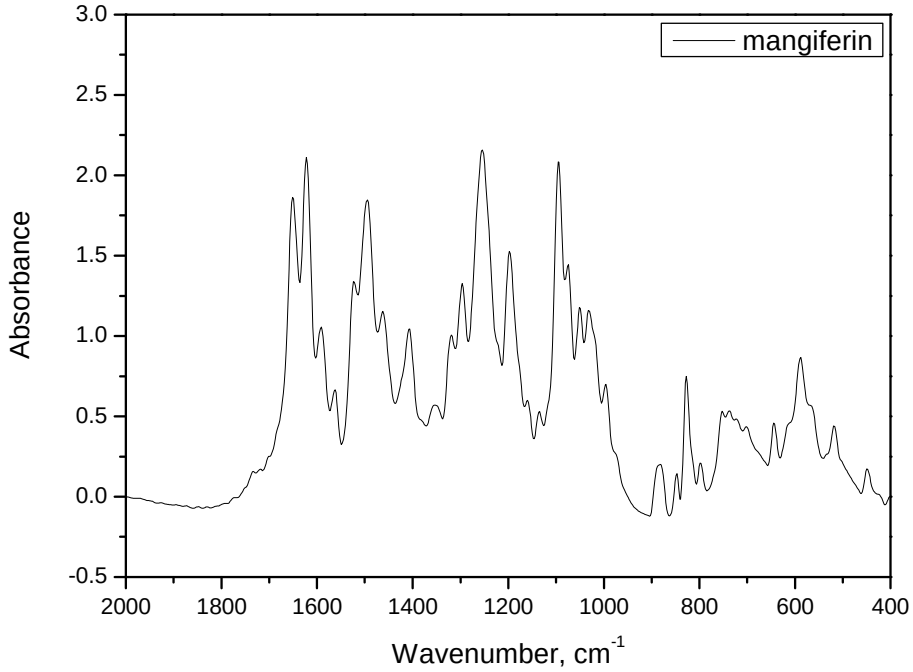

Figure 6 – FTIR for mangiferin between 400 - 2000 cm^{-1}.

The presence of mangiferin in the encapsulated samples was confirmed by the appearance of a high intensity peak at around 1560 cm^{-1} in all polysaccharide samples (Figure 5) which is likely a shifted absorbance band of mangiferin at 1520 cm^{-1}. This band is not present in the pectin (Souza *et al.,* 2012) or chitosan (Souza *et al.,* 2009) spectra what it is another confirmation for mangiferin. The mangiferin band at approximately 1650 cm^{-1} may also have an influence on the ionized carboxylic acid band for pectins which may explain why in the spectrum of SD3 this band was more intense than 1735 cm^{-1} as observed by Souza *et al.,* (2012) for the high methoxyl pumpkin pectin sample. Another observation (Figure 5) is the intensification of the band at app. 1100 cm^{-1} in all encapsulated sample spectra compared to that of chitosan or pectin itself what may be due to the high absorbance band at 1094 cm^{-1} for mangiferin.

3.2. Electronic photographs of the encapsulated materials

Figure 7 shows some photographs of the powder material obtained after spray-drying process. We can observe at naked-eye the differences between the materials obtained. Such as amount, colour, surface and particles shapes and sizes.

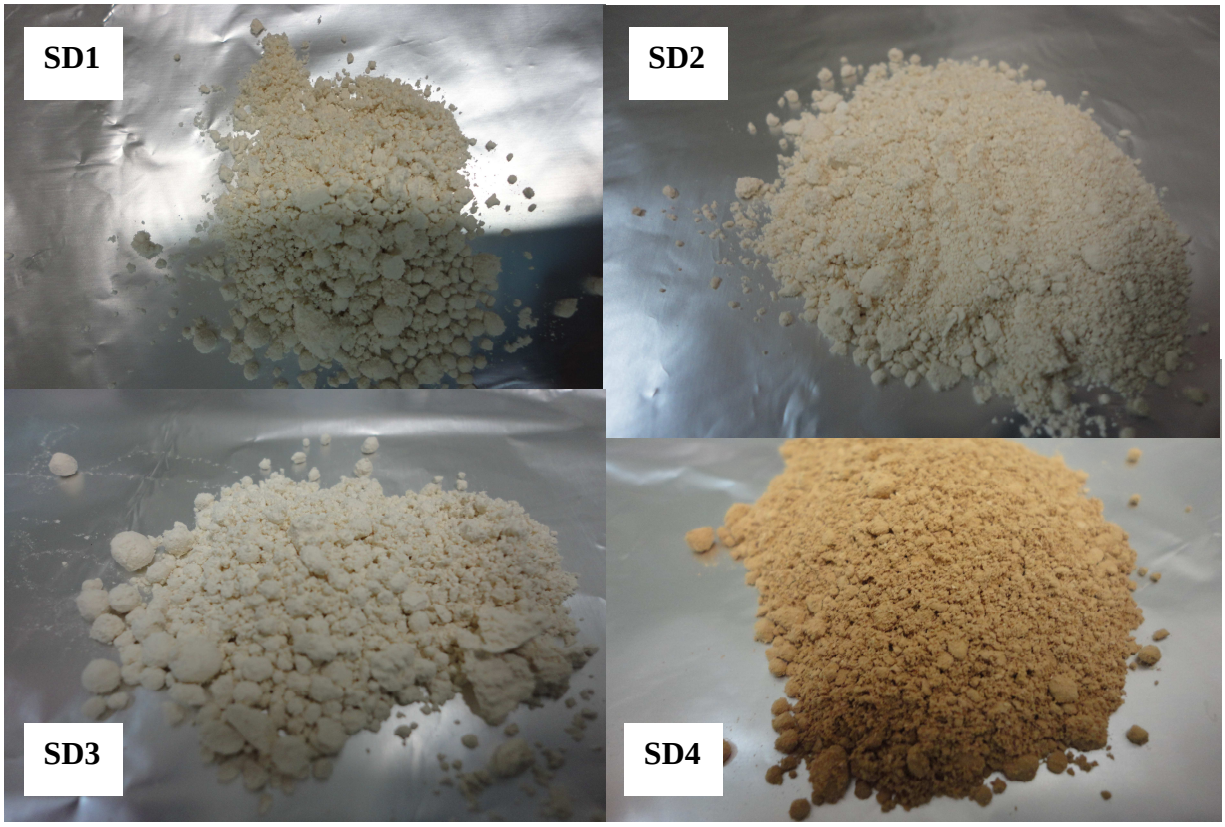

Figure 7 – Photographs for the encapsulated materials obtained after the atomization by spray-drying.

The pectin formulations SD1, SD2 and SD3 exhibit a white color while chitosan formulation SD4 exhibit strong brown coloration typical from the material. All formulation presented an amorphous appearance with different particle sizes and presence of agglomerations. SD2 seems to be more finely divided when compared to SD1, probably due to the addition of the surfactant Tween 80 to the formulation. The same was not observed to SD3, but much more agglomerations, in which pumpkin pectin was used.

3.3. Scanning Electronic Microscopy - SEM

Spray-drying technology has been used to synthesize fine homogeneous and multicomponent powders. Spherical powder particles obtained by a spray-drying method exhibit from irregular to regular morphologies and can exhibit high packing density, which leads to a better energy density (Zhang *et al.,* 2012).

The morphology obtained for the encapsulated materials was observed by SEM as shown in Figures 8 and 9. The particles are submicron or micron in diameter. A small amount of the particles are broken due to the high temperature used for spray drying. The submicron particles fill in the spaces between the micron particles, which improves the tap density (Zhang *et al.,* 2012). We can observe that the resulting particles have different average diameters. The wide measured range was between 3 and 7 µm for the SD1 and SD3 samples, respectively, even though we can see smaller particles than that. A slight size difference between SD1 and SD2 (range of size) was observed due to the addition of Polysorbate 80. SD4 displayed the smallest diameter between 3 and 5 µm.

The particle surface observed for SD1 was smooth but irregular, while those of SD2 presented a much smoother and regular surface. Because they were prepared using the same matrix, this effect was probably due to the addition of Polysorbate 80 to SD2, which likely improves the intermolecular interactions between the bioactive-matrix and the matrix itself causing smoothing effects on the particles surface. SD3 showed irregular spherical particles with some aggregation. In this case, the higher degree of methoxylation in the pectin used for SD3 may have an effect on the particle formation. SD4 particles were spherical but they presented a rough surface as can be observed in Figure 9.

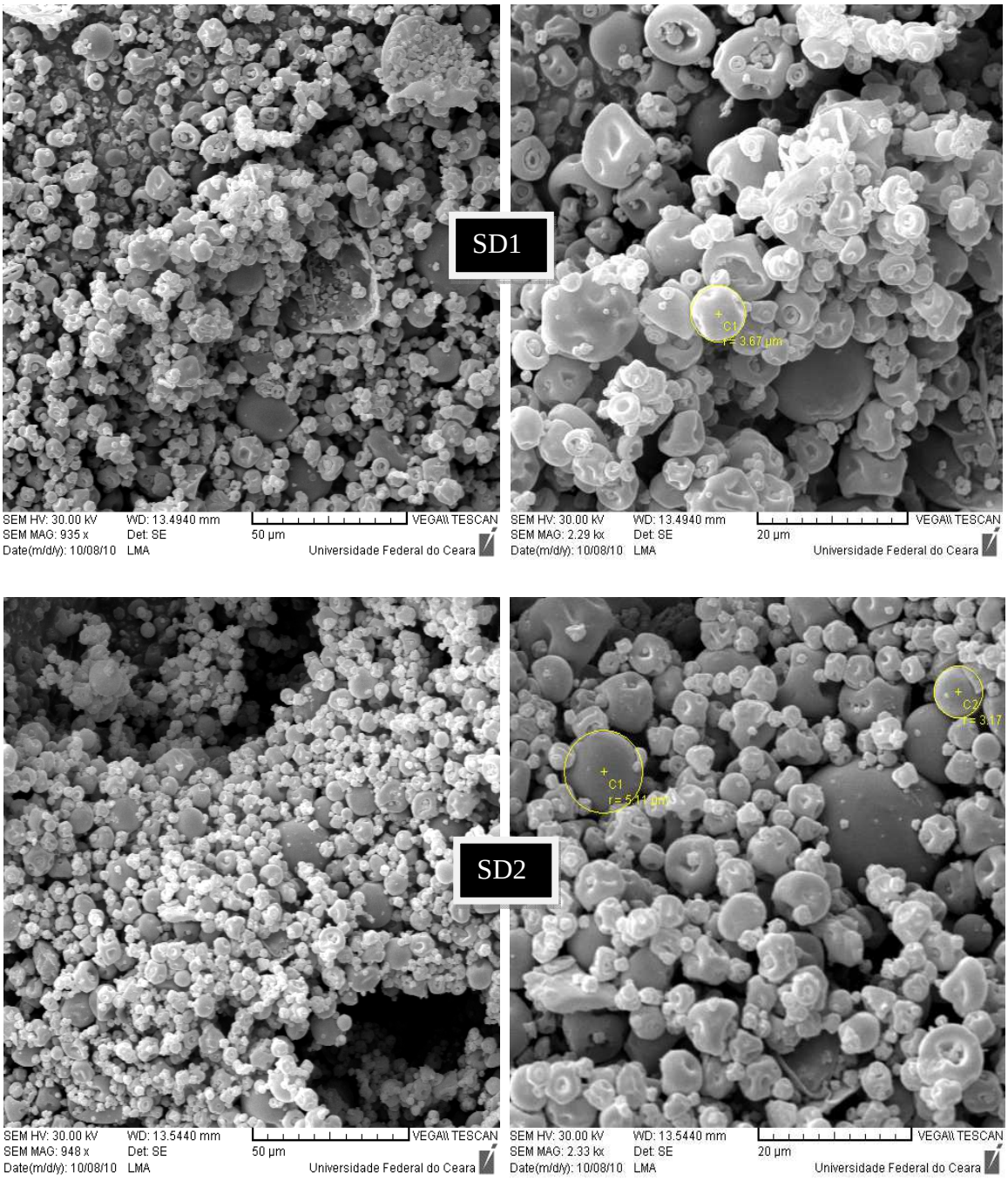

Figure 8 – SEM images for SD1 and SD2 samples.

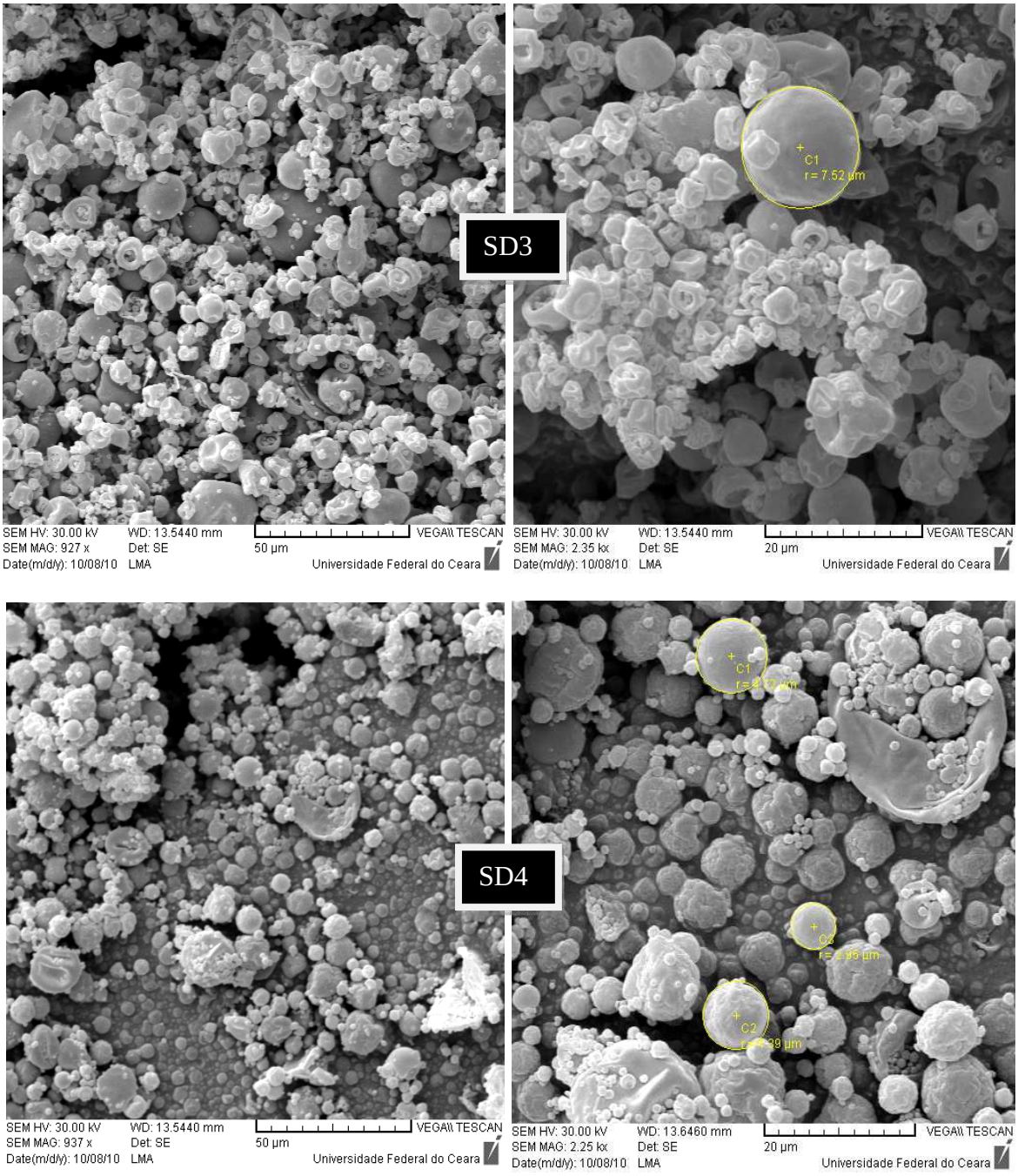

Figure 9 – SEM images for SD3 and SD4 samples.

3.4. Analysis of mangiferin in encapsulated materials by HPLC-ESI-MS

Mangiferin itself and in the encapsulated materials was detected and characterized by HPLC-ESI-MS. A commercial and purified mangiferin sample, obtained from the bark of *mangifera indica L.* as described by Barreto (2008), were compared (Figure 10). In the chromatograms of both purified and commercial mangiferin an intense peak with a retention time (t_r) of app. 21 min was observed. In the negative-ion mass spectra an intense peak $[M-H]^-$ typical of the mangiferin ion at *m/z* = 421 was observed. The HPLC-UV spectra of mangiferin displayed the following characteristic wavelengths at 240, 258, 274, 318 and 366 nm, in agreement with that published by Schieber *et al.,* 2003. A low intensity impurity peak at app. t_r = 22.2 min was identified by its $[M-H]^-$ at m/z = 435 as homomangiferin. The purity of the purified and commercial mangiferin was calculated as 99 and 91%, respectively. The peak around 40.0 min is related to column material and can be disregarded.

In the chromatograms of the polysaccharide formulations a low intensity mangiferin peak at t_r = 21 min in all samples is detected (Figures 11 and 12). This was confirmed by the characteristic mass spectra and UV spectra. From the peak integration values shown in Table 3 we can observe that mangiferin was detected at different amounts in the polymer matrix, even though the same amount of the mangiferin was used in the encapsulation procedure. This may be explained by the fact that mangiferin may have different intermolecular force interactions with the polymer polysaccharides used for encapsulation as well as the addition of the surfactant, so the mangiferin was retained differently in the matrix during the spray-drying procedure.

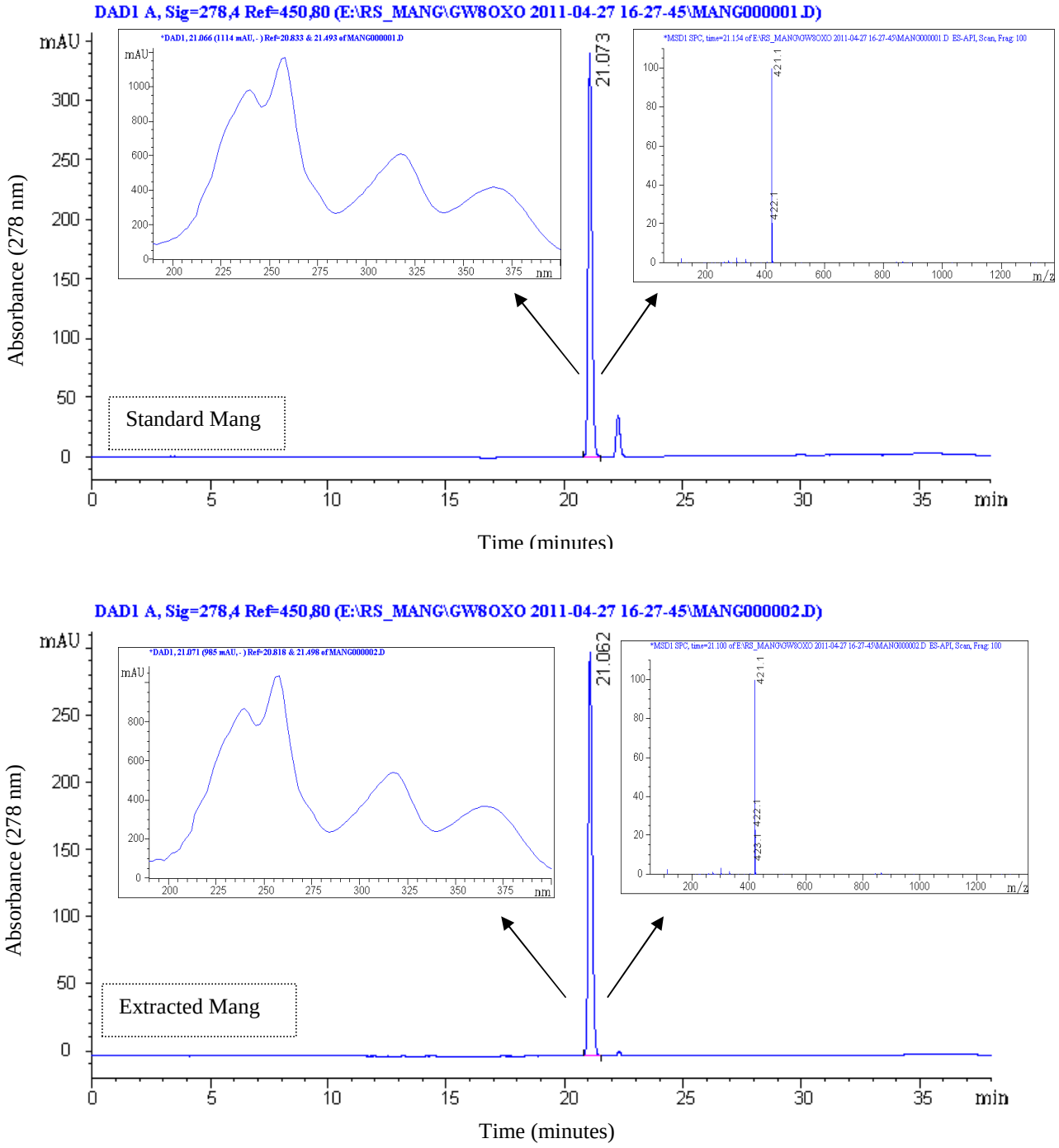

Figure 10 – HPLC chromatograms coupled with UV and MS spectra for standard and extracted mangiferin.

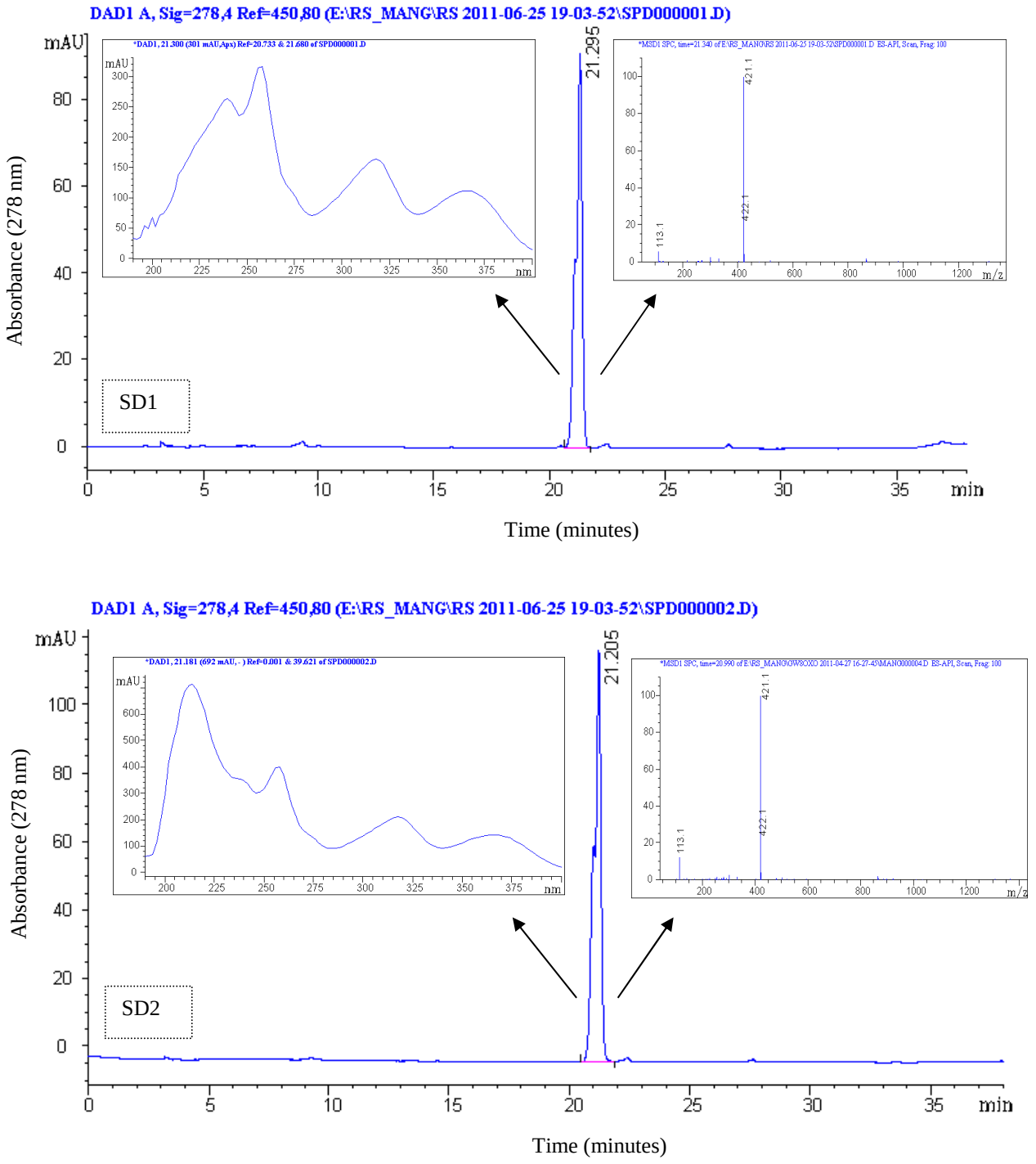

Figure 11 – HPLC chromatograms coupled with UV and MS spectra for SD1 and SD2 samples.

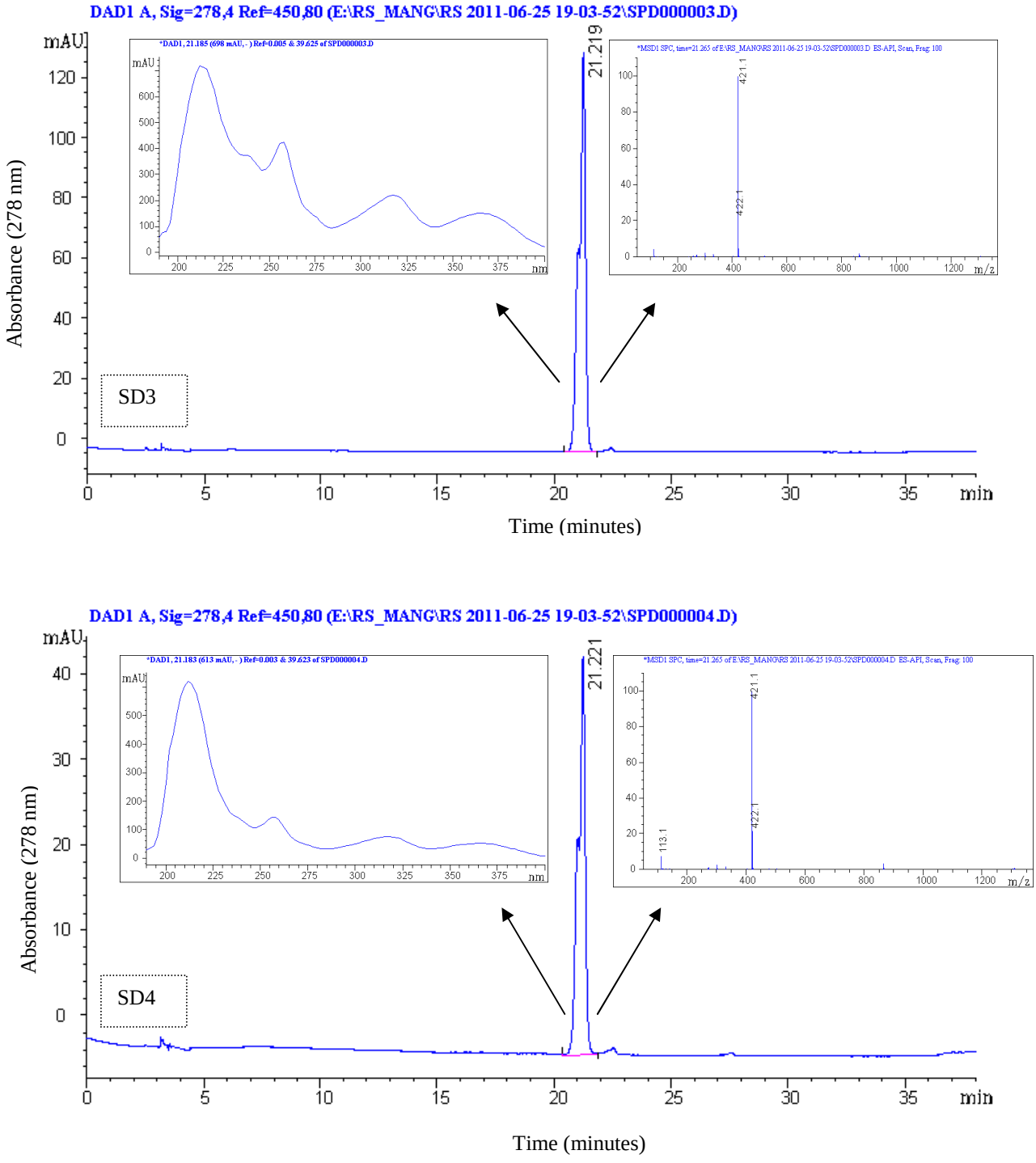

Figure 12 – HPLC chromatograms coupled with UV and MS spectra for the SD3 and SD4 samples.

The integrations of the signals for mangiferin from the absorbance at 278 nm are displayed in the Table 3 and are correlated with the concentration of mangiferin in the samples.

Table 3 – HPLC-ESI-MS data for the mangiferin and encapsulated samples. Signal absorbances at 278 nm and t_r at app. 21 min.

Sample	Peak Area [mAu*s]
Mang stand	3633.89
Mang ext	3262.87
SPD 1	1602.4
SPD 2	2236.8
SPD 3	2426.0
SPD 4	906.5

Differing amounts of mangiferin in the encapsulated materials were detected (Table 3). Even though the same pectin material was used for the preparation of SPD1 and SPD2, different amounts of mangiferin were encapsulated detected and this is probably related to the use of Tween 80 in the formulation of SPD2, which enhances the solubility of mangiferin in the polymer mixture. The highest value of mangiferin encapsulation was detected in the SPD3 formulation prepared from pumpkin pectin and the lowest for SPD4, prepared from chitosan.

3.5. Determination of Mangiferin in Encapsulated Materials

A mangiferin standard curve (Figure 13) was prepared in MetOH (optical absorbance (278 nm) vs. concentration, µM). The equation was calculated by linear fit (Y = 15.57181A + B*7.69902X) and the curve showed a good correlation coefficient R = 0.99979. Signal at 278 nm, retention time of 21.3 for mangiferin.

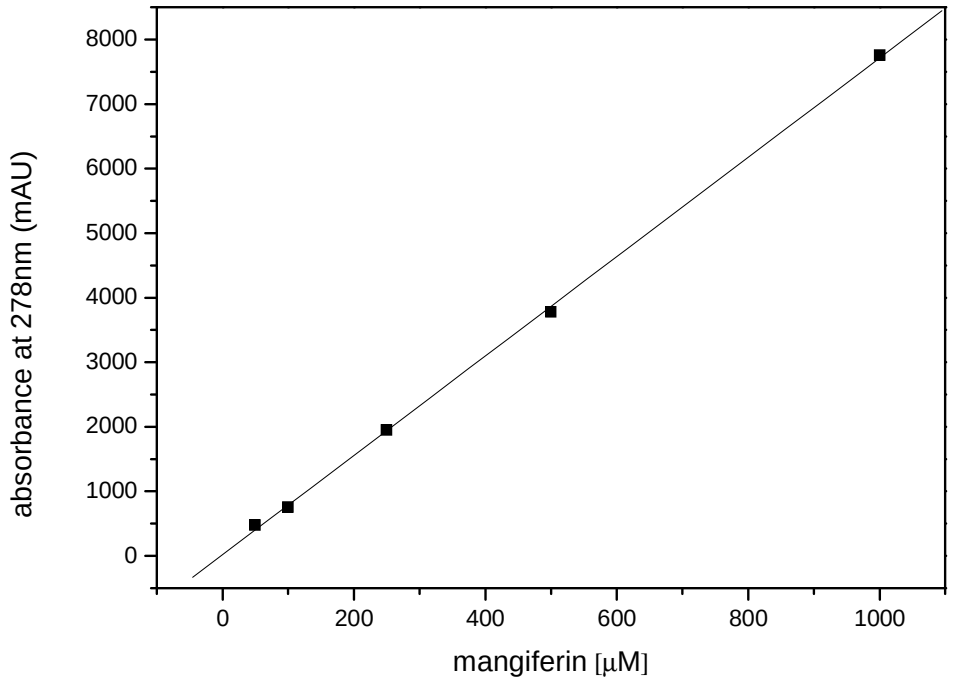

Figure 13 – Standard curve for mangiferin in MetOH.

After extraction in MetOH and injection in the HPLC-ESI-MS, the integration values were obtained and the amount of mangiferin in the encapsulated samples was then determined and quantified using the mangiferin standard curve equation. The data is displayed in Table 4. Taking into account the theoretical value of 100 µg mangiferin/mg of polysaccharide; we can consider that the concentration values obtained are the same as the encapsulation efficiency ones.

Table 4 – Values for the concentration of mangiferin in the capsules.

Samples	[mang] in encapsulated (µg/mg)	Encapsulation efficiency (%)*
SPD1	29	29
SPD2	41	41
SPD3	44	44
SPD4	16	16

*Calculation based on the theoretical value of 100 µg mangiferin/mg encapsulated material

The use of surfactant systems in the solubilization process of drugs has been reported (Patel & Patel, 2012). Adsorption of surfactant on a solid surface can modify their hydrophobicity, surface charge, and other properties related to interfacial processes such as dispersion, wetting, solubilization, detergency and these properties have attracted the attention of scientists when preparing solid dispersions and emulsions (Patel & Patel, 2012). Patel & Foss (1964) reported that the principal binding force between a phenolic compound and a non-ionic surfactant may be due to hydrogen bonds but a non-ionic surfactant can also contain a relatively large number of hydrophobic groups in the molecule contributing to hydrophobic interactions. From the results shown in Table 4 we can observe clearly the influence of the surfactant between the sample SD1 and SD2, which causes an increase of approx. 78 % in the solubility of mangiferin in the matrix. We can also observe that there was little difference between the citrus and pumpkin pectin formulations but a large difference between the use of pectin and chitosan (app. 3 times higher) even though the same conditions were used such as amount of mangiferin and surfactant.

4. Conclusions

The presence of polysaccharides used in the formulations was identified by FTIR as well as the bioactive mangiferin showing characteristics absorbance bands. SEM microphotographs presented different shapes and diameter sizes for the different particles obtained showing the influence of the polymer nature and the effect of the addition of surfactant to the samples. HPLC-ESI-MS was successfully used to detect the bioactive mangiferin in the particles as well as to determine the amount of incorporated mangiferin into each formulation. The pectin formulations generally gave higher (%) retention of mangiferin in the particles. This suggests that the nature of the polysaccharide as well as the surfactant used has a considerable influence on drug retaining ability during the spray-drying process. Another reason for this may be due to the nature of the non-ionic surfactant Tween-80 which may interact more hydrophobically (like dispersion forces) with the matrix even though hydrogen bonding is likely to occur. This explains why the highly positively charged chitosan polysaccharide had a lower drug retaining capacity followed by the negatively charged citrus pectin which has a lower methoxylation degree compared to the pumpkin pectin as determined in a previous publication (Souza *et al.,* 2012).

5. Acknowledgments

The authors would like to express their thanks for the financial support from CNPq, CAPES/Daad Sandwich Doctorate program.

6. References

Adamo, M., Junior, L. W. D., Qiu, D., Lee, A-H., Devincentis, J., Cheng, K-C. (2010). A simple reversed phase high-performance liquid chromatography method for polysorbate 80 quantitation in monoclonal antibody drug products. *Journal of Chromatography B*, 878, 1865–1870.

Barreto, J. C., Trevisan, M. T. S., Hull, W. E., Erben, G., de Brito, E. S., Pfundstein, B., Würtele, G., Spiegelhalder, B. Owen, R. W. (2008). Characterization and quantitation of polyphenolic compounds in bark, kernel, leaves and peel of mango. (*Mangifera indica* L.). *Journal of Agricultural and Food Chemistry, 56*, 5599-5610.

Beck-Broichsitter, Moritz,, Schmehl, T., Seeger W., Gessler, T. (2011). Evaluating the Controlled Release Properties of Inhaled Nanoparticles Using Isolated, Perfused, and Ventilated Lung Models. *Journal of Nanomaterials*, 2011, 1-16.

Bourgeois, S., Gernet, M., Pradeau, D., Andremont, A. & Fattal, E. (2006). Evaluation of critical formulation parameters influencing the bioactivity of β-lactamases entrapped in pectin beads. *International Journal of Pharmaceutics, 324*, 2-9.

Büchi website. Mini Spray Dryer B-290. (2012). Retrieved on May 10, from

http://www.buchi.com/Mini_Spray_Dryer_B-290.179.0.html

Carvalho, A. C. S., Guedes, M. M. de Souza, A. L., Trevisan, M. T. S., Lima, A. F., Santos, F. A. & Rao, V. S. N. (2007). Gastroprotective effect of mangiferin, a xanthonoid from *Mangifera indica*, against gastric injury induced by ethanol and indomethacin in rodents. *Planta Medica, 73*, 1372-1376.

Dar, A., Faizi, S., Naqvi, S., Roome, T., Zikr-ur-Rehman, S., Ali, M., Firdous, S., Moin, S. T. (2005). Analgesic and antioxidant activity of mangiferin and its derivatives: the structure activity relationship. *BPB: Biological and Pharmaceutical Bulletin*, 28, 596-600.

Duchateau, G. S. M. J. E. & Klaffke W. (2008). Product composition, structure, and bioavailability. *Food Biophysics*, *3*, 207-212.

Fang, Z., & Bhandari, B. (2010). Encapsulation of polyphenols – a review. *Trends in Food Science & Technology, 21*, 510-23.

Garcia, D., Escalante, M., Delgado, R., Ubeira, F. M. & Leiro, J. (2003). Anthelminthic and antiallergic activities of *Mangifera indica* L. stem bark components Vimang and mangiferin. *Phytotherapy Research, 17*, 1203-1208.

Gharsallaoui, A., Roudaut, G., Chambin, O., Voilley, A., Saurel, R. (2007). Applications of spray-drying in microencapsulation of food ingredients: An overview. *Food Research International, 40*, 1107–1121.

Gharsallaoui, A., Saurel, R., Chambin, O., Cases, E., Voilley, A., Cayot, P. (2010). Utilisation of pectin coating to enhance spray-dry stability of pea protein-stabilised oil-in-water emulsions. *Food Chemistry, 122*, 447–454

Guha, S., Ghosal, S. & Chattopadhyay, U. (1996). Antitumor, immunomodulatory and anti-HIV effect of mangiferin, a naturally occurring glucosylxanthone. *Chemotherapy*, *42*, 443-451.

Hou, S., Wang, F., Li, Y., Li, Y., Wang, M. , Sun, D., Sun, C. (2012). Pharmacokinetic study of mangiferin in human plasma after oral administration. *Food Chemistry, 132*, 289-294.

Jagetia, G. C. & Baiga, M. S. (2005). Radioprotection by mangiferin in DBAxC57BL mice: a preliminary study. *Phytomedicine*, 12, 209-215.

Kamnev, A. A., Colina, M., Rodriguez, J., Ptitchkina, N. M. & Ignatov, V. V. (1998). Comparative spectroscopic characterization of different pectins and their sources. *Food Hydrocolloids,* 12, 263-271.

Khossravi, M., Kao Y.-H., R.J. Mrsny, T.D. Sweeney. (2002). Analysis methods of polysorbate 20: A new method to assess the stability of polysorbate 20 and established methods that may overlook degraded polysorbate 20. *Pharmaceutical Research*, 19, 634.

Kim, T. H., Park, Y. H., Kim, K. J. & Cho, C. S. (2003). Release of albumin from chitosan-coated pectin beads in vitro. *International Journal of Pharmaceutics*, *250*, 371-383.

Kumari, A., Yadav, S. K., Yadav, S. C. (2010). Biodegradable polymeric nanoparticles based drug delivery systems. *Colloids and Surfaces B: Biointerfaces,* 75, 1–18.

Kurmi, B. D., Kayat, J., Gajbhiye, V., Tekade, R. K., Jain, N. K. (2010). Micro- and nanocarrier-mediated lung targeting. *Expert Opinion on Drug Delivery.* 7, 781–794.

Lawrie, G., Keen, I., Drew, B., Chandler-Temple, A., Rintoul, L., Fredericks, P. & Grøndahl, L. (2007). Interaction between alginate and chitosan biopolymers characterized using FTIR and XPS. *Biomacromolecules*, 8, 2533-2541.

Lebhardt, T., Roesler, S., Beck-Broichsitter, M., Kissel, T. (2010). Polymeric nanocarriers for drug delivery to the lung. *Journal of Drug Delivery Science and Technology*. 20, 171–180.

Liu, L. S., Fishman, M. L., Kost, J. & Hicks, K. B. (2003). Pectin-based systems for colon-specific drug delivery via oral route. *Biomaterials, 24*, 3333-3343.

Lüllmann, H., Mohr, K., Ziegler, A., Bieger, D., Wirth J. Color Atlas of Pharmacology. 2nd Edition, Thieme, 2000, 296-297.

Madziva, H., Kailasapathy, K. & Phillips, M. (2006). Evaluation of alginate-pectin capsules in cheddar cheese as a food carrier for the delivery of folic acid. *LWT-Food Science and Technology, 39*, 146-151.

Magalhães Jr., G. A., Santos, C. M. W., Silva, D. A., Maciel, J. S., Feitosa J. P. A., Paula, H. C. B, & de Paula, R. C. M. (2009). Microspheres of chitosan/carboxymethyl cashew gum (CMCG): effect of chitosan molar mass and CMCG degree of substitution on the swelling and BSA release. *Carbohydrate Polymers,* submitted.

Matute, A.C., Sanchez G. M. V. Campos, E. R., Alberti, A. E., Gottlieb, M., Ibarretxe, B. G., Delgado, G. J. M., Gruart, I. M. A. & Leal C. R. (2007). Food products for treating and preventing neurodegenerative diseases and ageing symptoms, contain morin or mangiferin. WO2007077279-A1 ; ES2277567-A1 Spanish Patent.

Nedovic, V., Kalusevic, A., Manojlovic, V., Levic S., Bugarski B. (2011). An overview of encapsulation technologies for food applications. *Procedia Food Science, 1*, 1806 – 1815.

Olano-Martin, E., Rimbach, G. H., Gibson, G. R., Rastall R, A. (2003). Pectin and pectic-oligosaccharides induce apoptosis in *in vivo* human colonic adenocarcinoma cells. *Anticancer Research,* 23, 341-346.

Patel, T. B. & Patel, L. D. (2012). Formulation and development strategies for drugs insoluble in gastric juice*. International Research Journal of Pharmacy*, 3, 106-113.

Patel, N. K. & Foss, N. E. (1964). Effect of temperature on the binding of parabens and phenols by polysorbate 80 and polyethylene glycol 4000. *Journal of Pharmaceutical Sciences,* 53/1, 94-97.

Rao, J. P., Geckeler, K. E. (2011). Polymer nanoparticles: preparation techniques and size-control parameters. *Progress in Polymer Science,* 36, 887–913.

Rashidova, S. Sh., Milusheva, R. Yu, Semenova, L. N., Mukhamedjanova, M. Yu., Voropaeva, N. L., Vasilyeva, S., Faizieva, R. & Ruban, I. N. (2004). Characteristics of interactions in the pectin-chitosan system. *Chromatographia,* 59, 779-782.

Rivera, D. G., Balmaseda, I. H., Leon,. A. A., Hernandez, B. C., Montiel, L. M., Garrido, G. G., Cuzzocrea, S. & Hernandez. R. D. (2006). Anti-allergic properties of *Mangifera indica L*. extract (Vimang) and contribution of its glucosylxanthone mangiferin. *Journal of Pharmacy and Pharmacology*, 58, 385-392.

Roy, I., Vij, N. (2010). Nanodelivery in airway diseases: challenges and therapeutic applications. *Nanomedicine,* 6, 237–244.

Schieber, A., Berardini, N., Carle, R. (2003). Identification of flavonol and xanthone glycosides from mango (*Mangifera indica L*. cv. ‘Tommy Atkins’) peels by high-performance liquid chromatography-electrospray ionisation mass spectrometry. *Journal of Agricultural and Food Chemistry,* 51, 5006.

Souza, J. R. R., Carvalho, J. I. X., Trevisan, M. T. S., Paula, R. C. M., Ricardo, N. M. P. S., Feitosa, J. P. A. (2009). Chitosan-coated pectin beads: characterization and in vitro release of mangiferin. *Food Hydrocolloids,* 23/8, 2278-2286.

Souza, J. R. R., Feitosa, J. P. A., Ricardo, N. M. P. S, Brito, E. S. (2012). Obtaining and Characterization of Regional Pumpkin Pectin by Acid Hydrolysis, (in corrections).

Wang, Z., Deng, J. Li, X. & Wang, Q. (2007). Dissoluble mangiferin inclusion compound and its preparation method. CN101019877-A Chinese Patent.

Wada, M. (2007). Foodstuffs compounding agent for treating diabetes comprises glycoside having xanthone structure. JP2007204462-A Japanese Patent.

Weiss, J. Decker, E. A., McClements, J., Kristbergsson, K., Helgason, T. & Awad, T. (2008). Solid lipid nanoparticles as delivery systems for bioactive food components. *Food Biophysics, 3*, 146-154.

Willats, W. G. T., Knox, J. P., Mikkelsen D. J. (2006). Pectin: new insights into an old polymer are starting to gel. *Trends in Food Science & Technology,* 17, 97-104.

Yoosook, C., Bunyapraphatsara, N., Boonyakiat, Y. & Kantasuk, C. (2000). Anti-herpes simplex virus activities of crude water extracts of Thai medicinal plants. *Phytomedicine, 6*, 411–419.

Zhang X., Guo H., Li X., Wang Z., Wu L. (2012). High tap-density Li3V2(PO4)3/C composite material synthesized by sol spray-drying and post-calcining method. *Electrochimica Acta*. 64, 65–70.

CHAPTER 3

Production and Characterization of Mangiferin Metabolites by Intestinal Environment Simulation

Souza, J. R. R.[1,2], Feitosa, J. P. A.[1], Ricardo, N. M. P. S[1], Trevisan, T. S.[1], Ulrich C. M.[2], Owen, R. W.[2]

[1]Departament of Organic and Inorganic Chemistry, Federal University of Ceará P. O. Box: 6.021, ZIP-Code: 60455-760, Fortaleza, Ceará, Brazil
[2]Division of Preventive Oncology, National Center for Tumor Diseases, Im Neuenheimer Feld 460/German Cancer Research Center, Im Neuenheimer Feld 581, Heidelberg, Germany

Mangiferin, a natural antioxidant and potential anticancer drug, has been investigated by several research groups in several countries in order to establish its pharmacological and biological properties. Due to its low bioavailability, already reported in many scientific publications, mangiferin is more available in the gut, where it will be metabolized into other compounds. The aim of this study was to produce and identify mangiferin metabolites simulating intestinal conditions as well as their isolation and characterization using different techniques such as HPLC-ESI-MS, Semipreparative HPLC, Nano-ESI-MS and ^{1}H / ^{13}C NMR.

Keywords: mangiferin, metabolism, intestine, microbiota, HPLC-ESI-MS.

1. Introduction

1.1. Consideration about drugs and natural compounds

In the mid-19th century, pharmacology was established as a science and since then many pharmacologists have studied the effects of drugs on the function of living systems. Nowadays a drug can be defined as a chemical substance of known structure, other than a nutrient or an essential dietary ingredient, wich, when administered to a living organism, produces a biological effect. Drugs may be synthetic chemicals, chemicals obtained from plants or animals, or products of genetic engineering (Rang *et al.*, 2007; Lüllmann *et al.,* 2010).

The National Cancer Institute (NCI) have promoted large-scale anticancer drug discovery and screening programs playing an important role in the development of anticancer natural compounds. Natural-product-based drug discovery is increasing based on new technologies, such as combinatorial synthesis, high-throughput screening and other approaches. Vincristine, irinotecan, etoposide and paclitaxel are famous examples of plant-derived compounds; actinomycin D, mitomycin C, bleomycin, doxorubicin and l-asparaginase are drugs coming from microbial sources, and citarabine is the first drug from a marine source. New generations of taxanes, anthracyclines, Vinca alkaloids, camptothecins, as well as the novel class of epothilones have been developed. Some of these are in clinical use, others in clinical trials. The anticancer activities of these drugs are characterized by different mechanisms of action (Lansky & Newman, 2007; Jeong *et al*., 2008; Nobili *et al.,* 2009):

- Interaction with microtubules (e.g. Vinca alkaloids);
- Inhibition of topoisomerases I (e.g. camptothecins - irinotecan, topotecan) or II (epopodophyllotoxins - etoposide and teniposide) and the microbial-derived anthracyclines (e.g. doxorubicin, epirubicin);
- Interference with tumour signal transduction pathways (e.g. sulforaphane, curcumin, resveratrol);
- Interference with tumour cell proliferation, cell cycle, invasion and angiogenesis (pomegranate - *Punica granatum*).

Some of these many botanical compounds which have positive effects in cancer therapy, have a long history behind them. As an example, the green tea antioxidant EGCG (epigallocatechin-3-gallate) showed significantly slow breast cancer growth in female mice and its use is attested in ancient Japanese texts. Promising and selective anti-cancer effects have been observed with Saffron (*Crocus sativus L.*) *in vitro, in vivo* and now also in clinical trials (Abdullaev, 2005; Schmidt *et al.,* 2007; Effect of Safron in ClinicalTrials.gov, 2012).

Myrrh comes from Arabia, Abyssinia, Turkey and Somali coast of eastern Africa. Myrrh is derived from the dried resin from the tree *Commiphora myrrha* and other species. In biblical history, it was chosen along with frankincense and gold, as a gift of the Three Wise Men to the newborn Christ. One very interesting thing about Myrrh in the anti-cancer field is not only how well it kills cancer cells in general, but how it kills those that are resistant to other anti-cancer drugs. It is reported to work by inactivating a protein called Bcl-2, a natural factor that is overproduced by cancer cells, particularly in the breast and prostate. Although myrrh compound does not appear to be as powerful as other anti-cancer drugs derived from plants – such as, vincristine, vinblastine and paclitaxel – its advantage seems to lie in the fact that it can harm cancer cells without harming healthy cells, something these other drugs do not do (Kinghorn *et al.,* 2003; Ariga & Seki, 2006; Nobili *et al.,* 2009).

Prodrugs are drug molecules that undergo an enzymatic and/or chemical transformation *in vivo* to release the active parent drug, which can then exert a pharmacological activity. About 5–7% of drugs approved worldwide are reported to be or classified as prodrugs (Rautio *et al.,* 2008). Many glycosides are reported as potential prodrugs and some natural glycosides are in fact prodrugs. Examples are the sennosides, which have been used since a long time as laxatives. Sennosides taken orally are hydrolyzed by colonic microflora, to liberate the active rhein anthrones. Given the high activity of the gut microflora in various glycosidases, a number of synthetic glycosides were examined as potential colonic delivery systems, in particular corticoids. The same strategy was applied to the colon-specific delivery of corticosteroids used to treat inflammatory bowel disease (Rautio *et al.,* 2008; Sinha & Kumria, 2001)

1.2. Mangiferin - a xanthone glycoside prodrug

Glycosides are widely distributed among plants. The knowledge of the chemistry, ocurrence and biogenesis of glycosydes has grown substantially with the development of natural product chemistry and has led to the isolation of a wide variaty of secondary metabolites. C-Glycosides are a special type of glycosides since the aglycone is directly attached to carbon 1 of a pyranose ring of a sugar while O-glycosides posessess a hemiacetal linkage (Franz & Grün, 1983). Xanthones are secondary metabolites that occurr in a few higher plant families and microorganisms. Xanthone C-glycosides appear to be biogenetically related to C-glycosyl flavonoid compounds. Xanthones have a large variety of biological and pharmacological activities including antihypertensive, antioxidative, antithrombotic, and anticancer activity. Especially, the effective inhibitory activity against human cancer cell lines has attracted considerable attention (Shen *et al*., 2010).

The xanthone glycoside Mangiferin (1, 3, 6, 7-tetrahydroxyxanthone-C2-beta-D-glucoside) was already reported to have several activities (Barreto *et al.,* 2008; Dar *et al.,* 2005; Garcia *et al.,* 2003; Rivera *et al.,* 2006; Carvalho *et al.,* 2007; Yoosook *et al.,* 2000; Guha *et al.,* 1996 ; Wada, 2007; Matute *et al.,* 2007). Since 1980´s mangiferin has been marketed by the Institute of Medical and Aromatic Plants (VILAR) in Russia as the main component of the drug named “Alpizarin” which shows antiviral activity against herpes DNK-viruses. The drug was reported to stimulate cell-mediated and humoral immunity, to induce gamma-interferon production in blood cells, it was characterized by low toxicity and did not produce undesired side effects. (Sokolov et al., 1987; Geodakyan et al., 1992; Smirnova et al., 2000; Kalmykova et al., 2003). Recently, García-Rivera et al. (2011) published that mangiferin, which is the predominant component of the Vimang extract, is a strong determinant of immunosuppressive anti-tumor effects in MDA-MB231 breast cancer cells.

As many other glycosides, mangiferin may exert its activity as a prodrug when mangiferin itself is metabolized in a specific site in the body into other several metabolites which may have stronger biological activities than the parent drug itself. In that way mangiferin may be classified as a prodrug.

1.3. Mangiferin - bioavailability, pharmacocynetics and pharmacodynamics

Several researchers have reported that the oral bioavailability of mangiferin was very low (Geodakyan *et al.,* 1992; Han *et al.,* 2010), and in rats it has been shown to be as low as 1.2% (Han *et al.,* 2010). Hou *et al.,* (2012) tried to use the HPLC-UV based method for detection of mangiferin in human plasma obtained from the human trial in our study but the method was not sensitive enough for detection of relative low level of mangiferin requiring a sensitive and selective method for the human trial. For that they used high sensitivity quadrupole mass spectrometry-HPLC method for determination of pharmacokinetic study of mangiferin in human plasma following oral administration with a lower limit of quantification (LOQ).

For that study, 21 healthy male in the 3 groups were given a single oral dose of mangiferin (0.1, 0.3 and 0.9 g, respectively) with 200 ml of water. Blood samples were collected, mangiferin was separated from the human plasma and analyzed by HPLC-MS using the negative ion mode for detection and quantitation of $[M-H]^-$ ion at m/z 421 for mangiferin. The mangiferin concentration in the human trial conducted in the study was found to be very low: Tmax (time point of maximum plasma concentration of mangiferin (38.64 $ng.mL^{-1}$) in the 0.9 mg group is an extremely small amount compared to the administration dose (Hou *et al.,* 2012). That suggests that most of mangiferin, when taken orally, will not pass hepatic metabolism but will be more avaiable in the intestine, where it can be converted to other metabolites by human intestinal bacteria in the gut.

1.4. Cleavage of the glucosyl bond of C-glucosides by human intestinal bacteria

One of the main characteristics of C-glycosides is that they are more resistant towards acid, alkaline and enzyme hydrolysis than O-glucosides. Even prolonged exposure to acid does not cleave the glucosyl bond of C-glucosides, in which glucose is attached by a carbon–carbon bond to the aglycone, to give the aglycone. Sanugul et al. (2005a,b) have isolated a novel strain of the genus Bacteroides (Bacteroides spedies MANG) responsible for the conversion of mangiferin to its aglycone, norathyriol. However, intestinal bacteria from human feces can cleave C-glucosyl bonds in various C-glucosides as reported before (Li et al., 2000; Sanugul et al., 2005a,b).

Aromatic C-glycosides have gained increasing interest as drug candidates due to their stability and biological activities (Braune & Blaut, 2011) but not much investigation has been done about eukaryotic C-glycosidases. One example is the enzyme preparation from dyer's saffron (Carthamus tinctorius), which catalysed the deglycosilation of the flavone C-glucoside orientin (Saito, 1990). Other plant-derived C-glycosides that are representatives of this group of natural compounds include the anti-tumour antibiotic pluramycin from Streptomyces spp. (Bililign *et al.,* 2005; Hultin, 2005). Human gut bacteria deglycosylate C-glucosidic derivatives of flavones (Li *et al.,* 2000), xanthones, for example, norathyriol from mangiferin glucoside (Sanugul *et al.,* 2005a; Sanugul *et al.,* 2005b) and anthrones (Hattori *et al.,* 1993).

The bacterial metabolic activity on C-glucosides in the gut may result in aglycones and further metabolites whose biological activities differ from that of the parent compound and may affect the bioavailability of bioactive polyphenolic C-glucosides in humans or modulate their effects in the body.

1.5. Norathyriol – the mangiferin aglycone

Norathyriol, the aglycone of a xanthone C-glycoside mangiferin, was isolated from the aerial parts of *Tripterospermum lanceolatum* (Hayata) Hara ex Stake (Gentianaceae) by Lin *et al.* (1982). Some biological activies have been reported for norathyriol such as inhibition of rabbit platelet aggregation and antithtombotic effects (Teng *et al*., 1989; Teng *et al*., 1991), relaxing of the rat thoracic aorta (Ko *et al*., 1991), inhibition of mediators release from rat peritoneal mast cells *in vitro*, and to suppress pleurisy and cutaneous plasma extravasation caused by inflammatory mediators in mice in vivo (Wang *et al.* 1994a; Wang *et al.* 1994b)

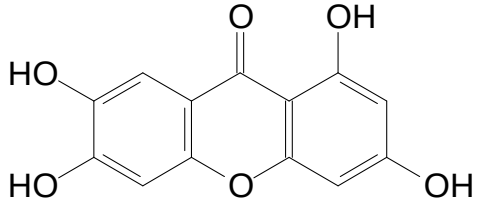

Figure 1 – Structure of norathyriol drew using chemwin software.

Inhibition of kinases by norathyriol has been reported as pathway mechanisms for several activities. Norathyriol markedly attenuated the fMLP/Cb induced tyrosine phosphorylation of 62 kDa and several other tyrosine phosphorylation bands suggesting that the Tirosine Kinase pathway is probably involved in the inhibition by norathyriol in fMLP-activated rat neutrophils (Hsu *et al*., 1997). Norathyriol also suppressed neutrophil cytosolic protein kinase C as well as rat brain protein kinase C over the same range of concentrations at which it inhibited respiratory burst (Wang *et al.*, 1997). Norathyriol attenuated the serotonin-induced permeability of rat heart endothelial cells to macromolecules in association with inhibition of protein kinase C activation, suggesting, that may be one signal transduction pathway for the protective effects of norathyriol against edema formation in response to inflammatory agonists in vivo (Lee *et al*., 1998).

Recently, Li *et al.* (2011) reported that norathyriol suppressed skin cancers induced by solar ultraviolet radiation in mice. Mechanistic investigations determined that norathyriol acted as an inhibitor of extracellular signal-regulated kinases ERK1/2 activity to attenuate UVB-induced phosphorylation in MAPK (Mitogen-activated protein kinases) signaling cascades. They confirmed the direct and specific binding of norathyriol with ERK2 through a co-crystal structural analysis (Figure2).

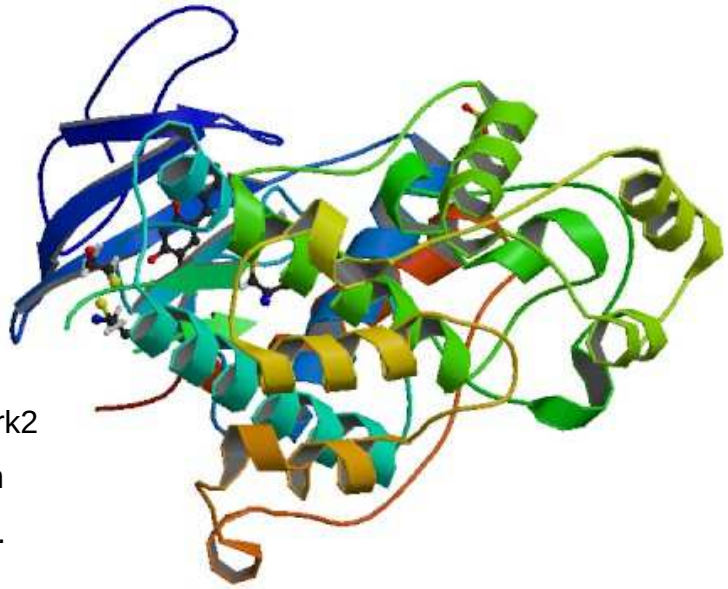

Figure 2 - Complex of Erk2 With Norathyriol. From NCBI and PDB (2011).

The xanthone moiety in norathyriol acted as an adenine mimetic to anchor the compound by hydrogen bonds to the hinge region of the protein ATP-binding site on ERK2. Norathyriol also inhibited in vitro cell growth in mouse skin epidermal JB6 P+ cells at the level of G2-M phase arrest. They concluded also that norathyriol mediates its chemopreventive activity by inhibiting the ERK dependent activity of transcriptional factors AP-1 and NF-kB during UV-induced skin carcinogenesis (Li *et al.,* 2011).

The Erk1/2 cascade is one among the major MAPK (mitogen-activated protein kinases) pathways in mammals. These proteins translate extracellular cues into changes in gene expression and protein activity. Erk1/2 exert pleiotropic effects, which are perturbed in many disease states, including human cancers, of which 30% show Erk hyperactivation (Dumesic *et al*., 2009, Chambard *et al*., 2007).

1.6. The Human gastrointestinal microbiota and its biotransformation activity

The term microflora describes microorganisms residing on body surfaces including the gastrointestinal tract generally named “flora” even though the term microbiota is preferred. The members of the human intestinal microbiota are reported to be very important to maintain human health and well-being since they are implicated in developmental, immunological and nutrition host functions. In numerical terms, from the total human and bacterial cells making up the body, only 10 % are eukaryotic (Egert *et al*., 2006).

At birth the human gut is sterile, shortly after that, a number of microbial strains/species, either from mother´s vagina or skin, find their way on to body surfaces and into the alimentary canal and, initially, facultatively anaerobic bacterial species, such as *Escherichia coli* and *streptococci* populate the gut. These bacteria create an adequate enviroment for the development of the anaerobic species that later dominate the gut (Cummings *et al.,* 2004; Macfarlane & Macfarlane, 1997).The mouth, pharynx, oesophagus, stomach, small intestine and large intestine correspond to the primary anatomical regions found in the human gastrointestinal tract. The caecum, colon, rectum and anal canal are collectevely referred to as the large intestine. Into different sections of

the gut, pH and redox potential undergo extreme variations. These variations will have an impact on the microbiotal colonisation of the digestive tract (McConnell *et al*., 2008a; Varum *et al.,* 2008).

Bacteria are reported to live adherent to the mucosal epithelium or in microhabitats (trapped in the mucous gel layer or in the intestinal lumen probably associated with either food particles or with each other) (Fanaro et al., 2003; Tannock, 1999). In the ascending colon, microorganisms, having plentiful supply of dietary nutrients, tend to grow rapidly, while in the transverse and descending colon substrate availability is lower and bacteria growth slows (Figure 3).

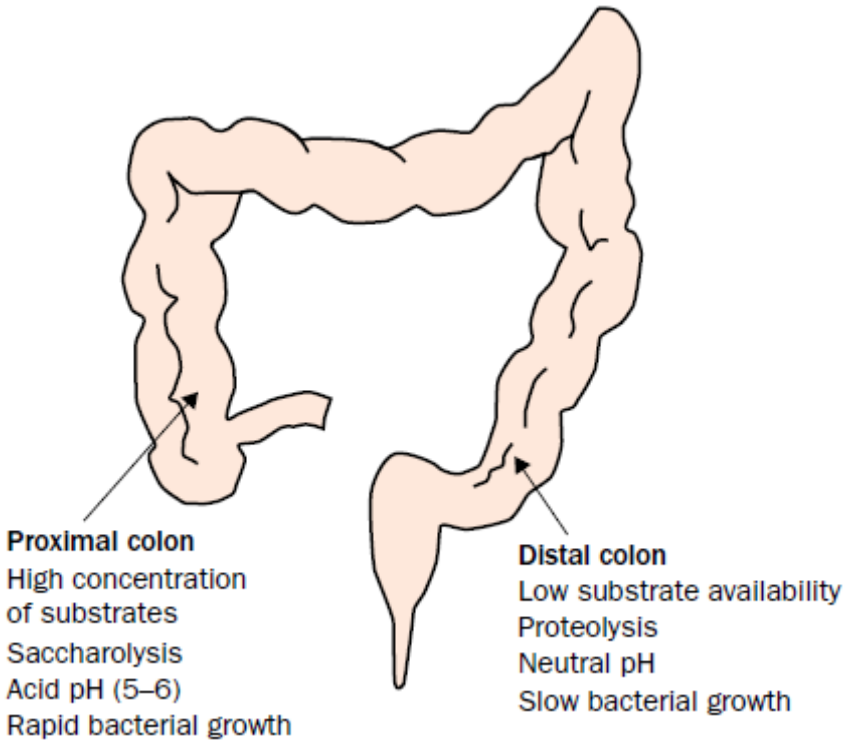

Figure 3 – Fermentation in the Colon. In the caecum and right colon, fermentation is very intense with a rapid bacterial growth while in the left or distal colon, bacterial populations are close to static. (from Guarner & Malagelada, 2003).

The first observations of faecal microbes described them as some “apparently randomly appearing bacteria”. The current estimate for the total

number of prokaryotes that inhabit the human gut is reported to be up to 100 trillion (10^{14}) microbes, so that makes the human GI tract one of the most populated microhabitats on earth. It is not known exactly how many bacterial cells exist in the human gut and wich species they all belong to, in fact, the identification and classification of microbes is one of the challenges of modern microbiology (Escherich, 1885; Whitman *et al.*, 1998; Savage, 2001; Ley *et al*., 2006). Finegold *et al.* proposed in 1983 an estimated of 400 bacterial species in the human gastrointestinal tract. Modern advances have made it possible to study bacterial populations by culture-independent appoaches using molecular genetic methodology like ribosomal RNA gene sequences for the classification of organisms since they are uniques versally distributed among all cellular life forms and they possess very slow genetic evolution wich allows the comparison between genetic sequences (domains) that have remained the same and sequences that have evolved. A new species is found when less than 98 % of domains are similar. Rajilic-Stojanovic et al. (2007) have compiled different ribosomal RNA studies together with culture-dependent studies, they reported a total of 1183 distinct bacterial species in the human gut (898 species using ribosomal RNA studies alone) and based on the variability seen so far between individuals they predicted an estimated diversity of the human gastrointestinal microbiota in excess of 3000 species.

Ribosomal RNA gene sequencing techniques have been used for species identification by alignment of the sequences with sequences stored in databanks. The technique has been used to identify species (from healthy subjects using mucosal and faecal samples) that belong to eight dominant phylogenetic phyla: *Firmicutes, Bacteroidetes, Proteobacteria, Fusobacteria, Verrucomicrobia, Cyanobacteria, Spirochaeates* and *Actinobacteria*. *Firmicutes* are reported to be the most abundant followed by Bacteroidetes that are also present in high numbers (Eckburg *et al.*, 2005; Wang *et al.*, 2005).

1.7. Biotransformation activity of the Gastrointestinal Microbiota (GIM)

The primary function of the GIM is to ferment carbohydrate and protein that escape digestion in the upper gut into absorbable energy. In addition, the metabolic reactions performed by these bacteria and their respective enzymes have the ability to metabolise drugs and other xenobiotics far more extensively than any other part of the body (Figure 4) (Sousa *et al.,* 2008; Scheline, 1973; Shamat, 1993; Mikov, 1994).

Scheline (1973) has even suggested that the GIM has the ability to act as an organ with a metabolic potential at least equal to the liver but there are, however, important differences between hepatic and bacterial metabolism. The liver is primarily responsible for metabolism via oxidation and conjugation producing polar high molecular weight metabolites, while the gastrointestinal microbiota is involved in reductive and hydrolytic reactions generating non-polar low molecular byproducts.

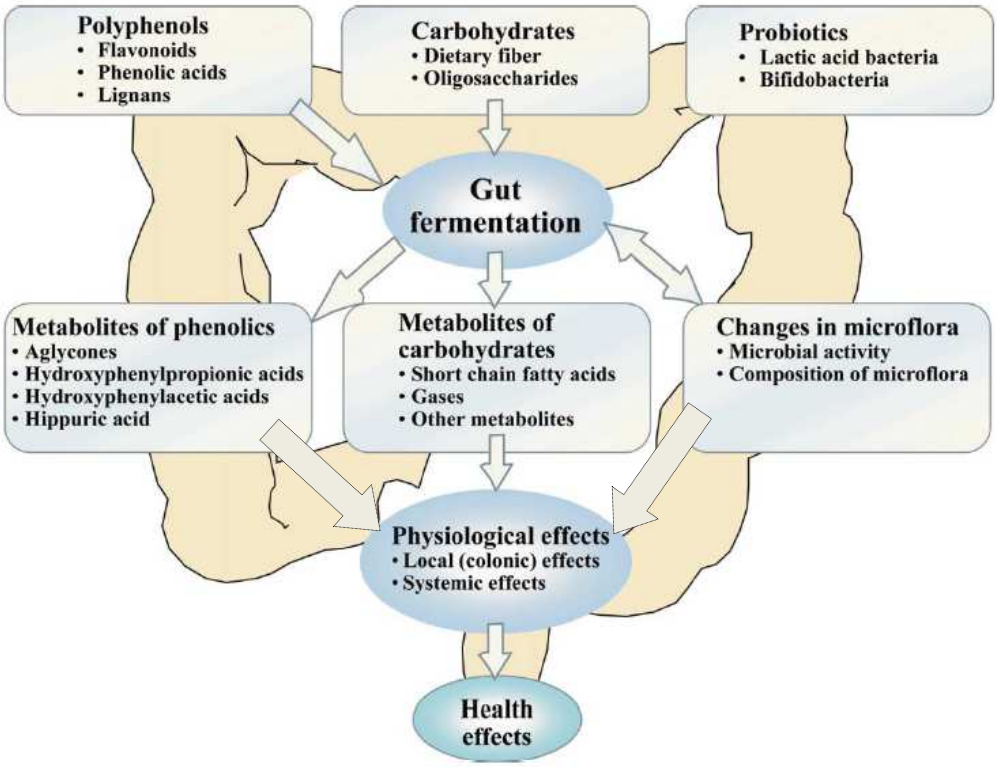

Figure 4 – Impact of colonic microflora in reactions on polyphenols, carbohydrates and other food ingredients. Adapted from Puupponen-Pimiä *et al.* (2002).

Davis (2005) reported that all drugs that are delivered to, or absorbed into, the blood stream, are subject to hepatic metabolism. Neverthless, rate and extent of bacterial metabolism will influence the amount of drug that reaches the distal gut. Most drugs are rapidly and completely absorbed in the upper gut so they are not much affected by intestinal bacteria but the biopharma of new drugs candidates is providing an increasing number of compounds that suffer from low solubility, low permeability or both. Drugs that display these properties will reach the lower confines of the gastrointestinal tract, presenting themselves to the microbiota. Drugs that are delivered via the intravenous route or that are fully absorbed from the upper parts of the gastrointestinal tract may still reach the lower gut by secretion or diffusion from the systemic circulation into the intestinal lumen, or may be excreted in the bile, possibly as conjugates following a recycling process known as enterohepatic recirculation. There is an increasing trend to develop modified release preparations (colon specific or extended release systems) to improve therapy via the oral route. In such cases, most if not all the entire drug load will be deposited in the large intestine, providing further opportunity for exposure to the microbiota (Basit, 2005; Rubinstein, 2005; Ibekwe *et al.,* 2006; Ibekwe *et al.,* 2008).

1.8. Bacterial metabolism, enzymes and polymorphism

Metabolic activity is reported to be a factor that influence drug metabolism and seem to depend on enzyme polymorphisms due to genetic differences among individuals. Studies of the metabolic activity of the intestinal bacteria and enterocytes have showed contribution to the metabolism of xenobiotics (Grundmann, 2010).

The microbial metabolism can render a drug pharmacologically active, inactive or toxic. Polyphenols, for example, are substrates for several enzymes (Figure 5) located in the small intestine and colon (Rechner et al., 2004). In some cases, this metabolic conversion actually leads to the generation of the active metabolite that is then readily absorbed for systemic effects or acts locally in the intestines. Oral prodrugs of 5-Fluoracil such as tegafur are metabolized via CYP 450 enzymes in the enterocytes and liver to the active drug (Grundmann, 2010).

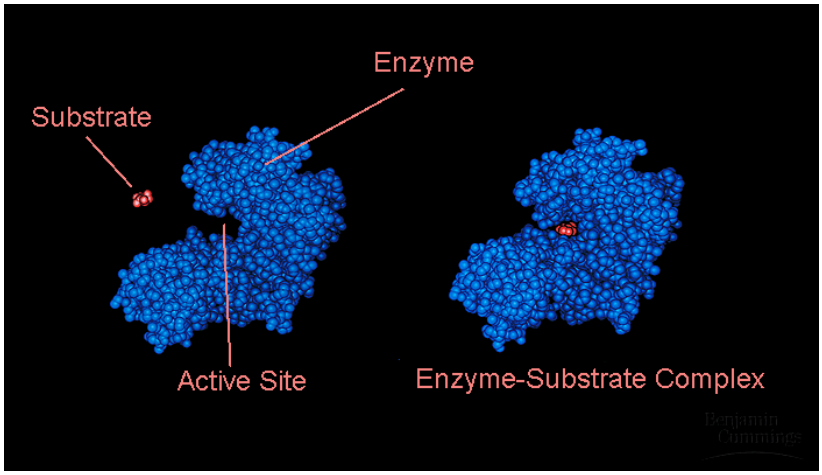

Figure 5 – Complex Enzyme-Substrate. Metabolic mechanism for activation of prodrugs. From Living Science, 2011.

The main bacterial metabolic processes are reduction and hydrolysis reactions and some minor fraction are cleavage, degradation, and coupling reactions. The most species on the gastrointestinal tract are facultative anaerobic bacteria, like Escherichia and streptococci, or entirely anaerobic species and because of that reduction is the most common metabolic bacterial reaction (Cummings *et al*., 2004). Glycosides, for example, are initially hydrolyzed by gut bacteria to the respective aglycone which is able to be absorbed into enterocytes through passive absorbance or however, can be actively transported into enterocytes by sodium glucose transporter protein 1 (SGLT1) (Grundmann, 2010).

Pharmacogenetics, a field whereby the genetics of the individual patient is taken into consideration during drug development and for individualized therapies, has shown that variability in genes encoding drug metabolizing enzymes often affects outcome in drug treatment to a very high extent and that the polymorphism of enzymes. Cytochromes P450 enzymes members are reported to be highly polymorphic. Because of such variability, the populations could be classified into 3 major phenotypes (Lewis & Wiseman, 2005; Ingelman-Sundberg *et al.,* 2007):

• The ultrarapid metabolizers, with more than 2 active genes encoding a certain P450;

• The extensive metabolizers, carrying 2 functional genes;

• The intermediate metabolizers, usually carrying 1 functional and 1 defective allele but may also carry 2 partially defective alleles;

• The poor metabolizers, lacking functional enzyme due to defective or deleted genes.

Bacteroides species (Phylum *Bacteroidetes*) are obligately anaerobic, non-sporeforming, gram-negative bacilli normally found associated with the intestinal tracts of humans and animals (Smith & Callihan, 1992). Gutacker *et al.* (2000), performed 16S rRNA sequencing using PCR assay of 93 Bacteroides fragilis strains and observed polymorphism in fourteen of the 15 genetic loci analysed.

2. Experimental

2.1. Reagents and Materials

- Acetic acid, acetonitrile, dichloromethane (DCM), brain heart infusion (BHI), K_2HPO_4, KH_2PO_4 were obtained from Merck (Darmstadt, Germany);
- Silica gel 60 from ICN Biomedicals (Eschwege, Germany);
- Sephadex^{TM} LH-20 lot # 303352 from Amersham Biosciences AB (Uppsala, Sweden);
- Sachets of ascorbic acid, AnaeroGen^{TM} (Nr. 68061) and Indicators of anaerobiosis (Nr. BR0055B) from Oxoid Ltd. (Basingstoke, UK);
- SPE (Solid Phase Extraction) C_{18} 5g / 45 mL Cardridges (Nr. 1061) of octadedyl-modified silica and endcapped obtained from Chromabond® (Düren, Germany);

2.2. *Equipaments*

- Eppendorf Mixer from Thermomixer Comfort N. 5355 01185 (Eppendorf-Netheler-Hinz GmbH 22331, Hamburg, Germany);
- Eppendorf centrifuge model N. 11210801 from Thermoelectron Industries SAS (Chateau-Gontier-France);
- Ultrasound Bath Elina Transsonic T450 N. 1185401 from Hans Schidbauer KG. N. 1185401 (Singen, Germany);
- Anaerobic container (Big Modell Typ DIAB 10003) from Dinkelberg Analytics (Gablingen, Germany);
- Vortex-2 Genie model G-560E Serial N. 85234 from Scientific Industries Inc. (Bohemia, USA);
- SPE (Solid Phase Extraction) C_{18} 5g / 45 mL Cardridges (Nr. 1061) of octadedyl-modified silica and endcapped obtained from Chromabond® (Düren, Germany);
- Balance Kern EW from Kern & Sohn GmbH S# 057770226 (Balingen, Germany);
- Analytical Balance Metler Toledo BP211D-OCE (0.00 mg) from Sartorius AG (Göttingen, Germany);
- Incubator N. 990430 from WTC Binder (Tuttlingen, Germany);
- Water bath SS40-D from Grant Instruments (England);
- Stirrer Yellow Line MSH Basic From IKA-Werke GmbH & Co. KG (Staufen, Germany);
- ELX 800 Universal Microplate Reader from Bio-tek Instruments Inc. (Overath, Germany);
- Freeye-dryer Christ alpha 1-4 N. 6441 from Martin Christ, An der Unteen Söse 50 (Osterode, Germany);
- Vacuum Concentrator from Bachofer GmbH (Reutlingen, Germany)

2.3. Instrumental Methods

2.3.1. Analytical HPLC

High performance chromatography-electrospray-ionization-mass spectrometry (HPLC-ESI-MS) analysis was conducted on a Hewlett-Packard (HP) 1090 liquid chromatograph (Agilent Technologies, Waldbronn, Germany) using a reverse-phase C18 Phenomenex column 250 mm × 4 mm (i.d.), 5 µm, (Latek, Eppelheim, Germany). The mobile phase consisted of 2% acetic acid in water (solvent A) and methanol (solvent B) with the following gradient profile: 95% A for 2 min; reduced to 75% A over 10 min; to 60% A over 20 min; to 50% A over 30 min; to 0% A over 5 min; continuing at 0% A until completion of the run. The flow rate of the mobile phase was 1.0 mL/min. Phenolic compounds in the eluant were detected at 257, 278, and 340 nm with a diode-array UV detector (HP 1040M). About 1 mL sample was colletected in each time point, centrifuged for 5 min at 14,000 r.p.m. and the supernatants (20 µL) were analysed by HPLC-ESI-MS.

2.3.2. Electrospray Ionization Mass Spectrometry (ESI-MS)

HPLC-ESI-MS was conducted on an Agilent 1100 HPLC, coupled to an Agilent single-quadrupole, mass-selective detector (HP 1101; Agilent Technologies, Waldbronn, Germany). Chromatographic separation of methanolic extracts was conducted using a column of the same type and dimensions as for analytical HPLC (Phenomenex, Latek, Eppelheim, Germany). The mobile phase consisted of 2% acetic acid in water (solvent A) and acetonitrile (solvent B) with the following gradient profile: initially 95% A for 10 min; to 90% A over 1 min; to 60% A over 9 min; to 80% A over 10 min; to 60% A over 10 min; to 0% A over 5 min and continuing at 0% A until completion of the run. Phenolic compounds were detected by their UV absorbance (A) at 257, 278 and 340 nm at room temperature. Mass spectra in the negative-ion mode were generated under the following conditions: fragmenter voltage = 100 V, capillary voltage = 2500 V, nebulizer pressure = 30 psi, drying gas temperature = 350 °C, mass range = 100 - 1500 D. Instrument control and data handling were performed with the same software as for analytical HPLC.

2.3.3. Semi-Preparative HPLC

Semi-preparative HPLC was conducted on a HP 1100 liquid chromatograph (Agilent Technologies, Waldbronn, Germany) fitted with a C18 column (10 mm i.d.) similar to that used for analytical HPLC. Separations were then programmed using the CC – module coupled to the Agilent LC-MSD Chemstation. For the separation of individual compounds, the mobile phase (3 mL/min) consisted of 0.2% acetic acid in water (solvent A) and acetonitrile (solvent B), utilizing the following solvent gradient profile over a total run time of 50 min: initially 95% A for 1 min; reduced to 90% A over 9 min; to 85% A over 10 min; to 80% A over 10 min; to 0% A over 5 min and continuing at 0% A until completion of the run. Peaks eluting from the column were collected on a HP 220 Microplate Sampler and subsequently lyophilized.

2.3.4. Nano-electrospray Ionization Mass Spectrometry (Nano-ESI-MS)

Nano-ESI-MS was performed with purified samples dissolved in methanol on a Finnigan MAT TSQ-7000 triple-quadrupole mass spectrometer (Finnigan, San Jose, California, USA) equipped with a nanoelectrospray source (EMBL, Heidelberg, Germany) using both the positive- and negative-ion modes. The collision gas was argon at a nominal pressure of 2.5 mTorr. Gold-plated glass capillaries for sample spraying were prepared in-house using a microcapillary puller (Type-87-B, Sutter Instruments, Novato, California, USA). The applied voltage was 40-70 V, and the m/z scan range was 20-2600.

2.3.5. ^{1}H and ^{13}C Nuclear Magnetic Resonance Spectroscopy

^{1}H and ^{13}C NMR spectra were recorded at 14.1 T (600.13 and 150.9 MHz, respectively), using 5-mm sample tubes on a Bruker Avance AV-600 spectrometer (Bruker BioSpin GmbH, Rheinstetten, Germany). All measurements were performed using CD3OD (99.96% D) as solvent and chemical shifts are reported relative to TMS for both nuclei. A variety of temperatures were used ranging from 288 to 328 K, depending on sample properties (dynamics and chemical exchange), and the appropriate temperatures for the data reported are given in the Tables.

2.4. Anaerobic Fermentation Set up

2.4.1. Preparation of Brain Heart Infusion (BHI) Solution

BHI broth was prepared dissolving the material in double distilled water (DDW) at a concentration of 37 g/L. After that the solution was sent for sterilization at 120 °C for 20 min and allowed to cool before inoculation with freshly faecal matrix.

2.4.2. Set up of Anaerobic Fermentation of Mangiferin (AFM)

An anaerobic fermentation study of mangiferin was performed (n = 7) simulating the intestinal environment conditions from human volunteers (n=3) (Table 1 and 2). For that, the test substance (e.g.: 50 or 100 mg of mangiferin) was suspended in ethanol (2.0 mL), mixed with app. 100 mg of the fecal sample in 100 mL of sterilized BHI solution inside a 100 mL sterilized and uncovered Duran bottles. The bottle was put along with two AnaeroGen cushions and an indicator of anaerobiosis in the anaerobic container that was hermetically closed. The container was incubated for/until 5 days (120h) at 37 °C and the solution was occasionally stirred. Samples (app. 1 mL) were taken from Duran bottles inside the container using a syringe connected to a tubular system coupled to the anaerobic container, centrifuged in eppendorfs at 14.1 RCF for 5 minutes and afterwoods, an aliquot of sample (10 or 20 µL) was injected in the LC-ESI-MS for inspection.

The anaerobic environment is created by the AnaeroGen^{TM} system that consists of a paper gas generating sachet. The paper sachet contains ascorbic acid and activated carbon which reacts on with air. Oxygen is rapidly absorbed and carbon dioxide is produced. When the paper sachet is placed in a sealed plastic pouch or container, this reaction will create ideal atmospheric conditions for the growth of anaerobes (Oxoid Microbiology Products, 2012).

Two different methodologies were used to set up the anaerobic fermentation studies (Table 2). The first one is described in *2.4.1* and the second methodology was used in AFM V1-3, AFM V2-2, AFM V3-2 which produced novel metabolites that are under investigation and due to that they will not be reported yet.

Table 1 – Fermentations for mangiferin with different volunteers' samples.

Anaerobic Fermentations of mangiferin (AFM)	
AFM V1-1	AFM with Volunter 1 sample first
AFM V1-2	AFM with Volunter 1 sample second
AFM V1-3	AFM with Volunter 1 sample third
AFM V2-1	AFM with Volunter 2 sample first
AFM V2-2	AFM with Volunter 2 sample second
AFM V3-1	AFM with Volunter 3 sample first
AFM V3-2	AFM with Volunter 3 sample second

Table 2 – Human volunteers profiles (n=3).

Parameters	**Volunteer 1**	**Volunteer 2**	**Volunteer 3**
Gender	male	male	male
BMI	22.8	24	21
Diet	low-fat	normal	normal
Smoker	no	no	yes
Drink alcohool	no	moderately	yes
Sports	Yes	Yes	moderately
Medications	No	Beta blocker	No

Body mass index (BMI) is reported by the U. S. Department of Health & Human Services (2012) as a measure of body fat based on height and weight that applies to both adult men and women.

BMI Categories:

- Normal weight = 18.5-24.9
- Overweight = 25-29.9
- Obesity = BMI of 30 or greater

2.4.3. Processment and fractionation of Fermentated Broth on SPE - C18 Cartridges

After the fermentation process the mixture had to be purified and fractionated using the SPE-C18 cartridges. Firstly, the SPE-C18 cartridges were preconditioned with 50 mL methanol and equilibrated with 50 mL DDW. The fermentated broth was then applied in two C-18 cartridges (50 mL / 5000 mg) as can be seen in diagram 1.

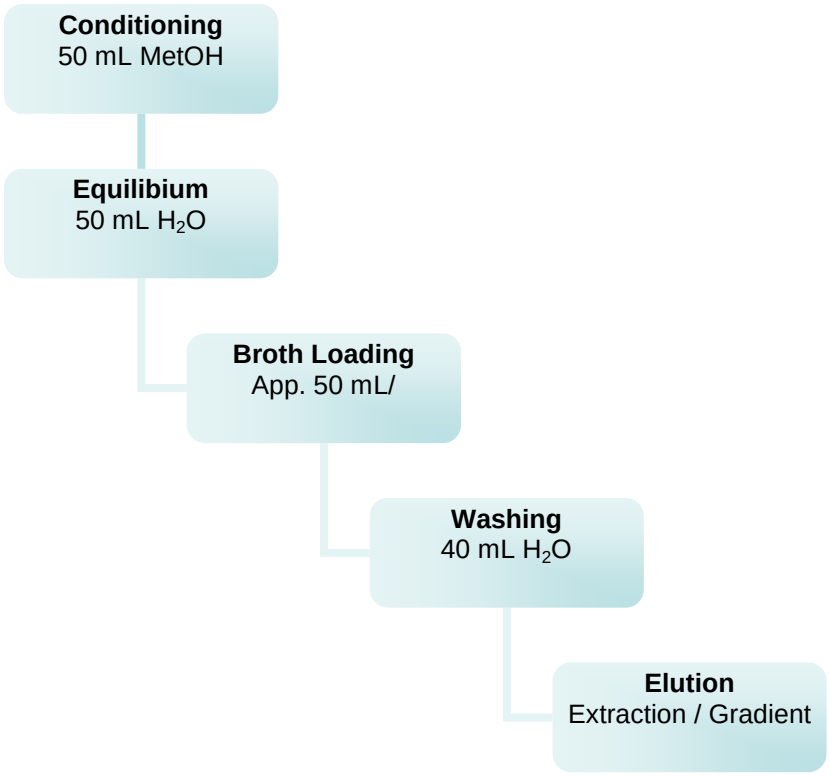

Diagram 1 – General use of SPE C-18 columns for fermented broth processment.

Along the fermentations, different methods were developed during the fermentation studies in order to find out which one should be the best for purification and fractionation of metabolites.

In the first fermentation study, AFM V1-1, the broth was divided in 3 falcon tubes just after the fermentation process was finished and centrifuged at

4500 U/min (3629 x g). The aqueous supernatant was collected and purified using the SPE-C18 cartridge as shown on the diagram 1. After that 40 mL of methanol was eluted and the eluate concentrated on rotaevaporator until it became dry. The sample was then dissolved in water and an aliquot of 20 µL was injected in the HPLC-ESI-MS for analysis.

In case of the AFM V1-2, AFM V2-1 and AFM V3-1fermentations, a further elution step was performed with solvent mixtures containing increasing concentrations of methanol in 2% acetic acid, resulting in five fractions as can be seen in Table 3.

Table 3 – Fractionation of the fermented BHI in the SPE-C18 Cartridges.

50 mL volume	**% of methanol in 2 % acetic acid**
Fraction 1	0
Fraction 2	5
Fraction 3	25
Fraction 4	50
Fraction 5	100

After the fractionation process the samples were freeze-dryed and then dissolved in 5.0 mL methanol. 20 µL of each sample was injected in the LC-MS to screen the compounds. The samples were then transferred to pre-weighted bottles and dryed under nitrogen. Fractions containing metabolites of interest were then afterwood purified by semipreparative HPLC. The AFM V3-1 broth was not processed but analysed just by the end of the fermentation.

Silica (gradient of methanol in dichloromethane) and Sephadex (gradient of methanol in ethanol) columm chromatographies were tested in comparison do semipreparative HPLC in order to purify the metabolites from AFM V1-2. Semipreparative HPLC showed better results and was used in further purifications.

3. Results and Discussion

3.1 Anaerobic Fermentation of Mangiferin – Volunteer 1 (AFM V1-1) Sample

3.1.1 Fermentation analysis by HPLC- ESI- MS

The first fermentation study of mangiferin was performed using 50 mg of mangiferin with volunteer 1 sample. Samples were collected at 0h point and after 12, 24, 36, 48 and 120 h of reaction, spinned and then injected (20 µL) on the HPLC-ESI-MS (Figures 6 to 11) for further analysis. In Figure 6 we can observe the chromatogram for the sample collected at 0 h of reaction. We can see a high peak for mangiferin (Ma) at a retention time of app. 21 min as well as a peak at 22.5 min showing some amount of a metabolite (M-1). At 0h time, M-1 may be probably some impurity present in the mangiferin sample. Other unlabelled peaks refer to compounds from the BHI solution.

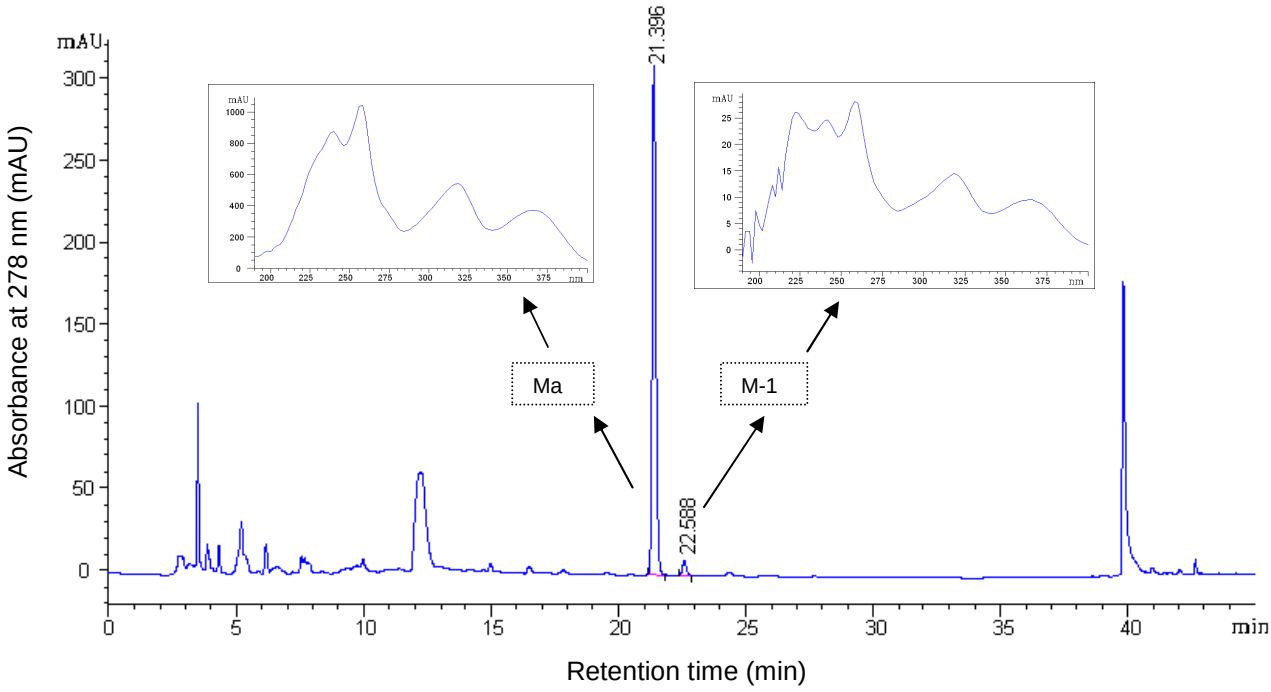

Figure 6 – HPLC chromatogram for 0 h of mangiferin anaerobic fermentation.

In Figure 7 we can observe that already at 12h of reaction, almost all mangiferin was metabolized and a high peak appeared at app. 36 min for another metabolite (M-2). The Figures 7 to 11 show the progression of the reaction with the consumption of mangiferin and the production of the metabolites.

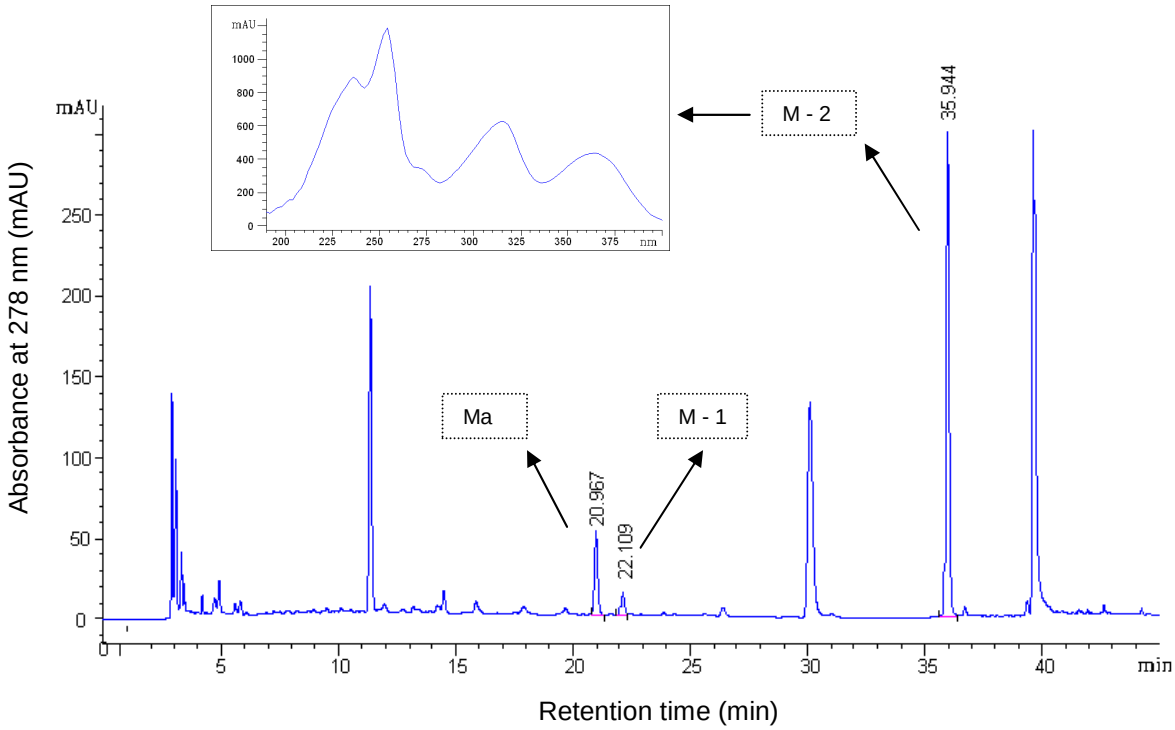

Figure 7 – HPLC chromatogram for 12h of mangiferin anaerobic fermentation.

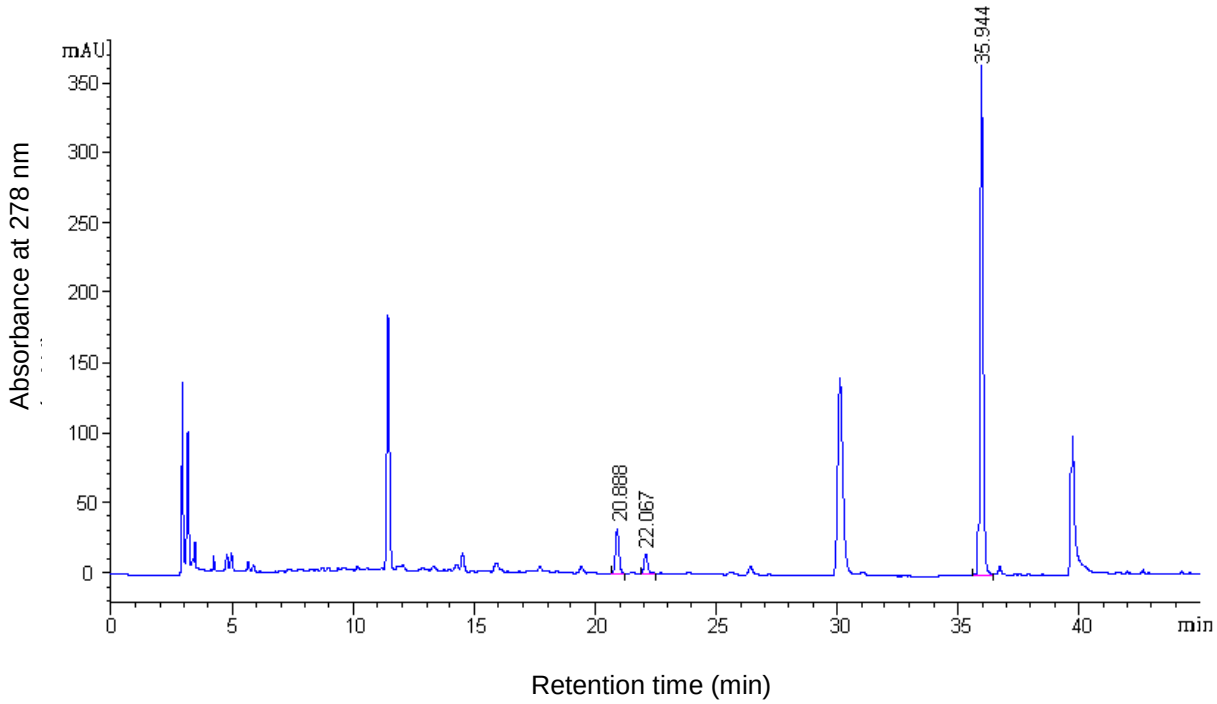

Figure 8 – HPLC chromatogram for 36h of mangiferin anaerobic fermentation.

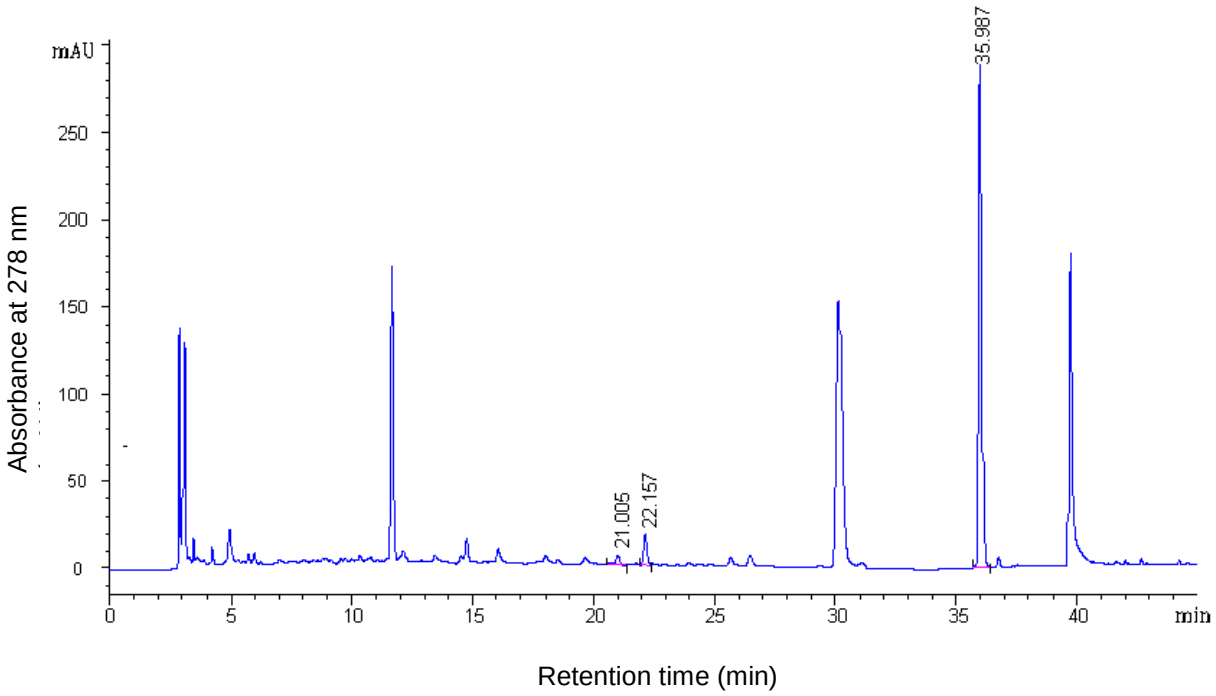

Figure 9 – HPLC chromatogram for 48h of mangiferin anaerobic fermentation.

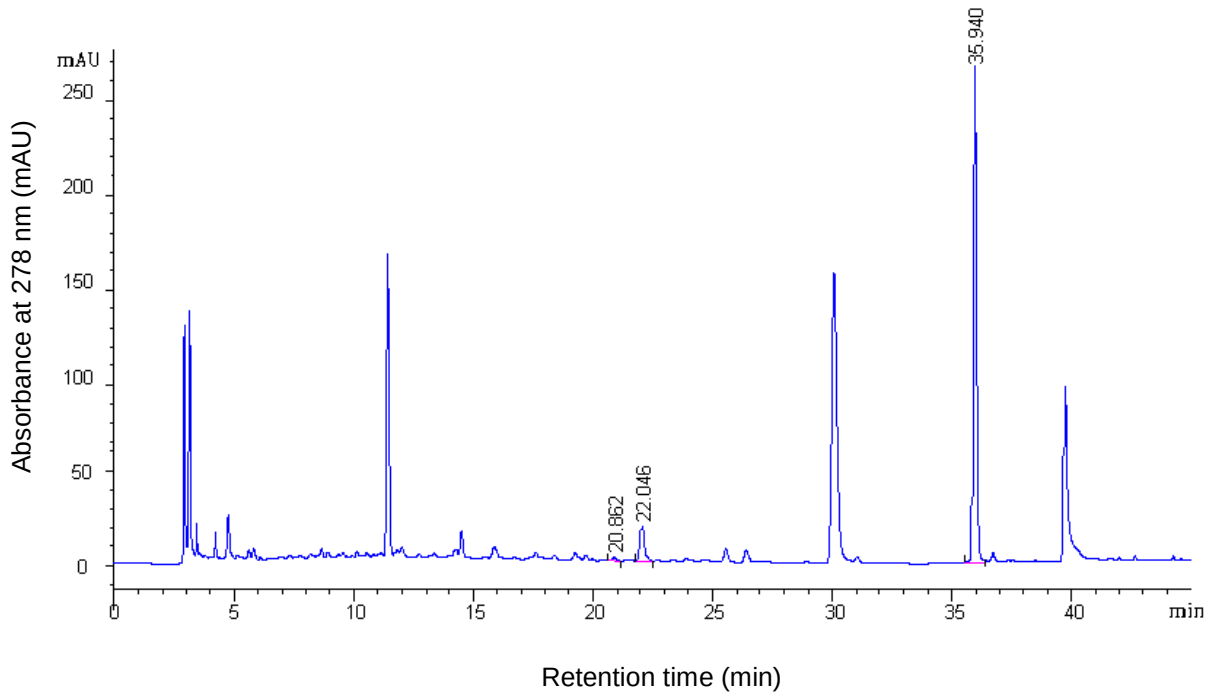

Figure 10 – HPLC chromatogram for 96h of mangiferin anaerobic fermentation.

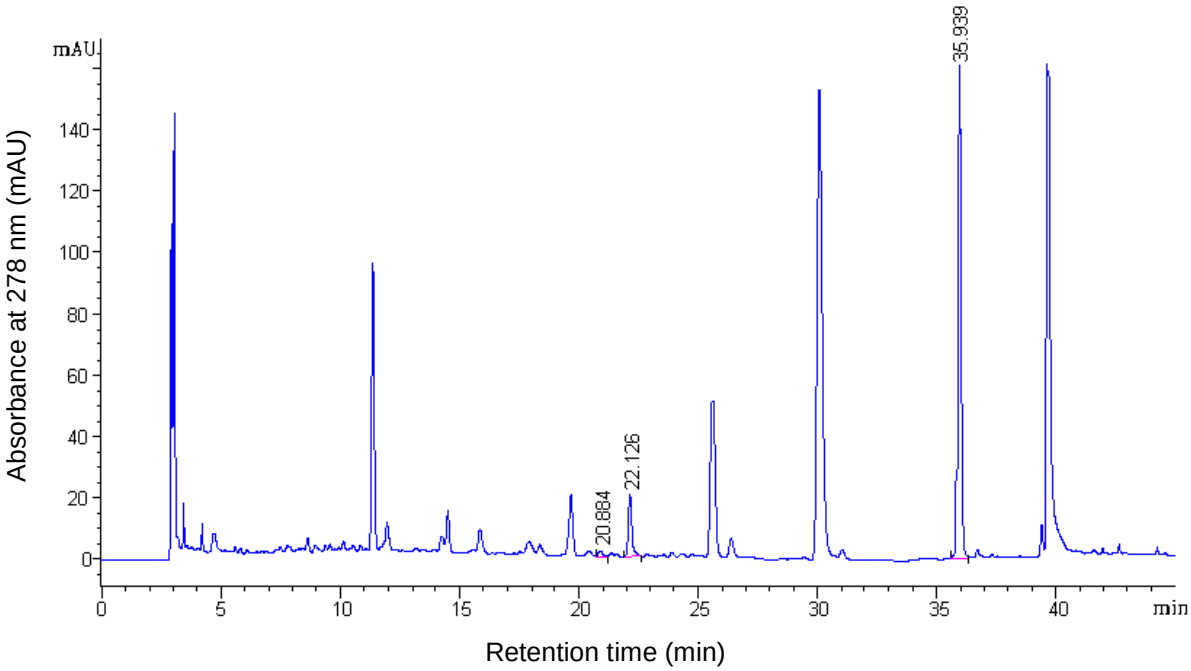

Figure 11 – HPLC chromatogram for 120h of mangiferin anaerobic fermentation.

For AFM V1-1 we can observe that at 36h fermentation time point, almost all mangiferin was converted to metabolites. In this case we see a fast metabolizing pattern that may be classified as an ultrarapid or extensive metabolizer.

3.1.2. HPLC-UV Spectra for mangiferin and metabolites

HPLC-UV Spectra of mangiferin at 12h of reaction and metabolites at 120h of anaerobic fermentation are shown in Figure 12. The UV spectra for mangiferin, homomangiferin and norathyriol show absorbance bands in agreement with that published by Schieber *et al*. (2003), Sanugul *et al*. (2005) and Qin et al. (2008), respectively, as can be seen in Table 4.

Table 4 – HPLC-UV wavelengths from DAD 278 nm for mangiferin and metabolites.

Compound	HPLC-UV λmax [nm]	HPLC-UV λmax [nm] published
Ma	240, 258, 274, 318, 366	241, 258, 275, 318, 366
M-1	226, 240, 258, 274, 318, 364	238, 258, 319, 367
M-2	236, 254,274, 316, 364	237, 254, 312, 362

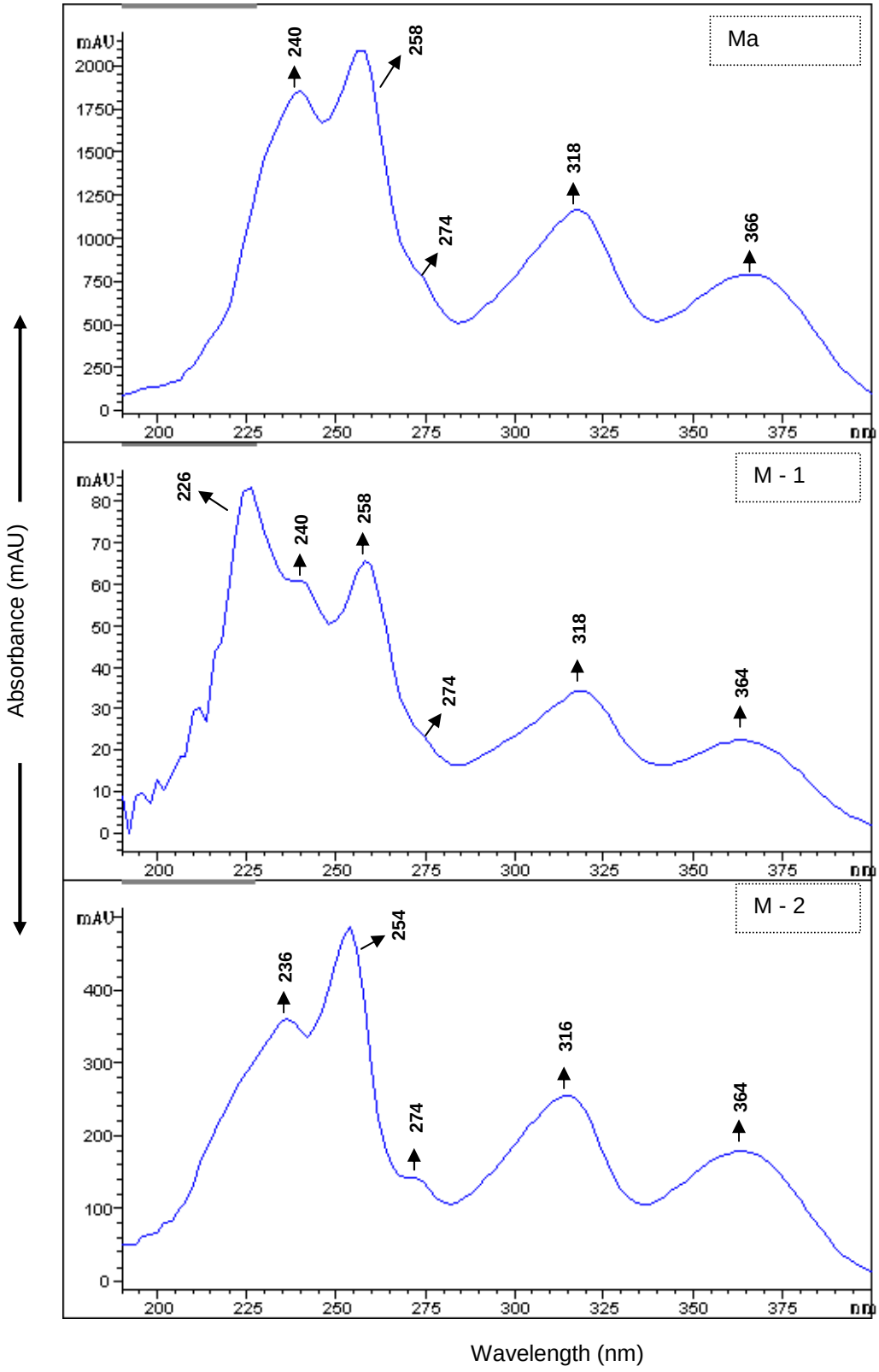

Figure 12 – HPLC-UV Spectra of mangiferin at 12h and metabolites at 120h of anaerobic fermentation.

3.1.3. *Mass Spectra for mangiferin and metabolites*

The figures 13 and 14 shows the mass spectra obtained from the HPLC-ESI-MS for mangiferin at 12h of fermentation and its metabolites homomangiferin and norathyriol at 120 h fermentation time point.

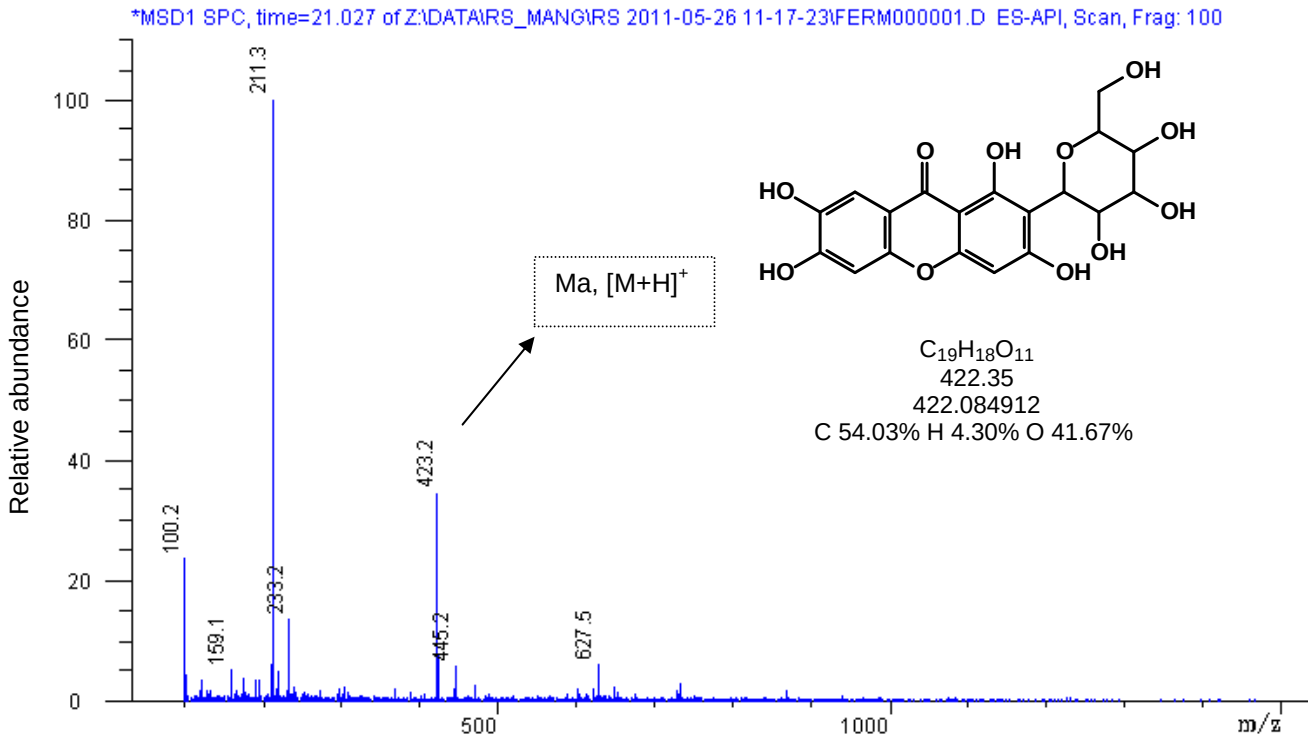

Figure 13 – MS Spectrum of mangiferin at 0h of anaerobic fermentation.

In the spectra shown in Figure X it was observed in the positive-ion mode mass spectra an intense peak $[M+H]^+$ typical of the mangiferin ion at m/z = 423.2 and it was observed as well as some other peaks related probably due to impurities compounds from the broth. The mass spectra for the metabolites shown in the Figure X we can observe an intense peak $[M-H]^-$ of the homomangiferin ion at m/z = 435.2 and for norathyriol at m/z = 259.2. Those measured in negative ion mode.

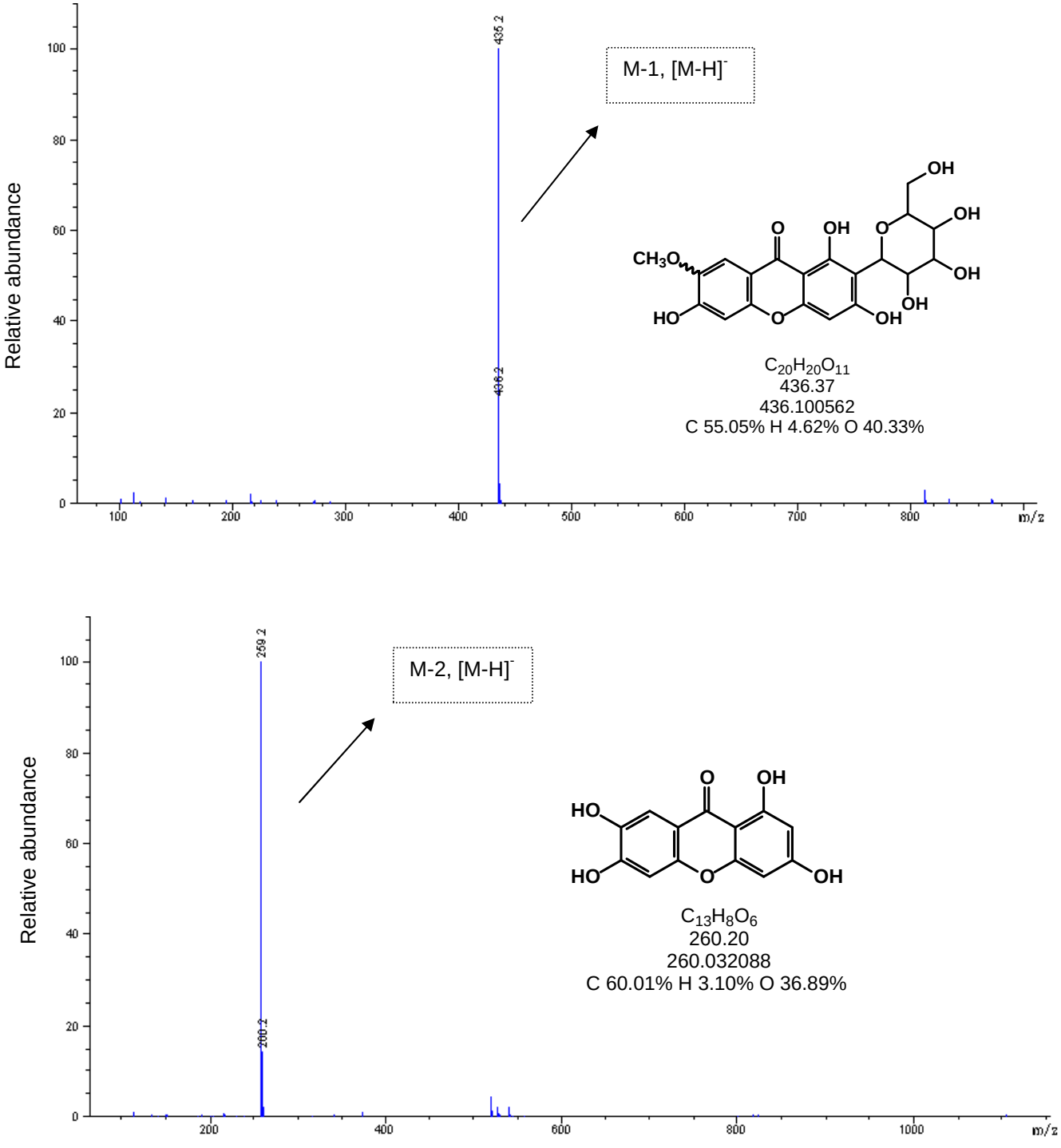

Figure 14 – MS Spectra of M-1 and M-2 at 120h of reaction.

3.1.4. Semipreparative HPLC – Purification of Mangiferin Metabolites from anaerobic Fermentation of Mangiferin with V1-1 sample

Firstly, a previous screening of the sample was performed using a semipreparative HPLC as can be seen in the chromatogram (Figure 15). A separation was then programmed in 10 runs using the CC – module coupled to the Agilent LC-MSD Chemstation. A number of 3 fractions were collected on assay tubes, transferred to round-bottomed flasks, freeze-dried and weighted in green-top bottles (Table 5).

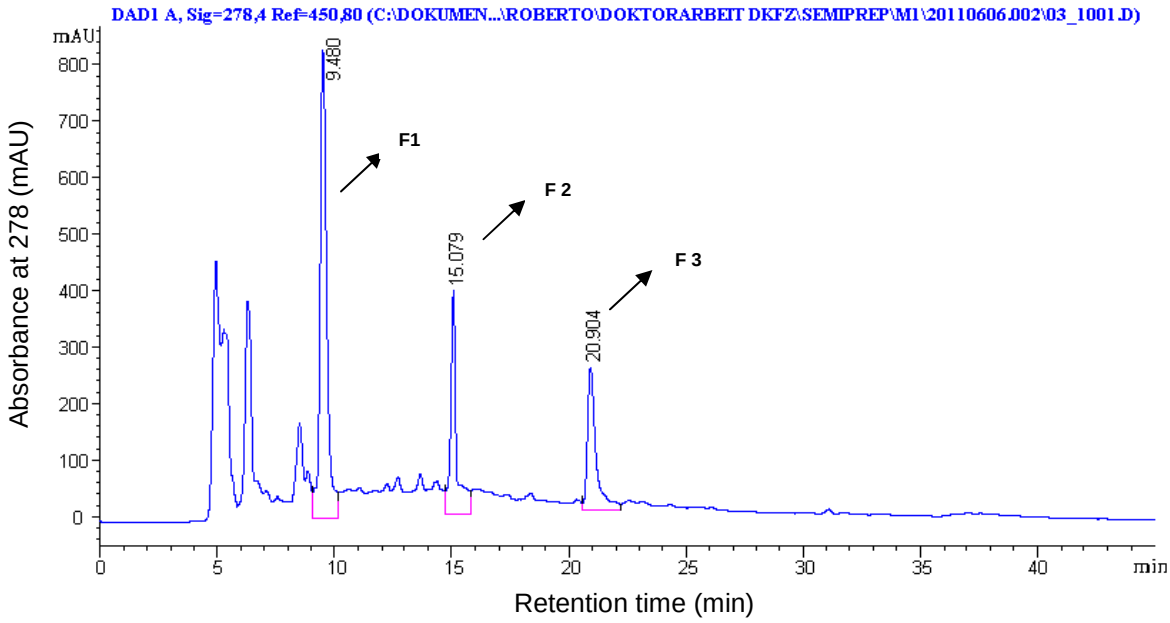

Figure 15 – Separation of mangiferin metabolites by semipreparative HPLC from V1-1 fermentation study.

The fractions showed different colors as can be seen in Figure 16. No metabolite was found in fraction F1, so the characterization steps were done only for fractions F2 and F3 which were found to be homomangiferin and norathyriol, respectively. Wu et al. (2010) obtained homomangiferin as a yellow powder. Sanugul et al. (2005) have obtained norathyriol as a yellow amorphous powder.

Table 5 – Fractions separated from AFM V1-1 by semipreparative HPLC.

Fractions	Mass (mg)	Color
F1	15.31	colorless
F2	4.23	greenish
F3	3.04	Yellowish

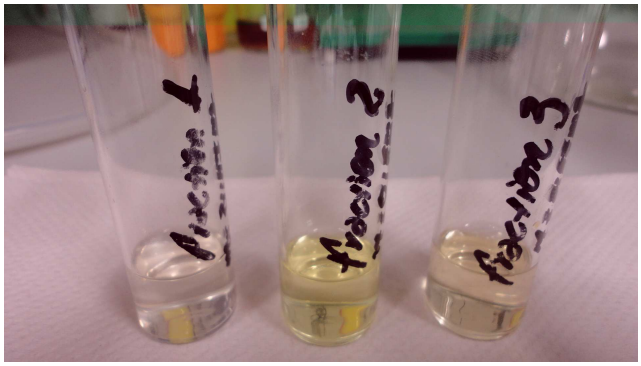

Figure 16 – Fractions separated by semipreparative HPLC from AFM V1-1.

The HPLC-UV Spectra of the metabolites separated by semipreparative HPLC are shown in Figure 17. The UV spectra for homomangiferin and norathyriol show absorbance bands in agreement with that observed before by analytical HPLC but with the difference of the appereance of a band around 210 nm.

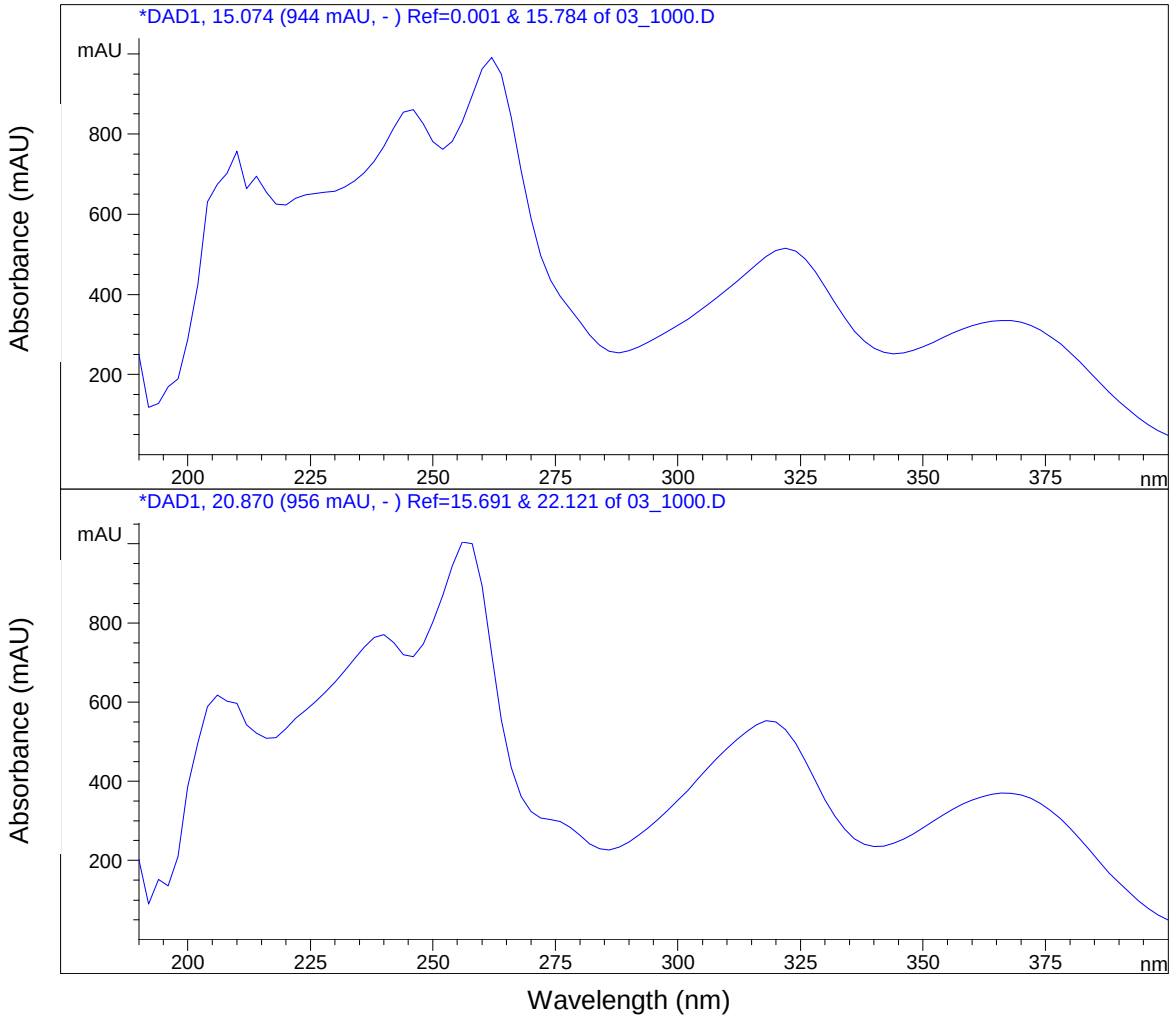

Figure 17 – UV spectrum for fraction 2: retention time at 15.08 min and absorbances at, 214, 224, 244, 262, 278, 322, 368 nm; and for fraction 3: retention time at 20.8 min and absorbances at , 210, 222, 240, 256, 276, 318, 368 nm.

3.1.5. Analysis of the fraction 2 by HPLC-ESI-MS

From the analysis of the HPLC chromatogram for the fraction 2 (Figure 18) it is possible to observe two main peaks which represent the metabolite homomangiferin at a retention time of app. 22 min and a second big peak at 39,6 min for impurities of the BHI solution.

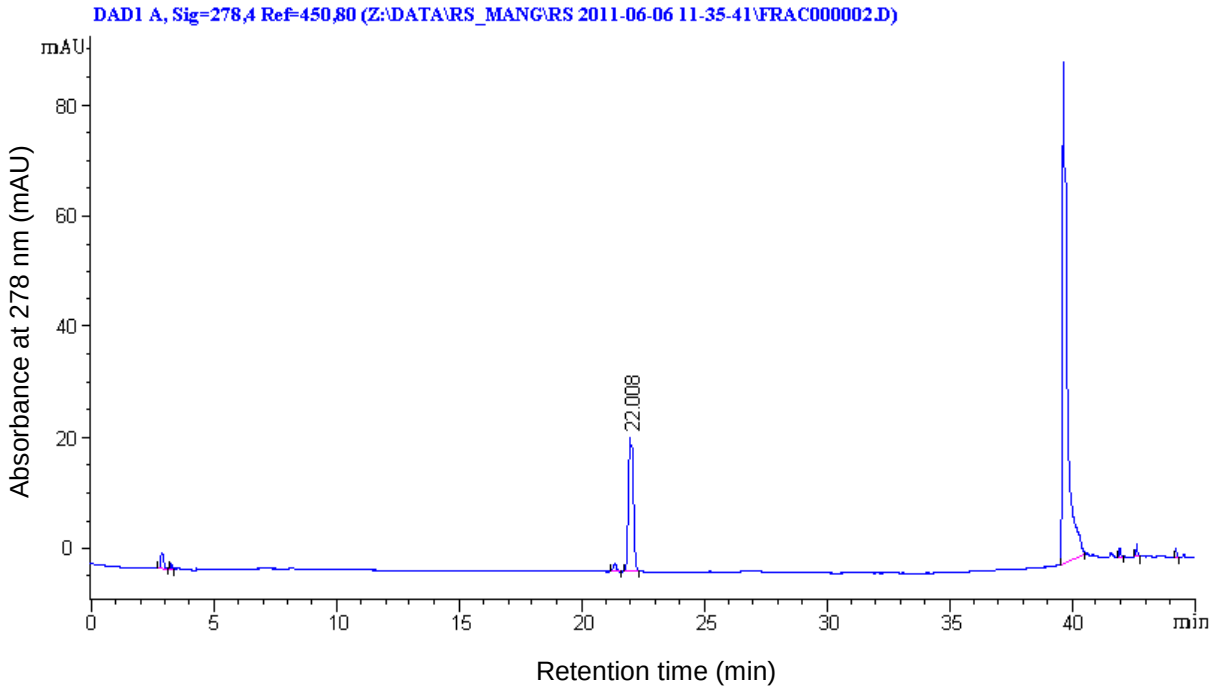

Figure 18 – HPLC chromatogram of the semiprep fraction 2 from V1-1study.

The Figures 19 and 20 show the UV and MS spectra for the fraction 2, respectively. The MS spectra shows the ion fragment $[M-H]^-$ for homomangiferin (m/z 436.2) and the UV spectra shows the absorbances bands for homomangiferin that matched with the results obtained from the semipreparative HPLC separation confirming the presence of the compound.

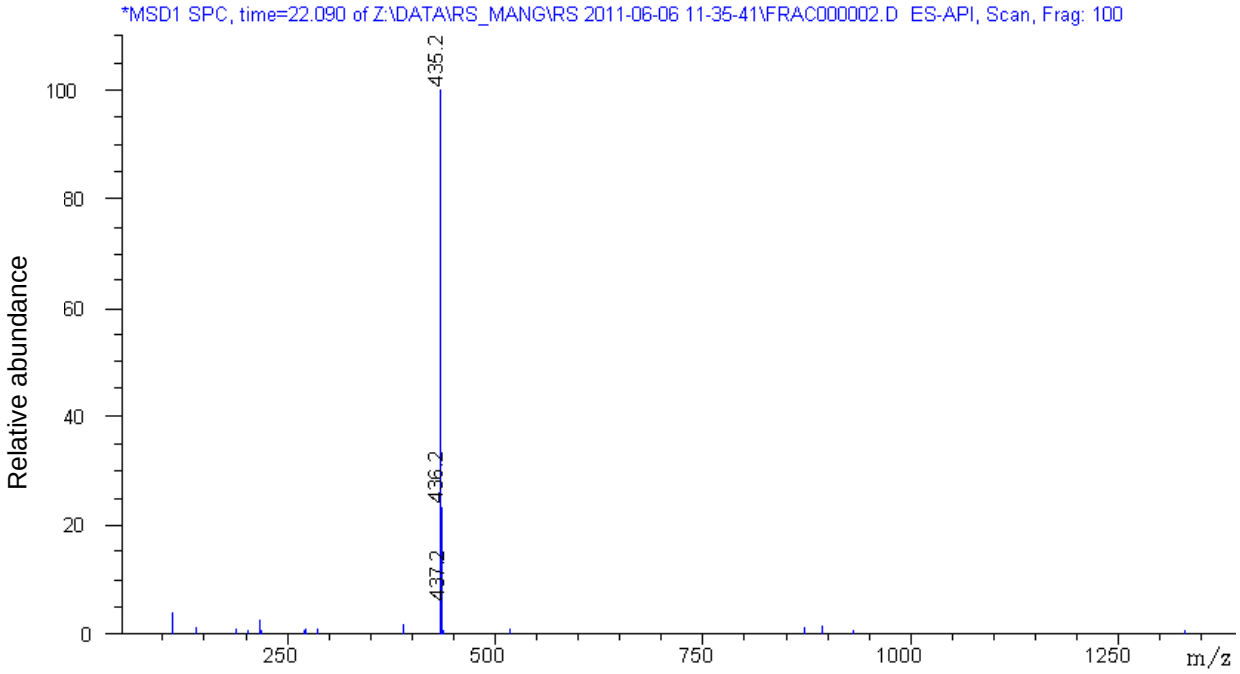

Figure 19 – MS spectra of fraction 2 separated by semipreparative HPLC.

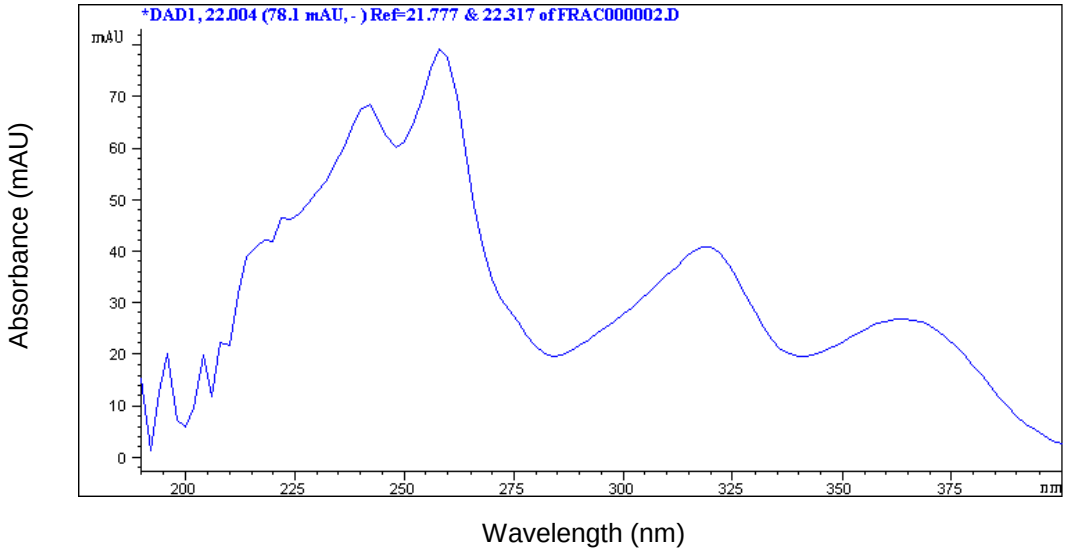

Figure 20 – UV Spectra of fraction 2. Absorbances at 208,218, 222, 242, 258, 274, 318, 366 nm.

3.1.6. Analysis of the fraction 3 by HPLC-MS-MS

From the analysis of the HPLC chromatogram for the fraction 3 (Figure 21) it is possible to observe two main peaks which represent the metabolite norathyriol at a retention time of app. 35,9 min and a second big peak at 39,6 min for impurities of the BHI solution.

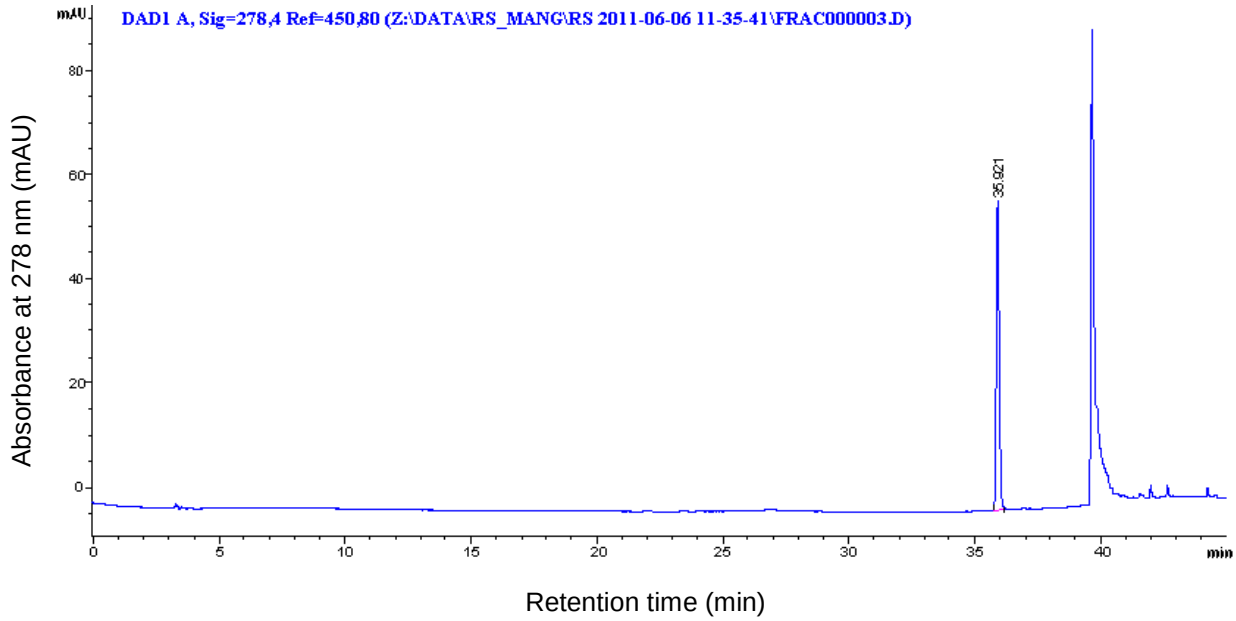

Figure 21 – HPLC chromatogram of the semiprep fraction 3 from V1-1study.

.

The Figures 22 and 23 show the UV and MS spectra for the fraction 3, respectively. The MS spectra shows the ion fragment $[M-H]^-$ for norathyriol (m/z 260.1) and the UV spectra shows the absorbances bands for norathyriol that matched with the results obtained from the semipreparative HPLC separation corfirming the presence of the compound.

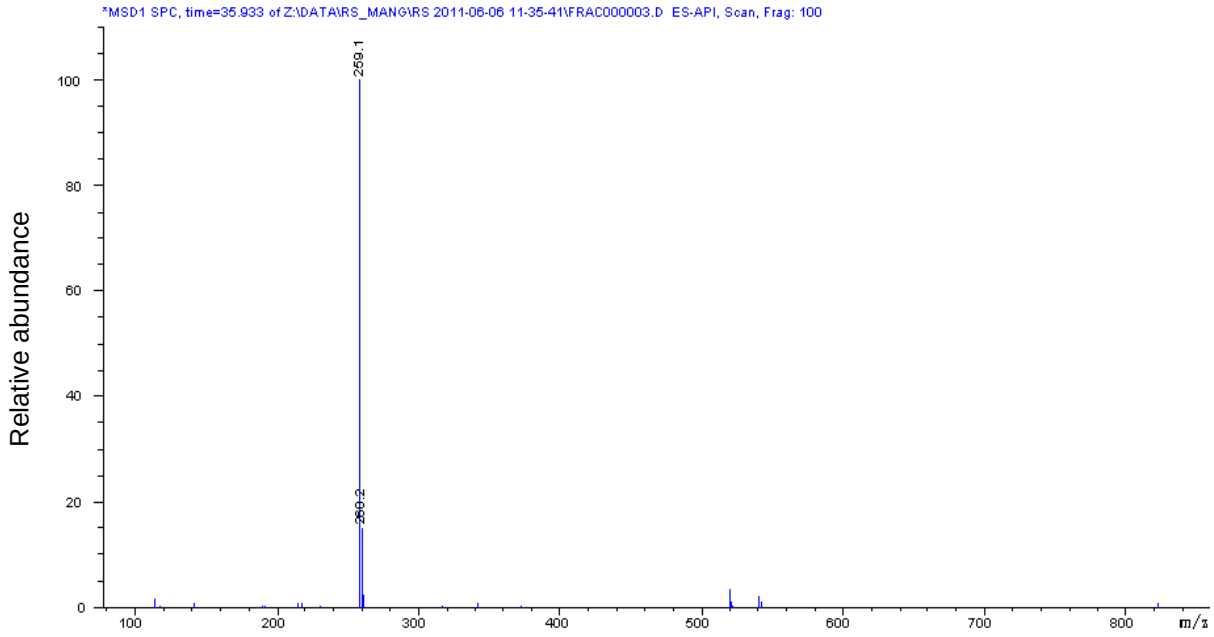

Figure 22 – MS spectrum of fraction 2 separated by semipreparative HPLC.

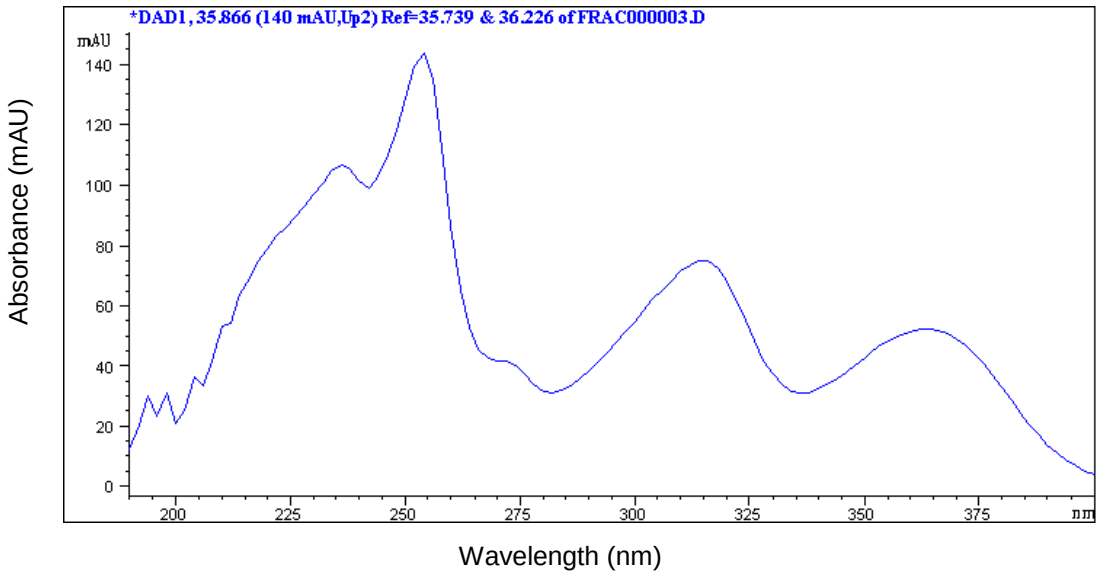

Figure 23 – UV Spectrum of fraction 2. Absorbances at 210, 214, 222, 236, 254, 272, 316, 364 nm.

3.2 Anaerobic Fermentation of Mangiferin – Volunteer 1 (AFM V1-2) Sample

3.2.1 Fermentation analysis by HPLC- ESI- MS

A second anaerobic fermentation of mangiferin with volunteer 1 sample was performed (Figure 24) in order to produce and isolate more metabolites and set up a new purification method for metabolites. From the chromatogram shown in Figure X we can observe that at 120h of fermentation, mangiferin was almost completely reacted producing M-2 and little amount of M-1.

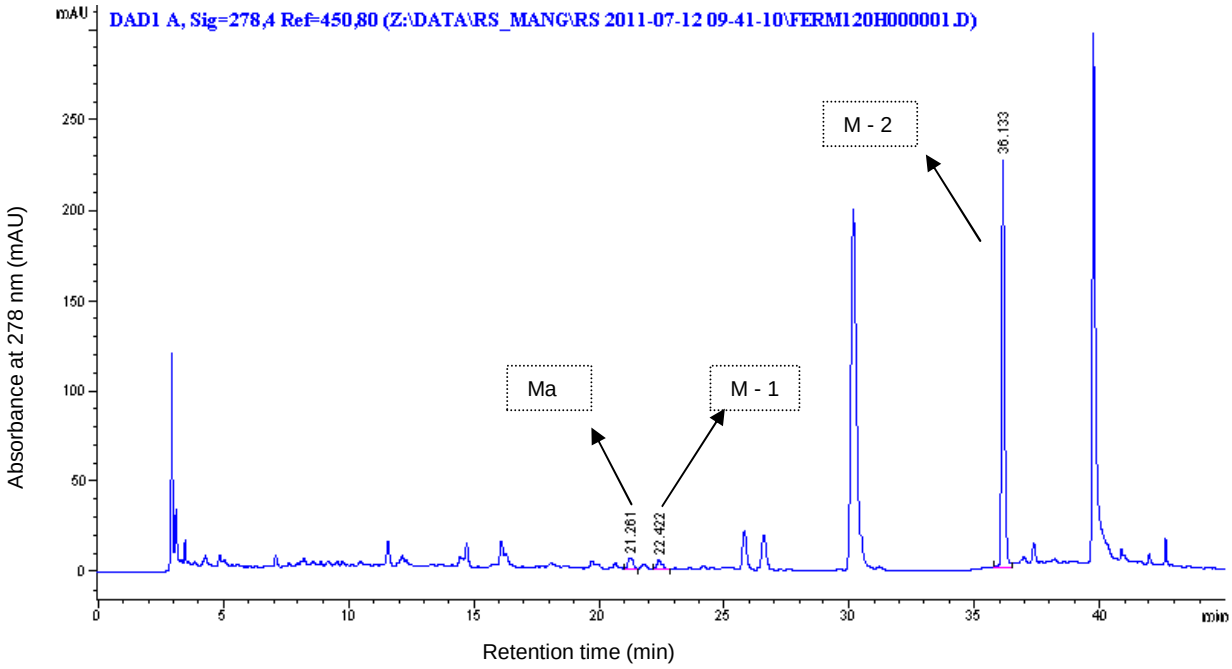

Figure 24 – HPCL chromatogram for 120h of mangiferin anaerobic fermentation.

In Figure 25 we can observe the MS Spectra of mangiferin at 0 h time point of fermentation to produce the metabolites screened at 120 h time point. The measures in negative ion mode shows the ion peaks m/z = 421.1, 435.1 and 259.1.

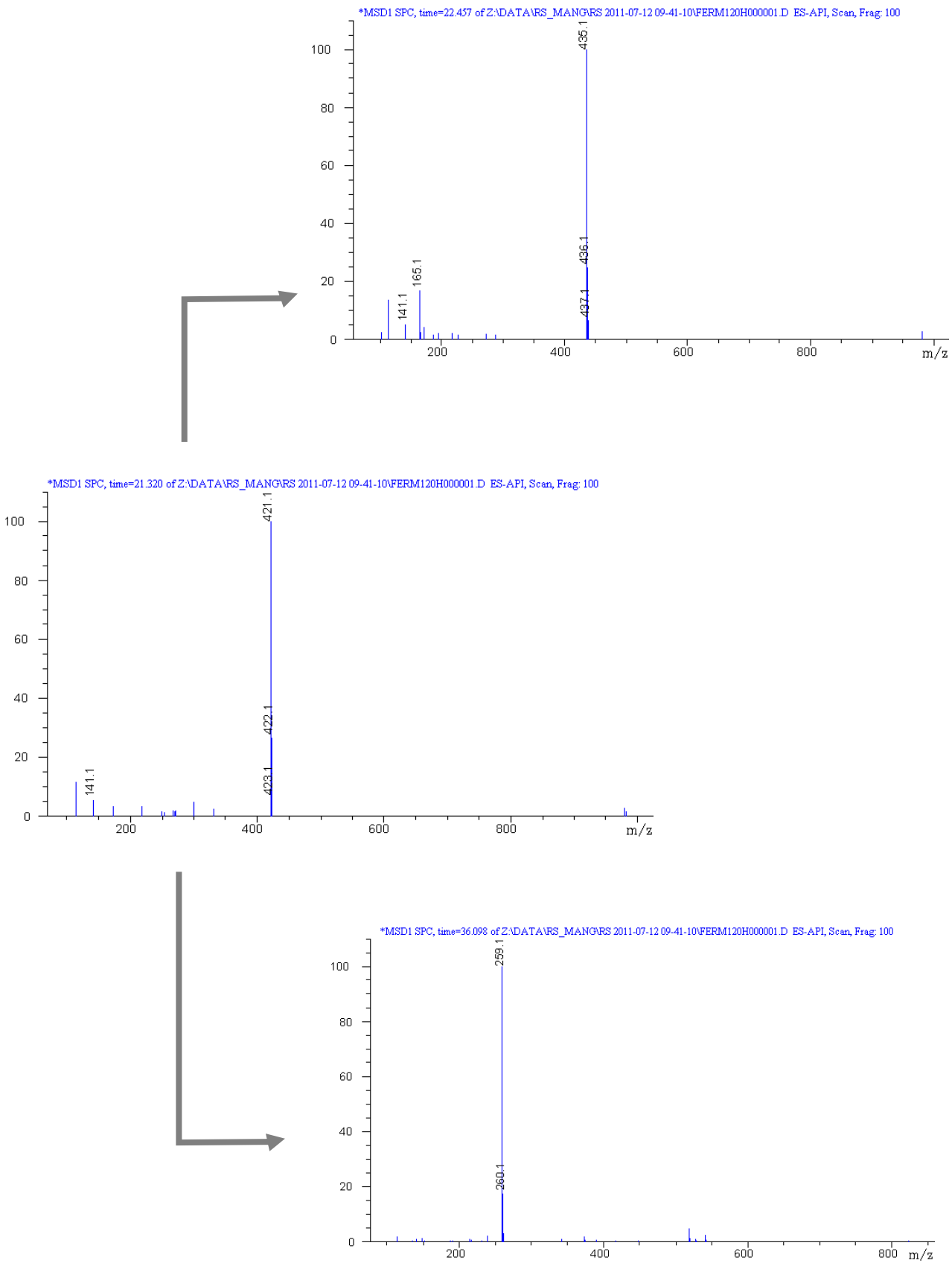

Figure 25 – MS Spectra showing the consumption of mangiferin (0 h) to produce the Metabolites (120 h).

After the fermentation process of mangiferin with V1-2 sample, the fermented broth was passed through two 5 g SPE Columns for purification and fractionation. After elution with the gradient MetOH/Acetic acid as described in methods 2.2.3, the fractions (n = 5) were obtained (Table 6). The fractions were freeze-dried, after that dissolved in 5.0 mL MetOH, transferred to green-top bottles and analyzed by HPLC-ESI-MS.

Table 6 – SPE gradient fractionation for AF of mangiferin with V1-2 sample.

SPE fractions	mass (mg)
Fraction 1	-
Fraction 2	-
Fraction 3	65.0
Fraction 4	63.5
Fraction 5	27.3

From the HPLC-ESI-MS analysis, no presence of mangiferin or metabolites was found in fractions 1 and 2 so they were discarded. The fraction 3 was found to be mainly unreacted mangiferin. for fractions 4 was found mainly norathyriol that after semipreparative purification was obtained in good purity and used for NMR. In Fraction 5 it was also found a good amount of norathyriol as well as its monodehydroxyl as can be seen in Figures 35 and 36. The chromatograms and spectra were then analyzed as follows.

3.2.2. Analysis of SPE fractions from AF of mangiferin fermentation V1-2

SPE Fraction 3

The fraction three obtained from the fractionation of V1-2 sample into SPE columm showed a very heterogenous mixture mangiferin and metabolites M-1 and M-2 and also impurities from the broth (Figure 26).

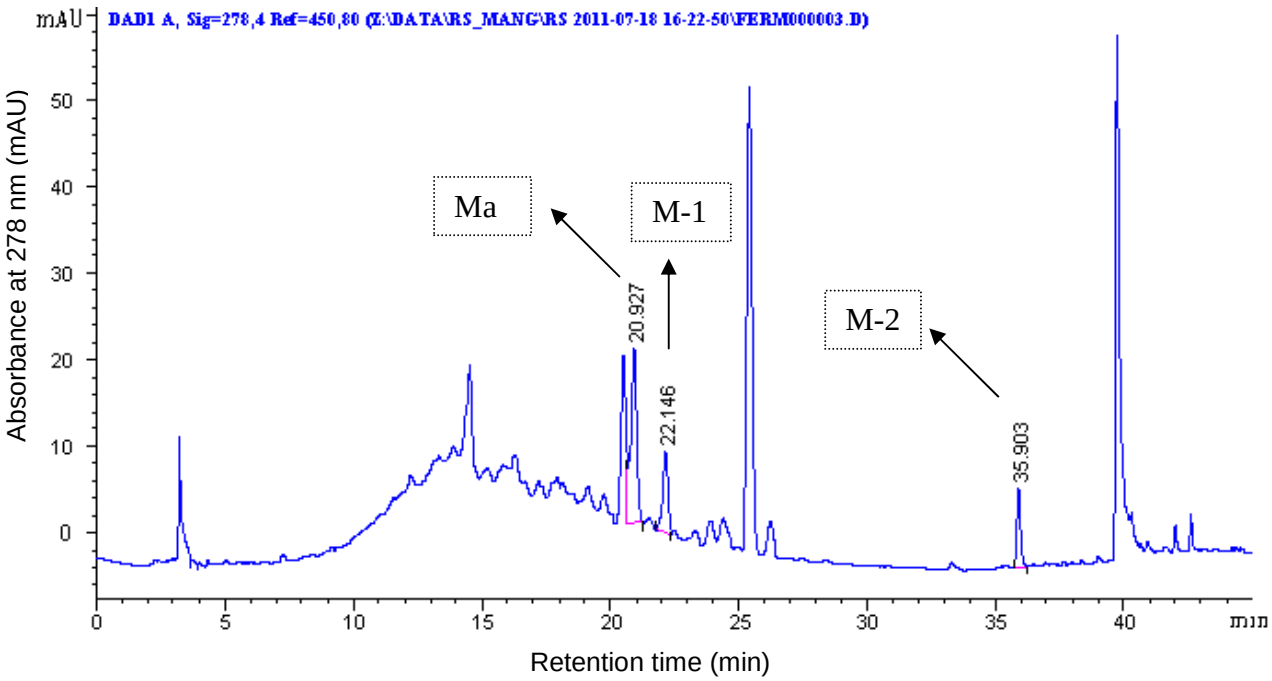

Figure 26 – HPCL chromatogram of SPE fraction 3 from AFM V1-2.

HPLC-UV Spectra of mangiferin and metabolites at in SPE fraction 3 are shown in Figure 27. The UV spectra absorbances for mangiferin, homomangiferin and norathyriol show absorbance bands in agreement with that shown before. Due to low intensity peak at the chromatogram, the UV spectrum for homomangiferin shows little differences but approximately the same absorbance bands.

In Figure 28 we can observe the MS Spectra of mangiferin and the metabolites. The measures in negative ion mode shows the main ion peaks m/z = 421.1, 435.1 and 259.1 and presence of some impurities.

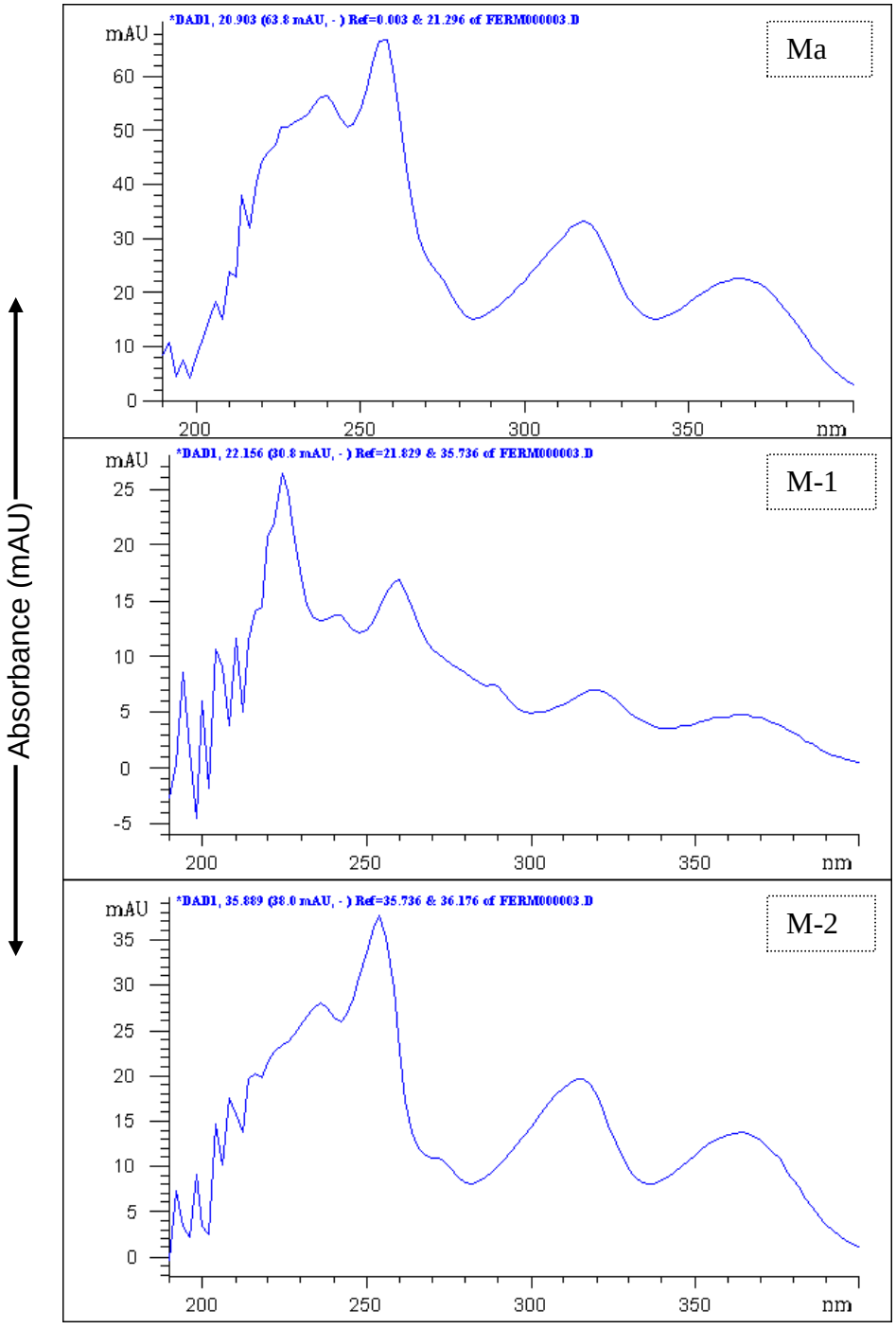

Figure 27 – UV Spectra for mangiferin and metabolites detected in fraction 3.

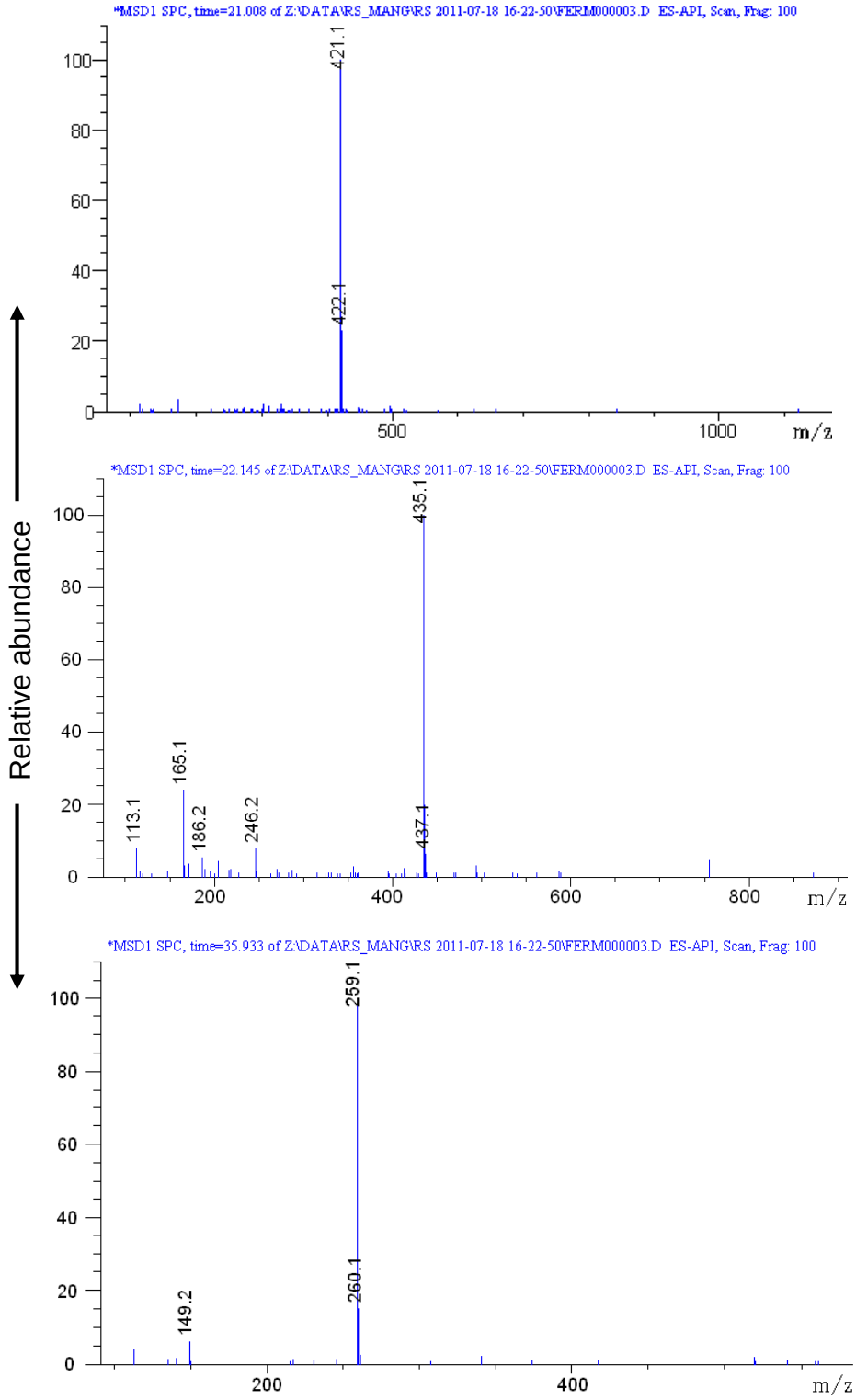

Figure 28 – MS Spectra for mangiferin and metabolites detected in fraction 3.

SPE Fraction 4

The fraction four obtained from the fractionation of V1-2 sample into SPE columm showed basically the metabolites M-2 in high concentration. Due to that we see distorted and high intense bands at the UV spectrum as well as the molecular ion peak at 259.1 in MS spectrum for norathyriol measured in negative ion mode (Figure 29).

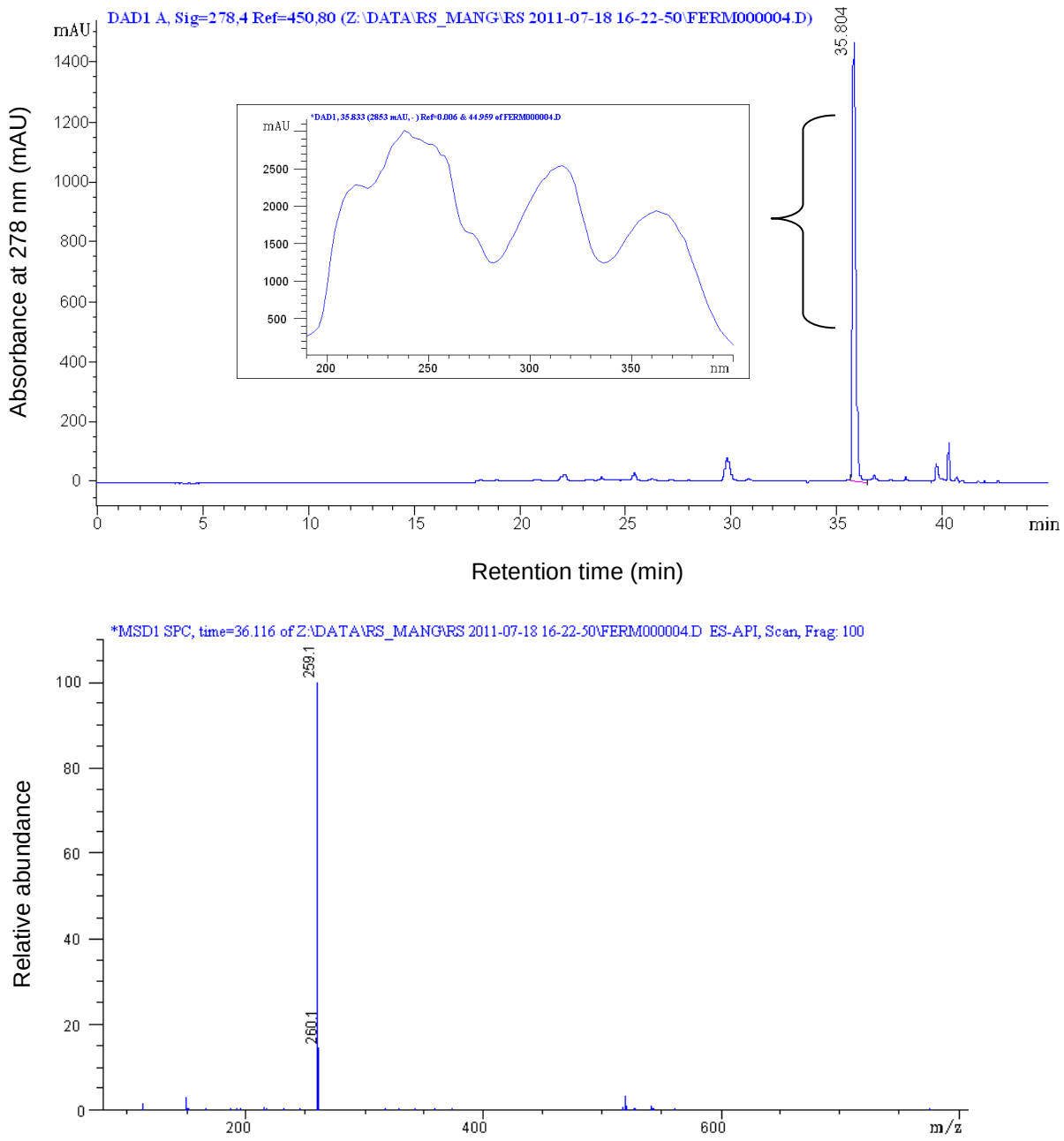

Figure 29 – HPCL chromatogram and UV-MS spectra for norathyriol metabolite detected in SPE fraction 4 from AFM V1-2.

SPE Fraction 5

The fith fraction obtained from the fractionation of V1-2 sample into SPE columm showed M-2 in higher concentration but also another metabolite M-3 (Figures 30 and 31). We can observe the molecular ion peak at 259.1 in MS spectra for norathyriol and at 243.1 for the monodehydroxyl norathyriol, obtained by dehydroxylation of norathyriol, probably gentisein (Liu *et al*., 2011; Matsushima *et al.*, 1985)

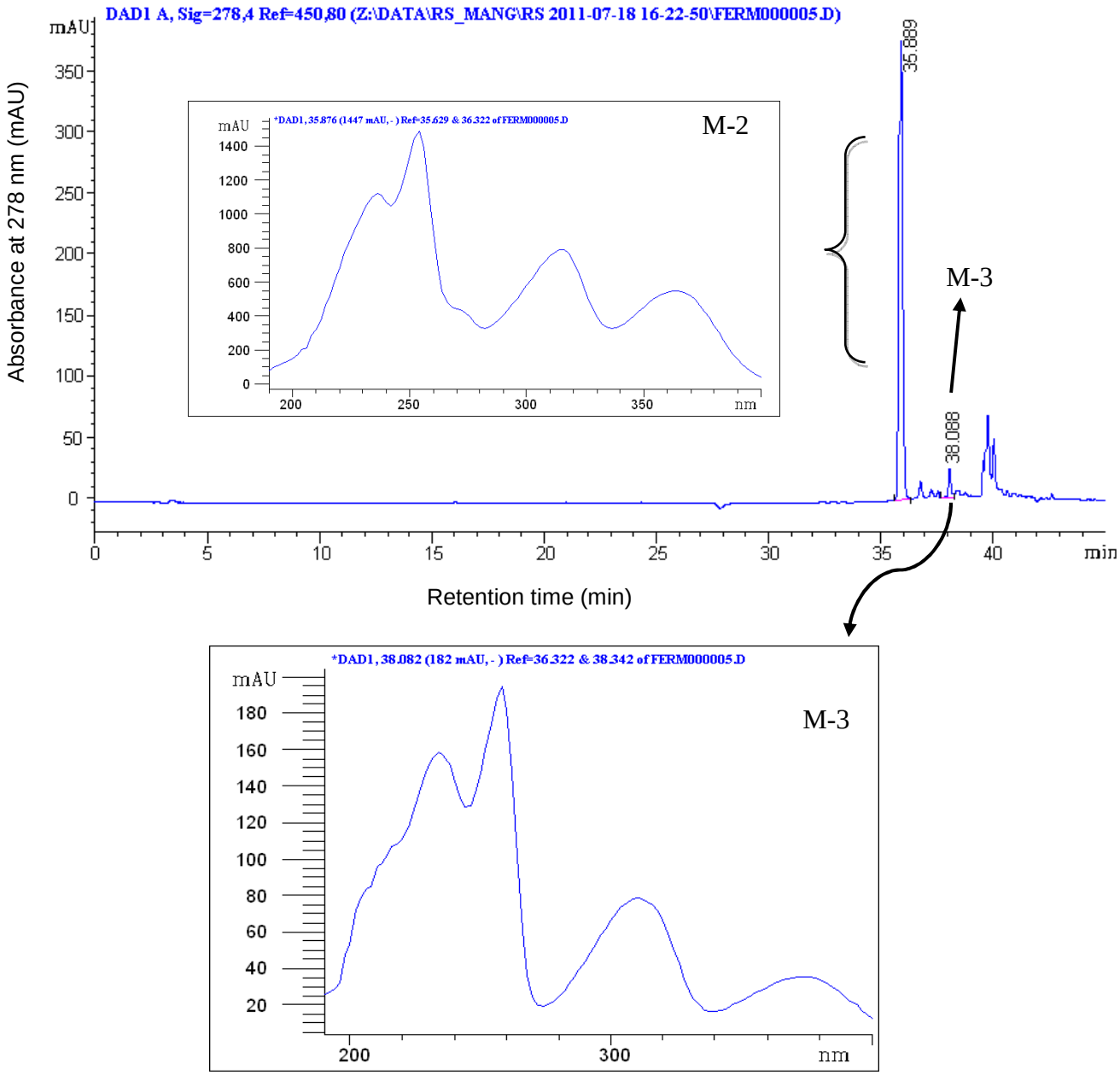

Figure 30 – HPCL chromatogram and UV spectra for norathyriol and M-3 detected in SPE fraction 5 from AFM V1-2.

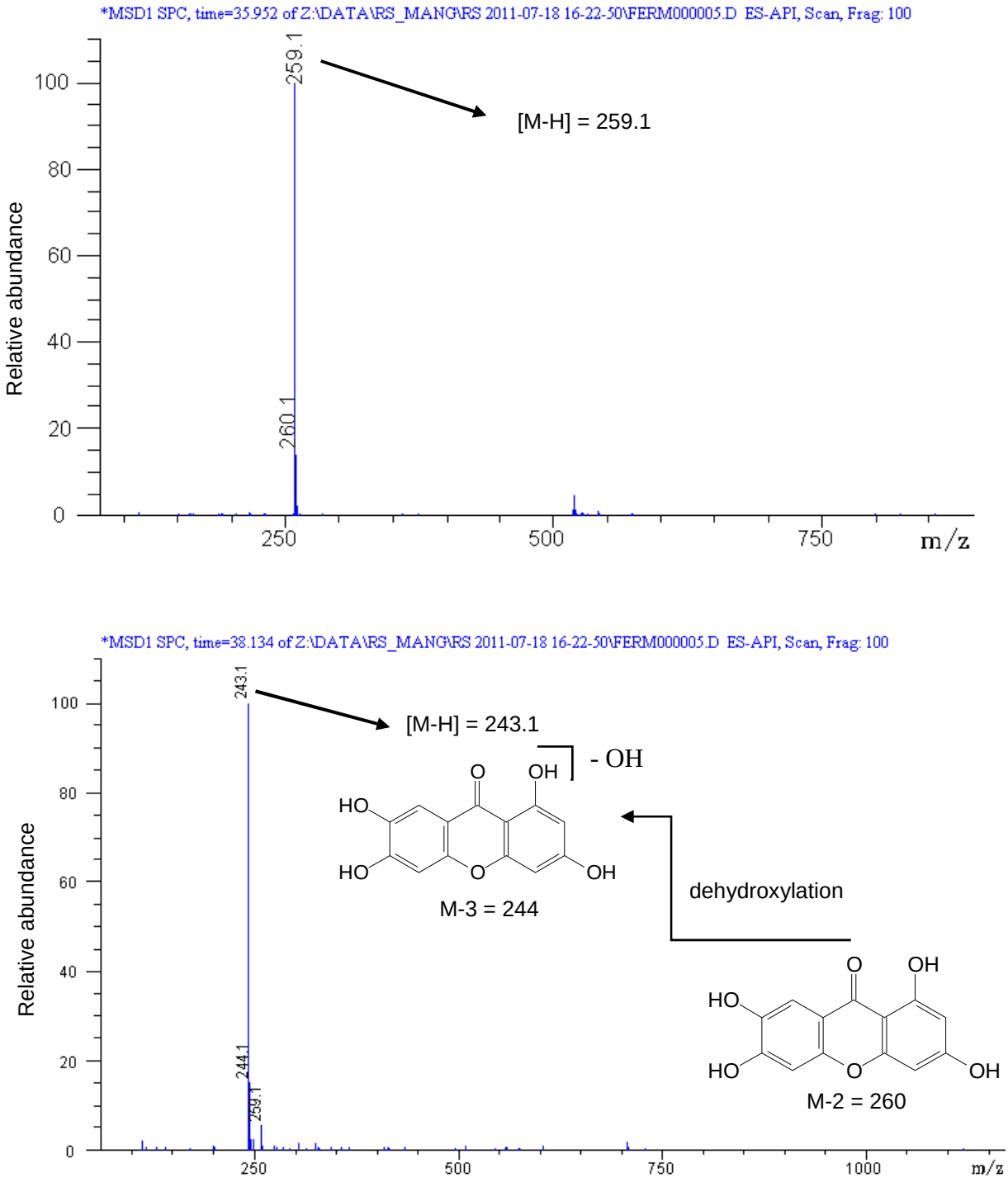

Figure 31 – MS Spectra for norathyriol and its monodehydroxyl metabolites detected in fraction 5.

3.3 Anaerobic Fermentation of Mangiferin – Volunteer 2 (AFM V2-1) Sample

3.3.1 Fermentation analysis by HPLC- ESI- MS

The first fermentation study of mangiferin with volunteer 2 sample was performed using 50 mg of mangiferin. As for AFM V1-1, samples were collected but at different time points: 0, 24, 48, 72, 96 and 120 h of reaction, spinned and then injected (20 µL) on the HPLC-ESI-MS (Figures 32 to 37) for further analysis. In Figure 37 we can observe the chromatogram for the sample collected at 0 h of reaction. We can see a high peak for Ma at a retention time of app. 21.3 min as well as a peak at 22.5 min showing some amount of M-1 at 0h time. Other unlabelled peaks refer to compounds from the BHI solution.

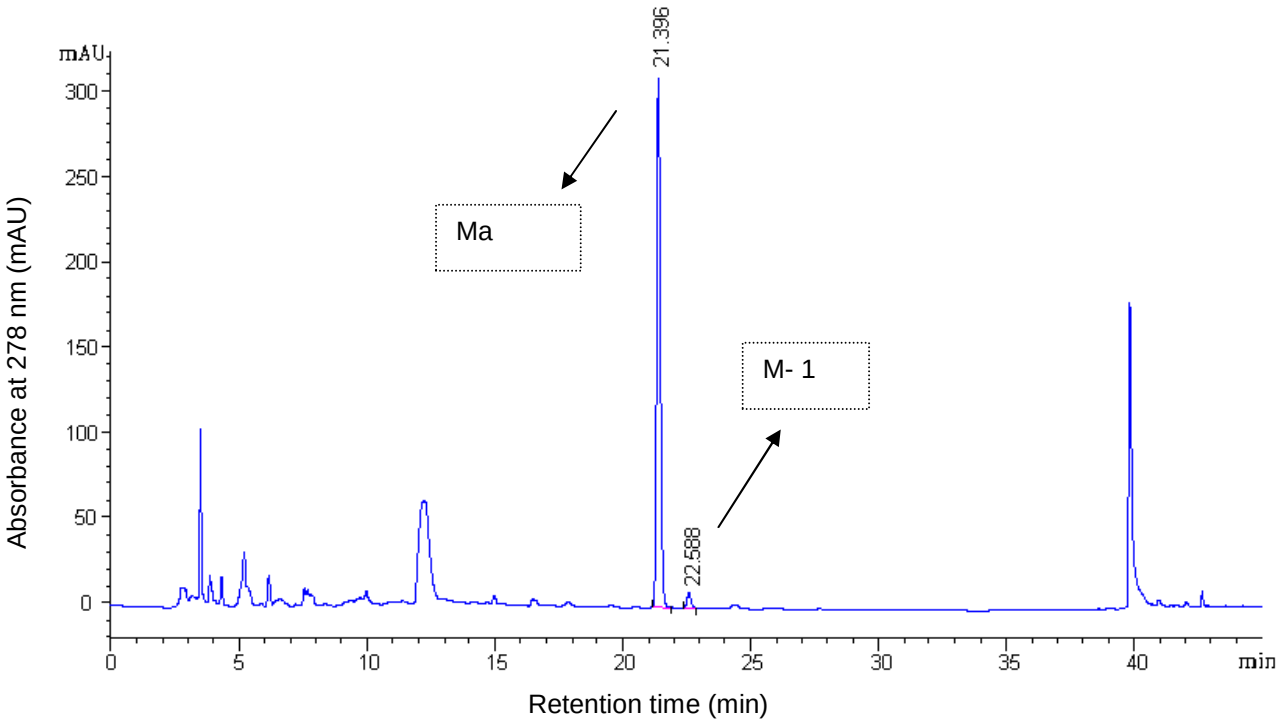

Figure 32 – HPCL for 0h of mangiferin anaerobic fermentation.

We can observe that even after 24h no much mangiferin had reacted (Figure 32), differently of that observed in AFM V1-1, where almost all mangiferin had reacted after 12h (Figure 7). After 48h, some amount of mangiferin was metabolized into M-1 and M-2 which remained almost constant until 120h as can be in Figures 32 to 37.

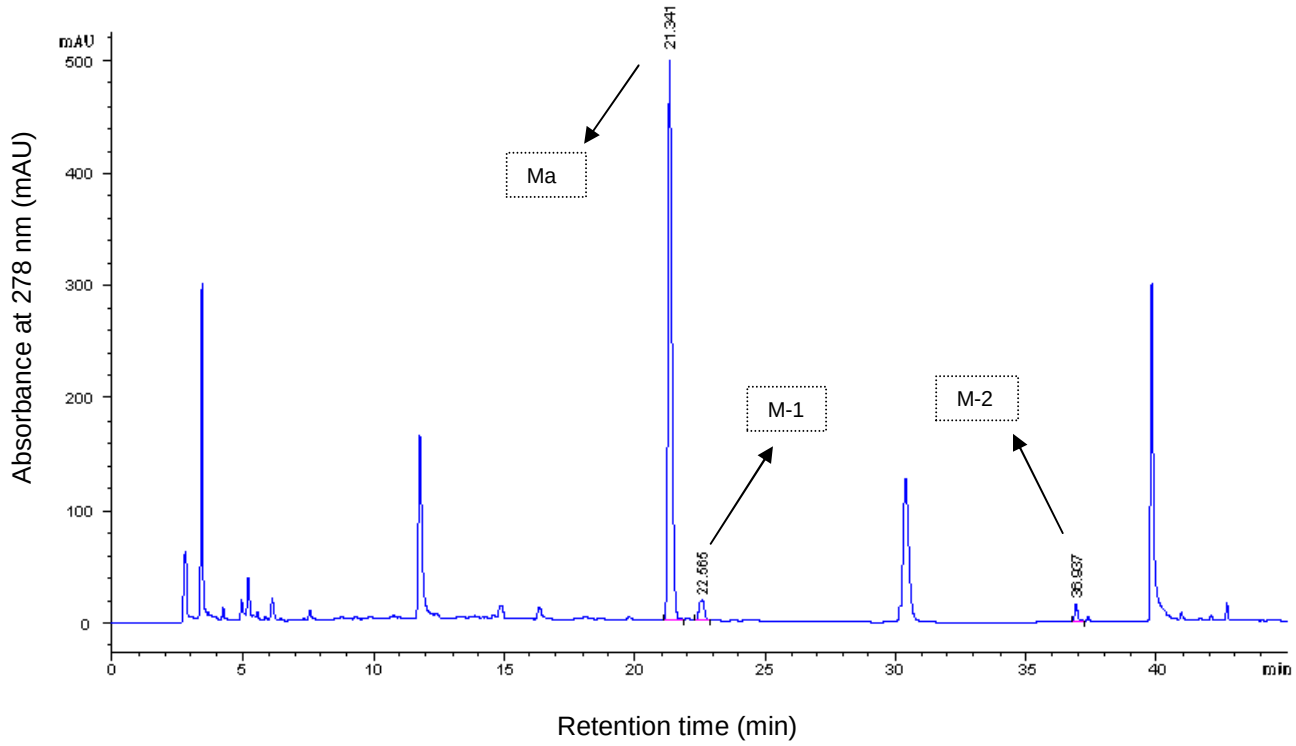

Figure 33 – HPCL for 24h of mangiferin anaerobic fermentation.

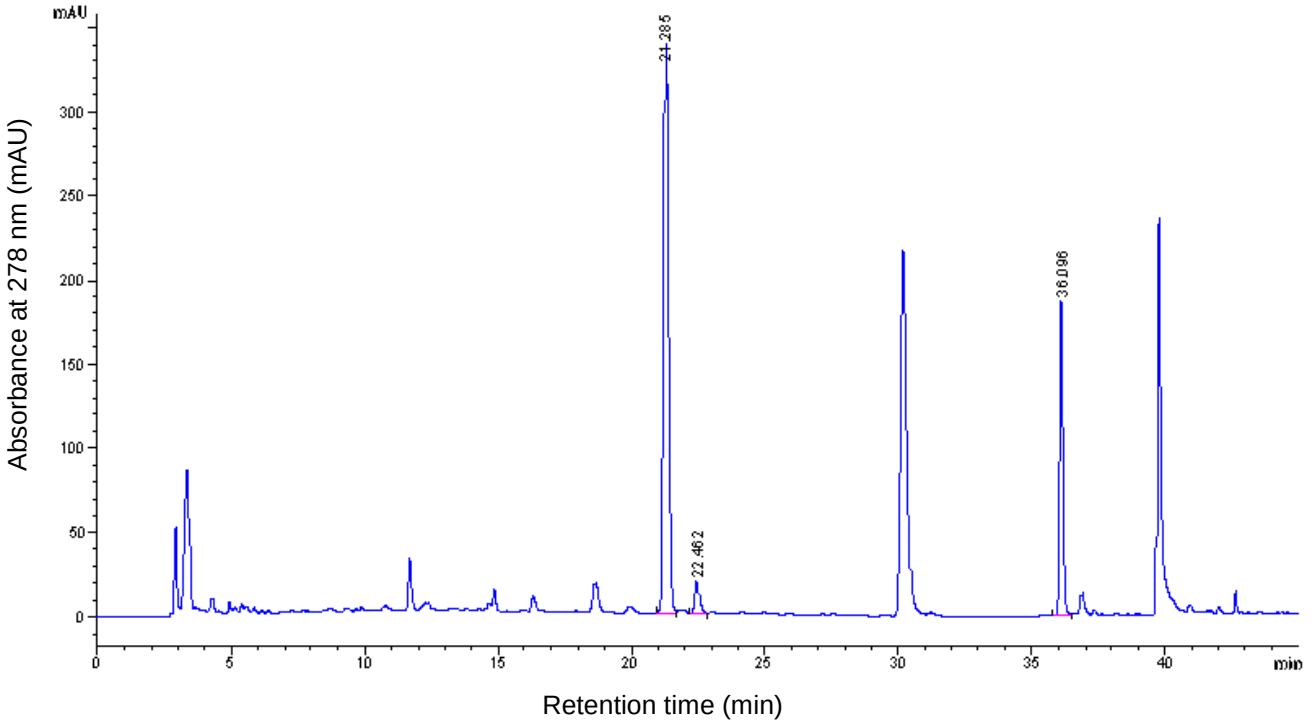

Figure 34 – HPCL for 48h of mangiferin anaerobic fermentation.

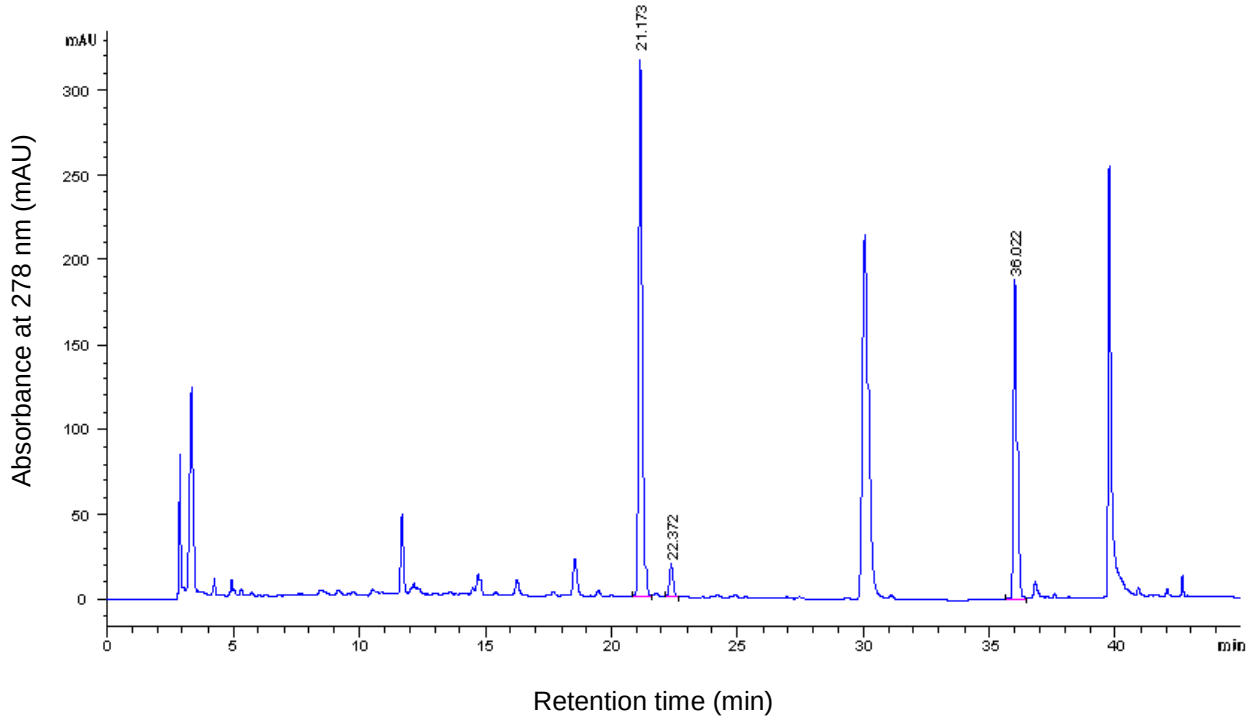

Figure 35 – HPCL for 72h of mangiferin anaerobic fermentation.

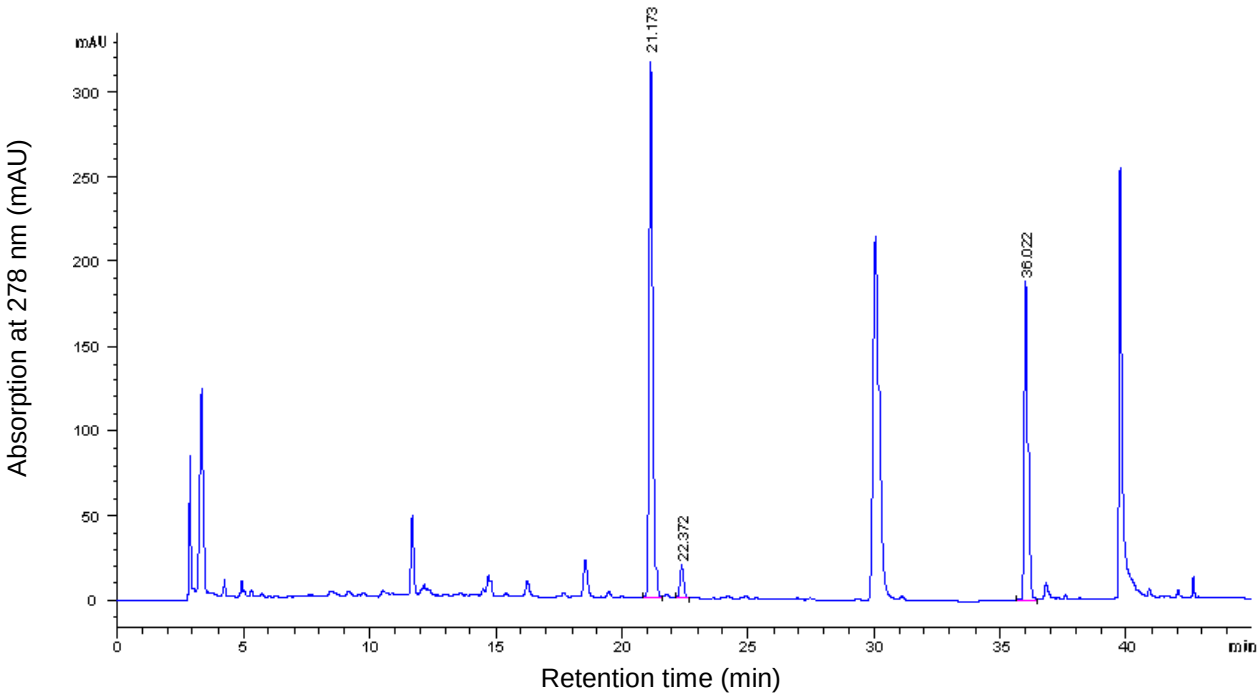

Figure 36 – HPCL for 96h of mangiferin anaerobic fermentation.

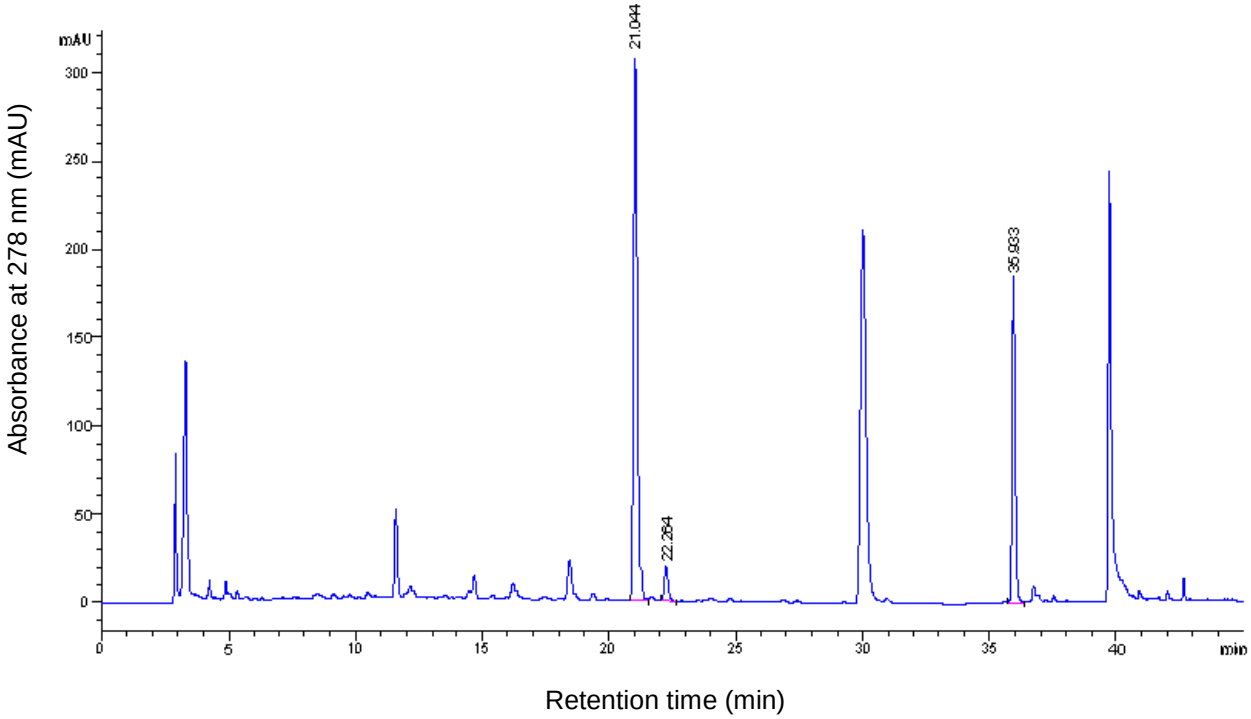

Figure 37 – HPCL for 120h of mangiferin anaerobic fermentation.

After the fermentation process of mangiferin with volunteer 2 sample, the fermented broth was passed through two 5 g SPE Columns for purification and fractionation. After elution with the gradient MetOH/Acetic acid as described in methods 2.2.3, the fractions (n = 5) were obtained (Table 7). The fractions 3-5 were freeze-dried, after that dissolved in 5.0 mL MetOH, transferred to green-top bottles and analysed by HPLC-ESI-MS.

Table 7 – SPE gradient fractionation for AF of mangiferin with V2-1 sample.

SPE fractions	mass (mg)
Fraction 1	-
Fraction 2	-
Fraction 3	38.22
Fraction 4	41.57
Fraction 5	9.45

From the HPLC-ESI-MS analysis, no presence of mangiferin or metabolites was found in fractions 1 and 2 so they were discarded. The fraction 3 was found to be mainly unreacted mangiferin. The chromatograms and spectra were then analyzed for fractions 4 and 5 as follows.

3.3.2. Analysis of SPE fractions from AFM V2-1

Fraction 3

The analytical HPLC analysis for fraction three revealed presence of unreacted mangiferin shown in the chromatogram (Figure 38 and 39) at 20.9 min retention time and by the UV spectra.

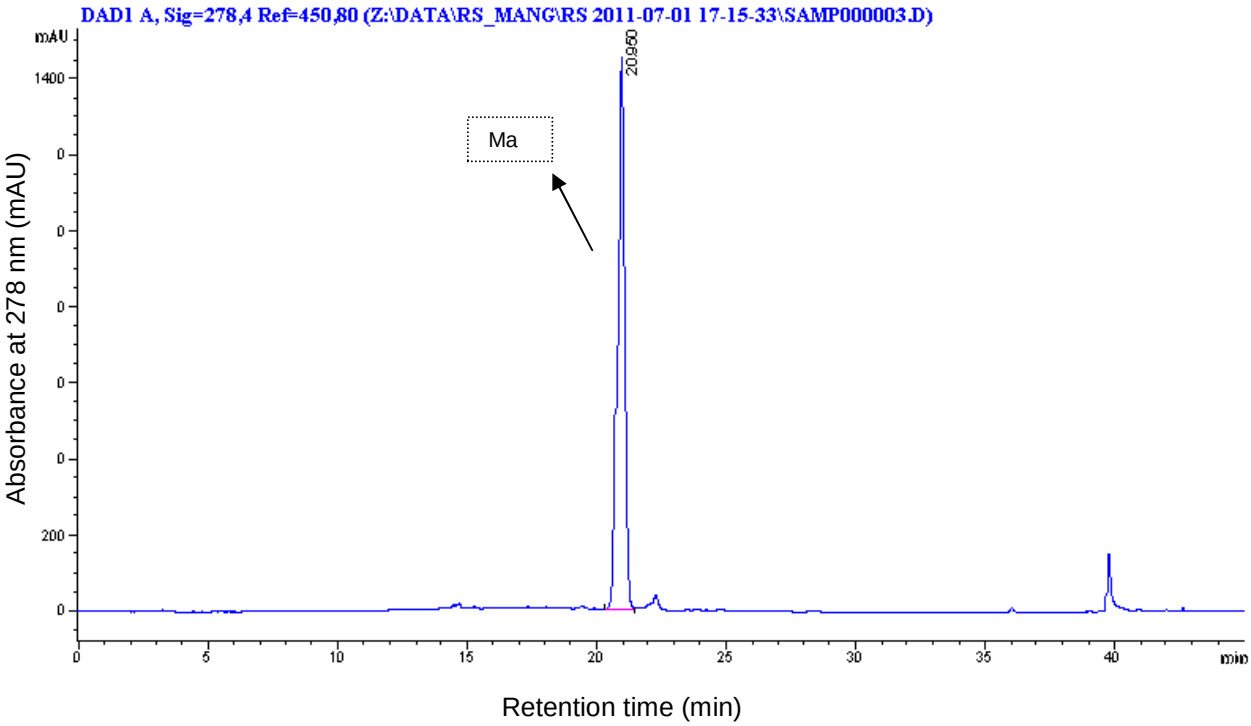

Figure 38 – HPCL chromatogram for mangiferin detected in SPE fraction 3 from AFM V2-1.

This fraction confirmed that a high amount of mangiferin remained unreacted in this fermentation study, contrary to that observed in AFM V1-1, whose fermentation worked almost up to one hundred per cent.

The presence of mangiferin in fraction three was also confirmed by the MS spectra showing the molecular ion peak m/z at 421.1 as seen in Figure 39.

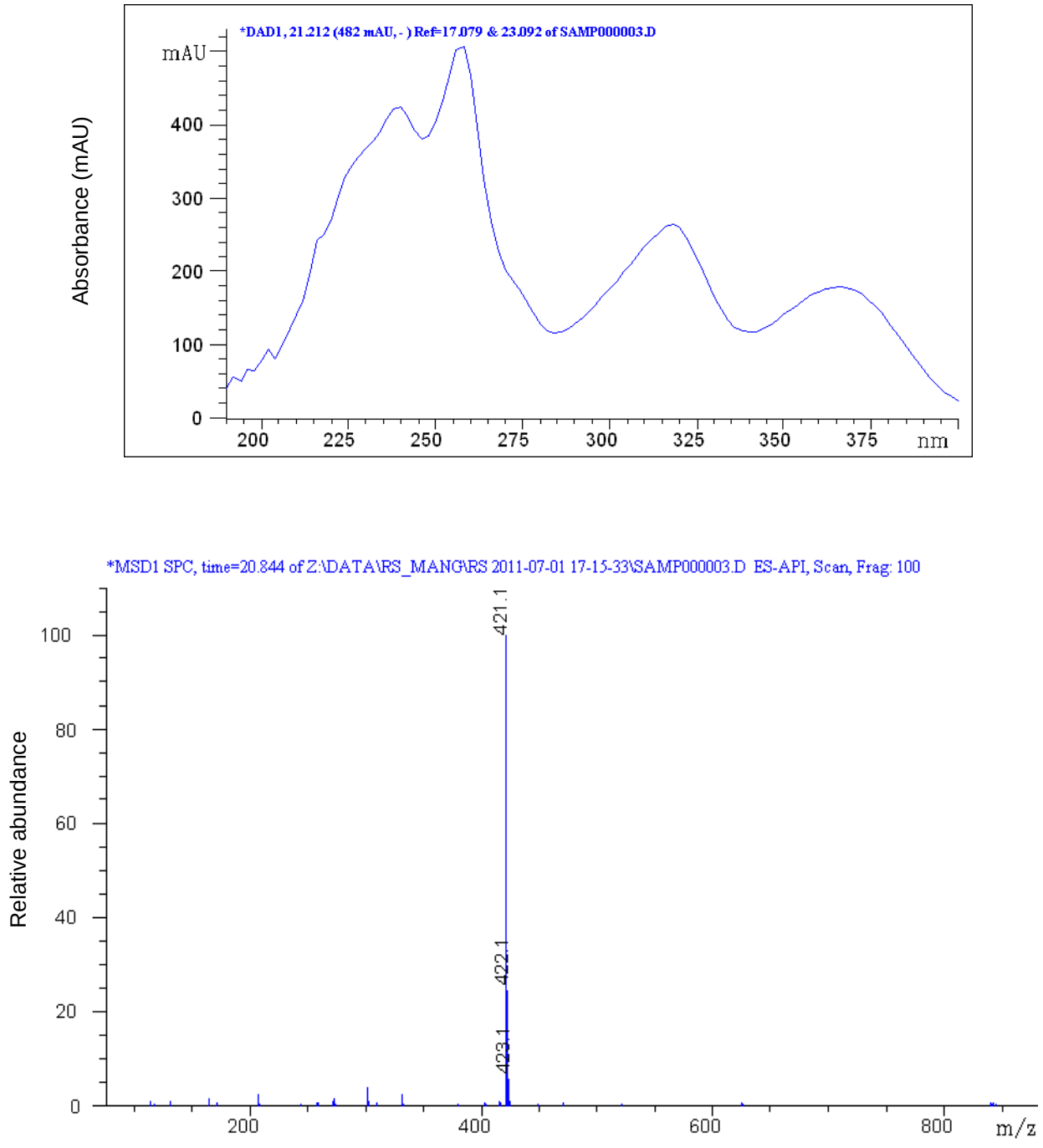

Figure 39 – MS and UV spectra for mangiferin detected in fraction 3.

Fraction 4

The HPLC analysis for fraction four revealed presence of norathyriol shown in the chromatogram (Figure 40) at 20.9 min retention time and by the UV spectra, The presence of norathyriol in fraction three was also confirmed by the MS spectra showing the molecular ion peak m/z at 259.1.

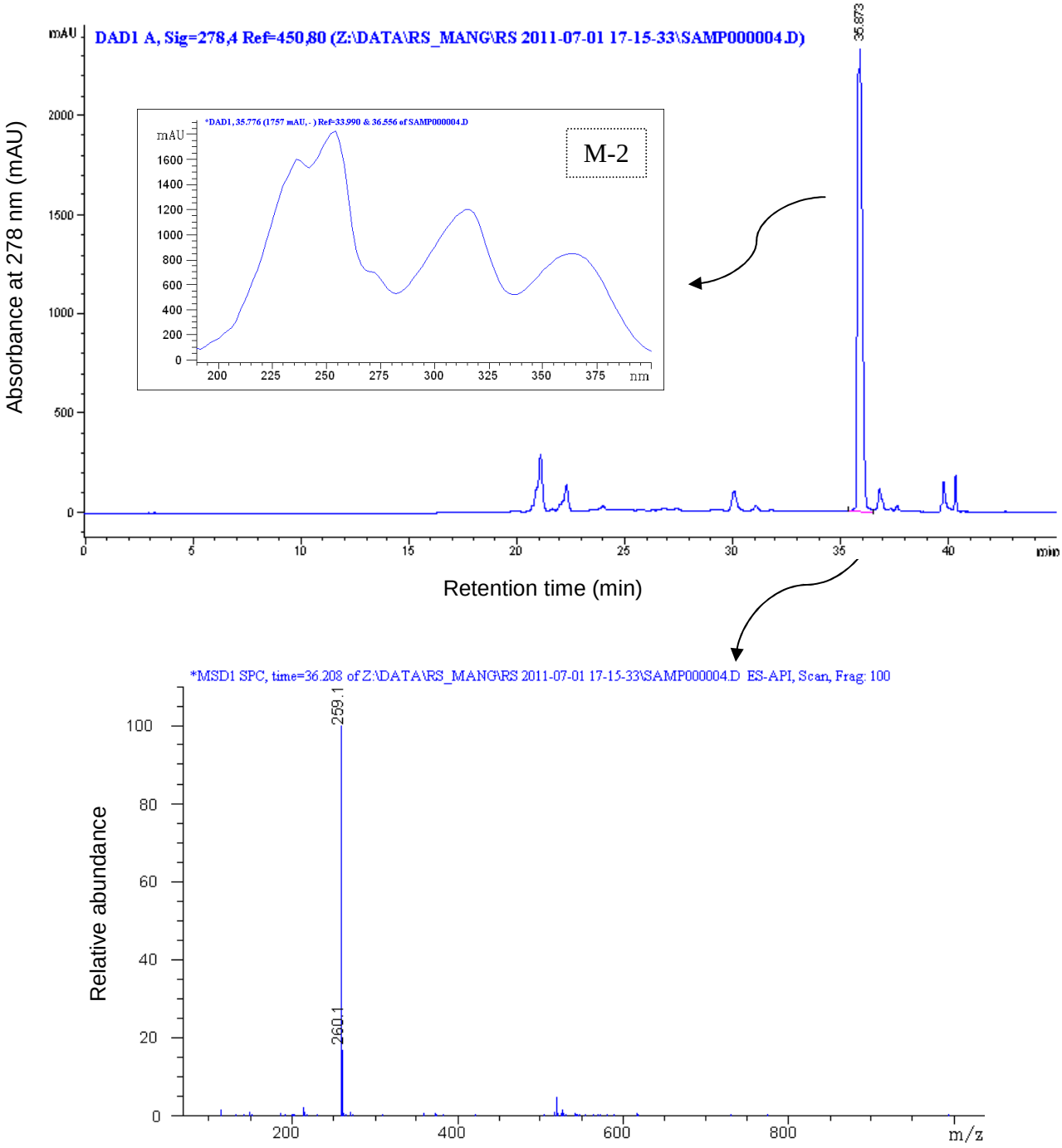

Figure 40 – HPCL chromatogram, UV and MS spectra M-2 detected in SPE fraction 4 from AFM V2-1.

Fraction 5

The HPLC analysis for fraction five revealed presence of M-2 and M-3 shown in the chromatogram (Figure 41) at 36.0 and 38.5 min retention time and by the UV spectra, The presence of metabolitesl in fraction five was also confirmed by the MS spectra showing the molecular ion peak m/z at 259.1 and 273.1 (Figure 42).

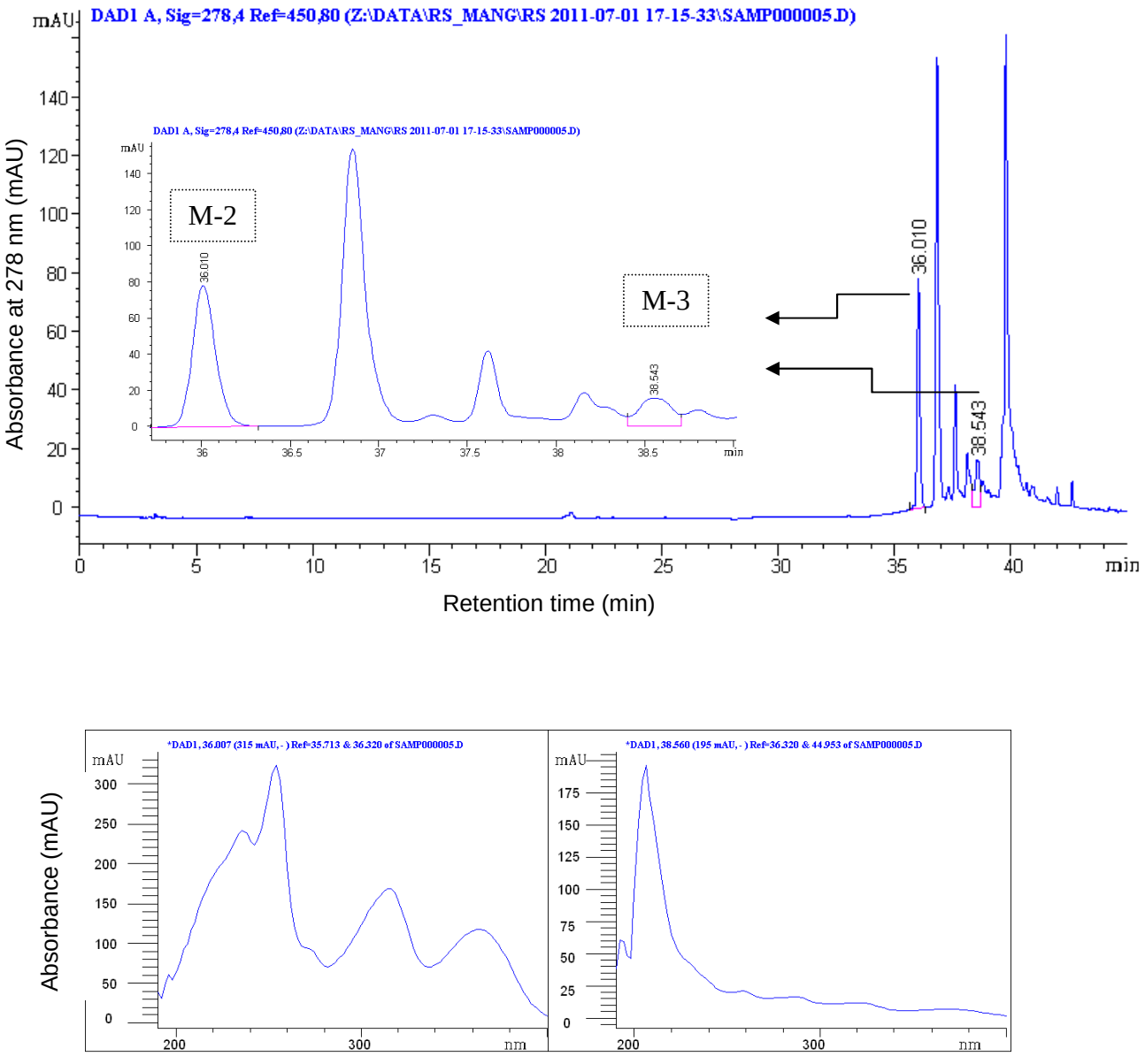

Figure 41 – HPCL chromatogram and UV spectra for M-2 and M-3 detected in SPE fraction 5 from AFM V2-1.

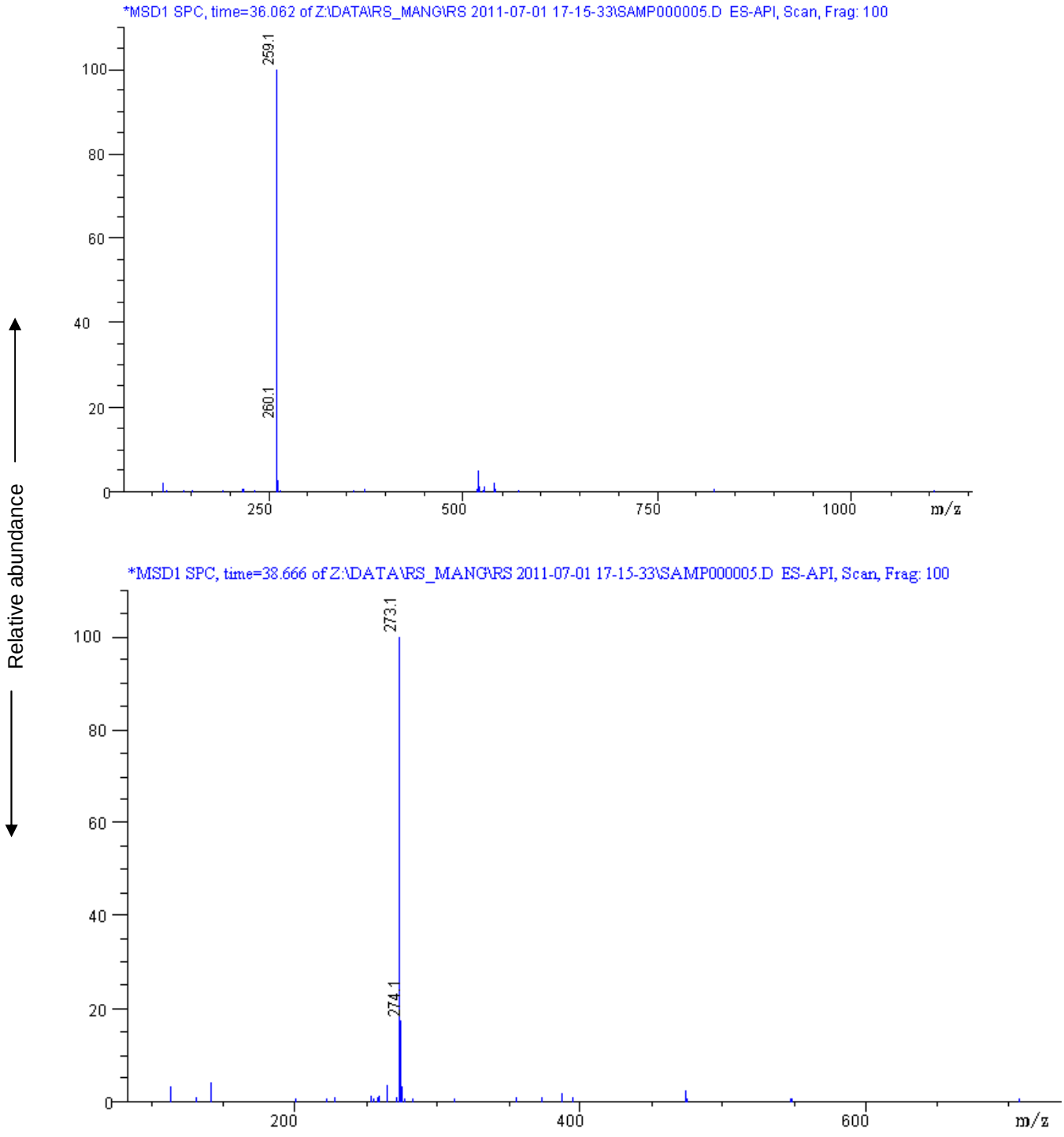

Figure 42 – MS spectra for M-2 and M-3 detected in SPE fraction 5 from AFM V2-1.

3.3.3. *Semipreparative HPLC – Purification of Mangiferin Metabolites from anaerobic Fermentation of Mangiferin with V2-1 SPE-F4 sample*

The V2-1 SPE-F4 sample was analyzed and fractionated by semipreparative HPLC (100µL injection) showing 6 main peaks (Figure 43). A number of six subfractions were collected for further analysis. The fraction at app. 16,4 min was found to be mangiferin and was not collected.

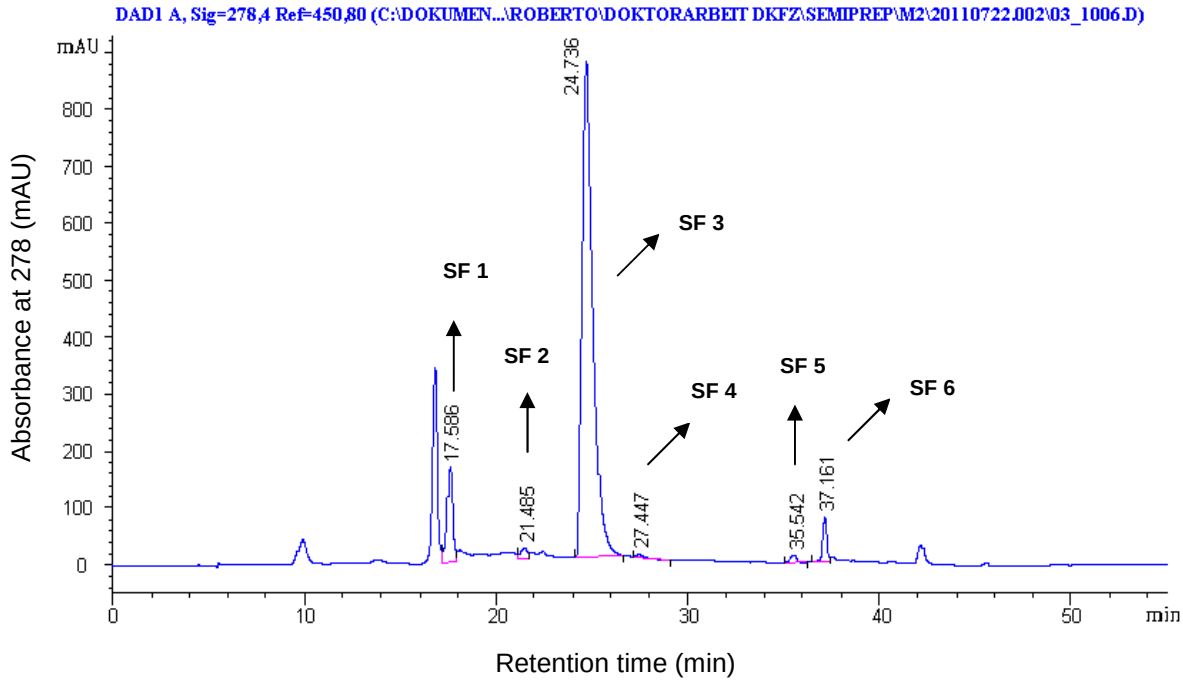

Figure 43 – Separation of mangiferin metabolites by semipreparative HPLC from V2-1 fermentation study.

The fractions isolated from V2-1 SPE-F4 sample were transfered to greentop bottles, weighted, dissolved in MetOH and 10 µL of each one was injected for control analysis using the HPLC-ESI-MS and the data are shown in Table 8 and Figures 44 to 49.

Table 8 - Fractions isolated from V2-1 SPE-F4 sample.

Subfractions(SF)	Mass (mg)	MS Detector Response (m/z ion peaks) in Analytical HPLC
1	2.01	421.1; 435.1; 259.1
2	0.97	421.1; 435.1
3	4.51	259.1
4	1.22	259.1
5	0.33	NR
6	0.2	NR

NR – Not Reported

The HPLC analysis of the subfraction is shown in Figures 44 to 49. The subfractions 1 and 2 were not observed to be pure but a mixture of compounds due probably to intermolecular interations. In subfractions 3 and 4, norathyriol was obtained in good purity.

3.3.4. HPLC-ESI-MS Analysis of semipreparative HPLC subfractions from V2-1

Subfraction 1

In this subfraction, three compounds were detected: Ma, mainly M-1 and some M-2 (m/z = 421.1, 435.1, 259.1) as can be observed in Figures 44 and 45.

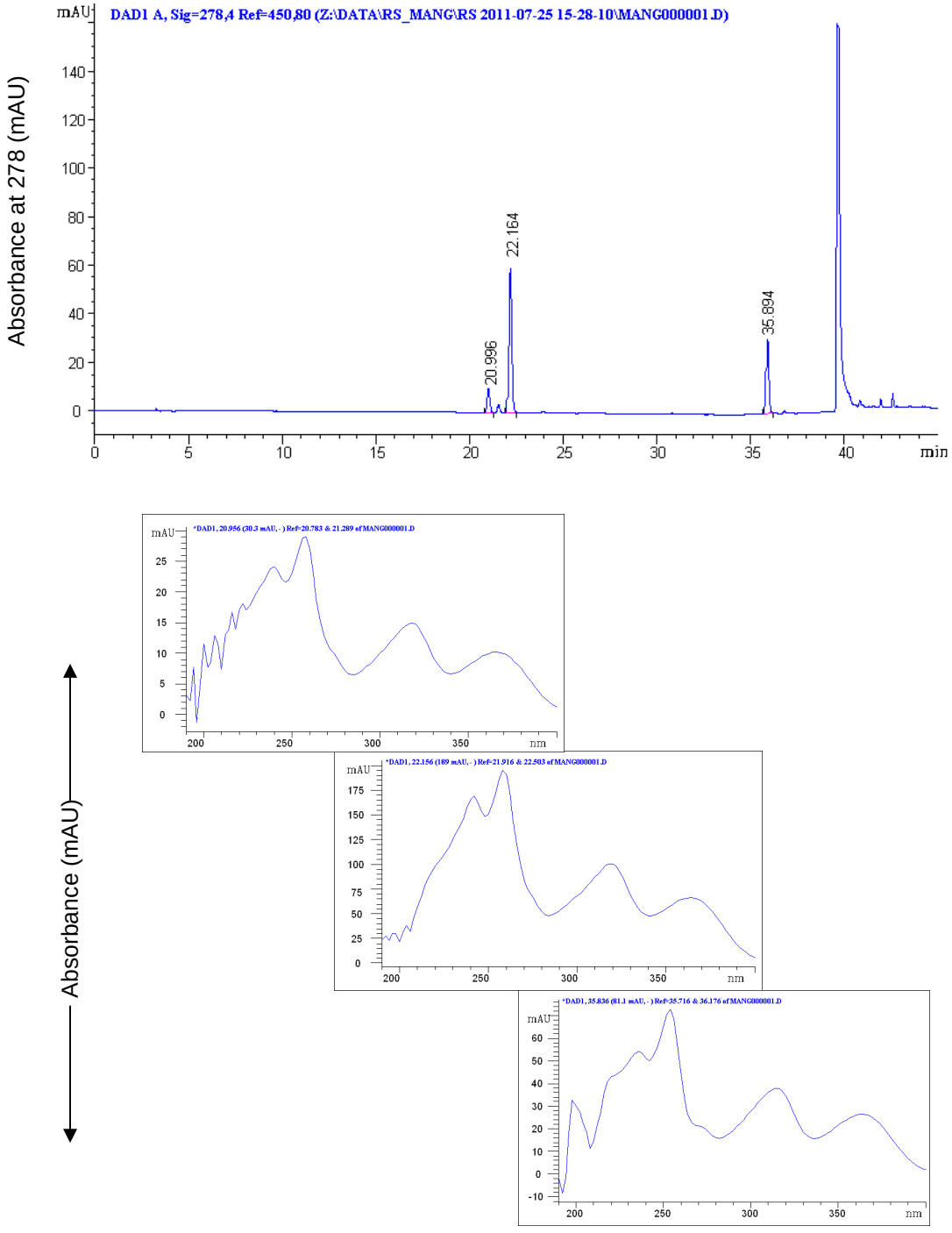

Figure 44 – HPCL chromatogram, and UV spectra M-2 detected in SPE fraction 4 from AFM V2-1.

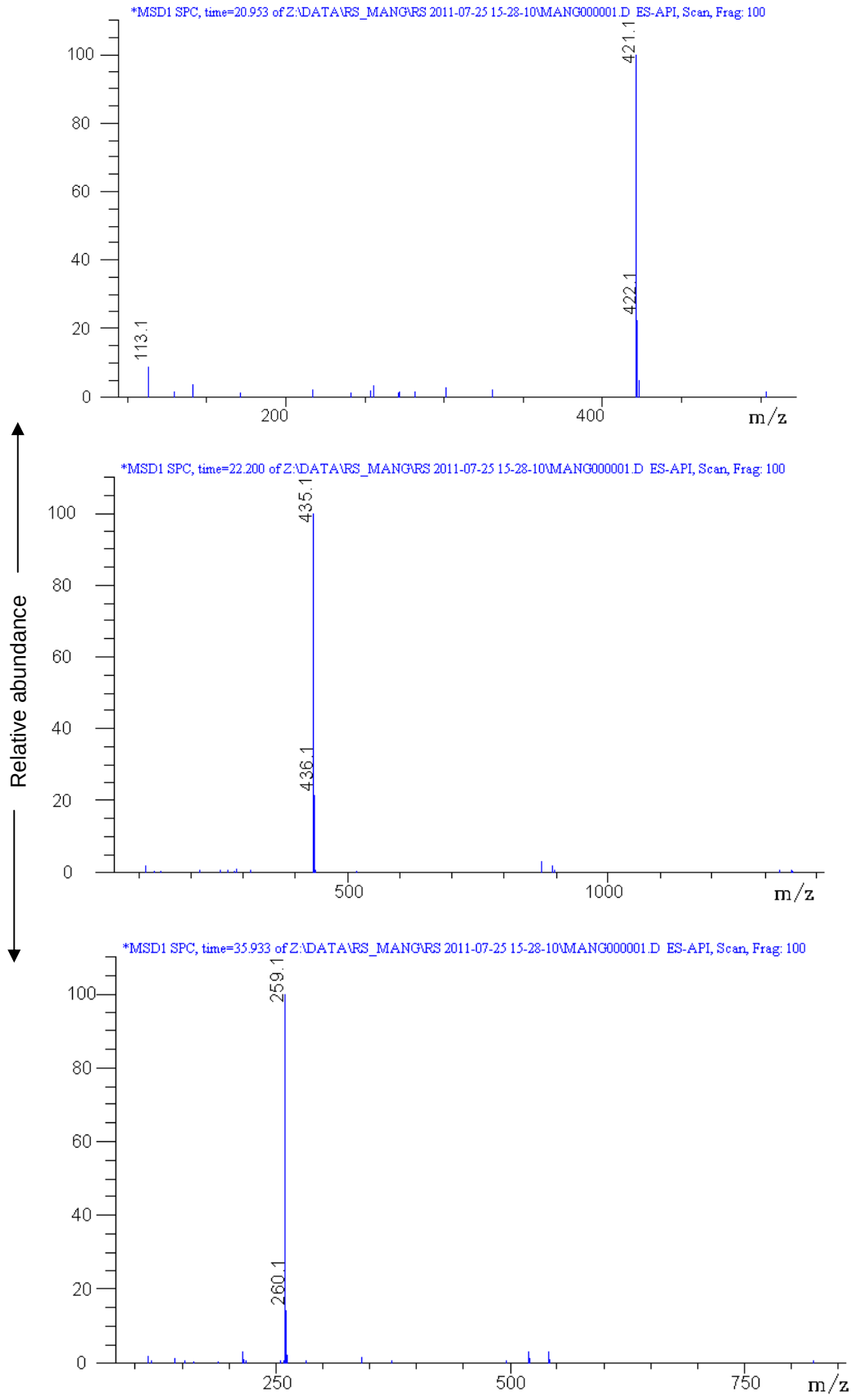

Figure 45 – MS spectra for compounds detected in subfraction 1.

Subfraction 2

In subfraction 2, mainly M-1 and some little amounts of M-3 (m/z = 421.1, 435.1) were detected as can be observed in Figures 46 and 47.

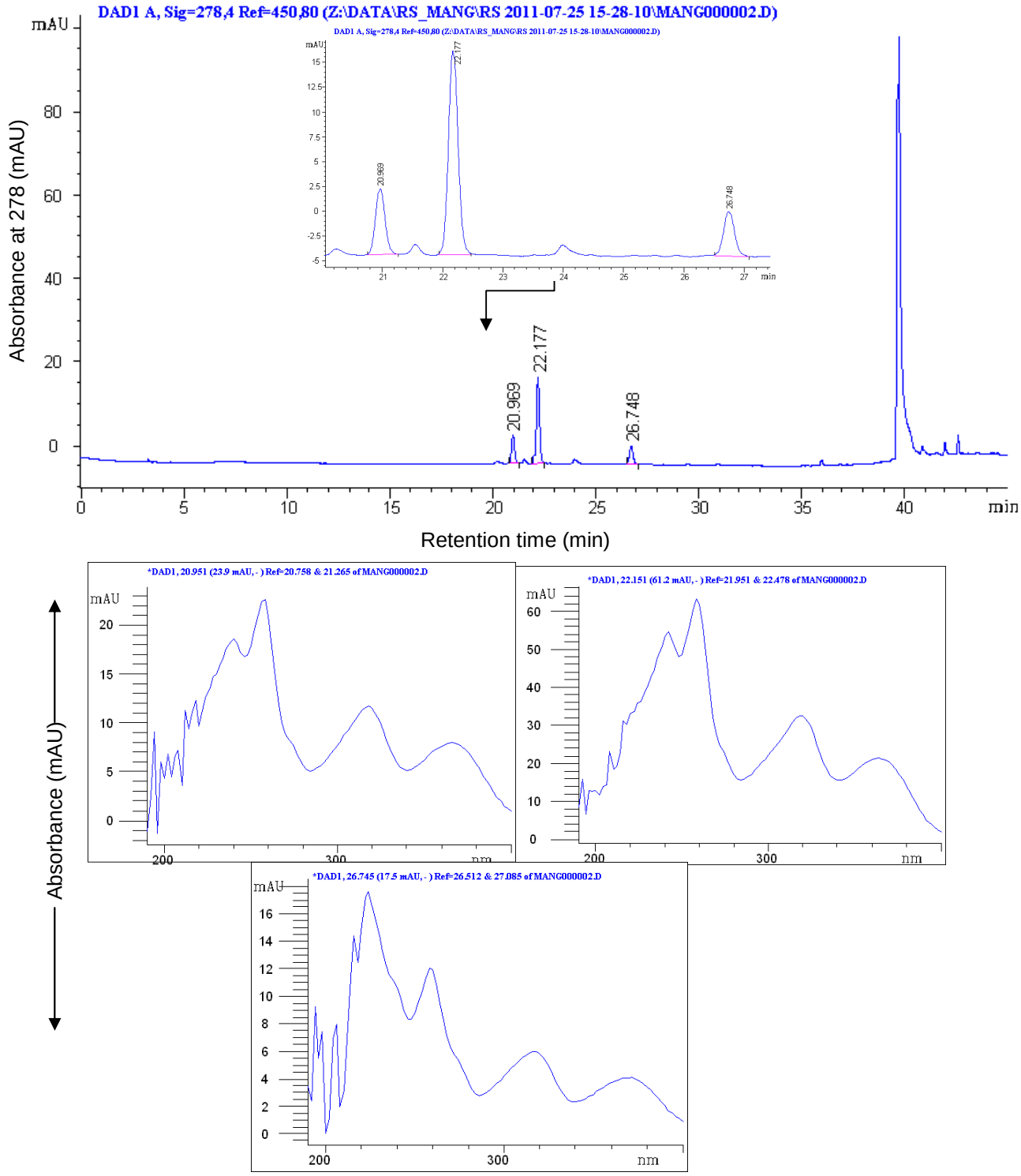

Figure 46 – HPCL chromatogram and UV spectra for compounds detected in subfraction 2.

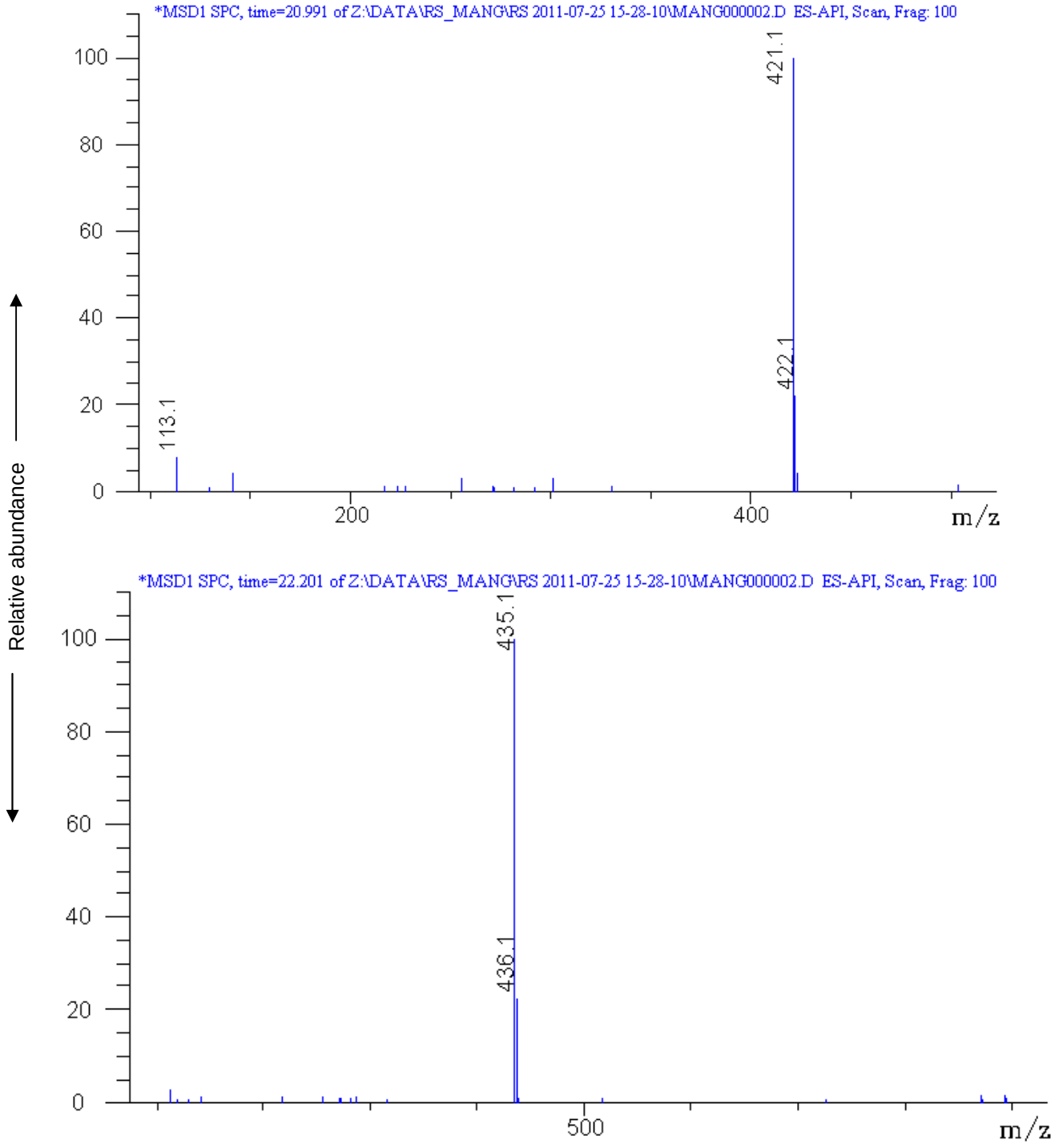

Figure 47 – MS spectra for compounds detected in subfraction 2.

Subraction 3

In subfraction, M-2 (m/z = 259.1) was detected in high amount as can be observed in Figures 48 and 49.

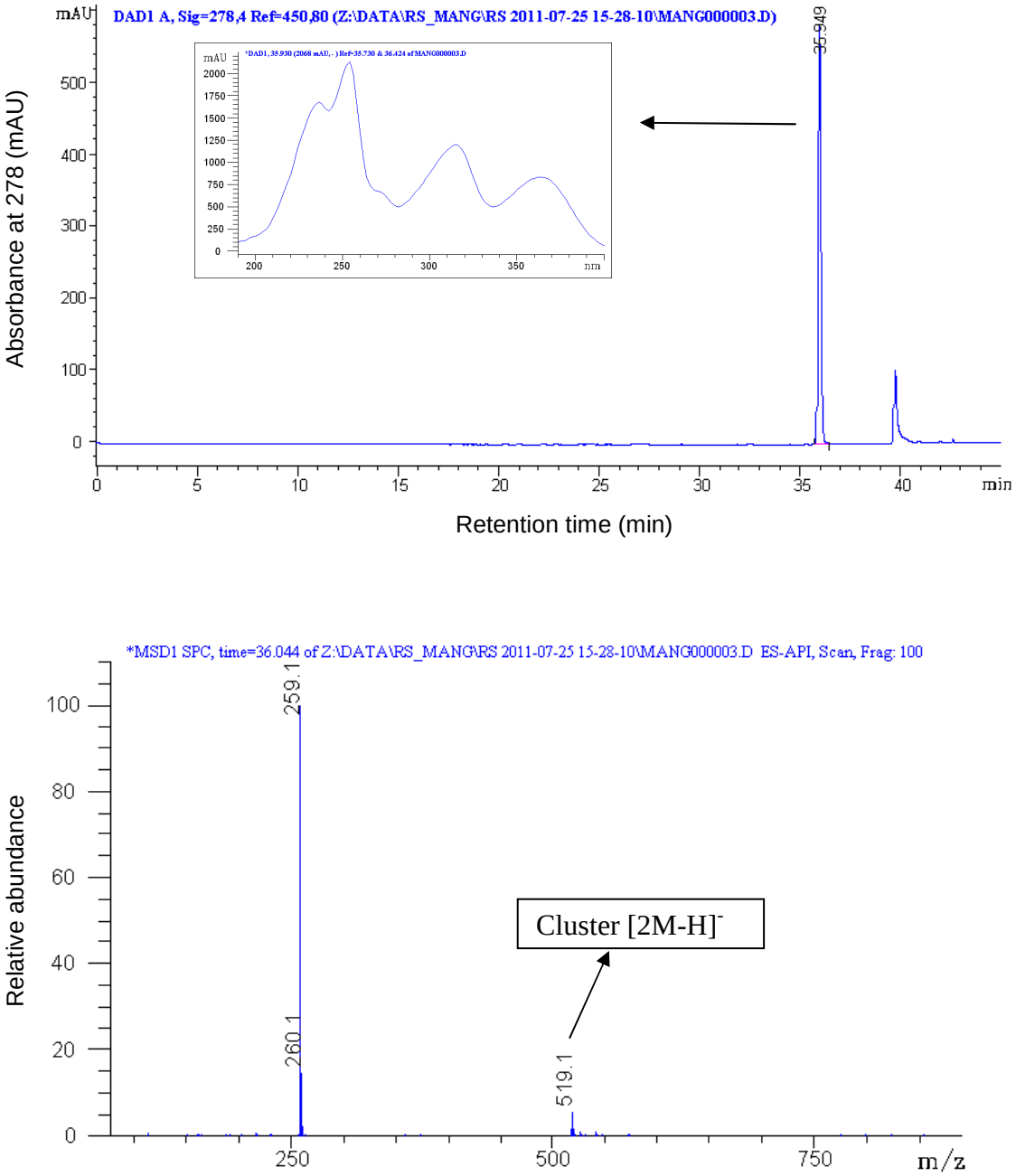

Figure 48 – HPCL chromatogram, UV, and MS spectra for compounds detected in subfraction 3.

Subfraction 4

As for subfraction 3, in subfraction 4, M-2 (m/z = 259.1) was detected in high amount as can be observed in Figure 54.

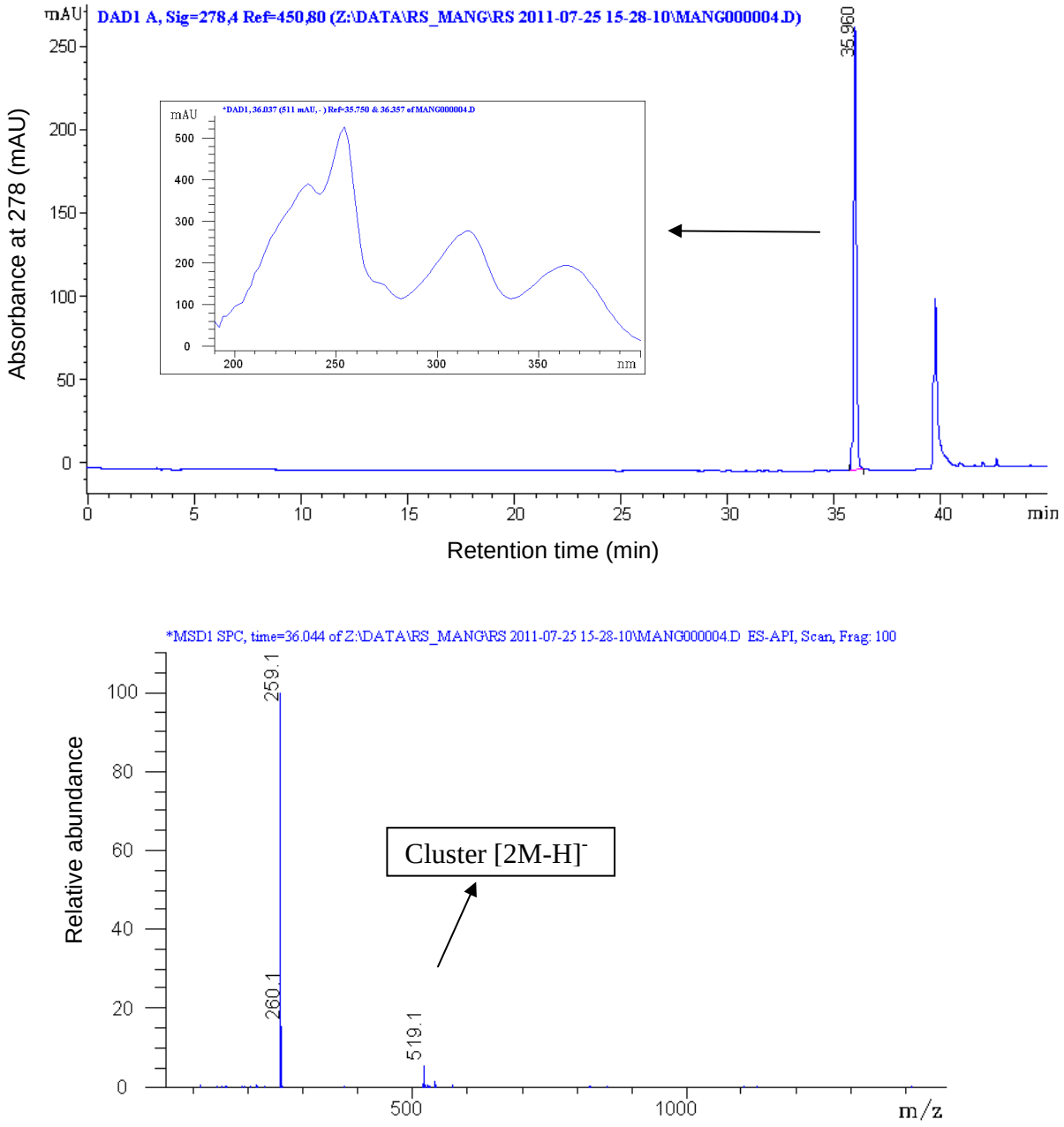

Figure 49 – HPCL chromatogram and UV, MS spectra for compounds detected in subfraction 4.

3.3.5. *Semipreparative HPLC – Purification of Mangiferin Metabolites from V2-1*

The V2-1 SPE-F5 sample was also analyzed and fractionated by semipreparative HPLC showing 7 main peaks (Figure 50). A number of seven subfractions were collected for further analysis (Table 9).

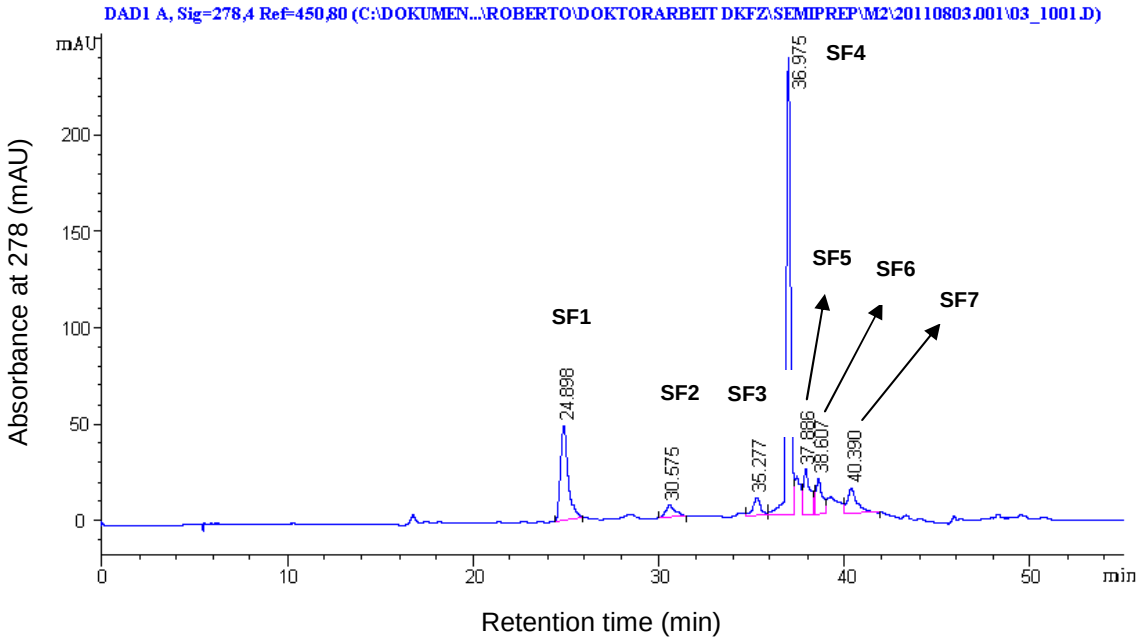

Figure 50 – Separation of compounds by semipreparative HPLC from V2-1 SPE-5.

The two first fractions were found to be M-2 and M-3 as can be seen in the UV and MS spectra (Figures 51). No metabolite was found in 6th or 7th ones.

Table 9 - Fractions isolated from V2-1 SPE-F5 sample.

Fractions	Mass (mg)	MS Detector Response (m/z ion peaks)
1	0.32	259.1
2	0.37	259.0; 273.1;
3	0.25	NR
4	0.32	NR
5	0.12	NR
6	0.21	-
7	0.05	-

3.3.6. HPLC-ESI-MS analysis of semipreperative HPLC subfractions from V2-1SPE-F5

Subfraction 1

In the first one, M-2 (m/z = 259.1) was detected in a good amount as can be seen in Figure 51.

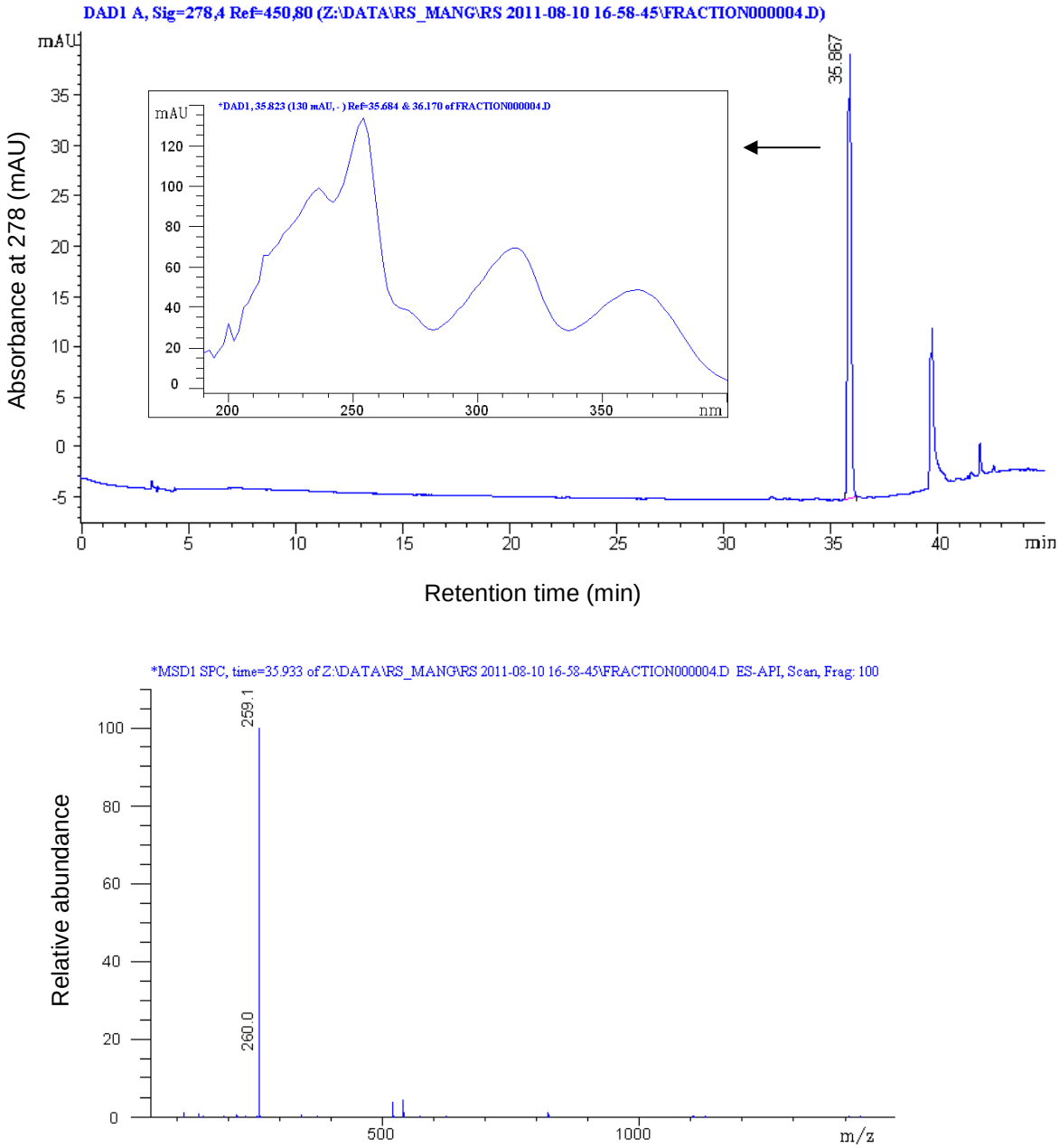

Figure 51 – HPCL chromatogram, UV and MS spectra M-2 detected in SPE fraction 4 from AFM V2-1.

Subfraction 2

In the second one, M-2 and M-3 (m/z = 259.1, 273.1) were detected in a good amount as can be seen in Figures 52 and 53.

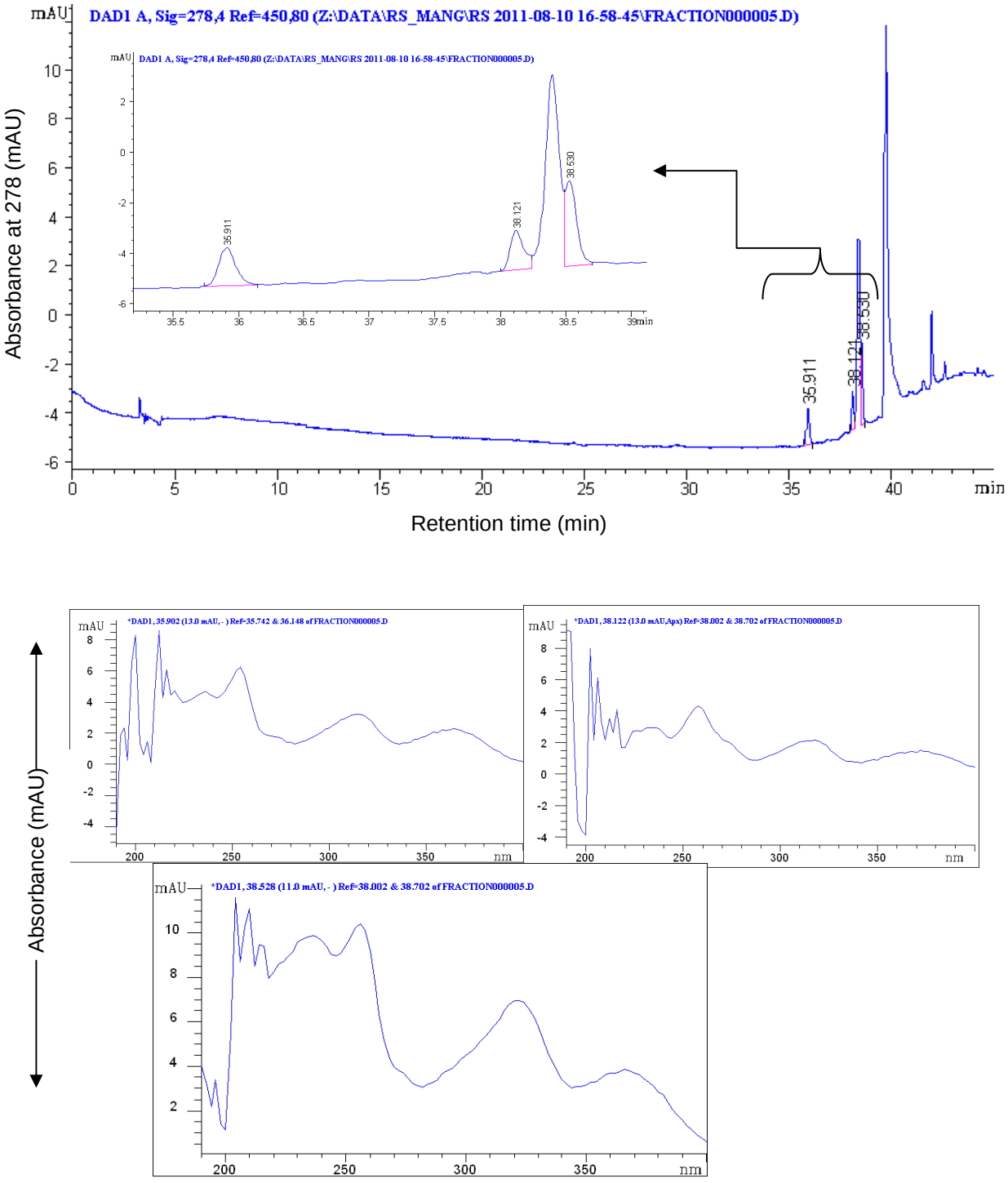

Figure 52 – HPCL chromatogram and UV spectra for M-2 and M-3 detected in subfraction 2 from V2-1 SPE-F5.

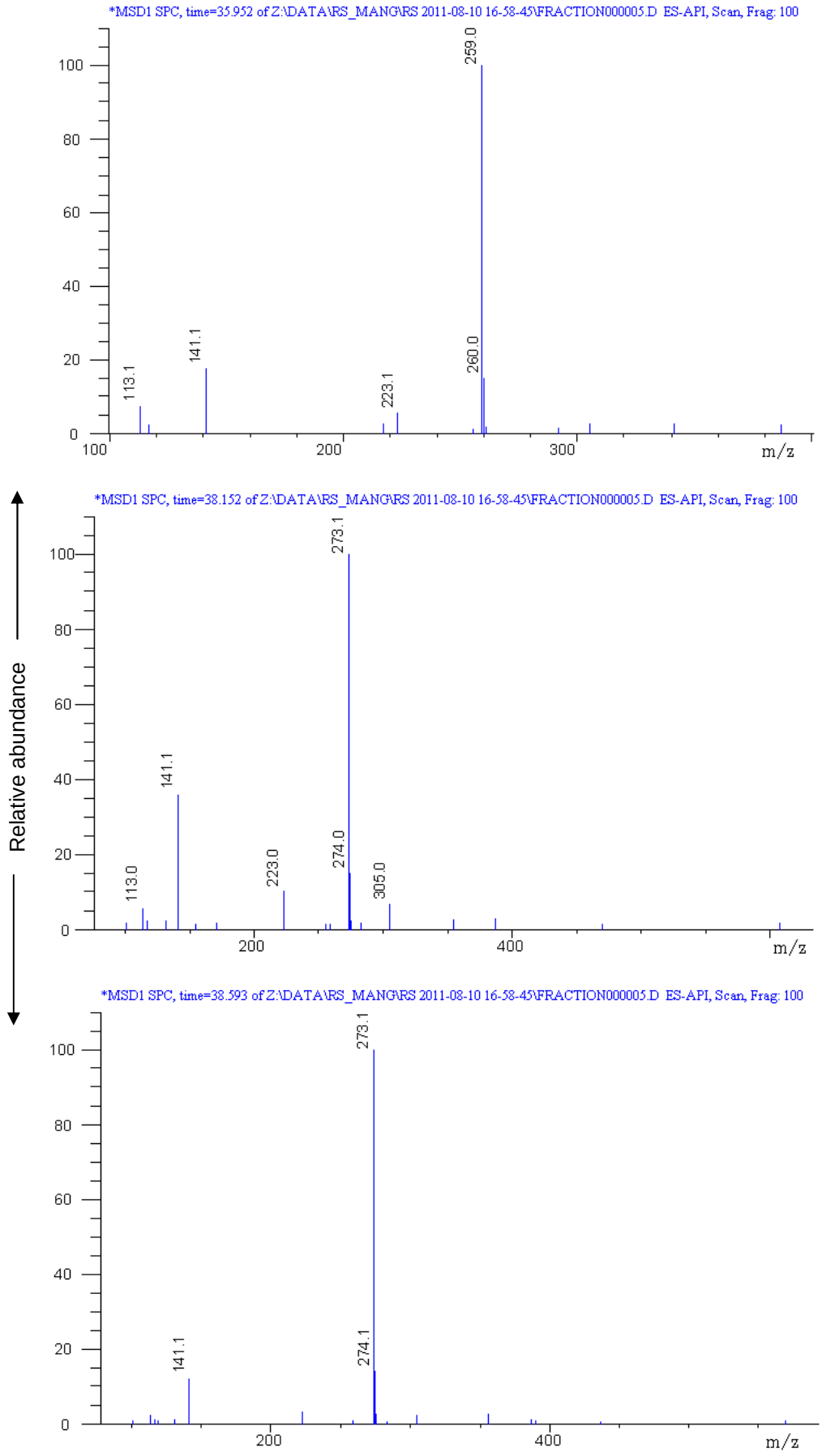

Figure 53 – MS spectra for compounds detected in subfraction 2 from V2-1 SPE-F5.

3.4. Anaerobic Fermentation Study – Volunteer 3 (V3-1) Sample

An anaerobic fermentation of mangiferin was set up with volunteer 3 sample. The method used was the same described for the other trials. For this experiment, two bottles with 100 mL BHI were set up at once and one of those was screened every 24 hour reaction. No reaction was observe in this fermentation study with volunteer 3 sample (Figure 54)

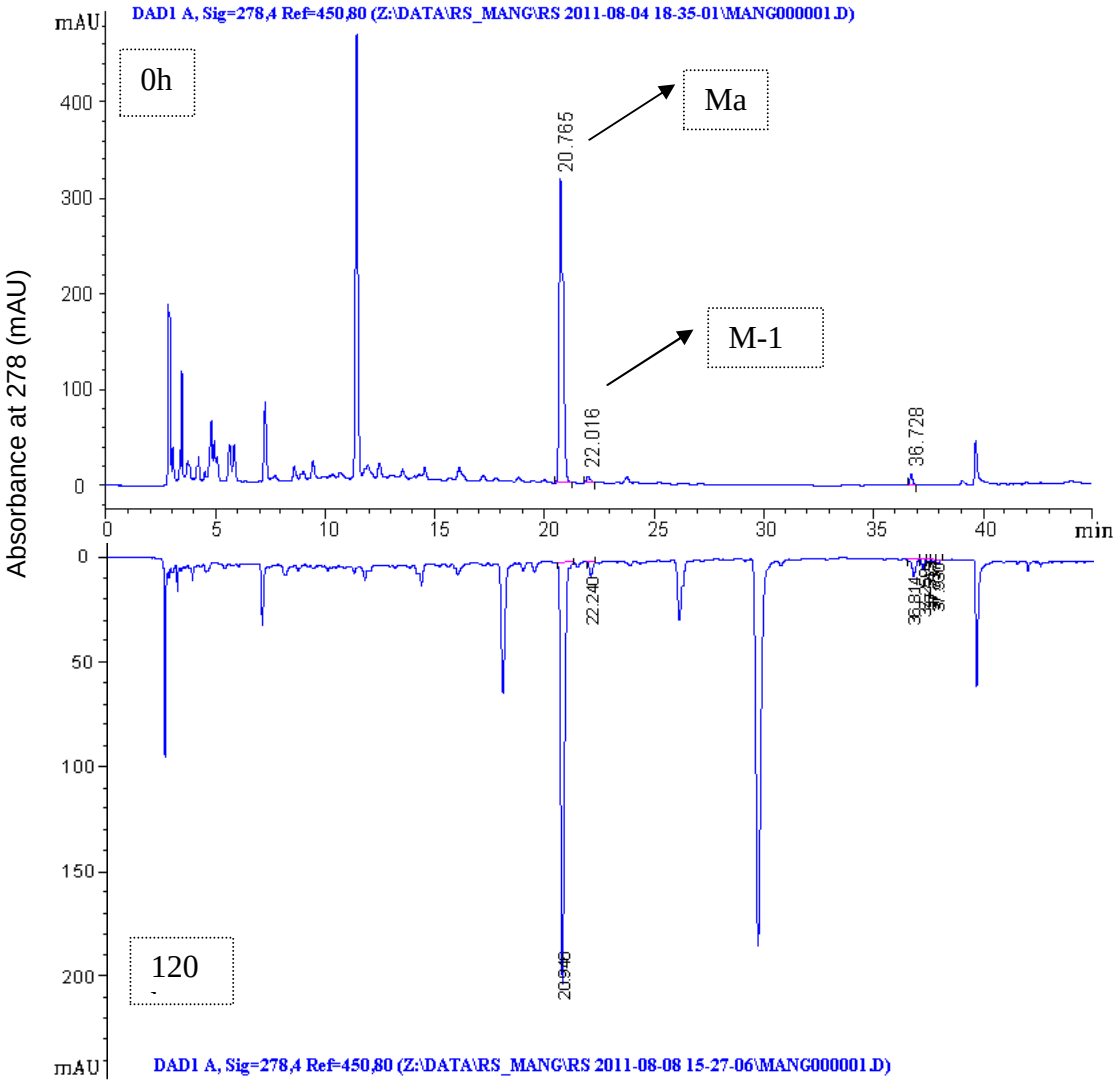

Figure 54 – HPCL chromatogram for 0 h and 120 h of mangiferin anaerobic fermentation.

We can observe that after 120, no production of metabolites was found for this volunteer sample. Probably due to lack of that specific bacteria species or bacteria enzymes.

3.5. Blanks for Anaerobic Fermentation of Mangiferin

3.5.1. Anaerobic Fermentation without Bacteria

After 5 days (120 h) of a blank anaerobic fermentation of mangiferin, a 20 µL from the broth was injected in the HPLC-MS to check for a background analysis. This blank experiment means no presence of fecal samples in the broth medium (Figure 55).

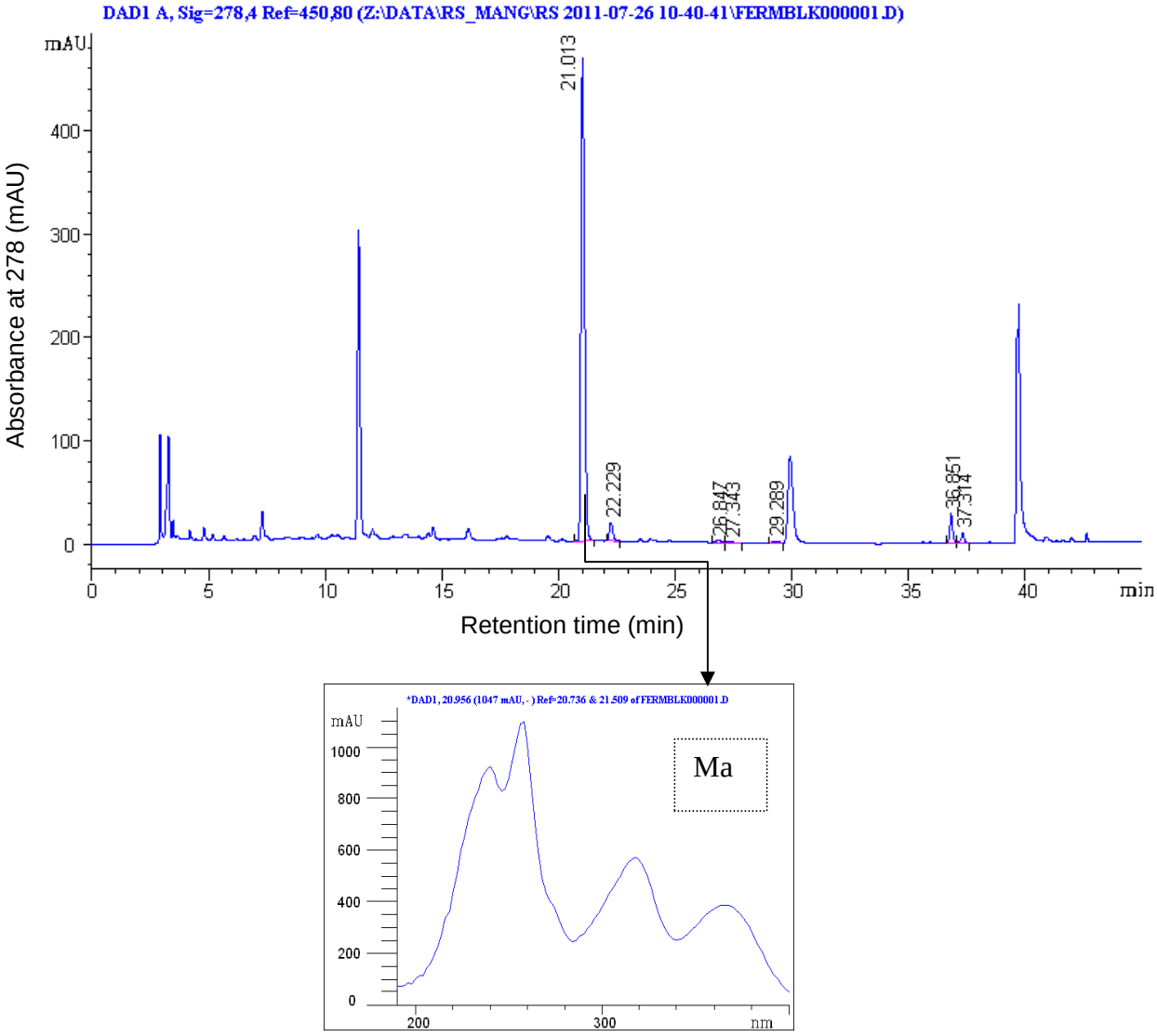

Figure 55 – HPCL chromatogram for 0h of mangiferin blank fermentation without gut bacteria.

As well as we had expected, unreacted mangiferin was found in high amount. Probably because of some contamination from another earlier fermentation in the anaerobic container, some little amount of metabolites were detected in the blank.

3.5.2. *Anaerobic Fermentation without mangiferin sample*

An anaerobic blank fermentation was set up without any presence of mangiferin to look into the reaction background. The main peaks are related to fermentation of the broth itself (Figure 56).

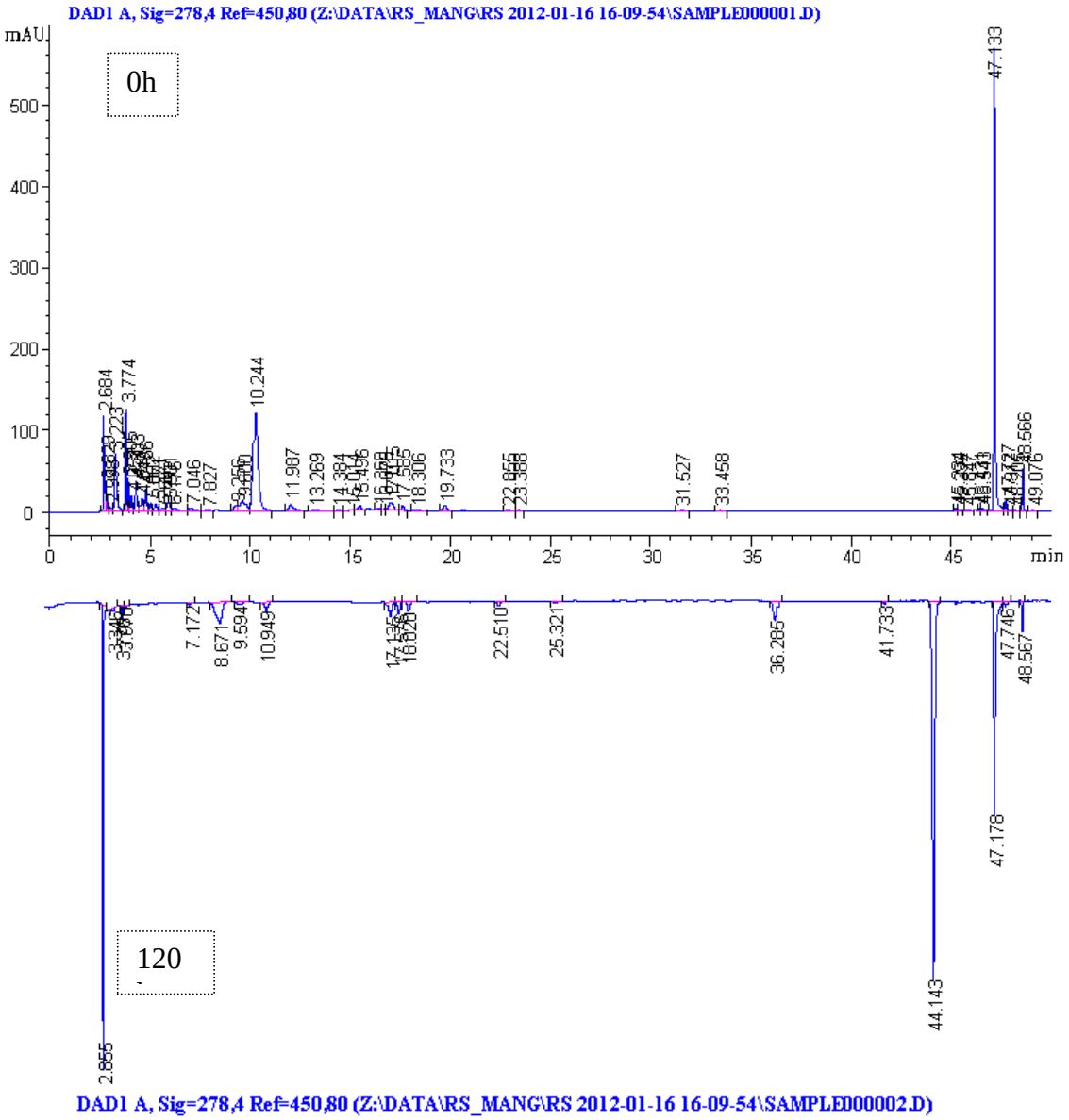

Figure 56 – HPCL chromatogram for 0 and 120h of blank anaerobic fermentation without mangiferin.

3.6. Kinects for the gut simulation reactions of mangiferin

The Figure 57 shows the reaction progress for mangiferin anaerobic fermentation for volunteers 1 and 2. We can see clearly that for V1, the reaction reached up to almost 100 % after 48h. For V2, it showed to be different and the reaction did not reached up to 50 % even after 120 h.

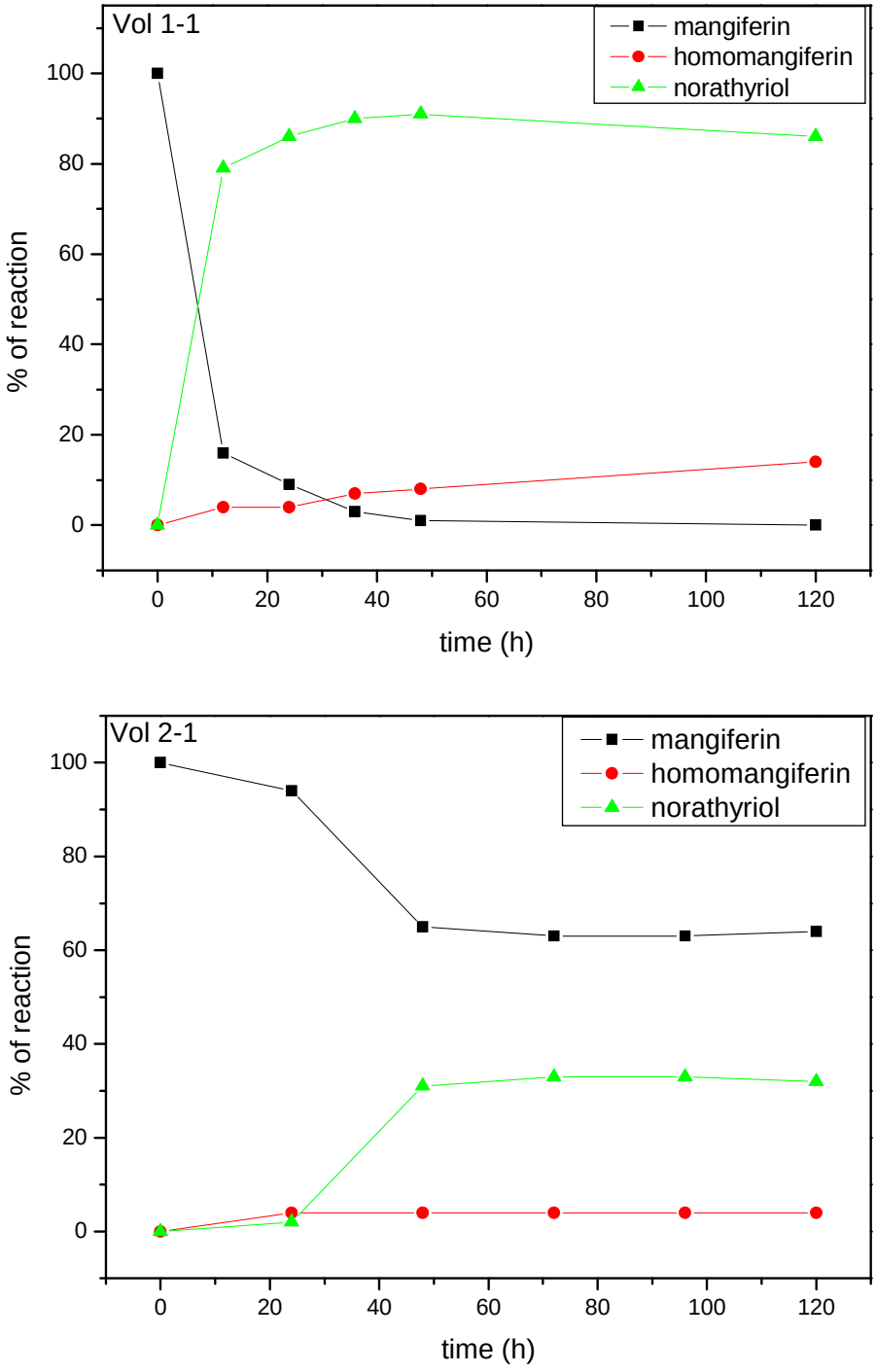

Figure 57 – Reaction progress of mangiferin anaerobic fermentation with volunteer 1 sample.

3.7. Analysis of mangiferin and metabolites by Nano-ESI-MS^{2,3}

From the spectra for V2 F4 SP1 we can observe molecular ion peaks for norathyriol (259.1), mangiferin (421.2) and homomangiferin (435.2) shown in Figure 58 (Appendix 3-6). We can also observe the nano-ESI-MS-MS fragmentation spectrum of the molecular ion m/z peak 259.1 for norathyriol which shows the following íons in degradation: 215.1, 187.1, 159.1, 151.0 (Figure 59) and the molecular ion m/z peak 421.1 for Ma which shows the following íons in degradation: 331.1, 301.1, 259.1 in negative ion mode (Figure 60). The spectrum for homomangiferin is shown in positive ion mode with the molecular ion peak 437.1 and the following main degradation peaks: 286.9, 217.0, 312.9, 340.8 (Figure 61).

3.8. Analysis of mangiferin and metabolites by ^{1}H and ^{13}C NMR

The Figures 62 shows the numbered structures for norathyriol and mangiferin which were plotted as well as correlated with the signals in order to confirm the structure determination. We can observe in Figures 63 to 66 (Appendix 7-10) the ^{1}H and ^{13}C NMR spectra with the chemical shifts signals (Tables 10 and 11) for the numbered structures of the compounds.

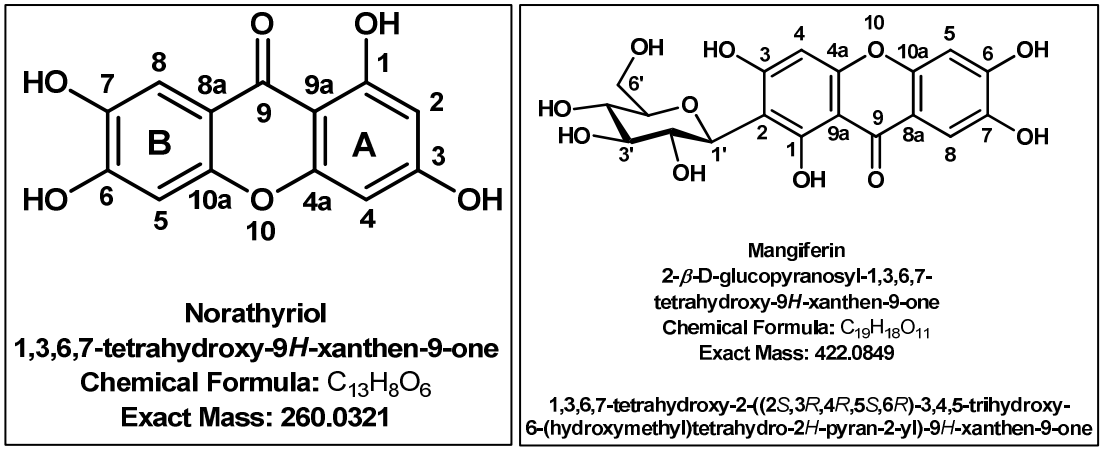

Figure 62 – Numbered structures for norathyriol, mangiferin and homomangiferin.

The chemical shift data are in agreement with that observed by Barreto *et al.* (2008) and Gómez-Zaleta *et al.* (2006) for the xanthone skeleton type of norathyriol, mangiferin and homomangiferin. The ^{13}C NMR spectra for norathyriol and mangiferin (600 MHz) showed thirteen signals referring to an aglycone portion that are consistent with those presented for a skeleton xantonic type (Figure 62), which has a carbonyl group between the two aromatic rings, with chemical shift consistent to those observed for the chelated carbonyl at approx. 180.1 (Miura et al., 1978). For mangiferin, the spectrum shows the signals even in the region of six carbons oxygen metínicos between 62 and 74 ppm, referring to a glycosidic moiety.

Table 10 - ^{1}H and ^{13}C NMR data for norathyiol; chemical shifts in ppm relative to TMS (multiplicity, coupling J in Hz).

in DMSO-d6 /CD3OD (1 : 2.2 mol ratio), 303K						
pos.	**^{13}C shift**	**^{13}C Mult.**	**^{1}H shift**	**^{1}H Mult.**	**J(H,H)**	**^{1}H linewidth**
	ppm		ppm		Hz	Hz
1	163.61	Cq				
2	98.37	CH	6.165	d	1.9	2.8
3	165.54	Cq				
4	94.34	CH	6.321	d, br	1.9	3.8
4a	158.60	Cq				
5	103.28	CH	6.852	s, vbr		5.7
6	154.88	Cq				
7	144.42	Cq				
8	108.79	CH	7.426	s, br		2.7
8a	113.05	Cq				
9	180.12	C=O				
9a	102.69	Cq				
10a	152.33	Cq				
CD3OD	48.45	CD3	3.240	CHD2		
DMSO-d6	39.54	CD3	2.581	CHD2		
TMS	0.00		0.000			

Table 11 - ^{1}H and ^{13}C NMR data for mangiferin; chemical shifts in ppm relative to TMS (multiplicity, coupling J in Hz).

in DMSO-d6 /CD3OD (1 : 0.63 mol ratio), 303K						
pos.	**^{13}C shift**	**^{13}C Mult.**	**^{1}H shift**	**^{1}H Mult.**	**J(H,H)**	**^{1}H linewidth**
	ppm		ppm		Hz	Hz
1	162.36	Cq				
2	107.85	Cq				
3	164.42	Cq				
4	94.26	CH	6.392	s		2
4a	157.51	Cq				
5	103.19	CH	6.868	s		2
6	154.56	Cq				
7	144.26	Cq				
8	108.81	CH	7.435	s		2
8a	112.95	Cq				
9	180.18	C=O				
9a	102.35	Cq				
10a	151.96	Cq				
1'	74.25	CH	4.748	d	9.8 (H2')	
2'	71.48	CH	4.077	dd	8.2 (H3')	
3'	79.53	CH	3.342	dd	9.2 (H4')	
4'	71.19	CH	3.308	m	NR	
5'	82.07	CH	3.301	m	NR	
6'a	62.13	CH2	3.576	dd	; -11.9 (H6'b), 5.0 (H5')	
6'b			3.770	dd	1.2 (H5')	
CD3OD	48.29	CD3	3.216	CHD2		
DMSO-d6	39.53	CD3	2.565	CHD2		
TMS	0.00		0.000			

NR = not resolved for multiplet analysis

The Figures 67 shows the numbered structures for homomangiferin (3-O-methyl mangiferin) plotted as well as correlated with the signals in order to confirm the structure determination. We can observe in Figures 68 and 69 (Appendix 11 and 12) the ^{1}H and ^{13}C NMR spectra with the chemical shifts signals (Table 12) for the numbered structures of the compounds.

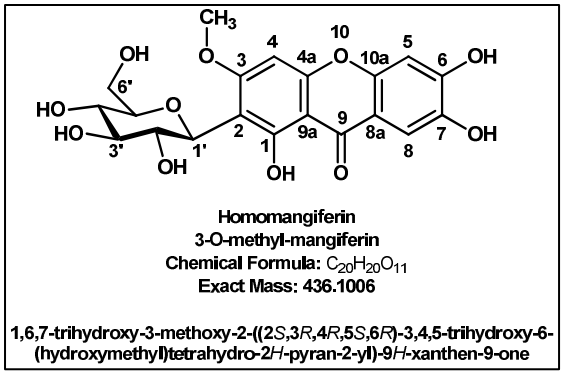

Figure 67 – Numbered structures for homomangiferin.

Homomangiferin exhibits slow hindered rotation of glucose and – OMe groups: two rotamers A and B are resolved with approximately equal populations. The Figure 70 shows the rotamers.

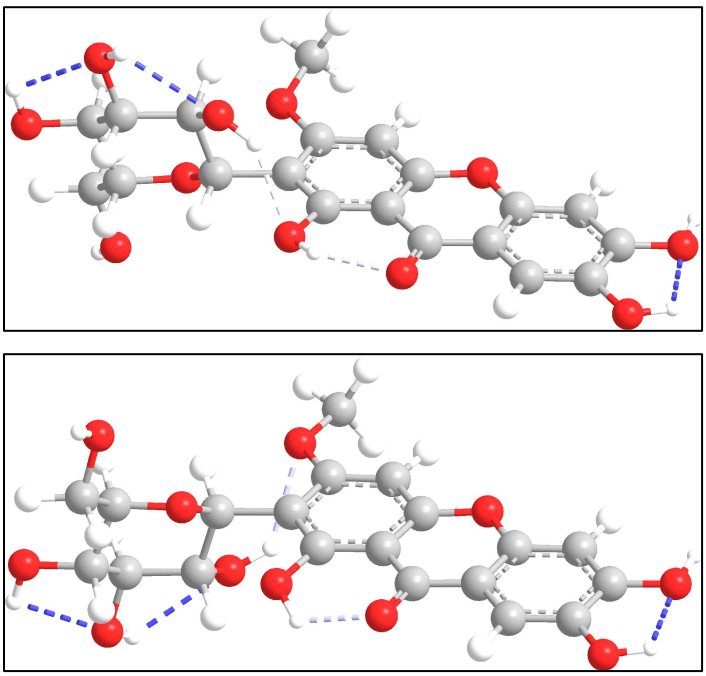

Figure 70 – Rotamers for homomangiferin structure.

Table 12 - ^{1}H and ^{13}C NMR data for homomangiferin; chemical shifts in ppm relative to TMS (multiplicity, coupling J in Hz).

in DMSO-d6 /CD3OD (1 : 0.63 mol ratio), 303K

Rotamer A

pos.	**13C shift**	**13C Mult.**	**1H shift**	**1H Mult.**	**J(H,H)**
	ppm		Ppm		Hz
1	161.120	Cq			
2	108.676	Cq			
3	165.886	Cq			
4	90.975	CH	6.610	s	
4a	157.602	Cq			
5	102.734	CH	6.853	s	
6	155.807	Cq			
7	144.619	Cq			
8	107.892	CH	7.411	s	
8a	112.013	Cq			
9	179.617	C=O			
9a	102.498	Cq			
10a	152.054	Cq			
3-OMe	56.295	CH3	3.882	s	
1'	73.270	CH	4.710	d	9.9 (H2')
2'	70.913	CH	4.065	dd	8.1 (H3')
3'	79.519	CH	3.275	m	NR
4'	71.397	CH	3.159	m	NR
5'	82.095	CH	3.235	m	NR
6'a	62.311	CH2	3.446	dd	NR
6'b			3.745	dd	NR
CD3OD	48.03	CD3		CHD2	
DMSO-d6	39.52	CD3		CHD2	
TMS	0.00				

Rotamer B

pos.	13C shift	13C Mult.	1H shift	1H Mult.	J(H,H)
	ppm		ppm		Hz
1	161.782	Cq			
2	108.676	Cq			
3	164.783	Cq			
4	90.170	CH	6.616	s	
4a	157.514	Cq			
5	102.707	CH	6.853	s, br	
6	155.807	Cq			
7	144.619	Cq			
8	107.892	CH	7.406	s	
8a	112.013	Cq			
9	179.927	C=O			
9a	102.979	Cq			
10a	151.989	Cq			
3-OMe	56.578	CH3	3.907	s	
1'	73.544	CH	4.655	d	9.8 (H2')
2'	70.276	CH	4.283	dd	8.5 (H3')
3'	79.560	CH	3.252	m	NR
4'	71.312	CH	3.200	m	NR
5'	81.981	CH	3.216	m	NR
6'a	62.288	CH2	3.467	dd	NR
6'b			3.743	dd	NR

4. Conclusions

Intestinal simulations studies with mangiferin showed that mangiferin will be most metabolized to norathyriol in different extent and rate dependently to the human gut bacterial population, even though some little amount of other metabolites were also detected by HPLC-ESI-MS and characterized by Nano-ESI-MS and NMR spectroscopy.

Hung *et al.,* (2011) studied the metabolism of mangiferin by human intestinal bacteria in vitro and observed that content of mangiferin metabolite, norathyriol, reached the maximum at 12h incubation. That is in agreement with V1 human sample which metabolized most of mangiferin after 12h of mangiferin anaerobic fermentation. Sanugul *et al.,* (2005) identified the bacteria, *Bacteroides* species MANG, responsible for the conversion of mangiferin to its aglycone, norathyriol. As *Bacteroides* species (Phylum *Bacteroidetes*) are found in the colon (Figure 71), we can conclude that this is the site of conversion of mangiferin and where norathyriol will be most avaiable.

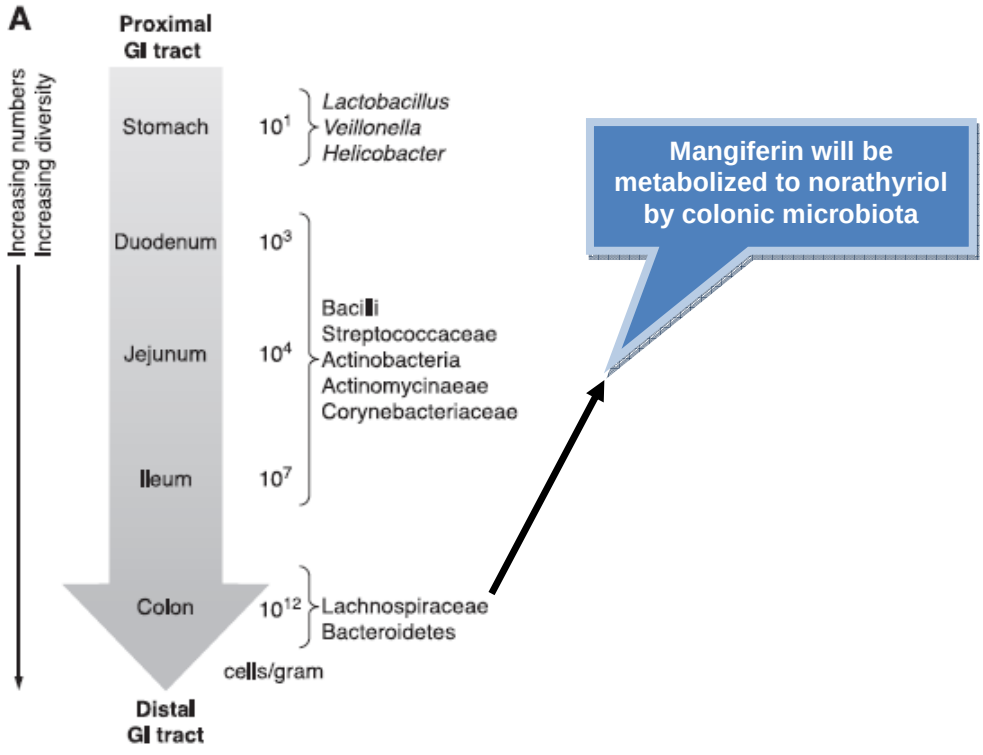

Figure 71 - Variations in microbial numbers and composition across the length of the gastrointestinal tract and association with mangiferin colonic metabolism by *Bacteroides* species MANG. Adapted from Sekirov et al. (2010).

It is not surprising that mangiferin has shown different metabolism rates by different people. Many scientific papers report the effect of drugs by human gut microbiota and how much that affects the parent drug to form metabolites. One famous example is the metabolism of 5-fluorocytosine to 5-fluorouracil. Huber et al. (1994) have cloned the bacterial enzyme cytosine deaminase responsible for the conversion and saw that the nonmammalian enzyme can metabolically activate a nontoxic prodrug to the cytotoxic anabolite.

5. Acknowledgments

The authors would like to express their thanks for the financial support from CNPq, CAPES/Daad Sandwich Doctorate program.

6. References

Abdullaev, F.I. (2005). Cancer chemopreventive and tumoricidal properties of saffron (Crocus sativus L.). *Experimental Biology and Medicine*, 227, 20–5.

Ariga T. & Seki T. (2006). Antithrombotic and anticancer effects of garlic-derived sulfur compounds: a review. *Biofactors*, 26, 93–103.

Basit, A. W. (2005). Advances in colonic drug delivery. *Drugs*, 65, 1991-2007.

Bililign, T., Griffith, B. R., Thorson, J. S. (2005). Structure, activity, synthesis and biosynthesis of aryl-C-glycosides. *Natural Product Reports*, 22, 742–760.

Braune, A., & Blaut, M. (2011). Deglycosylation of puerarin and other aromatic C-glucosides by a newly isolated human intestinal bacterium. *Environmental Microbiology,* 13(2), 482–494.

Carvalho, A. C. S., Guedes, M. M. de Souza, A. L., Trevisan, M. T. S., Lima, A. F., Santos, F. A. & Rao, V. S. N. (2007). Gastroprotective effect of mangiferin, a xanthonoid from *Mangifera indica*, against gastric injury induced by ethanol and indomethacin in rodents. *Planta Medica, 73*, 1372-1376.

Chambard, J. C., Lefloch, R., Pouysségur, J., Lenormand, P. (2007). ERK implication in cell cycle regulation. *Biochimica et Biophysica Acta,* 1773, 1299–1310.

Cummings, J. H., Antoine, J. M., Azpiroz, F., Bourdet-Sicard, R., Brandtzaeg, P., Calder, P. C., Gibson, G. R., Guarner, F., Isolauri, E., Pannemans, D., Shortt, C., Tuijtelaars, S., Watzl, B. (2004). Passclaim – gut health and immunity. *European Journal of Nutrition,* 43, 118-173.

Dar, A., Faizi, S., Naqvi, S., Roome, T., Zikr-ur-Rehman, S., Ali, M., Firdous, S. & Moin, S. T. (2005). Analgesic and antioxidant activity of mangiferin and its derivatives: the structure activity relationship. Biological & Pharmaceutical Bulletin, 28, 596-600.

Davis, S. S. (2005). Formulation strategies for absorbance windows. *Drug Discovery Today*, 10, 249-257.

Dumesic, P. A., Scholl, F. A., Barragan, D. I., Khavari, P. A . (2009). Erk1/2 MAP kinases are required for epidermal G2/M progression. *Journal of Cell Biology*, 185/3, 409–422.

Eckburg, P. B., Bik, E. M., Bernstein, C. N., Purdom, E., Dethlesen, L., Sargent, M., Gill, S. R., Nelson, K. E., Relman, D. A. (2005). Diversity of the human intestinal microbial flora. *Science*, 308, 1635-1638.

Effect of Saffron Supplementation on Macular Cone-mediated Function in Age related Macular Degeneration (safAMD). Retrieved on April 04, from http://clinicaltrials.gov/ct2/show/NCT00951288.

Egert, M., de Graaf, A. A., Smidt, H., de Vos, W. M., Venema, K. (2006). Beyond diversity: functional microbiomics of the human colon. Trends in microbiology, 14, 86-91.

Escherich, T. (1885). Die darmbakterien des neugeborenen und sauglings. *Fortschritte der Medizin*, 3, 447-547.

Fanaro, S., Chierici, R., Guerrini, P., Vigi, V. (2003). Intestinal microflora in early infancy: Composition and development. *Acta pediatrica*, 92, 48-55.

Finegold, S. M., Sutter, V. L., Mathisen, G. E. (1983). Normal and indigenous flora. In: Hentges, D. J. (Ed.), Human Intestinal Microflora in Health and Disease. Academic Press, New York.

Franz, G. & Grün, M. (1983). Chemistry, Occurrence and Biosynthesis of C-Glycosil Compounds in Plants. *Journal of Medicinal Plant Research,* 47, 131-140.

Garcia, D., Escalante, M., Delgado, R., Ubeira, F. M. & Leiro, J. (2003). Anthelminthic and antiallergic activities of *Mangifera indica* L. stem bark components Vimang and mangiferin. *Phytotherapy Research, 17*, 1203-1208.

García-Rivera, D., Delgado, R., Bougarne, N., Haegeman, G., Berghe, W. V. (2011). Gallic acid indanone and mangiferin xanthone are strong determinants of immunosuppressive anti-tumour effects of mangifera indica l. Bark in mda-mb231 breast cancer cells. *Cancer letters*, 305, 21-31.

Geodakyan, S. V., I. Voskoboinikova, V., Tjukavkina, N. A., Kolhir, V. K., Kolesnik, Y. A., Zjuzin, V. A., Glyzin, V. I. S. Sokolov, J. (1992). Experimental Pharmacokinetics of Biologically Active Plant Phenolic Compounds. I.Pharmacokinetics of Mangiferin in the Rat. *Phytotherapy research*, 6, 332-334.

Gómez-Zaleta, B., Ramírez-Silva, M. T., Gutiérrez, A., González-Vergara, E., Güizado-Rodríguez, M., Rojas-Hernández, A. (2006). UV/vis, ^{1}H, and ^{13}C NMR spectroscopic studies to determine mangiferin pKa values. *Spectrochimica Acta Part A*, 64, 1002–1009.

Guarner, F. & Malagelada J.-R. (2003). Gut flora in health and disease. *The Lancet*, 361, 512–19.

Guha, S., Ghosal, S. & Chattopadhyay, U. (1996). Antitumor, immunomodulatory and anti-HIV effect of mangiferin, a naturally occurring glucosylxanthone. *Chemotherapy*, *42*, 443-451.

Han, D., Chen, C., Zhang, C., Zhang, Y., & Tang, X. (2010). Determination of mangiferin in rat plasma by liquid-liquid extraction with UPLC-MS/MS. *Journal of Pharmaceutical and Biomedical Analysis*, 51(1), 260-263.

Hattori, M., Akao, T., Kobashi, K., Namba, T. (1993). Cleavages of the O- and C-glucosyl bonds of anthrone and 10,10′-bianthrone derivatives by human intestinal bacteria. *Pharmacology*, 47, 125–133.

Hou, S., Wang, F., Li, Y., Li, Y., Wang, M. , Sun, D., Sun, C. (2012). Pharmacokinetic study of mangiferin in human plasma after oral administration. *Food Chemistry*, 132/1, 289-294.

Hsu, M.-F., Raung, S.-L., Tsao, L.-T., Lin, C.-N., Wang, J.-P. (1997). Examination of the Inhibitory Effect of Norathyriol in Formylmethionyl-Leucyl-Phenylalanine-Induced Respiratory Burst in Rat Neutrophils. *Free Radical Biology & Medicine*, 23/7, 1035–1045.

Huber, B. E., Austin, E. A., Richards, C. A., Davis, S. T., Good, S. S. (1994). Metabolism of 5-fluorocytosine to 5-fluorouracil in human colorectal tumor cells transduced with the cytosine deaminase gene: Significant antitumor effects when only a small percentage of tumor cells express cytosine deaminase. *Proceedings of the National Academy of Sciences USA,* 91, 8302-8306.

Hultin, P.G. (2005). Bioactive C-glycosides from bacterial secondary metabolism. *Current Topics in Medicinal Chemistry*, 5, 1299–1331.

Ibekwe, V. C., Fada, H. M., McConnell, E. L., Khela, M. K., Evans, D. F., Basit, A. W. (2008). Interplay between intestinal pH, transit time and feed status on the in vivo performance of pH responsive ileo-colonic release systems. *Pharmaceutical Research*, 25, 1828-1835.

Ibekwe, V. C., Liu, F., Fada, H. M., Khela, M. K., Evans, D. F., Parsons, G. E., Basit, A. W. (2006). An investigation into the in vivo performance variability of pH responsive polymers for ileo-colonic drug delivery using gamma scintigraphy in humans. *Journal of Pharmaceutical Sciences,* 95, 2760-2766.

Ingelman-Sundberg, M., Sim, S. C., Gomez, A., Rodriguez-Antona, C. (2007). Influence of cytochrome P450 polymorphisms on drug therapies: Pharmacogenetic, pharmacoepigenetic and clinical aspects. *Pharmacology & Therapeutics,* 116, 496–526.

Jagetia, G. C. & Baiga, M. S. (2005). Radioprotection by mangiferin in DBAxC57BL mice: a preliminary study. *Phytomedicine*, 12, 209-215.

Jeong, W. S., Jun, M., Kong, A. N. (2006). Nrf2: a potential molecular target for cancer chemoprevention by natural compounds. *Antioxiditant & Redox Signaling,* 8, 99–106.

Jmol: an open-source Java viewer for chemical structures in 3D. Access on march 1st. http://www.jmol.org/

Kalmykova, T. P., Kermanian, F., Okhotnikova, V. F. (2003). Optimization of Composition and Production Technology of Alpizarin Liniment. *Pharmaceutical Chemistry Journal*, 37(5), 48-50.

Ko, F. N., Lin, C. N., Liou, S. S., Huang, T. F., Teng, C. M. (1991). Vasorelaxation of rat thoracic aorta caused by norathyriol isolated from Gentianaceae. *European Journal of Pharmacology*, 192, 133–139.

Kinghorn, A. D., Farnsworth, N. R., Soejarto, D. D., Cordell, G. A., Swanson, S. M., Pezzuto, J. M., Wani, M. C., Wall, M. E., Oberlies, N. H., Kroll, D. J., Kramer, R. A., Rose, W. C., Vite, G. D., Fairchild, C. R., Peterson, R. W., Wild, R. (2003). Novel Strategies for the Discovery of Plant-Derived Anticancer Agents. *Pharmaceutical Biology*, 41, 53–67.

Lansky, E. P. & Newman, R. A. (2007). Punica granatum (pomegranate) and its potential for prevention and treatment of inflammation and cancer. *Journal of Ethnopharmacology*, 19, 177–206.

Lee, H.-Z., Lin, W.-C., Yeh, F.-T., Lin, C.-N., Wu, C.-H. (1998). Decreased protein kinase C activation mediates inhibitory effect of norathyriol on serotonin-mediated endothelial permeability. *European Journal of Pharmacology*, 353, 303–313.

Lin, C. N., Chang, C. H., Arisawa, M., Shimizu, M., Morita, N. (1982). Two new xanthone glycosides from Tripterospermum lanceolatum. *Phytochemistry*, 21, 205–208.

Liu, H., Wang, K., Tang, Y., Sun, Z., Jian, L., Li, Z., Wu, B., Huang, C. (2011). Structure Elucidation of in vivo and in vitro Metabolites of Mangiferin. *Journal of Pharmaceutical and Biomedical Analysis*, 55, 1075-1082.

Lewis, D. F. V. & Wiseman A. (2005). A selective review of bacterial forms of cytochrome P450 enzymes. *Enzyme and Microbial Technology*, 36, 377–384.

Ley R. E., Peterson, D. A., Gordon, J. I. (2006). Ecological and evolutionary forces shaping microbial diversity in the human intestine. *Cell,* 124, 837-848.

Living Science. Dr Parrys Website. (2011) Retrieved on April 16, from http://www.livingscience.co.uk/joomla/index.php?option=com_content&view=article&id=57:enzymes&catid=42:enzymes&Itemid=54.

Li, Y., Meselhy, M. R., Wang, L. Q., Ma, C. M., Nakamura, N., Hattori, M. (2000) Biotransformation of a C-glycosylflavone, abrusin 2″-O-beta-D-apioside, by human intestinal bacteria. *Chemical & Pharmaceutical Bulletin (Tokyo)*, 48, 1239–1241.

Lüllmann, H., Mohr, K., Hein, L. (2010). Color Atlas of Pharmacology. 4th Edition, Thieme, 296-297.

Macfarlane, G. T. & Macfarlane, S. (1997). Human colonic microbiota: ecology, physiology and metabolic potential of intestinal bacteria. *Scandinavian Journal of Gastroenterology,* 222, 3-9.

Matsushima, T., Araki, A., Yagame, O., Muramatsu, M., Koyama, K., Ohsawa, K., Natori, S., Tomimori, H. (1985). Mutagenicities of xanthone derivatives in Salmonella typhimurium TA100, TA98, TA97, and TA2637. *Mutation Research*, 150, 141-146.

Matute, A. C., Sanchez G. M. V., Campos, E. R., Alberti, A. E., Gottlieb, M., Ibarretxe, B. G., Delgado, G. J. M., Gruart, I. M. A. & Leal C. R. (2007). Food products for treating and preventing neurodegenerative diseases and ageing symptoms, contain morin or mangiferin. WO2007077279-A1 ; ES2277567-A1 Spanish Patent.

McConnell, E. L., Fadda, H. M., Basit, A. W. (2008a). Gut instincts: explorations in intestinal physiology and drug delivery. *International Journal of Pharmaceutics*, 364/2, 213-226.

Mikov, M. (1994). The metabolism of drugs by the gut flora. *European Journal of Drug Metabolism and Pharmacokinetics*, 19, 201-207.

Miura, I.; Hostettmann, K.; Nakanishi, K. (1978). 13C-NMR of naturally occurring xanthone aglycones and glycosides. *Nouveau Journal de Chemie*, , 2, 6, 653.

NCBI – National Center for Biotechnology Information. Complex Of Erk2 With Norathyriol. (2011). Retrieved on April 17th, from http://www.ncbi.nlm.nih.gov/Structure/mmdb/mmdbsrv.cgi?Dopt=s&uid=95719 .

Nobili, S., Lippi, D., Witort, E., Donnini, M., Bausi, L., Mini E., Capaccioli S., Natural compounds for cancer treatment and prevention. Pharmacological Research 59 (2009) 365–378.

Oxoid Microbiology Products, 2012. Atmosphere generation system. Retrieved on January 31, from http://www.oxoid.com/UK/blue/prod_detail/prod_detail.asp?pr=AN0010&c=UK&lang=EN.

Pardo-Andreu, G. L., Aánchez-Baldoquín, C., Ávila-González, R., Delgado, R., Naal, Z., Curti, C. (2006). Fe(III) improves antioxidant and cytoprotecting activities of mangiferin. *European Journal of Pharmacology*, 547, 31-36.

PDB – Protein Data Bank. Complex of ERK2 with norathyriol. DOI:10.2210/pdb3sa0/pdb.(2011).Retrieved on April 17th, from http://www.rcsb.org/pdb/explore/explore.do?structureId=3SA0.

Puupponen-Pimiä, R., Aura, A.-M., Oksman-Caldentey, K.-M., Myllärinen, P., Saarela, M., Mattila-Sandholm, T. Poutanen, K. (2002). Development of functional ingredients for gut health. *Trends in Food Science & Technology*, 13, 3–11.

Qin, J., Deng, J., Feng, X., Wang, Q., Wang, S. (2008). Quantitative RP–LC Analysis of Mangiferin and Homomangiferin in Mangifera indica L. Leaves and in Mangifera persiciforma C. Y. Wu et T. L. Ming Leaves. *Chromatographia*, 68, 955–960.

Rajilic-Stojanovic, M., Smidt, H., de Vos, H. M. (2007). Diversity of the human gastrointestinal tract microbiota revisited. *Environmental Microbiology,* 9, 2125-2136.

Rang, H. P., Dale, M. M., Ritter, J. M., Flower, R. J. (2007). Pharmacology. Sixth edition. Churchill Livingstone Elsevier.

Rautio J., Kumpulainen, H., Heimbach, T., Oliyai, R., Oh, D., Järvinen, T., Savolainen, J. (2008). Prodrugs: design and clinical applications. *Nature Reviews*, 7, 255-270.

Rechner, A. R., Smith, M. A., Kuhnle, G., Gibson, G. R., Debnam E. S., Srai, S. K. S., Moore, K. P., Rice-Evans, C. A. (2004). Colonic Metabolism Of Dietary Polyphenols: Influence Of Structure On Microbial Fermentation Products. *Free Radical Biology & Medicine*, 36/2, 212 – 225. Saito, K. (1990) Enzyme-catalyzed cleavage of the C-glycosidic linkage to the aromatic ring-A of 3′,4′,5,7- tetrahydroxyflavone 8-C-glycoside. *Biochimica et Biophysica Acta*, 1035, 340–347.

Rivera, D. G., Balmaseda, I. H., Leon,. A. A., Hernandez, B. C., Montiel, L. M., Garrido, G. G., Cuzzocrea, S. & Hernandez. R. D. (2006). Anti-allergic properties of *Mangifera indica* L. extract (Vimang) and contribution of its glucosylxanthone mangiferin. *Journal of Pharmacy and Pharmacology, 58*, 385-392.

Rubinstein, A. (2005). Colonic drug delivery. *Drug discovery today*, 2, 33-37.

Sanugul, K., Akao, T., Li, Y., Kakiuchi, N., Nakamura, N., and Hattori, M. (2005a) Isolation of a human intestinal bacterium that transforms mangiferin to norathyriol and inducibility of the enzyme that cleaves a C-glucosyl bond. *Biological and Pharmaceutical Bulletin*, 28, 1672–1678.

Sanugul, K., Akao, T., Nakamura, N., and Hattori, M. (2005b) Two proteins, Mn2+, and low molecular cofactor are required for C-glucosyl-cleavage of mangiferin. *Biological and Pharmaceutical Bulletin*, 28, 2035–2039.

Savage, D. C. (2001). Microbial biota of the human intestine: A tribute to some pioneering scientists. *Current Issues in Intestinal Microbiology,* 2, 1-15.

Sanchez, G. M., Re, L., Giuliani, A., Nunez-Selles, A. J., Davison, G. P. & Leon-Fernandez, O. S. (2000). Protective effects of *Mangifera indica* L. extract, mangiferin and selected antioxidants against TPA-induced biomolecules oxidation and peritoneal macrophage activation in mice. *Pharmacological Research, 42*, 565–573.

Scheline, R. R. (1973). Metabolism of foreign compounds by gastrointestinal microorganisms. *Pharmacological Reviews*, 25, 451-523.

Schieber, A., Berardini, N., Carle, R. (2003). Identification of flavonol and xanthone glycosides from mango (Mangifera indica L. cv. 'Tommy Atkins') peels by high-performance liquid chromatography-electrospray ionisation mass spectrometry. *Journal of Agricultural and Food Chemistry*, 51, 5006.

Schmidt, M., Betti, G., Hensel, A. (2007). Saffron in phytotherapy: pharmacology and clinical use. *Wiener medizinische Wochenschrift,*157, 315–409.

Sekirov, I., Shannon, L., Russell, L., Antunes, C. M., Finlay, B. B. (2010). Gut Microbiota in Health and Disease. *Physiological Reviews*, 90, 859–904.

Shamat, A. M. (1993). The role of the gastrointestinal microflora in the metabolism of drugs. *International Journal of Pharmaceutics,* 97, 1-13.

Shen, R., Wang, P., Tang, N. (2010). Cytotoxic Activity and DNA-binding Properties of Xanthone Derivatives. *Journal of Fluorescence,* 20 1287–1297.

Sinha, V. R. & Kumria, R. (2001). Colonic Drug Delivery: Prodrug Approach. *Pharmaceutical Research*, 18, 557–564.

Smirnova, L. P., Sheichenko, V. I., Tokhtabaeva, G. M. (2000). Study of the Chemical Composition of Alpizarin from Mango Leaves. *Pharmaceutical Chemistry Journal*, 34(2), 22 – 25.

Smith, C. J. & Callihan, D. R. (1992). Analysis of rRNA Restriction Fragment Length Polymorphisms from Bacteroides spp. and Bacteroides fragilis Isolates Associated with Diarrhea in Humans and Animals. *Journal of Clinical Microbiology*, 806-812

Sokolov, S. Y., Belova, L. F., Baginskaya, A. I., Leskova, T. E. (1987) Pharmacological Properties of a New Antiviral Preparations Alpizarine. UDC 615.322:528.615/.015.4.07

Sousa, T., Paterson, R., Moore, V., Carlsson, A., Abrahamsson, B., Basit, A. W. (2008). The gastrointestinal microbiota as a site for the biotransformation of drugs. *International Journal of Pharmaceutics*, 363,1-25.

Tanock, G. W. (1999). Analysis of the intestinal microflora: a renaissance. *Antoine Van Leeuwenhoek*, 76, 265-278.

Teng, C. M., Ko, F. N., Wang, J. P., Lin, C. N., Wu, T. S., Chen, C. C., Huang, T. F. (1991). Antihaemostatic and antithrombotic effect of some antiplatelet agents isolated from Chinese herbs. *Journal of Pharmacy and Pharmacology*, 43, 667–669.

Teng, C. M., Lin, C. N., Ko, F. N., Cheng, K. L., Huang, T. F. (1989). Novel inhibitory actions on platelet thromboxane and inositol phosphate formation by xanthones and their glycosides. *Biochemical Pharmacology*, 38, 3791–3795.

U. S. Department of Health & Human Services, 2012. National Heart Lung and Blood Institute.Calculate your Body Mass Index. (2012) Retrieved on April 23 from http://www.nhlbisupport.com/bmi/bminojs.htm.

Varum, F. J., McConnel, E. L., Sousa, J. J., Veiga, F., Basit, A. W. (2008). Mucoadhesion and the gastrointestinal tract. *Critical Reviews in Therapeutic Drug Carrier Systems*, 25, 207-258.

Wada, M. (2007). Foodstuffs compounding agent for treating diabetes comprises glycoside having xanthone structure. JP2007204462-A Japanese Patent.

Wang, J. P., Ho, T. F., Lin, C. N., Teng, C. M. (1994a). Effect of norathyriol, isolated from Tripterospermum lanceolatum, on A23187-induced pleurisy and analgesia in mice. *Naunyn-Schmiedeberg's Archives of Pharmacology*, 350, 90–95.

Wang, J. P., Raung, S. L., Lin, C. N., Teng, C. M. (1994b). Inhibitory effect of norathyriol, a xanthone from Tripterospermum lanceolatum, on cutaneous plasma extravasation. *European Journal of Pharmacology*, 251, 35–42.

Wang, J.-P., Raung, S.-L., Tsao, L.-T., Lin, C.-N. (1997). Evidence for the involvement of protein kinase C inhibition by norathyriol in the reduction of

phorbol ester-induced neutrophil superoxide anion generation and aggregation. *European Journal of Pharmacology*, 336, 81–88.

Wang, M., Ahrne, S., Jeppsson, B., Molin, G. (2005). Comparison of bacterial diversity along the human intestinal tract by direct cloning and sequencing of 16S rRNA genes. *FEMS Microbiology Ecology,* 54, 219-231.

Wang, R.-R., Gao, Y.-D., Ma, C.-H., Zhang, X.-J., Huang, C.-G., Huang, J.-F., Zheng, Y.-T. (2011). Mangiferin, an Anti-HIV-1 Agent Targeting Protease and Effective against Resistant Strains. *Molecules*, 16, 4264-4277.

Whitman, W. B., Coleman, D. C., Wiebe, W. J. (1998). Prokaryotes: the unseen majority. *Proceedings of the National Academy of Sciences of the United States*, 95, 6578-6583.

Wu, Z., Wei, G., Lian, G., Yu, B. (2010). Synthesis of Mangiferin, Isomangiferin, and Homomangiferin. *Journal of Organic Chemistry*, 75, 5725–5728.

Yoosook, C., Bunyapraphatsara, N., Boonyakiat, Y. & Kantasuk, C. (2000). Anti-herpes simplex virus activities of crude water extracts of Thai medicinal plants. *Phytomedicine, 6*, 411–419.

CHAPTER 4

Cytotoxic Screen of Mangiferin and Metabolites In two Human Tumor Cell Lines

Souza, J. R. R.[1,2], Feitosa, J. P. A.[1], Ricardo, N. M. P. S[1], Trevisan, T. S.[1], Ulrich C. M.[2], Frei, E.[2], Owen, R. W.[2]

[1]Departament of Organic and Inorganic Chemistry, Federal University of Ceará P. O. Box: 6.021, ZIP-Code: 60455-760, Fortaleza, Ceará, Brazil

[2]Division of Preventive Oncology, National Center for Tumor Diseases, Im Neuenheimer Feld 460/German Cancer Research Center, Im Neuenheimer Feld 581, Heidelberg, Germany

Mangiferin, a natural antioxidant and potential anticancer drug, has been investigated by several research groups in several countries in order to establish its pharmacological and biological properties. Due to its low bioavailability values, already reported in many scientific publications, mangiferin is thought to be more available in the gut, where it will be metabolized into other several compounds. The aim of this study was to investigate the cytotoxic effects of mangiferin and its main metabolites in human cancer cell lines such as intestinal cancer cell line Caco-2 in order to observe the potential anticancer activity of these compounds *in vitro.*

Keywords: mangiferin, metabolites, cytotoxicity, cancer, human cell lines.

1. Introduction

1.1. Cancer and Chemoprevention – Basic concepts

Cancer is found to be a group of more than 100 diseases and it is defined as uncontrolled cellular growth as a result of changes in the genetic information in cells. Cells and tissues are complex systems with critical stages and checkpoints to ensure normal growth, development, and function. Normally the division, differentiation, and death of cells are carefully regulated and cancers start as a single cell that has lost control of its normal growth and replication processes.

Human adults are made up of around 10^{13} cells, which are renewed and replaced constantly. About 5–10 per cent of cancers are reported to result directly from inheriting genes associated with cancer, but the majority involves alterations or damage accumulated over time to the genetic material within cells. The causes of damage are both endogenous (internal) and exogenous (environmental). Approximately 85 per cent of adult cancers develop from the epithelial cells of the inner and outer linings of the body and are called carcinomas. Cancers of glandular tissue such as the breast are called adenocarcinomas; cancers from bone and muscle derived from mesoderm cells (embryonic cells that grow to form muscle, blood, bone, and connective tissue), are called sarcomas. Each type of cancer has different characteristics, but one feature in common in all these diseases is unregulated cell growth and/or cell death. Apart from haematological cancers such as leukaemias, this results in a tumour or mass, and cancerous cells often invade the surrounding tissue. Spread of cancer cells from the primary site to other parts of the body is called metastasis. Benign tumours do not invade or metastasise. Malignant tumours do not remain localised but can invade and/or metastasise.

Several phytochemicals present in plants, fruits and vegetables act as antioxidants, preventing oxidative damage to cells, proteins, and DNA. A few possible mechanisms of phytochemicals are reported: influence cancer risk through their antioxidant activities, modulation of detoxification enzymes, stimulation of the immune system, antiproliferative activities, and/or modulation of steroid hormone concentration and hormone metabolism. Understanding the action and mechanisms of phytochemicals on cancer development is important

to improve its prevention and treatment (World Cancer Research Fund / American Institute for Cancer Research, 2007; Chan & Giovannucci, 2010; Thapa & Gosh, 2012).

1.2. The lungs and occurrence of cancer

The lungs are a pair of cone-shaped breathing organs in the chest that brings oxygen into the body as you breathe in. They release carbon dioxide, a waste product of the body's cells, as you breathe out. Each lung has sections called lobes. The left lung has two lobes. The right lung is slightly larger and has three lobes. Two tubes called bronchi lead from the trachea (windpipe) to the right and left lungs. Tiny air sacs called alveoli and small tubes called bronchioles make up the inside of the lungs as can be seen in Figure 1. The bronchi are sometimes also involved in lung cancer (National Cancer Institute, 2011).

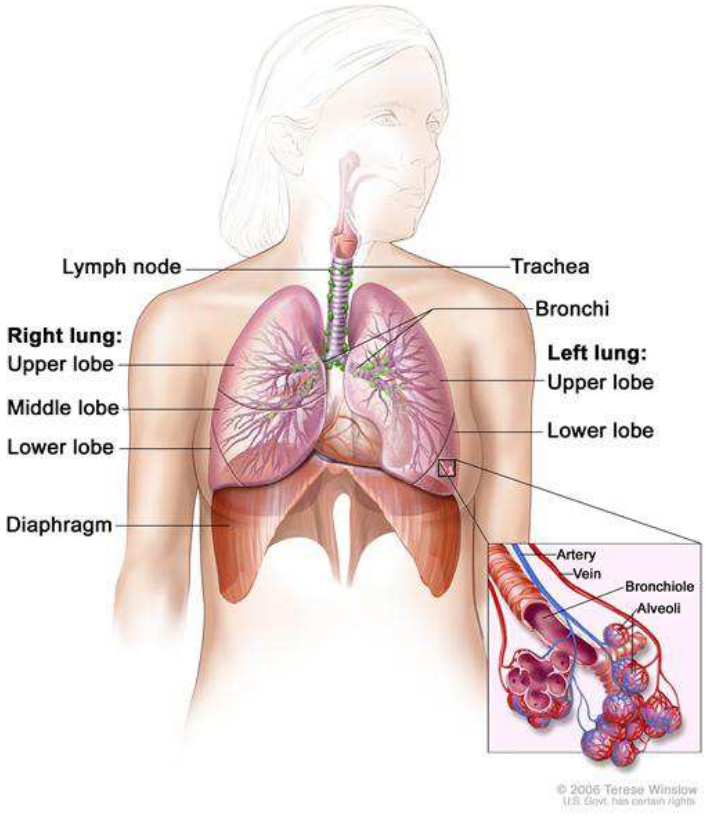

Figure 1 - Anatomy of the respiratory system, showing the trachea and both lungs and their lobes and airways. (National Cancer Institute. General Information About Non-Small Cell Lug Cancer 2011).

There are two main types of lung cancer: non-small cell lung cancer and small cell lung cancer. There are several types of non-small cell lung cancer and each type of non-small cell lung cancer has different kinds of cancer cells. The types of non-small cell lung cancer are named for the kinds of cells found in the cancer and how the cells look under a microscope (National Cancer Institute. General Information About Non-Small Cell Lug Cancer 2011):

- Squamous cell carcinoma: Cancer that begins in squamous cells, which are thin, flat cells that look like fish scales. This is also called epidermoid carcinoma.
- Large cell carcinoma: Cancer that may begin in several types of large cells.
- Adenocarcinoma: Cancer that begins in the cells that line the alveoli and make substances such as mucus.
- Other less common types of non-small cell lung cancer are: pleomorphic, carcinoid tumor, salivary gland carcinoma, and unclassified carcinoma.

1.3. The non-small bronchial carcinom cells

The non-small cell lung carcinoma (NSCLC) constitutes 75 % of primary lung cancers and comprises large-cell undifferentiated carcinomas, squamous carcinomas, and adenocarcinomas (Figure 2) (Mahaffey et al, 2009). The non-small cell bronchial carcinoma is a tumor with a considerable epidemiological significance.

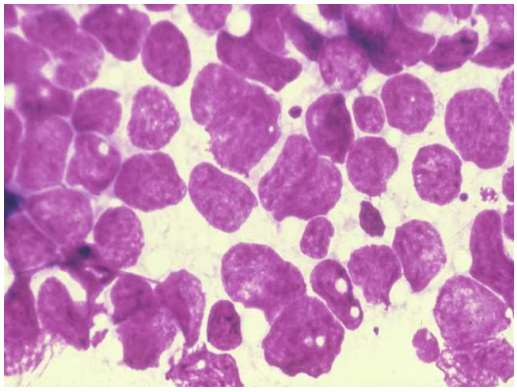

Figure 2 – Image of non-small cell lung cancer (Metrohealth, 2011).

Characteristics of the biology of non-small cell bronchial carcinomas are normally fast-growing tumors, wich takes untreated patients rapidly to generalized symptoms and cachexia. Therefore it is assumed that the bronchial carcinoma non-small cell is a tumor with high need of nutrients and substrates (Eschen, 2004).

Lung cancer is reported to be the most common cause of cancer deaths worldwide (Zhong et al, 2010) and it was the most commonly diagnosed cancer as well as the leading cause of cancer death in males in 2008 globally (Jemal et al., 2011).

The GLOBOCAN project published estimates of the incidence of, mortality and prevalence from major type of cancers, at national level, for 184 countries of the world. The GLOBOCAN estimates presented for 2008 in Figure 3 shows lung cancer with the highest incidence in the world (Ferlay et al., 2010).

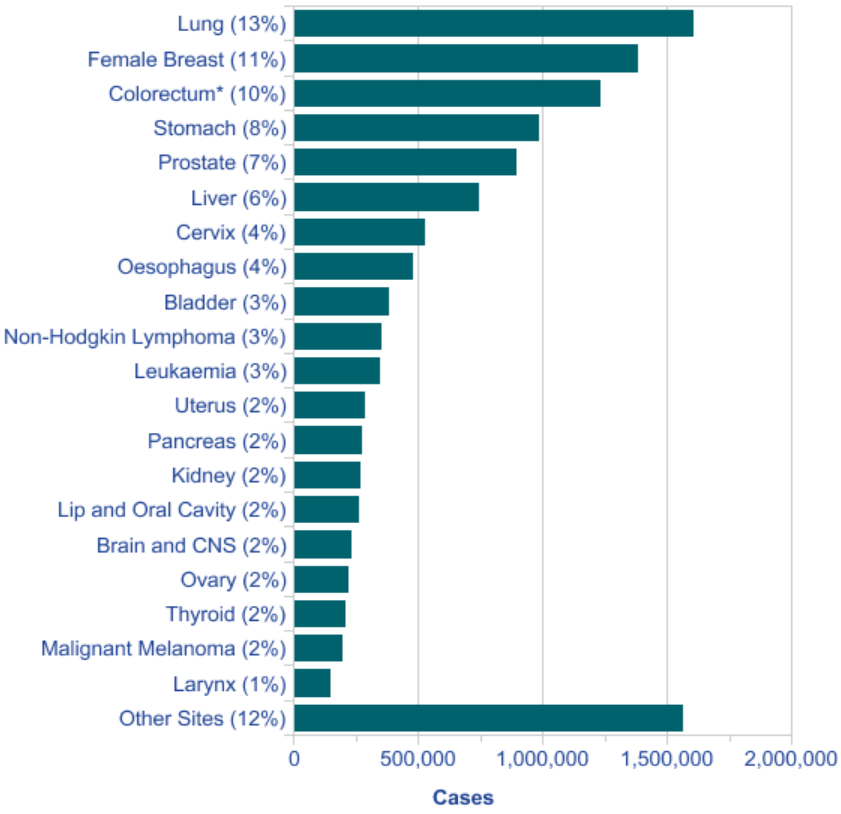

Figure 3 - The 20 Most Commonly Diagnosed Cancers in 2008. (*Colorectum including anus). Estimates from GLOBOCAN 2008. Prepared by Cancer Research UK, 2012).

It is estimated 17,210 new cases of lung cancer in men and 10,110 in women in Brazil in 2012. These values correspond to an estimated risk of 18 new cases per 100,000 men and 10 to every 100,000 women. Excluding the non-melanoma skin tumors, lung cancer in men is the second most frequent in the South (37 / 100,000) and Midwest (17 / 100,000). In the Southeast (20 / 100,000), Northeast (8 / 100,000) and North (8 / 100,000), ranks third. For women, is the third most common in the South (19 / 100,000), the fourth in the Midwest (9 / 100,000) and fifth in the Southeast (11 / 100,000), Northeast (6 / 100,000) and North (5 / 100,000) (Estimate/2012 – Cancer Incidence in Brazil, 2011).

1.4. The Colon, rectum and ocurrence of cancer

The colon and rectum are parts of the digestive system (Figure 4) . They form a long, muscular tube called the large intestine (also called the large bowel). The colon is the first 4 to 5 feet of the large intestine, and the rectum is the last several inches. Partly digested food enters the colon from the small intestine. The colon removes water and nutrients from the food and turns the rest into waste (stool). The waste passes from the colon into the rectum and then out of the body through the anus (National Cancer Institute. The Colon and Rectum, 2011).

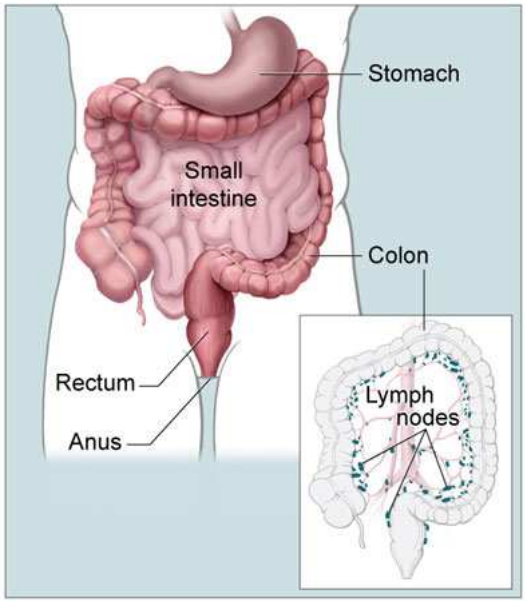

Figure 4 -This picture shows part of the digestive system (National Cancer Institute. The Colon and Rectum, 2011).

Colorectal cancer is a disease in which cells in the colon or rectum become abnormal and divide without control, forming a mass called a tumor. Colorectal cancer cells may also invade and destroy the tissue around them. In addition, they may break away from the tumor and spread to form new tumors in other parts of the body. Colorectal cancer is the third most common type of non-skin cancer in men (after prostate cancer and lung cancer) and in women (after breast cancer and lung cancer). It is the second leading cause of cancer death in the United States after lung cancer (National Cancer Institute. Surveillance Epidemiology and End Results 2011).

For Brazil, in 2012, it is expected 14,180 new cases of cancer of colon and rectum in men and 15,960 in women. These values correspond to an estimated risk of 15 new cases per 100,000 men and 16 women to every 100,000. Excluding the non-melanoma skin tumors, cancer of the colon and rectum in men is the second most common in the Southeast (22 / 100,000) and third in the South (18 / 100,000) and Midwest (14 / 100,000). In the North ranks fourth (4 / 100,000), and in the Northeast (5 / 100,000), the fifth. For women, it is the second most common in the Southeast (23 / 100,000) and South (20 / 100,000), the third in the Midwest (15 / 100,000) and Northeast (7 / 100,000), and sixth in the North (5 / 100,000) (Estimate/2012 – Cancer Incidence in Brazil, 2011).

1.5. The Caco-2 cell line

The Caco-2 cell line was developed by Dr. Jorgen Fogh at the Sloan-Kettering Institute for Cancer Research. It can be defined as a continuous line of heterogeneous human epithelial colorectal adenocarcinoma cells (Fogh & Trempe, 1975). In the 1970s, a collection of cell lines was established from gastrointestinal tumors, with the aim of performing studies on cancer mechanisms and related cytostatic therapies (Fogh et al., 1977). The Figure 5 shows Junctional staining of the colon cancer cell line Caco-2.

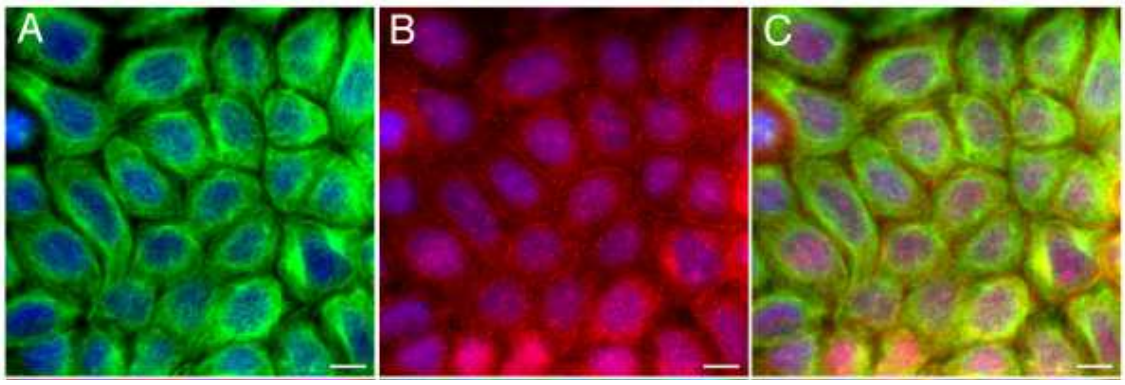

Figure 5 - Caco-2 cells co-immunostained with the polyclonal M-APC antibody for microtubules. A microtubule-independent junctional localisation is seen. Tubulin green, APC red and DAPI blue. Panel C is a merged image (Adapted from Lagford et al., 2006).

1.6. Citotoxicity Assays of compounds - Sulforhodamine B method

The sulforhodamine B assay is a cytotoxic assay developed by Skehan and colleagues to measure the cellular protein content of adherent and suspension cultures in 96-well microtiter plates. The method was developed for large-scales drug screens as for example the disease-oriented in vitro anticancer-drug discovery project of the National Cancer Institute (NCI). More than 10.000 samples were tested each year in this project with analysis of several million individual wells (Skehan et al., 1990; Voigt, 2005).

The method consists on the ability of the protein dye sulforhodamine B (Hydrogen 3,6-bis(diethylamino)-9-(2,4-disulphonatophenyl)xanthylium) to bind electrostatically and stoichiometrically, at mild acidic conditions, to protein basic amino acid residues of fixed cells (Figure 6). The protein dye can be extracted at mild basic conditions from the cells and be solubilized for optical density measurement using weak bases such as Tris base (Voigt, 2005).

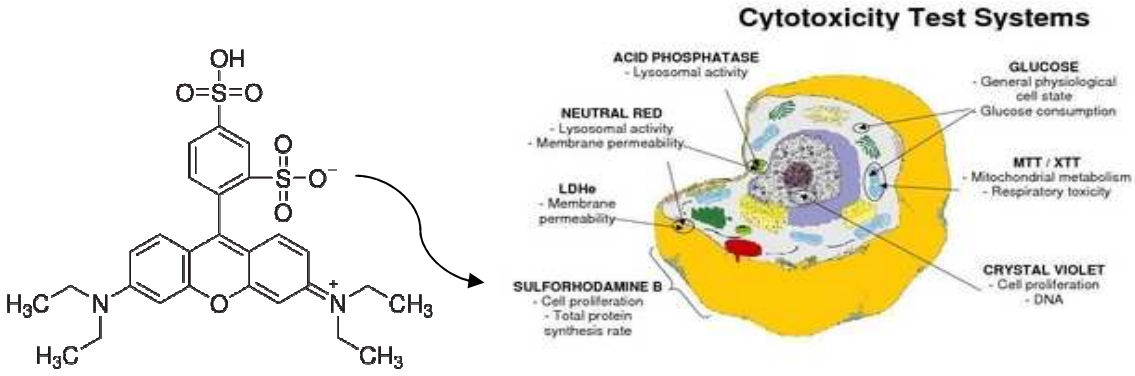

Figure 6 – Chemical structure of the anionic dye sulforhodamine B and possible binding site on cell proteins (Sigma-Aldrich, 2012; Aniara, 2012).

The aim of this work is the investigation of the action spectrum of mangiferin and its metabolites in cytotoxic studies *in vitro* using two cancer cell lines to identify the most promising substances in an *in vitro* anticancer-drug screen.

a) Non-small bronchial carcinoma cells (A240286S);
b) Colon cancer cells (Caco-2).

2. Materials and Methods

2.1. Materials

2.1.1. Biological Materials - Cells lines

The experiments were performed with human non-small lung carcinoma ephitelial tumor cells (A240286S) and epithelial Colon cancer cells (Caco-2) lines:

A240286S – This is a human bronchial adenocarcinoma cell line, isolated from an adrenal metastasis, prepared and avaiable by Prof. Dr. C. Granzow, Molecular Toxicology Department / DKFZ). It is known as p-glycoprotein mediated multidrug resistant (Granzow et al., 1998). The cell line grows adhering to the bottom of the culture vessel and acts as a monolayer culture. It is uncomplicated for subculturing.

Caco-2 – This is a human colorectal adenocarcinoma cell line. This line was isolated from a primary colonic tumor from a 72 years old male Caucasian, ATCC number: HTB-37. Upon reaching confluence, the cells express characteristics of enterocytic differentiation. The Caco-2 cells express also retinoic acid binding protein I and retinol binding protein II and are keratin positive. It is resistant against human immunodeficiency virus (HIV, LAV). The cell line grows adhering to the bottom of the culture vessel as a monolayer culture. It is uncomplicated for subculturing.

A contamination screen was performed for the cell lines using the Multiplex cell Contamination Test (McCT) at the DKFZ Core facilities. This facility developed and validated this novel high-throughput Multiplex cell Contamination Test, which is currently able to detect 37 contamination markers in a single reaction. Unnoticed cell culture contamination by viruses, mycoplasma, or other cell lines is not uncommon and a threat to laboratory safety and the quality of scientific results. The assay is based on multiplex PCR with targetspecific primers and subsequent hybridization of amplimers to specific oligonucleotide probes (Schmitt & Pawlita, 2009). This novel method solves problems in cell culture contamination multiplexing more than 37 primers pairs in a single PCR reaction detecting presence of mycoplasma, viruses or other cross-contaminations with other cells such as HeLa, HEK293(T), Namalwa and Cos7.

2.1.2. Glassware and plastics

Cell culture flask, 250 mL / 75cm^2, Schraghals, Falcon	Becton & Dickison, Heidelberg
Cell culture flask, 50 mL / 25cm^2, Schraghals, Falcon	Becton & Dickison, Heidelberg
Siryinge without needle 50 mL	Thermoeurope, Belgium
Falcon serological pipettes (2, 5, 10, 25 and 50 mL)	Becton & Dickison, Heidelberg
Falcon MicrotestTM 96 tissue culture plates, 96 well, flat bottom with low evaporation Lid	Becton & Dickison, Heidelberg
Onetouch Barrier, sterile tips 1-330 µL	Sorenson Biosciences, USA
Finntips®, 5 mL	Thermolab systems, USA
Distrip Mini syringes for DISTRIMAN® repetitive pipette 1250µL capacity for aliquots from 10 to 125 µL, wrapped and sterilized	GILSON S.A.S, France
Ready-to-use filter holders 0.2 µm	Renner Gmbh, Dannstadt
Centrifuge Tubes (15 mL), Falcon	Becton & Dickison, Heidelberg

2.1.3. Media and solutions

Fetal Bovine Serum (FBS) Seraplus	PAN Biotech, Aidenbach
Hepes buffer solution (1M)	PAA Laboratories, Austria
L-Glutamin 200 mM	PAN Biotech, Aidenbach
Phosphate-buffered saline (DPBS), Dulbeccos formula without magnesium and calcium	PAN Biotech, Aidenbach
RPMI 1640 Medium with 2,0 g/L NaHCO3, without L-Glutamine and low endotoxin	Biochrom AG, Berlin
RPMI 1640 Medium with 2,0 g/L $NaHCO_3$, without L-Glutamine and without Phenol Red	Biochrom AG, Berlin
MEM Earle´s Medium with 0.85 g/L $NaHCO_3$ and without L-Glutamine	Biochrom AG, Berlin
NEAA – Non essential amino acids (100 x)	Biochrom AG, Berlin
Sodium Pyruvate 100 mM	Biochrom AG, Berlin
Trypsin (0,05%) - EDTA (0,02%) in DPBS	PAA laboratories, Austria
Trypan blue 0.5 % (w/v) in phisiological saline	Biochrom AG, Berlin

2.1.4. Chemicals

Dimethylsulfoxid (DMSO), P.A	Merck, Darmstadt
Acetic acid, P. A	Merck, Darmstadt
Ethanol absolut	Sigma-Aldrich, Seelze
Sulforhodamin B	Sigma-Aldrich, Steinheim
Tris (hydroxymethyl) aminomethan (Tris)	Sigma-Aldrich, Steinheim

2.1.5. Equipaments

CO_2-Incubator from Integra Biosciences	Fernwald, Germany.
Digital Camera Powershot S50 from Canon PC1048 N. 6223057210	Japan.
Liebherr Comfort KSD 3542 (+4C/-20C)	Ochsenhausen, Germany.
Light Microscope Leitz DM IL with reverse optics from Leitz	Wetzlar, Germany.
Finnpipette BioControl (10µl - 300µl) Multichanal pipette from Labsystems	Frankfurt, Germany.
DISTRIMAN® Repeat pipettor 2-1000 µL from ABIMED	Langenfeld, Germany.
Shaker for 96 well plates DT-2 from Neolab	Heidelberg, Germany.
Spectrophotometer µ-Quant from Bio-Tek Instruments	Gödensdorf, Germany.
Laminar flow Hood BioGARD from Labotec	Göttingen, Germany.
Tweezers from Neolab	Heidelberg, Germany.
pH meter Beckmann from Neolab	Heidelberg, Germany.
Waterbath 1002 GFL	Burgwedel, Germany.
Hemocytometer Neubauer from Neolab	Heidelberg, Germany.
Casy® 1 Cell Counter, model TTC from Roche	Switzerland.
Centrifuge Mikro 22 from Hettich	Tuttlingen, Germany.

2.2. Cell Biological Methods

2.2.1. Production of the used cell culture media

The following standard culture media are used to cultivate cells *in vitro* and to adapt the cell culture conditions for the A240286S (Table 1) and Caco-2 (Table 2) cell lines in a tumor situation *in vivo*. For the production of the Cell culture media, all the additives were filtered-sterilized using sterilization filters (pore size 0,2 µm). The fetal bovine serum (FBS) was firstly heat-inactivated for 1h at 56 °C.

Table 1 – Composition of a standart cell culture medium with 10 % fetal bovine serum (Full medium) for the A240286S cell line.

End composition	End concentration	Volume
Liquid Medium RPMI 1640 (with 2,0 g/L $NaHCO_3$, without L-Glutamine, low endotoxin)	-	450 mL
FBS	10%	50 mL
L-Glutamin 200 mM	2 mM	5 mL
HEPES 1 M	20 mM	10 mL

Table 2 – Composition of a standart cell culture medium with 15 % fetal bovine serum (Full medium) for the Caco-2 cell line.

End composition	End concentration	Volume
Liquid Medium MEM Earle´s (with 0.85 g/L $NaHCO_3$, without L-Glutamine)	-	425 mL
FBS	15%	75 mL
NEAA (100X)	1 X	5 mL
Sodium Pyruvate 100 mM	1 mM	5 mL
L-Glutamin 200 mM	2 mM	5 mL

2.2.2. Preparation methods and general use of the used solutions

Ready-to-use Trypsin/EDTA Solution – This solution was used for the detaching of the cells from the ground of the culture flasks. When subculturing adherent cells, intercellular and cell-to-substrate links or connections must be gently dissociated. Proteolytic enzymes, such as trypsin (i.e. a serine peptidase), breaks or gently separates these bonds by creating a single-cell suspension from which new subcultures are realized. Trypsin solutions are widely used as cell dissociation reagents for continuous cell culture of adherent growing cells. Trypsin proteolysis or trypsinization is a process in which proteins have been digested or treated with trypsin and are thus said to be trypsinized. Trypsin is available in a varied array of formulations with or without EDTA. EDTA is a chelator that binds calcium and magnesium ions that may otherwise inhibit the trypsin activity, which then hydrolyzes and gains access to the intercellular bonds (BI Biological Industries, 2012).

.

Fixing solution for cells - Cells attached to the plastic substratum were fixed by gently layering 100 µL of ethanol/acetic acid 95/5% on the top of the growth medium in each well. The cultures were incubated at -20 °C for 5 min and then washed five times with tap water to remove the fixing solution, growth medium, low-molecular-weight metabolites, and serum protein. Plates were air dried and then followed to the protein dye step.

Sulforhodamine B Solution – This dye solution is used for the quantification of cellular protein (Sieger, 1999). The solution is prepared diluting sulforhodamine B at 0.4 % and acetic acid at 1 % in bidestilled water as can be seen in diagram 1.

Diagram 1 – Preparation of the Sulforhodamine B solution.

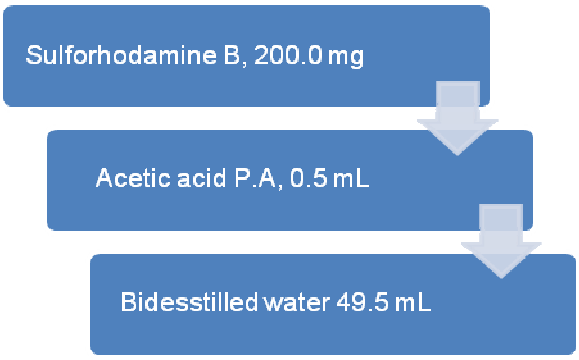

To the cells fixed to the plastic substratum were added gently 100 µL of Sulforhodamine B solution on the top of the growth medium in each well and then the cultures were incubated in a completely dark place for 30 min. After taking the sulforhodamine B solution out, the plate was washed four times with 1 % acetic acid and let in hood untill the cell layer was completely air-dried.

Tris (hydroxymethyl) aminomethan – This solution is used in the measurement process of the protein attached Sulforhodamine B that will be released from the cells after the addition of Tris. For the preparation, 1,2114 g of Tris is dissolved to a final volume of 1000.0 mL of bidestilled water at a final concentration of 10 mM. Just before reading the plates in the spectrophotometer, 100 µL of the solution is added to each well of the plate.

2.2.3. Detection of Cell Culture contaminations using McCT

In order to detect presence of cross-contamination by viruses, mycoplasma or with other human cell lines, the McCT was used. Firstly the cell sample was pre-prepared using the following steps recommended by the DKFZ genomics and proteomics core facility (Diagram 2).

Diagram 2 – Protocol for Cell lysate preparation through boiling extraction of genomic DNA from cultured cells.

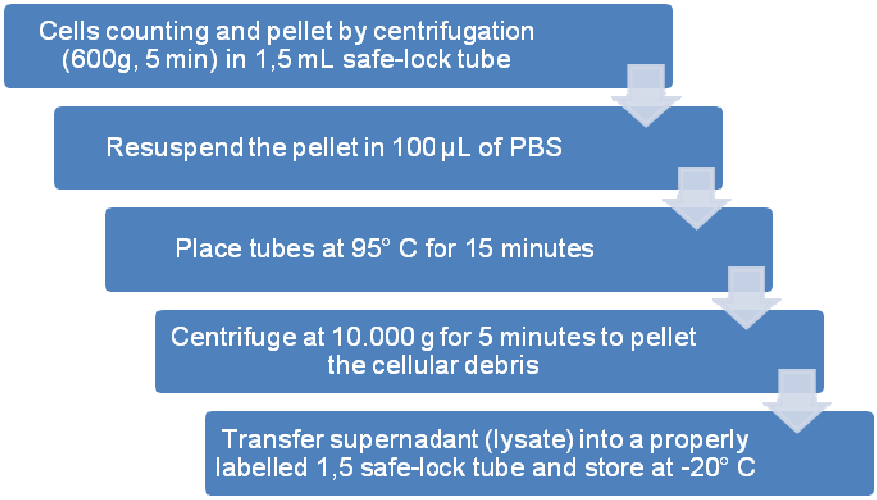

During the DNA extraction, filter tips were used to avoid cross-contamination. The procedure was done in Cabinet with circulating filtered air to protect the specimens from exogenous contaminations.

After the preparation described above in Diagram 2 the cell sample was sent to the Genomics and Proteomics core facility of DKFZ for the McCt assay to dectect contaminations as described by Schmitt & Pawlita (2009). The analyses are shown in Appendix 13 and 14.

2.2.4. Cryopreservation and thawing of cells

Cryopreservation of cells

For this a freezing medium was prepared at 37 °C using ready-to-use cell culture medium plus 20% FCS plus 10% DMSO.

Cells from an ongoing culture was firstly centrifuged in normal medium and then twice washed in freezing medium and after that centrifuged again. App. $1x10^6$ cells were suspended in freezing medium inserted in cryotubes, slowly freezed and stored at -196 °C in liquid nitrogen.

Thaw of cells

After the removal of the cryotube from the storage box, in which it was stored at -196 °C, the cell suspension was rapidly warmed up in a waterbath at 37 °C. The total volume (app. 1 mL) was removed and placed into culture medium prevously warmed at 37 °C (10 – 20 mL). After a first centrifugation (350 g for 10 min) of the cells, they were washed twice to achieve a complete removal of DMSO and resuspended in normal growth medium.

Then vitality of the cell was performed viable and dead cells determination with trypan blue in a hemocytometer. Here, the percentage of living cells should be on the total cell number of at least 80%. The cells were initially taken in a higher cell density than usual in culture, with a daily monitoring of the growth behavior and it was important a change of culture medium for the next few days.

2.2.5. Cultivation of cells

Cell passages of the adherent growing A240286S and Caco-2 cells lines

Before the passage of the cells, the color of the medium (containing phenol red) was assessed from red to yellow, what showed the strong comsuption of the medium ingredients. The cell culture flasks were inspected under the microscope to check confluency and any contaminations. This particular attention was paid to the density of the cell layer, which should be smooth and regular. For each cell line, there were passages of 30 and 10 mL culture flasks.

The A240286S cells there were passages every three to four days. For a 72-hour growth period, the density was 1.5 x 10^6 cells / 30 mL and 5 x 10^5 cells / 10 mL in tissue culture flasks with 75 and 25 cm^2 of ground surface, respectively. The lag time until the next passage of the cells was 96 hours, so a density of 9 x 10^5 cells / 30 mL was sufficient. The cultivation proved to be unproblematic, as the cells were not much sensitive. For the Caco-2 cells there were passages once a week and the densities were 2 x 10^6 cells / 30 mL and 7 x 10^5 cells / 10 mL. The medium was changed twice a week after 48h and 96h of growth.

The used cell culture medium was removed and the cell layer washed once with PBS. Following this, trypsin / EDTA solution (app. 1 mL / 10mL or 2 mL / 30 mL flask) was used to detach the cells, as to wet the bottom of the bottle (approx. 1 mL). Excess solution was immediately removed again and the flask was put in the incubator at 37 °C for 3 minutes to detachment the cells. For the Caco-2 cells it was necessary to incubate them for a longer time (15 min) for total detachment from the flask surface. The detached cells were completely added in 10 mL of culture medium (at 37 °C). By repeatedly pipetting up and down the cells could be avoided from cell clumps. By using an eletronic cell counter (Casy® 1), the density of the cell suspension was determined (50 or 100 µL cell suspension / 10 mL saline solution) as well as the diameter of the cells could be calculated and put in fresh medium.

2.2.6. Determination of the optimum growth density of the cell line A240286S

The cells were seeded at different cell densities in 150 mL culture medium / well and grown for 24h, 48h, 72h, and 96h and growth behavior was checked with the Sulforhodamine B method. Firstly, the culture medium was removed. The cells were then fixed with 100 µL fixing solution / well at - 20 ° C for 5 min, which after the fixation was removed. By several washes (5 times) with tap water that was flushed out as completely as possible, then the plate was let to dry under air stream of a work bench. To the fixed and dried cells was given 100 µL Sulforhodamine B-solution/well. The coloring was performed for 30 min in the dark. After treatment, the pink solution was removed and rinsed by at least four washes with 1% acetic acid. The Plate had to be tapped out vigorously on absorbent paper to remove the entire SRB supernatant, because this would distort the measurement result. After drying the cells under the air stream, the cellularly bound dye was brought back into solution with 100 µL Tris / well by shaking the plate for five minutes. The measurement was performed on a spectrophotometer (µ-Quant, Bio-Tek Instruments) at wavelengths of 520, 546, 565 and 680 nm.

2.2.7. Cytotoxicity experiments

All cytotoxicity experiments were performed in 96-well plates - according to the protocol of Sieger (1999). The cells were seeded at the optimal cell density determined above in 96-well plates in 150 µL culture medium / well and after 24 h of growth time, the substance (50 µL) to be tested was added to the medium. The evaluation was carried out 24h, 48h and 72h after the addition of the test compound with the method described above. For each measurement, controls with and without 0,4 % DMSO were run in which cells were grown without exposure to test compounds over the same period.

2.2.8. *Example of a Cell Culture Experiment Planning*

All the cell culture experiments were planned using the scheme shown in Table 3. The scheme is a standard model of a 96-well plate.

Table 3 – Scheme for planning cell culture assays using a 96-well plate.

	1	2	3	4	5	6	7	8	9	10	11	12
A												
B												
C												
D												
E												
F												
G												
H												

Because of variation in the absorption values observed before, the wells A1-A12, H1-H12, A1-H1 and A12-H12 were not used in the assays. For all experiments, each density of cells was seeded in 6 wells per 96 well plates and the experiments were carried out for five days. The different procedures for growth curves and cytotoxic assays are then described as follow.

The table 4 show an example of the first growth curve performed for the A240286S cells. For different plates were seeded with cells as shown.

Table 4 – First growth curve for the A240286S cells.

Wells	Cell density, cells/well
B2-G2	Medium (blank control)
B3-G3	1.0×10^3
B4-G4	2.0×10^3
B5-G5	5.0×10^3
B6-G6	1.0×10^4
B7-G7	2.0×10^4
B8-G8	5.0×10^4

For the first growth rate experiment for each cell line, it was important to check a wide range of cell densities and after that to check for an arrow density to find out the best density where the cells were growing in a better way (log phase). For all plates, the different density of cells were seeded on day one and after 24, 48, 72 and 96 h plates were analyzed under the microscope (to check presence of any contaminations) and the Sulforhodamine B assay was used to check the cell density.

The Table 5 shows the planning for the cytotoxicity assay for mangiferin in the A240286S cell line. All the assays were performed in 5 days.

Table 5 - Cytotoxicity assay for mangiferin.

Wells	Content
B2-G2	150 µL cells + 50 µL medium
B3-G3	150 µL cells + 50 µL DMSO/medium
B4-G4	150 µL cells + 50 µL 0.1 µM C1
B5-G5	150 µL cells + 50 µL 1.0 µM C1
B6-G6	150 µL cells + 50 µL 10 µM C1
B7-G7	150 µL cells + 50 µL 100 µM C1

For all assays, for plates were seeded with cells on the first day as shown in Table 5 but one of the plates was used as a control (blank) and was just seeded on B2-G2 and B3-G3 wells with 150 µL cells/well and Sulforhodamine B assay was performed after 24 g. The other three plates were seeded on the first day and on the second day, medium, DMSO/medium and mangiferin in different concentrations were added to the cells. After 24, 48 and 72h the plates were checked under microscope and the Sulforhodamine B assay was then performed.

3. Results and Discussion

3.1. Citotoxicity test for the cell lines A240286S and Caco-2 using the Sulforhodamine B – Staining Method

A differentiation between living and dead cells is not possible in this test method because the total protein content is determined. Microscopic observation have shown that dead cells from the adherent growing cell line A240286S lose the contact with the ground, and are removed from the culture flaks by removing the culture medium. The test, which is basically suitable for both adherent cells and suspension of cells, was used for the both adherent A240286S and Caco-2 cell lines to achieve a very high correlation between the parameters "total protein" and "vital cells".

Despite several implementation steps, the sulforhodamine B cytotoxicity assay can be well integrated with the laboratory routine, as there is a possibility of storage once the cells are fixed. This is a major advantage over other test methods that determine vitality of living cells, because the SRB test is independent of intermediary metabolism. After successful solvolysis of the dye in Tris solution, a measure must be conducted without much delay so that no evaporation takes place in the solution. The optical density can be determined over a wide range of visible wavelengths, where the maximum sensitivity is at 564 nm (Skehan et al., 1990).

We have also conducted an experiment using the LC-ESI-MS to screen the absorption spectra for Sulforhodamine B that achieved the maximum at 560 nm (Figure 7). Since the measured values up to 2.0 optical densities have a con linear behavior with the dye concentrations, a suboptimal wavelength of 520 nm was chosen for the experiments, which ensured the desired linearity.

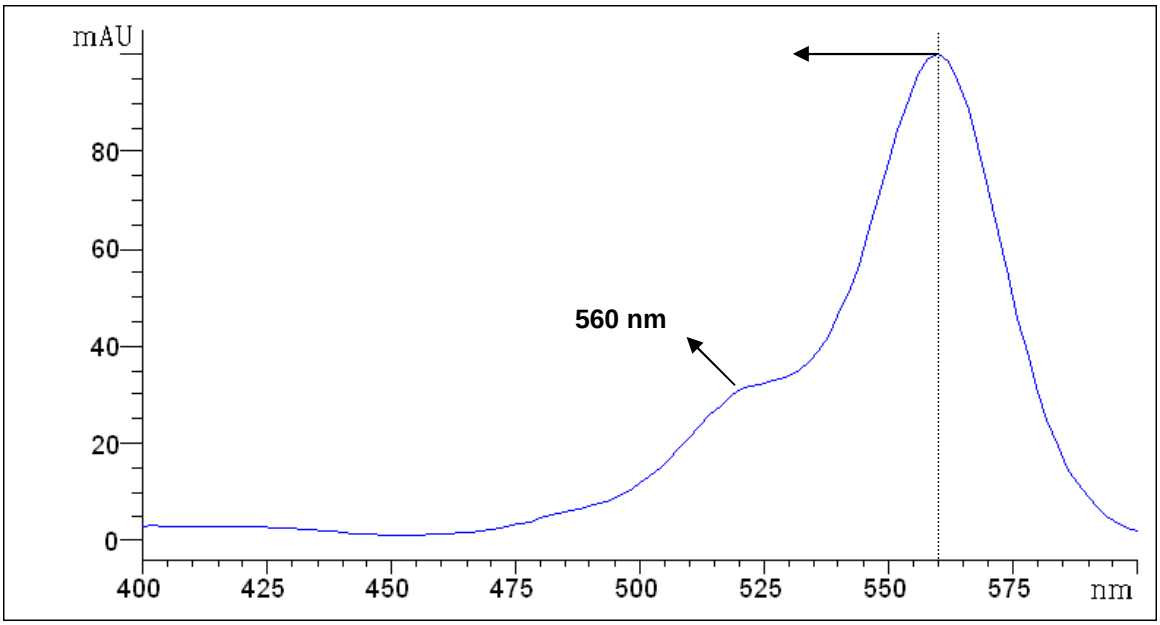

Figure 7 – UV Spectra for the Sulforhodamine B Solution.

For a discussion of the growth curves of cells A240286S find the following criteria:

- Increase in optical density (i.e growth) over 96h, because the cells should be observed in the planned cytotoxic experiment throughout this period;
- Largest possible slope of the curve to be able to differentiate easily among the planned cytotoxic experiments between cytostatic effects and death of the cells due to high cell densities;
- Optical density of at maximum 2 and low expression of standard deviation.

3.2.1. Growth Curves for the A240286S cells

The Figure 8 shows the growth curves performed for the A240286S cell line using the Sulforhodamine B dye as cell staining. The total number of cells was grown in 200 µL of medium and each density was seeded in 6 wells per 96 well plates.

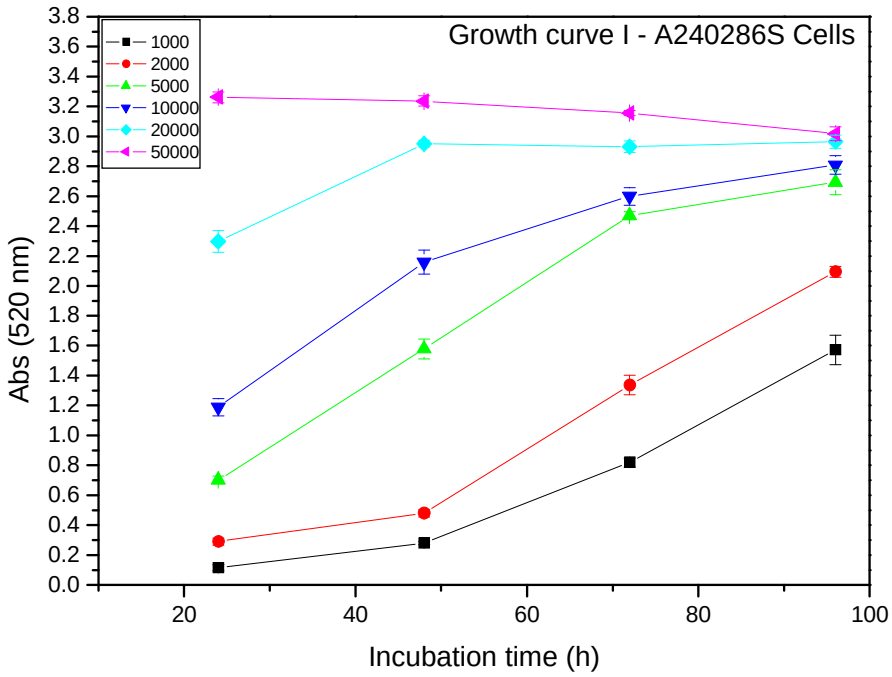

Figure 8 – First growth curve performed for the A240286S cell line.

The first growh curve (Figure 5) showed a wide growth spectrum at different cell densities. At 50,000 cells/well we see no growth of cells because of a too high cell density. Between 10,000 and 20,000 cells/well we can also observe a high density of cells. The best density showed to be at 2,000 cells/well but in order to investigate better conditions, a second growth curve was set up (Figure 9) to observe cell densities between 1,000 and 4,000 cells/well.

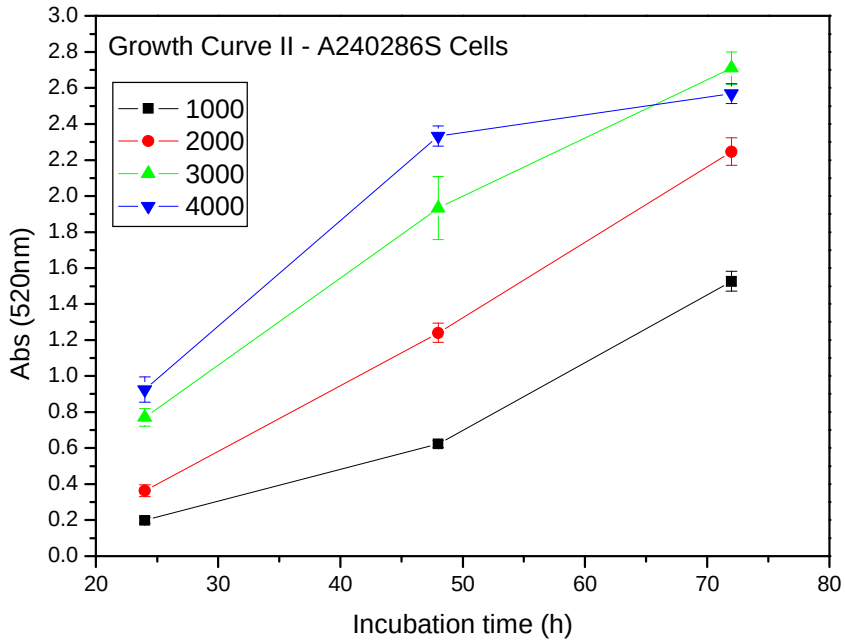

Figure 9 – Second growth curve performed for the A240286S cell line.

The best growing conditions were found to be at a cell density of 2 x 10^3 cells/200 µL. The cells were in log-phase over and showed up in very good growth, without passing into the stationary phase.

The log phase is characterized by active proliferation and during this phase the cell population is considered to be as its ´healthiest´ and that is why is preferred to use cells in log phase when assessing cell function (Davis, 2011).

With higher cell densities the measured values were at high absorbances (over 2), so that the significance of the results in these areas was unreliable. The growth behavior of the lowest cell density had to be judged to be growing slowly.

After the fourth experiment a third growth curve (Figure 10) was performed to investigate the growth behaviour of the cells. The best growth condition was set up to 1.5 x 10^3 / well for the fifth experiment. All the growth curves were determined using the SRB method assay.

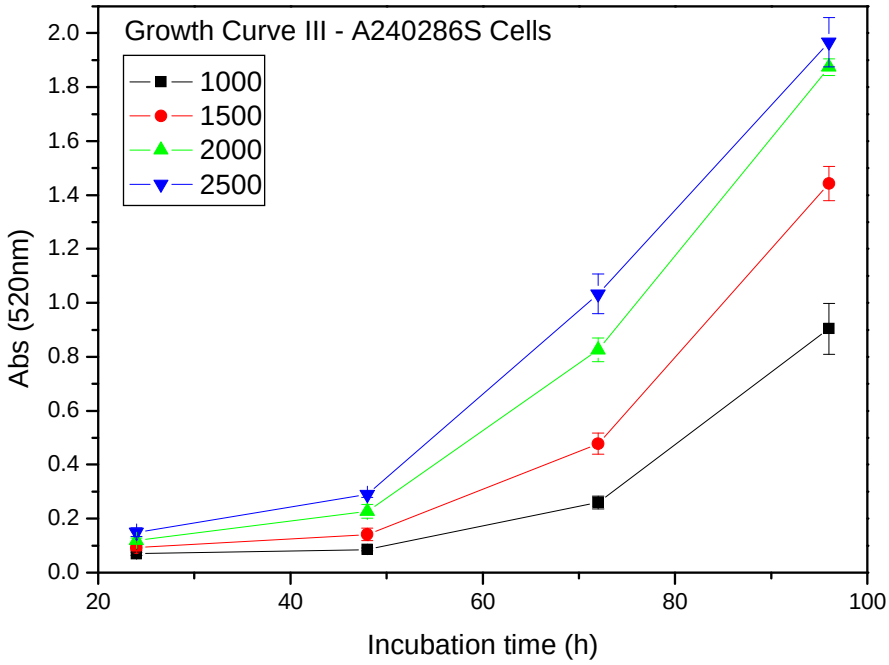

Figure 10 – Third growth curve performed for the A240286S cell line.

A Photo documentation of the growth behavior of the cells was performed. The Figures 11 and 12 shows the growth of the cell line A240286S.

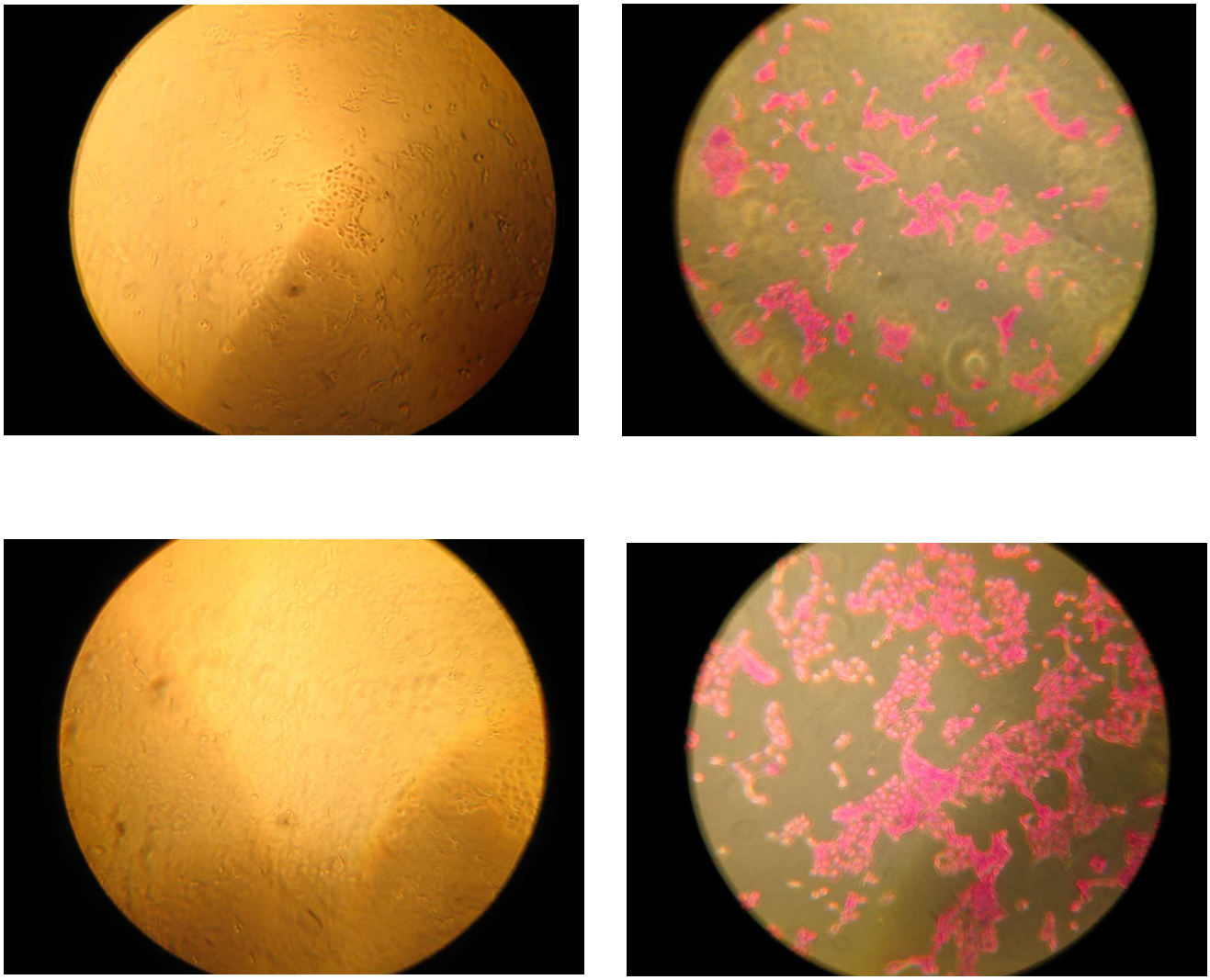

Figure 11 – Growth of the cell line A240286S after 24 (A) and 48h (B) without (1) and with (2) the staining SRB dye.

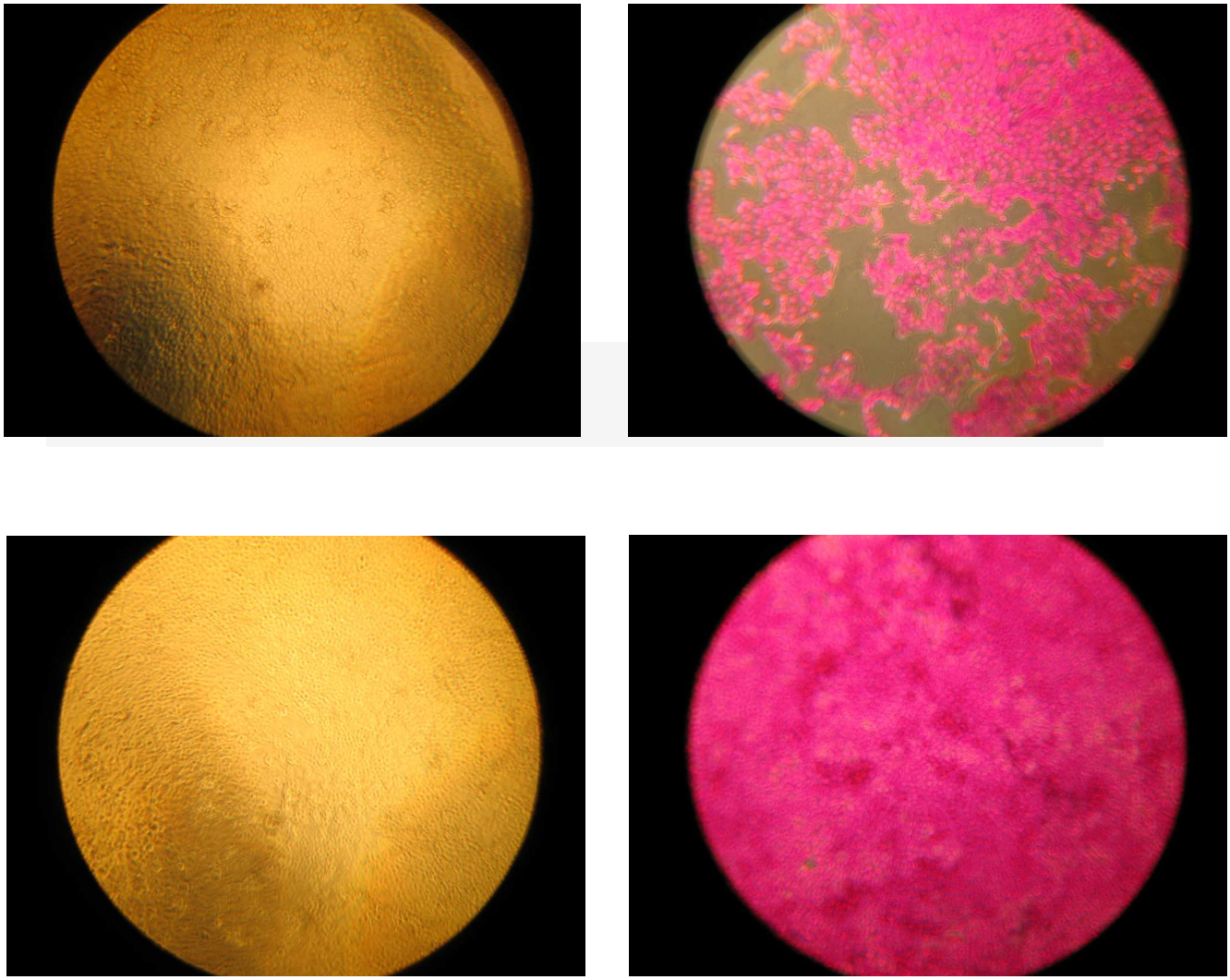

Figure 12 – Growth of the cell line A240286S after 72 (C) and 96h (D) without (1) and with (2) the staining SRB dye.

The cells of the cell line A240286S grows adherent to the bottom of the culture vessel. Where, after 24h observation, the cells were spread in the area until a single-cell layer almost completely covered the ground. The cell line A240286S grows as monolayers, ie there is no multilayered accumulation of tumor cells.

3.2.2. Growth Curves for the Caco-2 cells

Growth curves were also performed for the Caco-2 cell line (Figures 13) using the Sulforhodamine B dye as cell staining. As for the other cell line A240286S, the total number of cells was grown in 200 µL of medium.

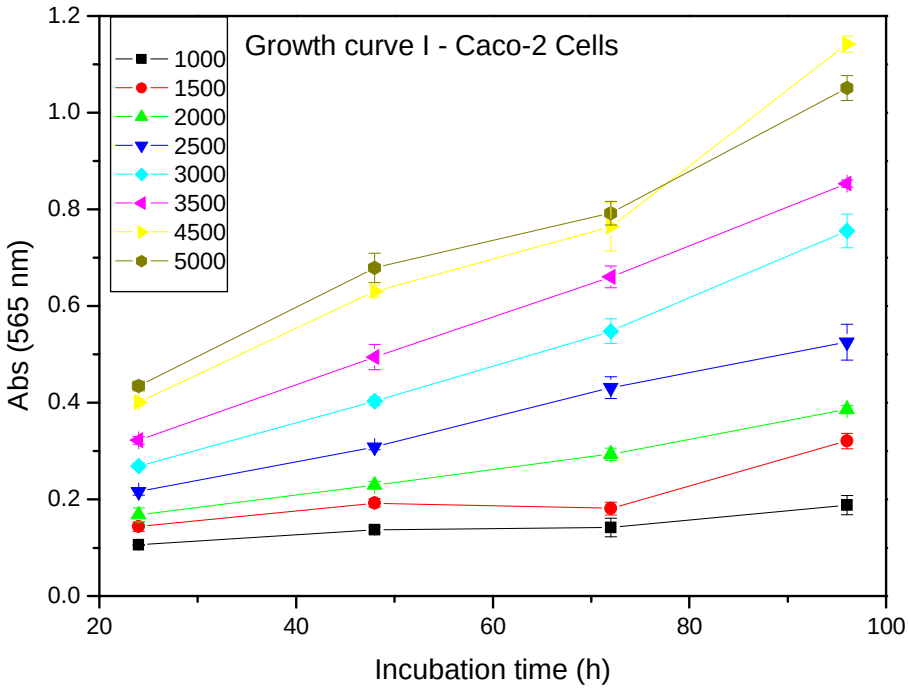

Figure 13 – First growth curve performed for the Caco-2 cell line.

The cell densities between 1,000 and 2,500 cells/well showed to have grown very slowly with a too long lag phase probably due to the low density of cells. The best growth behavior was found for 4,500 and 5,000 cells/well. A second growth curve assay was then set up to investigate higher densities between 2,500 and 6,500 cells/well (Figure 14).

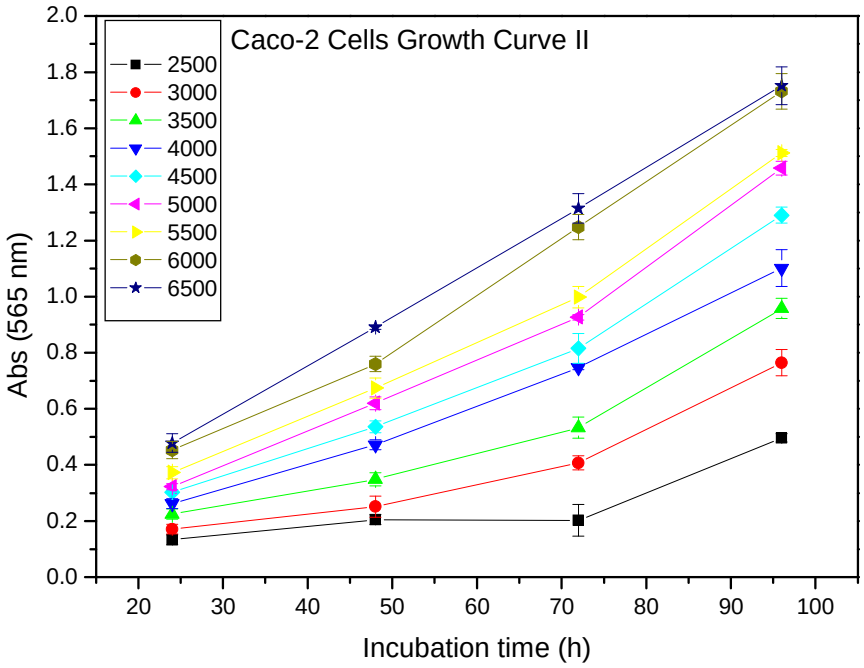

Figure 14 – Second growth curve performed for the Caco-2 cell line.

The best growing conditions were found to be at a cell density of 5 x 10^3 cells/200 µL where the cells were in log-phase and showed up in very good growth, without passing into the stationary phase. This cell density was then chosen to carry out the cytotoxicity experiments with the Caco-2 cell line.

A Photo documentation of the growth behavior was performed for the Caco-2 cells. The Figures 15 shows the growth of the cell line during the SRB Method.

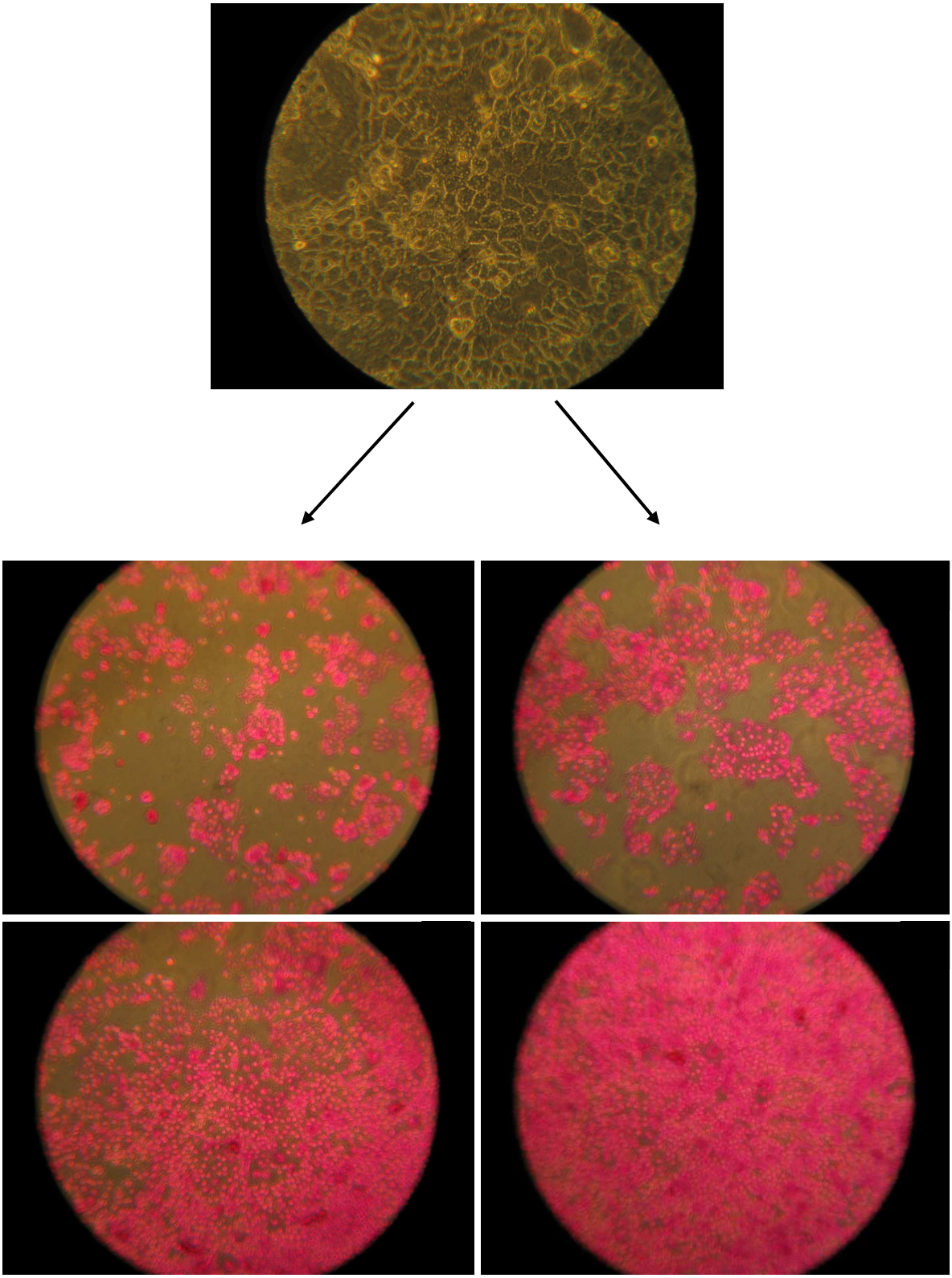

Figure 15 – Growth of the Caco-2 cell line before staining (A) and after 24 (B) and 48h (C) 72 (D) and 96h (E) with the staining SRB dye.

3.3. In vitro cytotoxicity assays with the cell line A240286S

3.3.1. Effect of mangiferin and metabolites on the cells

After establishing optimal testing procedures for the cell line A240286S and understanding of the growth behavior in a variety of preliminary tests, the results for the cytotoxyc experiments are presented below. In these experiments we investigated if either mangiferin (C1) or its metabolites norathyriol (C2) and homomangiferin (C4) are cytotoxic compounds. The experiments were all carried out in complete medium (10% FCS). The Figure 16 shows the dose-dependent toxicity of mangiferin after 24/48/72 hours of incubation.

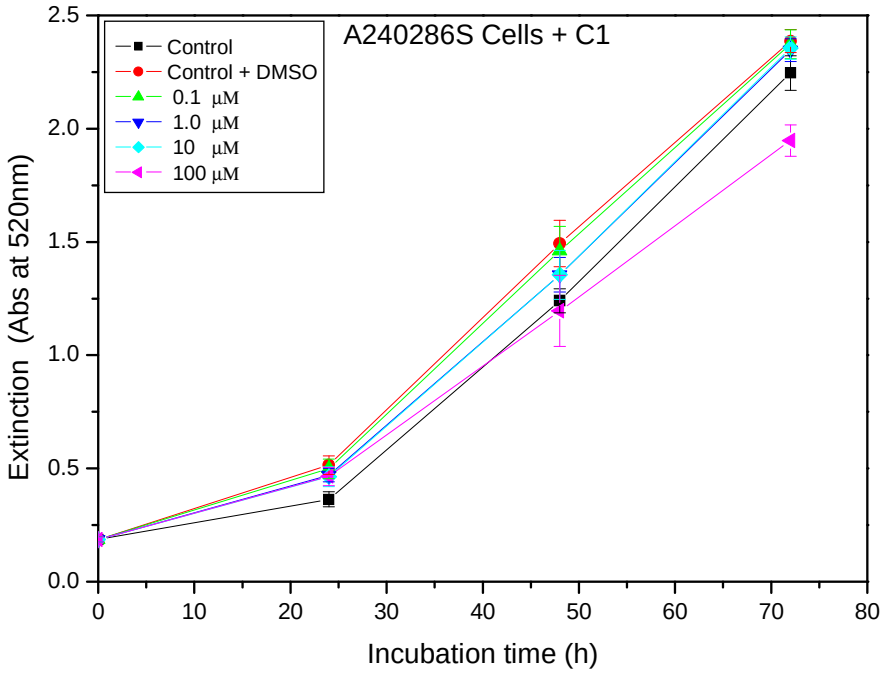

Figure 16 – Effect of mangiferin at different concentrations (0.1 µM, 1 µM, 10 µM, 100 µM) on the cell line A240286S. Cell density = 2.0 x 10^3 cells/well.

In the Figure 15 we can observe that mangiferin did not have strong activity on the growth rate of the cell line A240286S. Except for some inhibition at 100 µM we can see no effect and no IC_{50} calculation was possible for the substance.

The effect was observed to be different for the main metabolite of mangiferin, norathyriol, as can be seen in Figure 17.

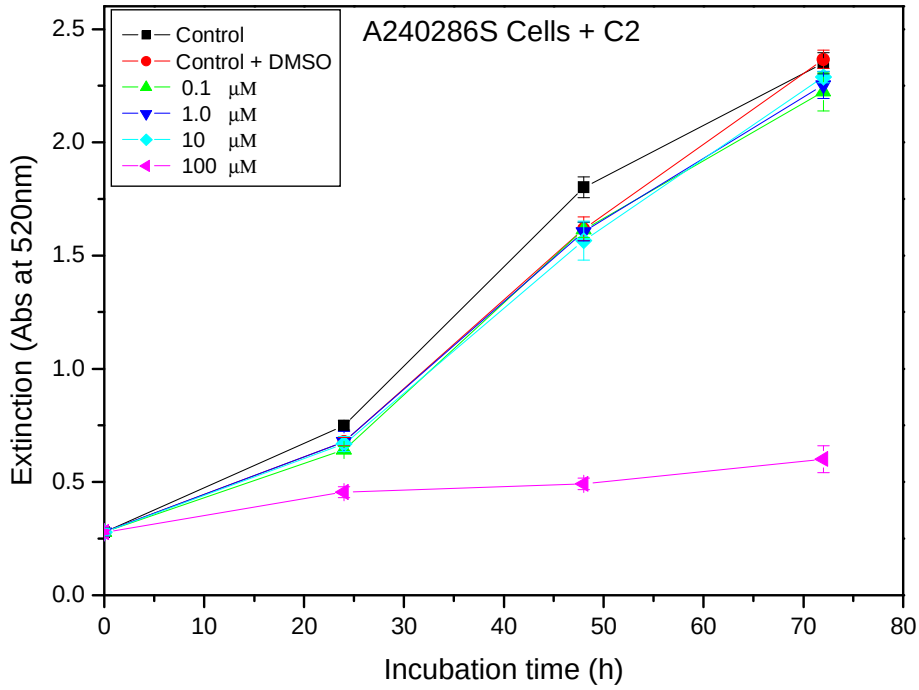

Figure 17 – Effect of norathyriol at different concentrations (0.1 µM, 1 µM, 10 µM, 100 µM) on the cell line A240286S. Cell density = 2.0 x 10^3 cells/well.

The substance showed good activity at concentration 100 µM in the growth inhibition of the cancer cell line investigated as can be observed above. As we cannot observe death of cells we may assume that norathyriol has a cytostatic effect against the lung adenocarcinoma cells.

Cytostatics are substances that particularly affect proliferating or dividing cells. Rapidly dividing malignant cells are preferentially injured. Damage to mitotic processes not only retards tumor growth but may also initiate apoptosis (programmed cell death). Tissues with a low mitotic rate are largely unaffected; likewise, most healthy tissues. This, however, also applies to malignant tumors consisting of slowly dividing differentiated cells. Tissues that have a physiologically high mitotic rate are bound to be affected by cytostatic therapy (Lüllmann et al, 2000).

In order to find out from which concentration would norathyriol have some activity and to determine the IC_{50} value for the compound in the cell line, a repeated assay with a different range of concentrations was performed (Figure 18). This time we could observe a concentration-dependence effect between 10 and 100 µM. In this experiment we could observe that even at a concentration of 40 µM, norathyriol showed some inhibition activity against the cells and much higher when at 60 µM. At a concentration of 80 µM the cytostatic activity was close to the concentrations of 100 µM already observed before.

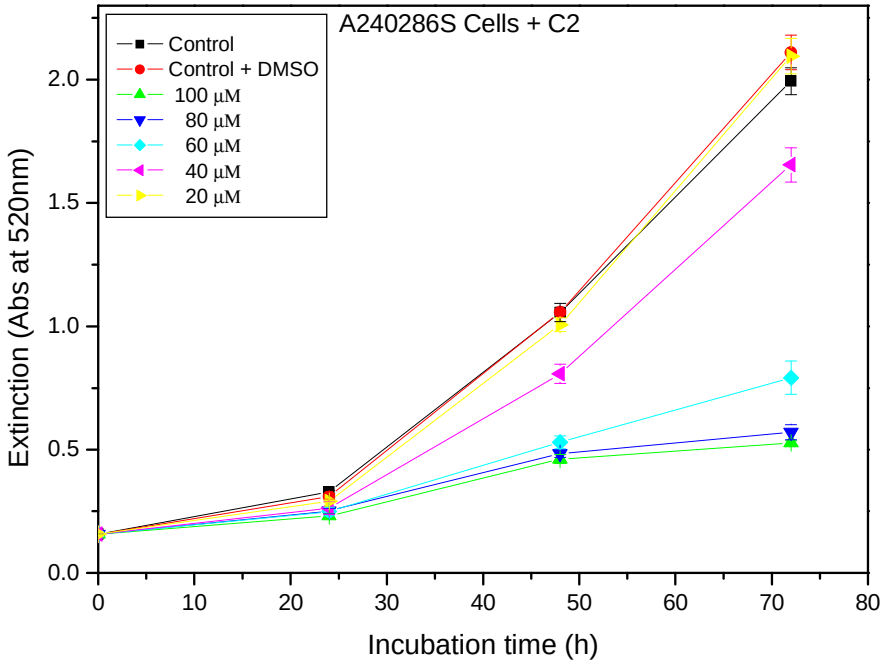

Figure 18 – Effect of norathyriol and at different concentrations (20 µM, 40 µM, 60 µM, 80 µM and 100 µM) on the cell line A240286S. Cell density = 2.0 x 10^3 cells/well.

One explanation for the cytostatic activity of norathyriol is that after the deglycosilation of mangiferin, the substance becomes more lypohilic and due to that it could penetrate better the cell membrane causing damages to the cells.

A cytotoxic essay was also performed for another mangiferin metabolite, homomangiferin, as can be seen in Figure 19.

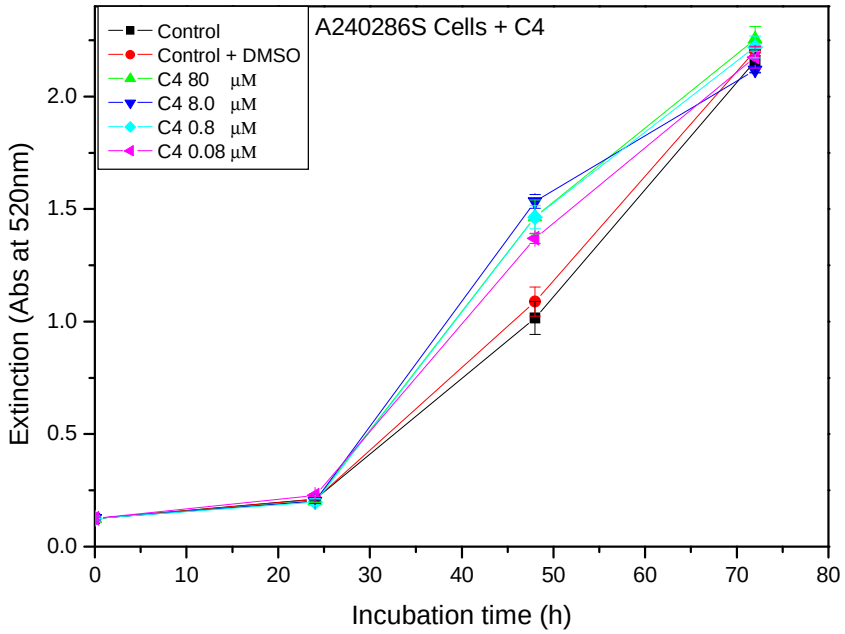

Figure 19 – Effect of homomangiferin and at different concentrations (0.1 µM, 1 µM, 10 µM, 100 µM) on the cell line A240286S in the SRB-Test. Cell density = 1.5 x 10^3 cells/well.

For this compound no cytotoxic activity was detected. The result was similar to that of mangiferin and this is probably due to the structure of homomangiferin which is similar to mangiferin with the difference that one hydroxyl groups is methylated.

3.3.2. Effect of gallic acid and synergy of mangiferin/gallic acid on the cell line A240286S

A cytotoxic essay was also performed to investigate the activity of gallic acid, wich is also one of the main compounds found in *mangiferina indica L.* extracts, on the cell line A240286S. The results can be seen in Figure 20.

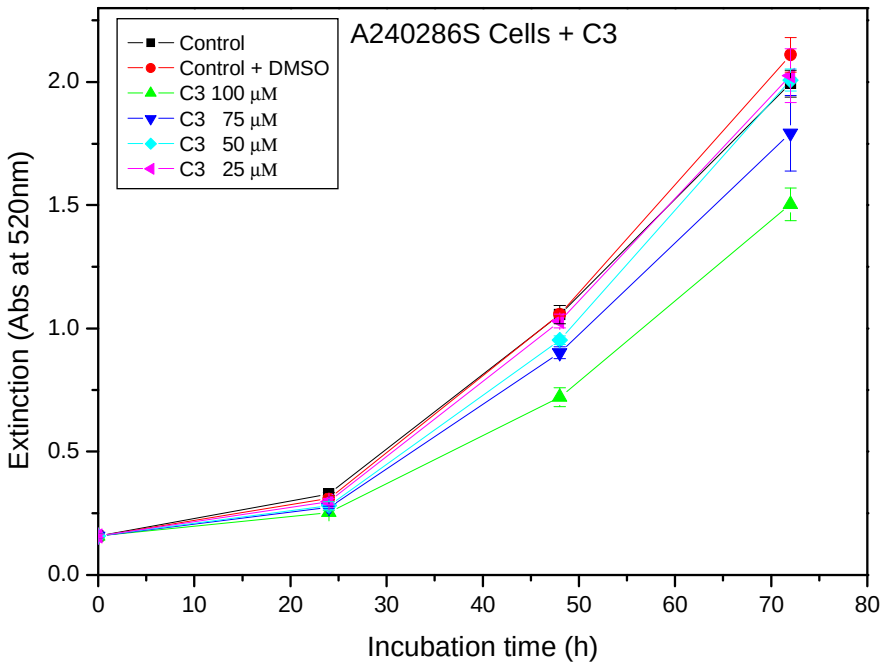

Figure 20 – Effect of gallic acid and at different concentrations (25 µM, 50 µM, 75 µM, 100 µM) on the cell line A240286S in the SRB-Test. Cell density = 2.0 x 10^3 cells/well.

For this essay, a cytotoxic screen was performed in a concentration range from 25 to 100 µM. Some cytostatic activity was observed at the concentration of 75 µM but at the highest concentration of 100 µM we could see a better activity of the substance against the cells.

A synergistic study was performed mixing the compounds mangiferin and gallic acid in order to investigate this effect on the cancer cells (Figure 21).

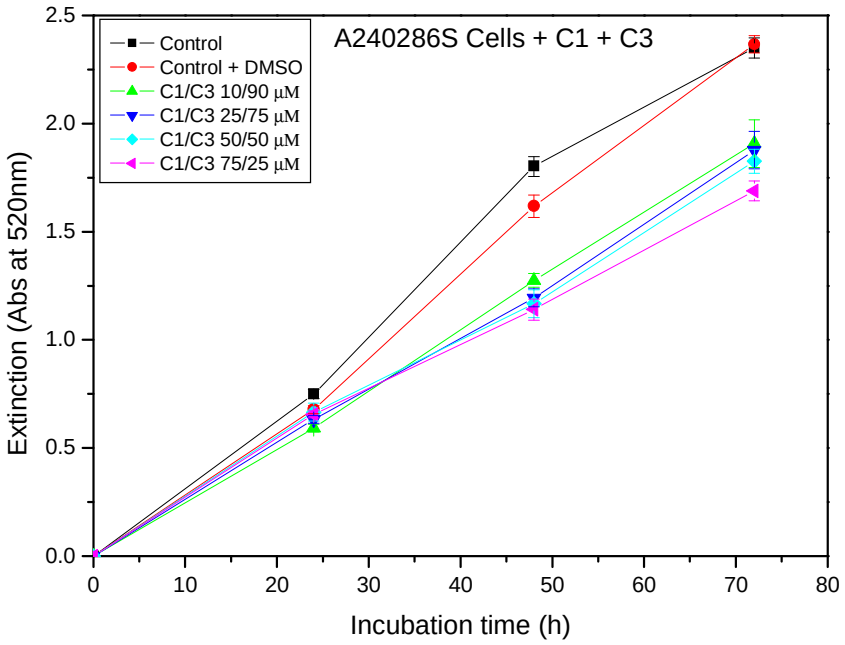

Figure 21 – Synergistic effect of mangiferin/gallic acid and at different concentrations (10/90 µM, 25/75 µM, 50/50 µM, 75/25 µM) on the cell line A240286S. Cell density = 2.0 x 10^3 cells/well.

A range of concentration was chosen in which we could observe the effect of a higher amount of each one of the compounds (e.g. 10/90 µM) as well as the effect of the same amount (50/50 µM) of each compound. We can observe that as long as the concentration of mangiferin enhances, better is the activity against the cells showing the best activity at 75/25 µM mangiferin/gallic acid. The result showed to be surprisingly as gallic acid alone had shown to have better activity compared to mangiferin itself.

3.3.3. Calculating IC_{50} values for the cytotoxic activity against the A240286S cell line

The IC_{50} parameter is defined as the concentration of compound that causes 50 % reduction in viable cell count (Gomes et al., 2007). A calculation of IC_{50} values was possible for the compound that showed better activity, norathyriol. The IC_{50} calculations were done using the program tablecurve-fitting routines in the software package (Jandel Scientific, Chicago, IL). The IC_{50} value for norathyriol was found to be the best, 51 µM, against the non-small lung carcinoma cell line A240286S (Figure 22).

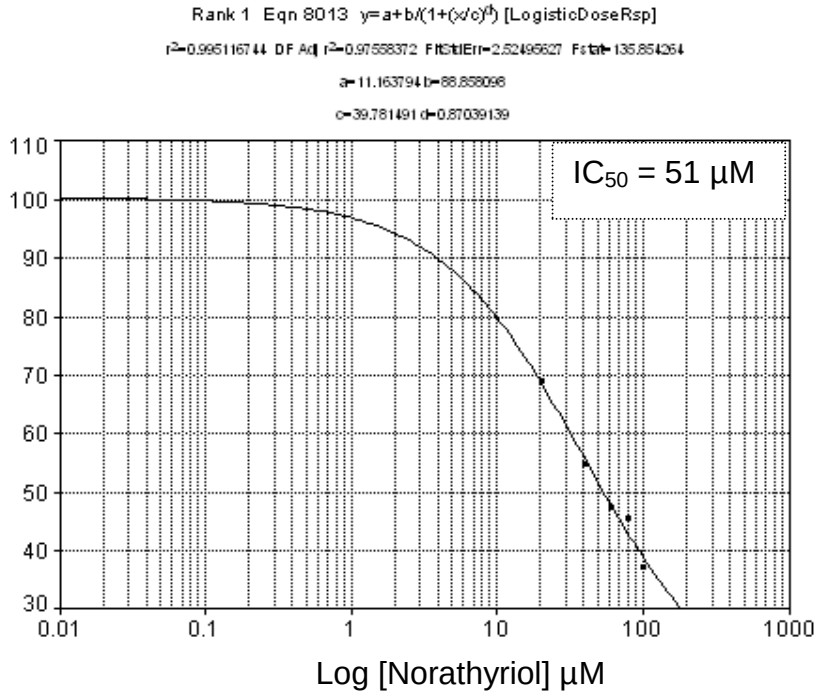

Figure 22 – IC_{50} calculation for Norathyriol at 72h assay with A240286S cell line.

3.4. In vitro cytotoxicity assays with the Caco-2 cell line

3.4.1. Effect of mangiferin and metabolites on the cells

As for the cell line A240286S, an understanding of the growth behavior of the Caco-2 cell line in a variety of preliminary tests was very important. The results for the cytotoxicity experiments are presented below. In these experiments we also investigated if either mangiferin (C1) or its major metabolite norathyriol (C2) are cytotoxic compounds. The experiments were all carried out in complete medium (15% FCS). The Figure 23 shows the dose-dependent activity of mangiferin after 24/48/72 hours of incubation.

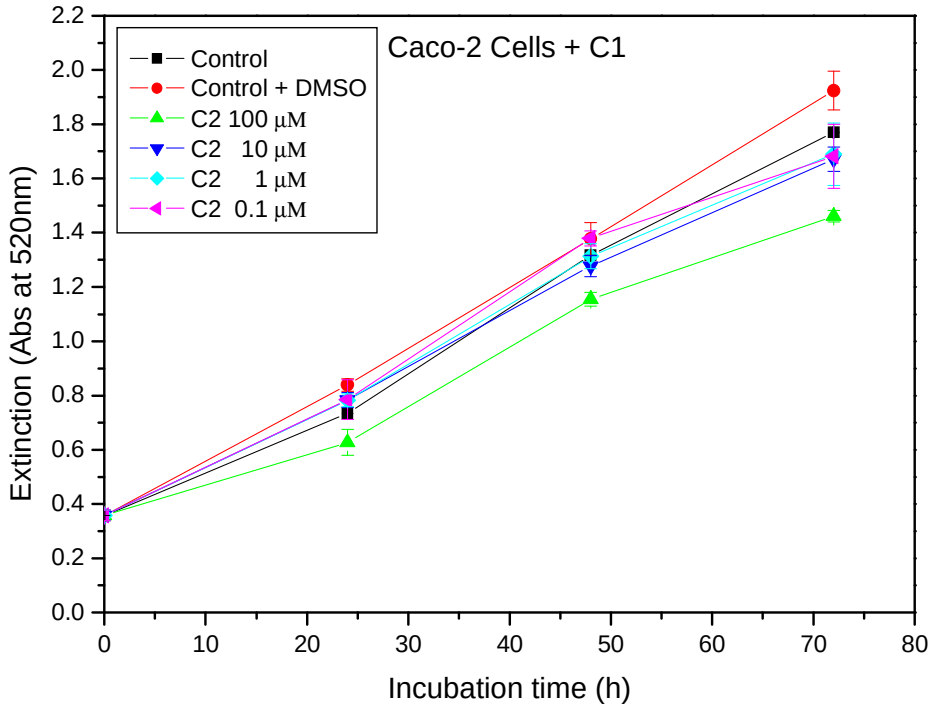

Figure 23 – Effect of mangiferin at different concentrations (0.1 µM, 1 µM, 10 µM, 100 µM) on the Caco-2 cell line. Cell density = 5.0 x 10^3 cells/well.

In the Figure 22 we can observe that mangiferin was not active on the growth rate of the Caco-2 cell line in the concentration range of 0,1 – 100 µM. Except for some a little growth inhibition at 100 µM and no IC_{50} calculation was possible for the substance.

As expected, the effect was observed to be much higher for the main metabolite of mangiferin, norathyriol, as can be seen in Figure 24. In the Figure we can observe an interesting concentration-dependence effect between 10 and 100 µM showing between cytostatic and cytotoxic activity

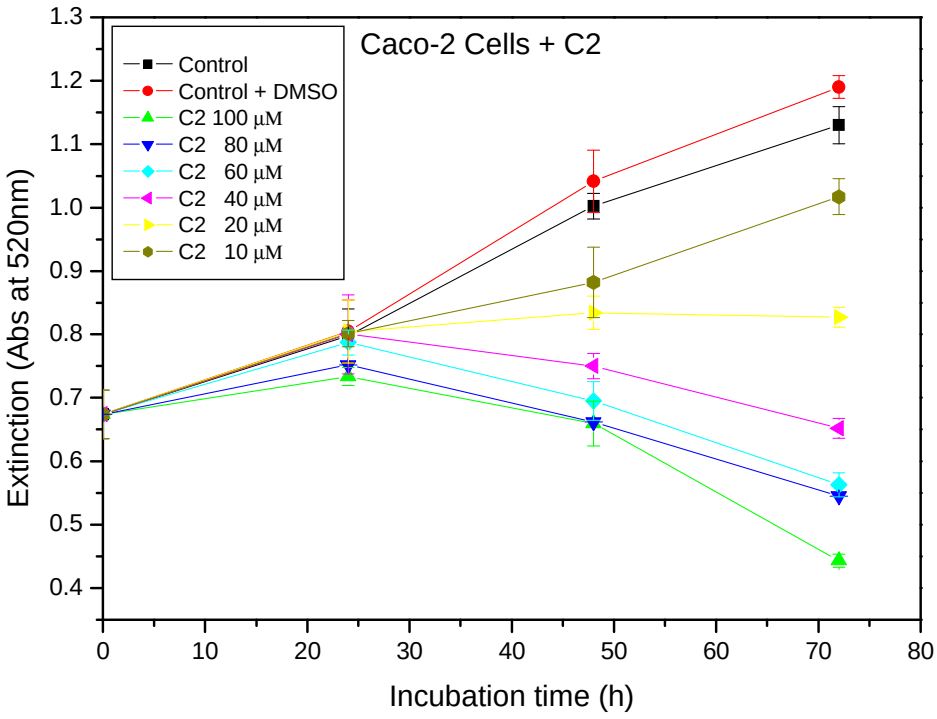

Figure 24 – Effect of norathyriol at different concentrations (10 µM - 100 µM) on the Caco-2 cell line. Cell density = 5.0 x 10^3 cells/well.

The substance norathyriol showed already some activity at concentrations of 10 µM and untill 40 µM we can observe the growth inhibition of the cancer cell line showing cytostatic activity. Above the concentration of 60 µM we can observe cytotoxicity effects close to that for 80 µM. The concentration of 100 µM showed the best cytotoxic effects killing Caco-2 cells.

3.4.2. Calculating IC_{50} values for the cytotoxic activity against the Caco-2 cell line

A calculation of IC_{50} value against the Caco-2 cell line was not possible for mangiferin but for the compound norathyriol (51 µM) which showed good activity and is shown in Figure 25. The IC_{50} calculations were done using the program tablecurve-fitting routines in the software package (Jandel Scientific, Chicago, IL).

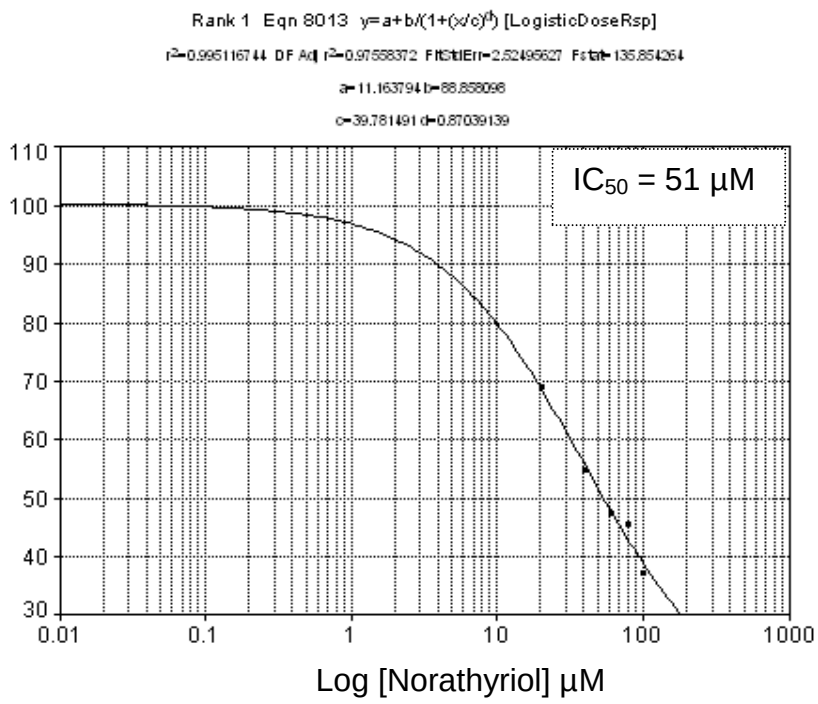

Figure 25 – IC_{50} calculation for norathyriol at 72h assay with Caco-2 cell line.

Norathyriol showed also a good anticancer activity against the Caco-2 cell line as for the bronchial carcinoma cell line with approximately the same values of IC_{50}. The main difference was that norathyriol exhibited cytotoxic in addition to cytostatic activity, a higher concentrations of 60-100 µM. That would be probably due to different mechanisms, inhibiting different pathways once it is thought to penetrate the cell membrane. A very important following step would be to investigate the cytotoxic effects on immortalized normal cell lines (such as immortalized intestinal cell lines) as well as to follow the investigation of norathyriol anticancer-tumor supression activities in mice.

4. Conclusions

Our in vitro experiments suggest that the compounds possess anticancer potential in different levels. Norathytiol showed cytostatic effect on the A240286S cell line and cytostatic/cytotoxic effects on the Caco-2 cell line.

García-Rivera *et al.* (2011) have identified various target molecules in different transcription factor NFkB cancer pathways in metastatic breast cancer cells, which are sensitive to treatment with Vimang extract and its constituents mangiferin and gallic acid. Their experiments regards the understanding the mechanism of action of this phytomedicine in cancer cells, basically for the modulation of NFkB activity at the crossroad of inflammation and cancer. They identify gallic acid as an essential component, besides mangiferin for the anticancer effects of Vimang extract. Those results are in agreement to the results observed, even thouth no much effect was observed for gallic acid on caco-2 cell line.

Li *et al.* (2012) have recently reported that norathyriol inhibited *in vitro* cell growth in mouse skin epidermal JB6 P+ cells at the level of G2-M phase arrest suppressing solar UV-induced skin carcinogenesis. The chemopreventive activity was found to be by inhibiting the ERK 1/2 Kinase dependent activity of transcriptional factors AP-1 and NF-kB during UV-induced skin carcinogenesis. They have identified norathyriol as a safe highly effective new chemopreventive agent against development of UV-induced skin cancer. Inhibition of kinases may be one of the possible mechanisms of norathyriol against the cell lines studied.

Our experiments suggests that norathyriol, the main metabolite of mangiferin, have a great impact on the activity of mangiferin in supressing tumor cancer cells as we observed for the non-small lung cells and colon cancer cells lines. Further experiments should be done on the mechanistic effects and on pathways inhibition of the compounds on the colon cancer cell lines studied.

5. Acknowledgments

The authors would like to express their thanks for the financial support from CNPq, CAPES/Daad Sandwich Doctorate program.

6. References

Aniara Screening Tools. SRB Sulforhodamine B (300). Retrived in April 10, 2012, from http://www.aniara.com/mm5/merchant.mvc?Store_Code=ANIA&Screen=PROD&Category_Code=srb&Product_Code=AKSR96-300.

BI Biological Industries. Trypsin & Cell Dissociation. Retrived in April 10, 2012, from http://www.bioind.com/product_list?c0=12274.

Cancer Research UK. Cancer Worldwide - the global picture. Retrieved April 10, 2012, from http://info.cancerresearchuk.org/cancerstats/world/the-global-picture/cancer-overall-world.

Chan, A. T. & Giovannucci, E. L. (2010). Primary Prevention of Colorectal Cancer. *Gastroenterology*, 138, 2029–2043.

Davis, J. M. Animal cell culture: essential methods. 2011 by John Wiley & Sons Ltd.

Eschen, N., (2004), Untersuchung zur Zytotoxizität und zum Wirkmechanismus der Antifolatkonjugate Aminopterin-Humanes Serumalbumin und Methotrexat-Humanes Serumalbumin an zwei humanen Tumorzellinien. Doktorarbeit, Universität Heidelberg.

Estimate 2012: incidência de câncer no Brasil / Instituto Nacional de Câncer José Alencar Gomes da Silva, Coordenação Geral de Ações Estratégicas, Coordenação de Prevenção e Vigilância. – Rio de Janeiro : Inca, 2011. 118.

Ferlay, J., Shin, H.R., Bray, F., Forman, D., Mathers, C., Parkin, D.M. GLOBOCAN 2008 v1.2, Cancer Incidence and Mortality Worldwide: IARC CancerBase No. 10. Lyon, France: International Agency for Research on Cancer, 2010. Available from: http://globocan.iarc.fr. Graph prepared by Cancer Research UK

Fogh, J., Fogh, J. M., Orfeo, T. One hundred and twenty seven cultured human tumor cell lines producing tumors in nude mice. Journal of the National Cancer Institute. 59 (1977) 221-6.

Fogh, J. & Trempe, G. Human Tumor Cells In Vitro. (J. Fogh, ed.), Plenum, 1975, 115-141.

Gomes, A., Choudhury, S. R., Saha, A., Mishra, R., Giri, B., Biswasa, A. K., Debnath, A., Gomes, A. (2007). A heat stable protein toxin (drCT-I) from the Indian Viper (Daboia russelli russelli) venom having antiproliferative, cytotoxic and apoptotic activities. *Toxicon*, 49, 46–56.

Jemal, A., Bray F., Center M. M., Ferlay, J., Ward E., Forman D. Global Cancer Statistics. (2011). *CA: A Cancer Journal for Clinicians*, 61, 69–90.

García-Rivera D., Delgado R., Bougarne N., Haegeman G., Berghe W. V. (2011). Gallic acid indanone and mangiferin xanthone are strong determinants of immunosuppressive anti-tumour effects of Mangifera indica L. bark in MDA-MB231 breast cancer cells. *Cancer Letters,* 305, 21–31.

Granzow, C., Drings, P., Kopun, M. (1998). Identifizierung von Chemosensitivität bei menschlichen Tumorzellen durch flavinschützende Tests in vitro, 328-332. Springer Verlag Berlin Heidelberg.

Langford, K. J., Askham, J. M., Lee, T., Adams, M. Ewan, E. M. (2006). Examination of actin and microtubule dependent APC localisations in living mammalian cells. *BMC Cell Biology*, 7(3), 1-18.

Li, J., Malakhova, M., Mottamal, M., Reddy, K., Kurinov, I., Carper, A., Langfald, A., Oi, N., Kim, M. O., Zhu, F., Sosa, C. P., Zhou, K., Bode, A. M., Dong, Z. (2012). Norathyriol suppresses skin cancers induced by solar ultraviolet radiation by targeting ERK kinases. *Cancer Research,* 72, 260-270.

Lüllmann, H., Mohr, K., Ziegler, A., Bieger, D., Wirth J. (2000). Color Atlas of Pharmacology. 2nd Edition, Thieme, 296-297.

Mahaffey, C. M., Zhang H., Rinna A., Holland W., Mack P. C., Forman H. J. (2009). Multidrug-resistant protein-3 gene regulation by the transcription

factor Nrf2 in human bronchial epithelial and non-small-cell lung carcinoma. *Free Radical Biology & Medicine,* 46, 1650–1657.

MetroHealth. Academic Health Care System. Lug Cancer. Retrieved December 07, 2011, from http://www.metrohealth.org/body.cfm?id=1635.

National Cancer Institute (US). General Information About Non-Small Cell Lug Cancer. Retrieved November 8, 2011, from http://www.cancer.gov/cancertopics/pdq/treatment/non-small-cell-lung/Patient/page1.

National Cancer Institute (US). The Colon and Rectum. Retrieved November 8, 2011, from http://www.cancer.gov/cancertopics/wyntk/colon-and-rectal/page2.

National Cancer Institute (US). Surveillance Epidemiology and End Results. Retrieved November 8, 2011, from http://www.cancer.gov/cancertopics/wyntk/colon-and-rectal/page2.

Schmitt, M., & Pawlita, M. (2009). High-throughput detection and multiplex identification of cell contaminations. *Nucleic Acids Research*, 37, 119.

Sigma-Aldrich. Sulforhodamine B, acid form. Retrieved in April 10, 2012, from http://www.sigmaaldrich.com/catalog/product/aldrich/341738?lang=de&region=DE.

Sieger, S., (1999), Kombinierte Wirkung zweier neuer Zytostatikakonjugate auf Tumorzellinien unterschidlicher Sensivität. Diplomarbeit, Universität Konstanz.

Skehan, P., Storeng R., Scudiero D., Monks A., McMahon J., Vistica D., Warren J. T., Bokesch H., Kenney S., Boyd M. R. (1990). New Colorimetric Cytotoxicity Assay for Anticancer-Drug Screening. *Journal of the National Cancer Institute*, 82, 13.

Thapa, D., & Ghosh, R. (2012). Antioxidants for prostate cancer chemoprevention: Challenges and opportunities. *Biochemical Pharmacology*, 83, 1319–1330.

Voigt, W. Sulforhodamine B Assay and Chemosensitivity. Methods in Molecular Medicine, vol. 110: Chemosensitivity: Vol. 1: In Vitro Assays. Edited by: R. D. Blumenthal. Humana Press Inc., Totowa, NJ.

World Cancer Research Fund / American Institute for Cancer Research. (2007). Food, Nutrition, Physical Activity, and the Prevention of Cancer: a Global Perspective.Washington DC: AICR.

Zhong, M., Ma, X., Sun C., Chen, L. (2010). MicroRNAs reduce tumor growth and contribute to enhance cytotoxicity induced by gefitinib in non-small cell lung cancer. *Chemico-Biological Interactions,* 184, 431–438.

Final Conclusions

Pectin samples were successfully isolated from pumpkin, characterized and used with chitosan to encapsulate mangiferin using spray-drying technique for oral drug delivery formulations.

Studies suggest that most of mangiferin content, when taken orally, will not reach hepatic metabolism but will be more available in the colon, where it can be converted by bacterial enzymes in the gut to other metabolites which some of them may have even more pronounced activities as the parent prodrug mangiferin. Intestinal simulations showed that mangiferin is most metabolized to norathyriol in different rates depending on the gut bacteria population. Cytotoxic studies showed that norathyriol has higher cytotoxic activity compared to mangiferin. In this context mangiferin can be classified as a prodrug which has as target a bacterial enyzme, which will convert it to its main metabolite, norathyriol (Figure 1).

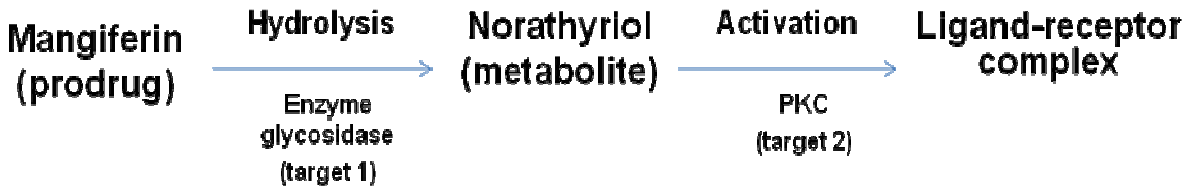

Figure 1 - Possible mechanism pathway for the anticancer activity of mangiferin.

One possible mechanism for norathyriol is inhibition of protein kinases such as that reported by Li et al. (2011). Another possible mechanisms reported by natural compounds are those like inhibition of DNA replication, interaction of microtubules, interference on signal transduction pathways or other ones. The investigation of the action mechanism of norathyriol on cancer cells would be, therefore, one of the next steps to be performed. Future studies could focus also on effects of mangiferin and its main metabolite, norathyriol, in mice.

Appendix 1 – Figure 8

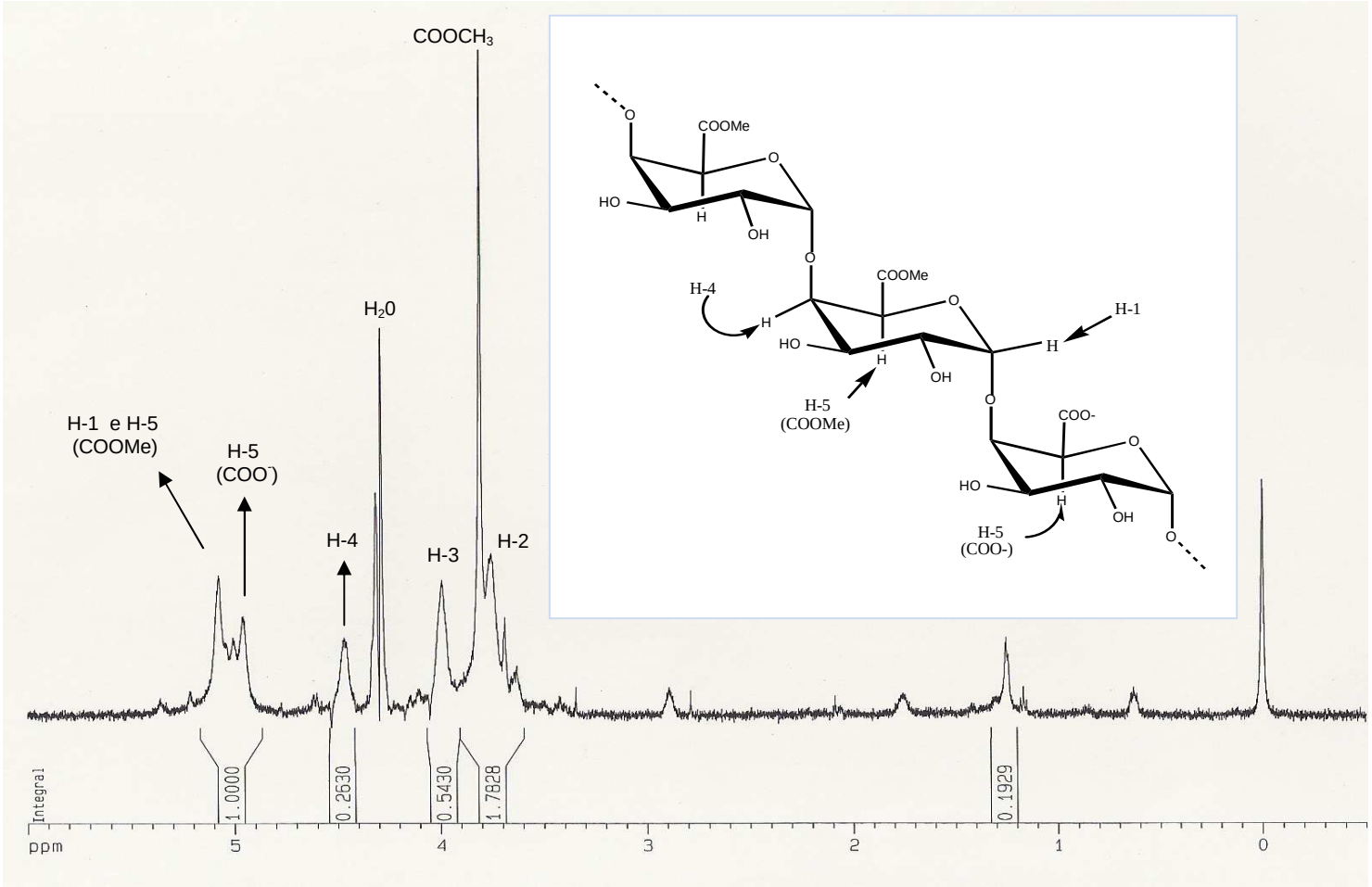

Figure 8 - ^{1}H NMR spectrum of pectin.

Appendix 2 – Figure 9

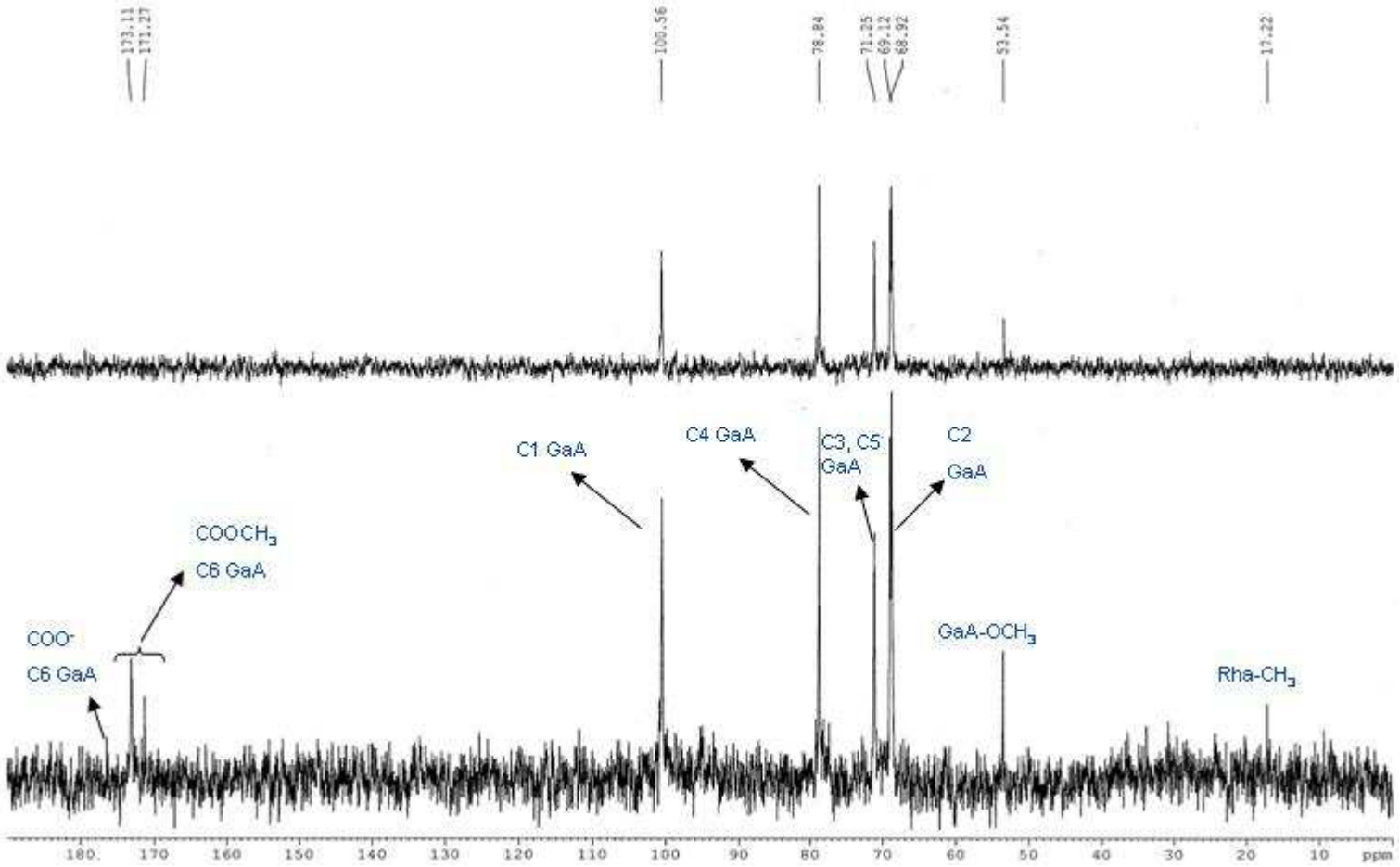

Figure 9 – ^{13}C NMR spectrum for sample of pectin.

Appendix 3 – Figure 58

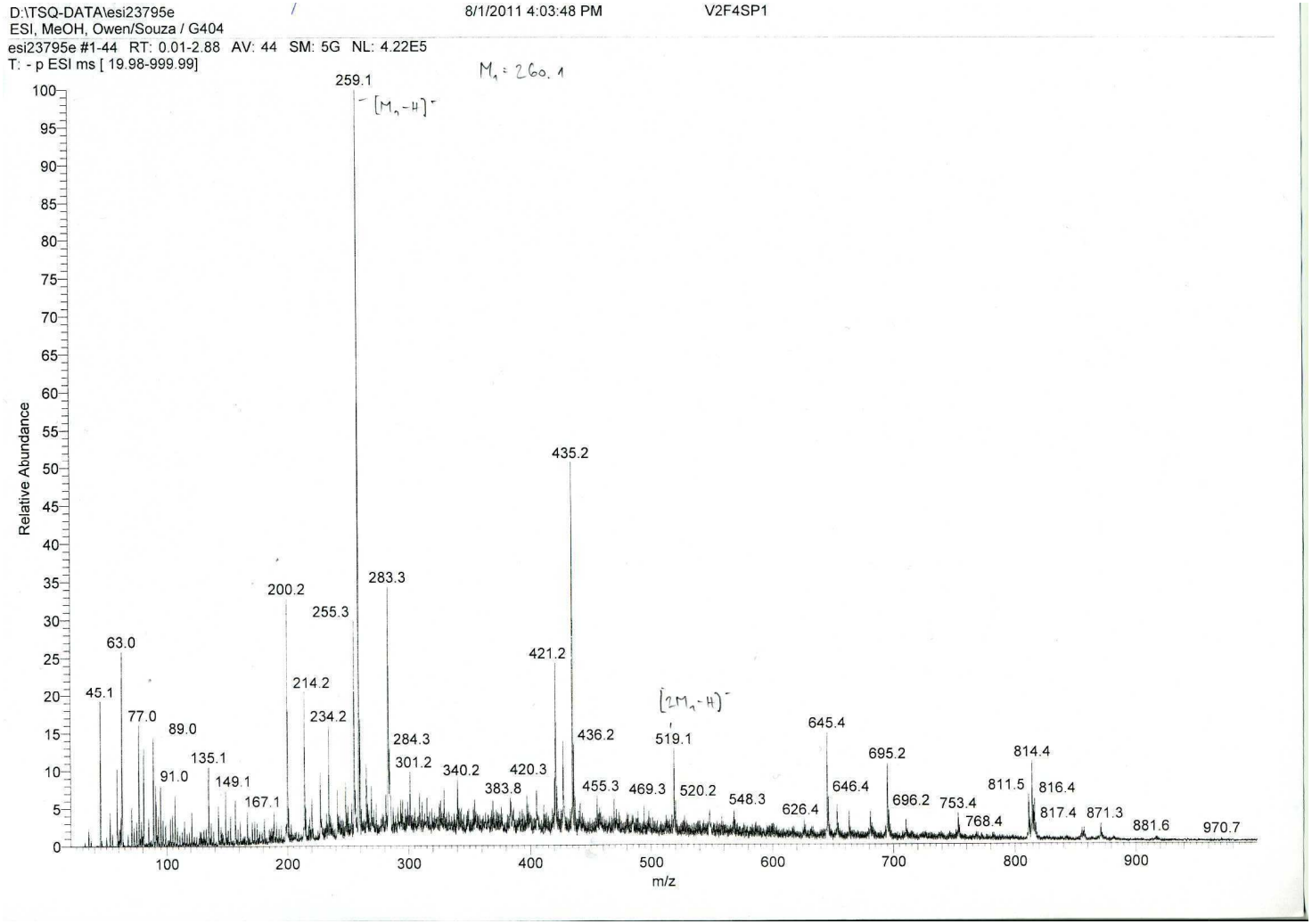

Figure 58 – Nano-ESI-MS spectrum for V2F4-SP1 in negative ion mode.

Appendix 4 – Figure 59

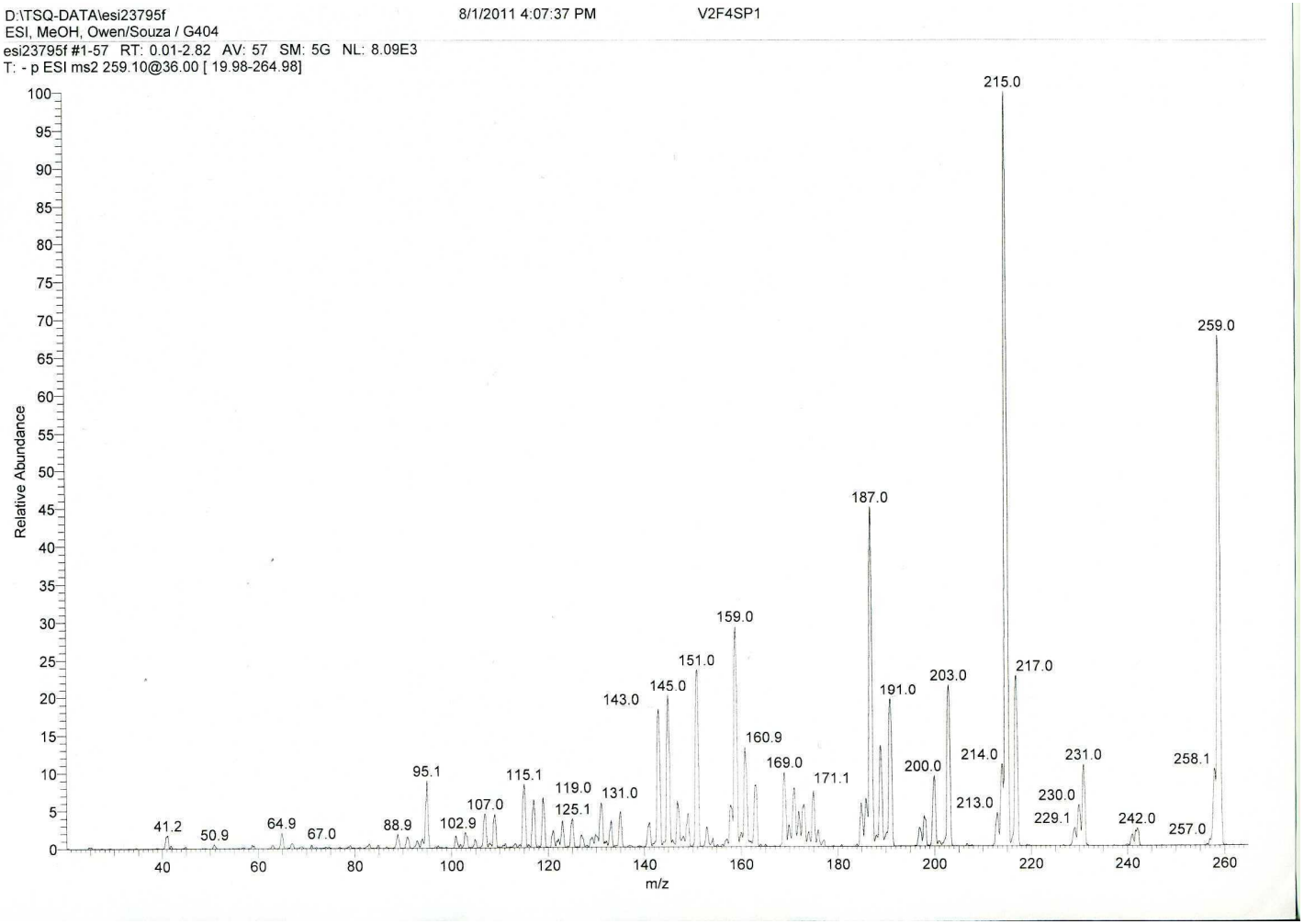

Figure 59 – Nano-ESI-MS^2 fragmentation spectrum of peak 259.1 for M-2.

Appendix 5 – Figure 60

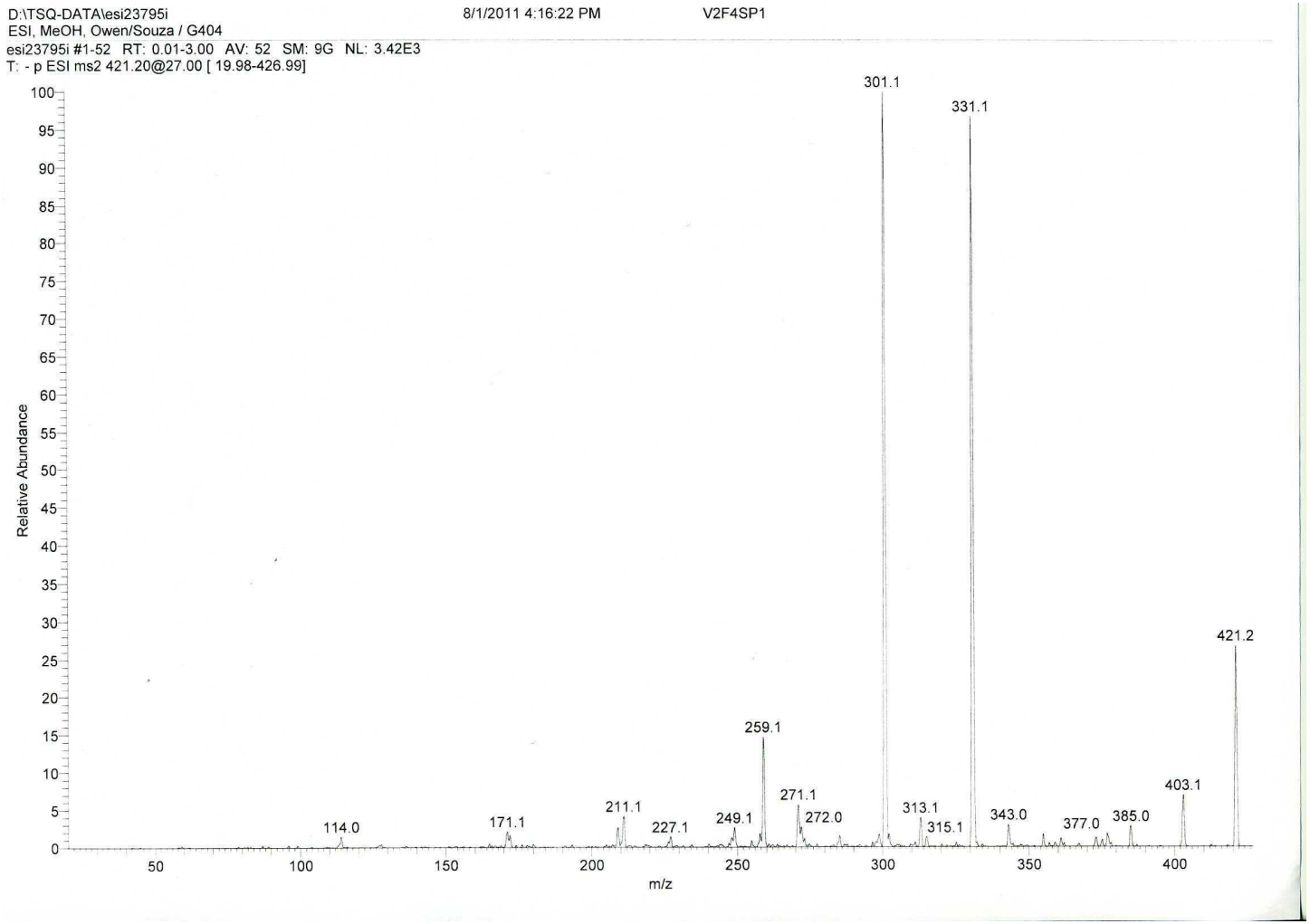

Figure 60 – Nano-ESI-MS^2 fragmentation spectrum of peak 421.2 for Ma.

Appendix 6 – Figure 61

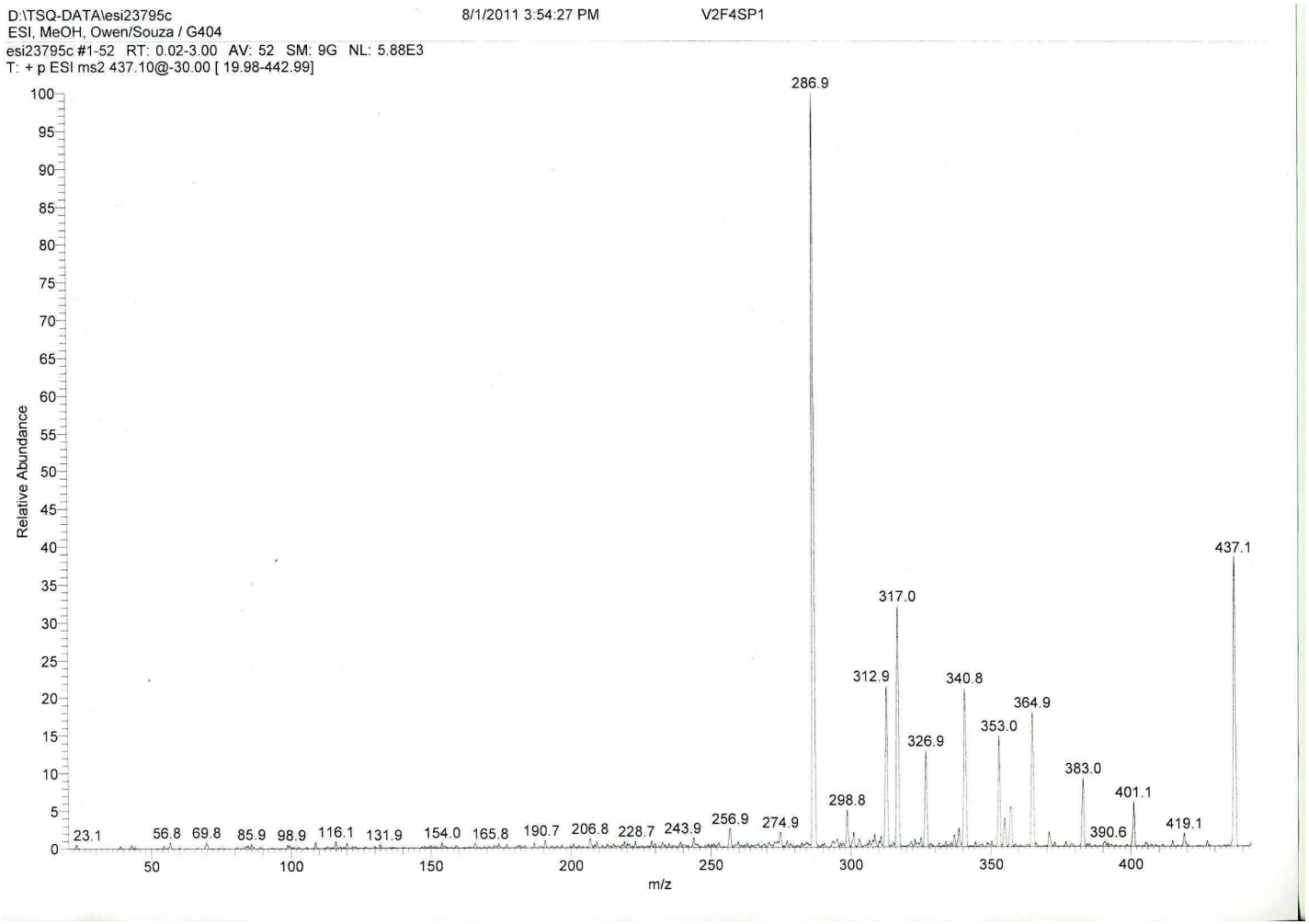

Figure 61 – Nano-ESI-MS^2 fragmentation spectrum of peak 437.1 for M-1.

Appendix 7 – Figure 63

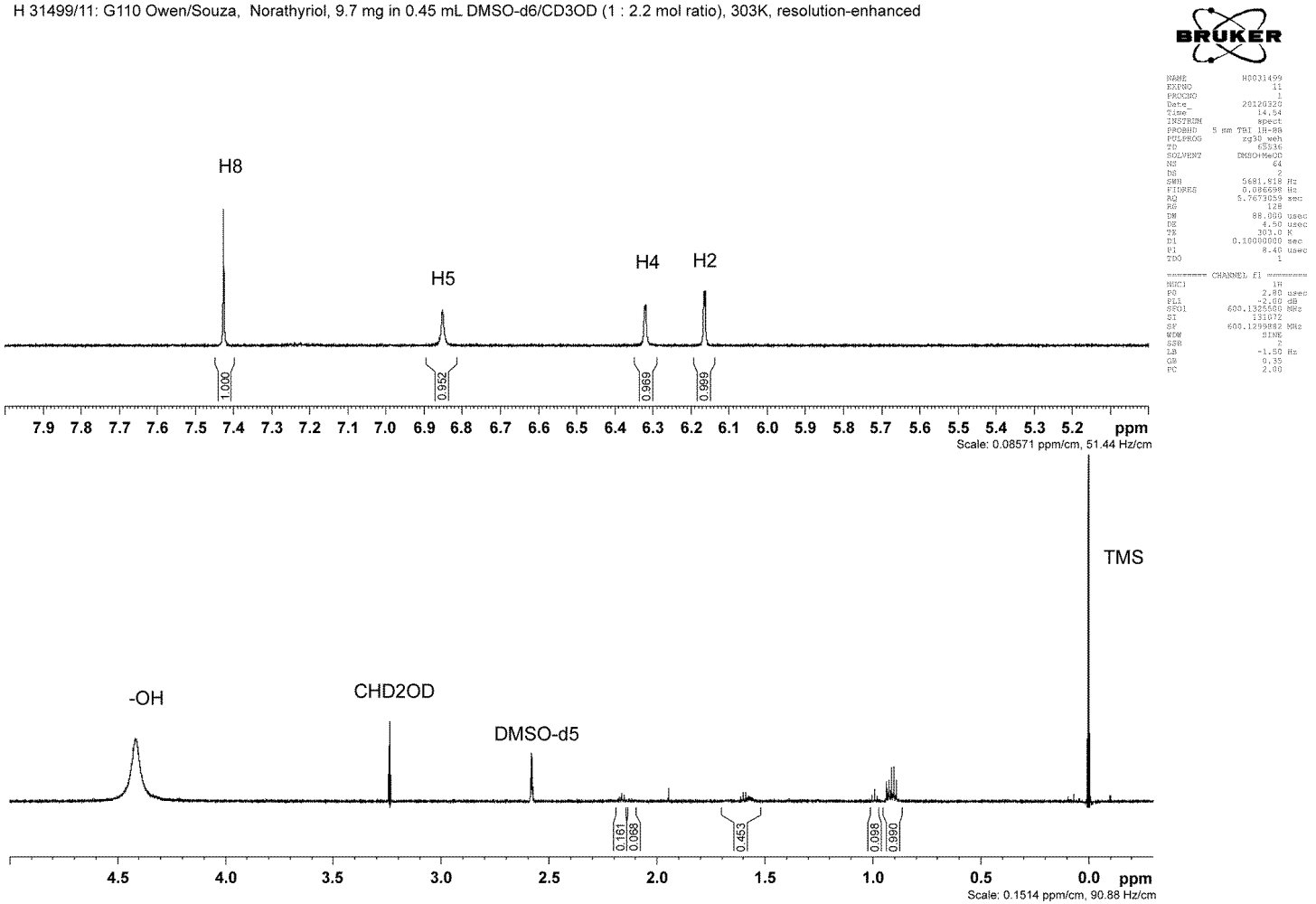

Figure 63 - ^{1}H RMN spectrum (600 MHz) for norathyriol in CD_3OD.

Appendix 8 – Figure 64

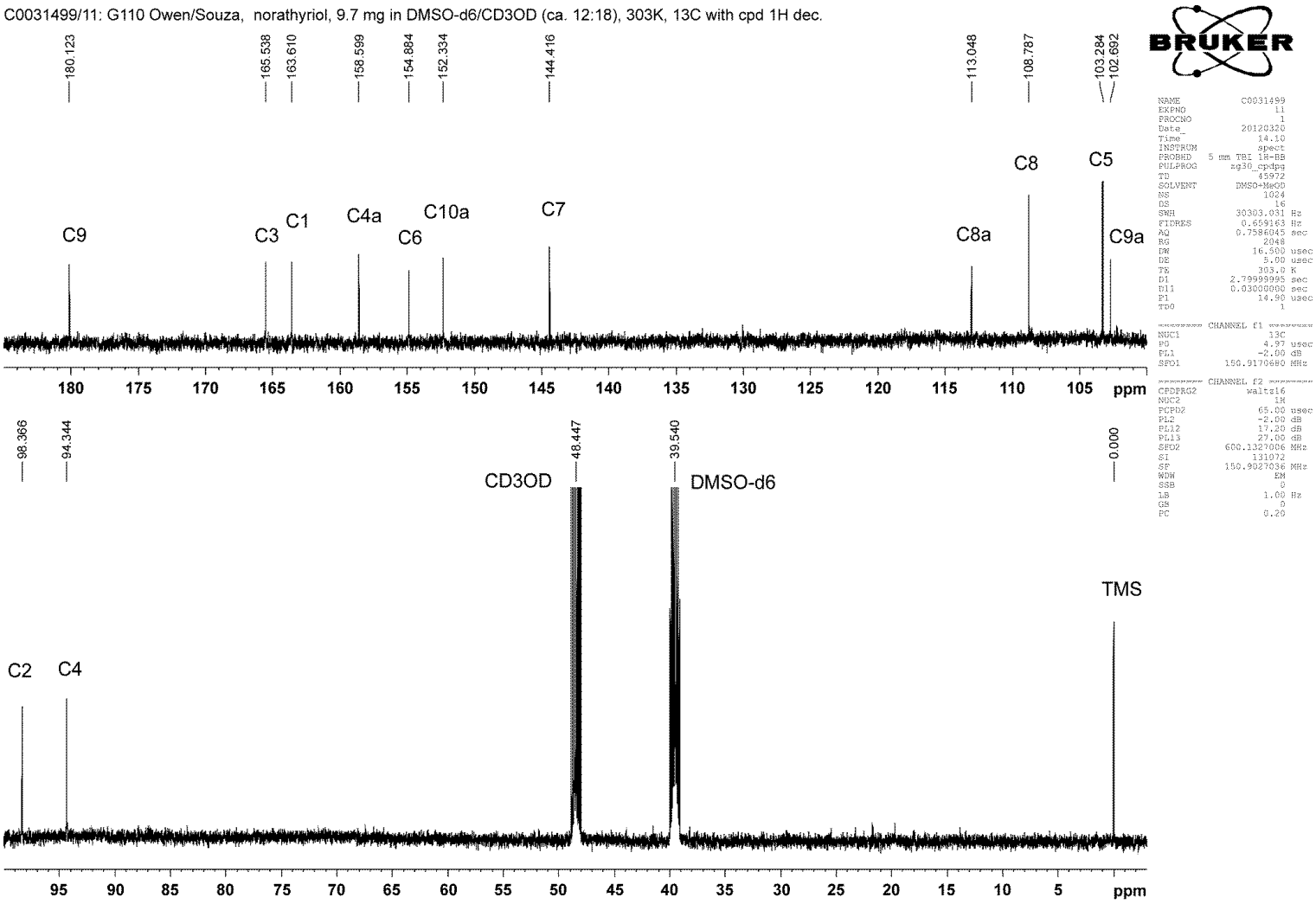

Figure 64 – ^{13}C RMN spectrum (600 MHz) for norathyriol in CD_3OD

Appendix 9 – Figure 65

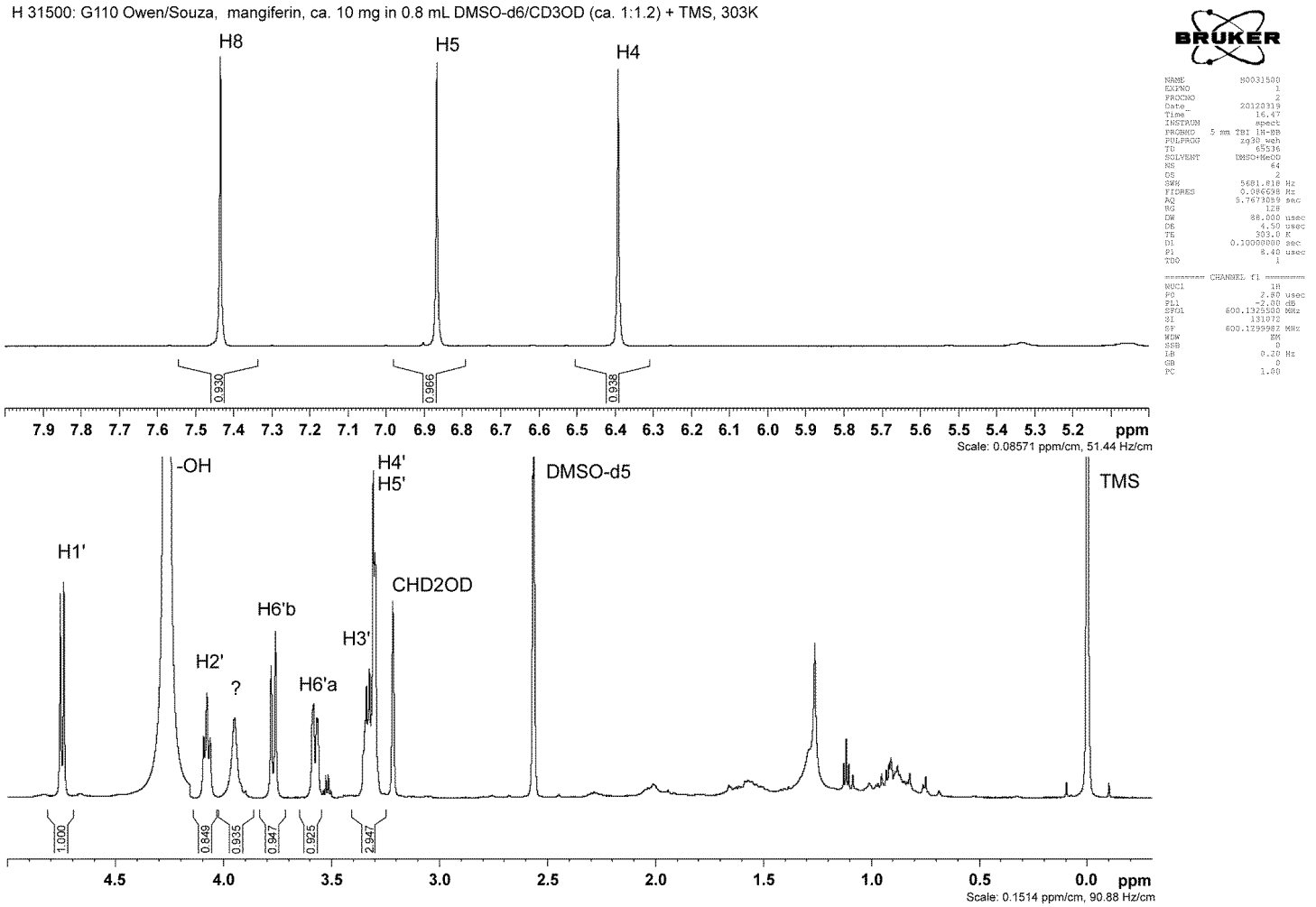

Figure 65 - ^{1}H RMN spectrum (600 MHz) for mangiferin in CD_3OD.

Appendix 10 – Figure 66

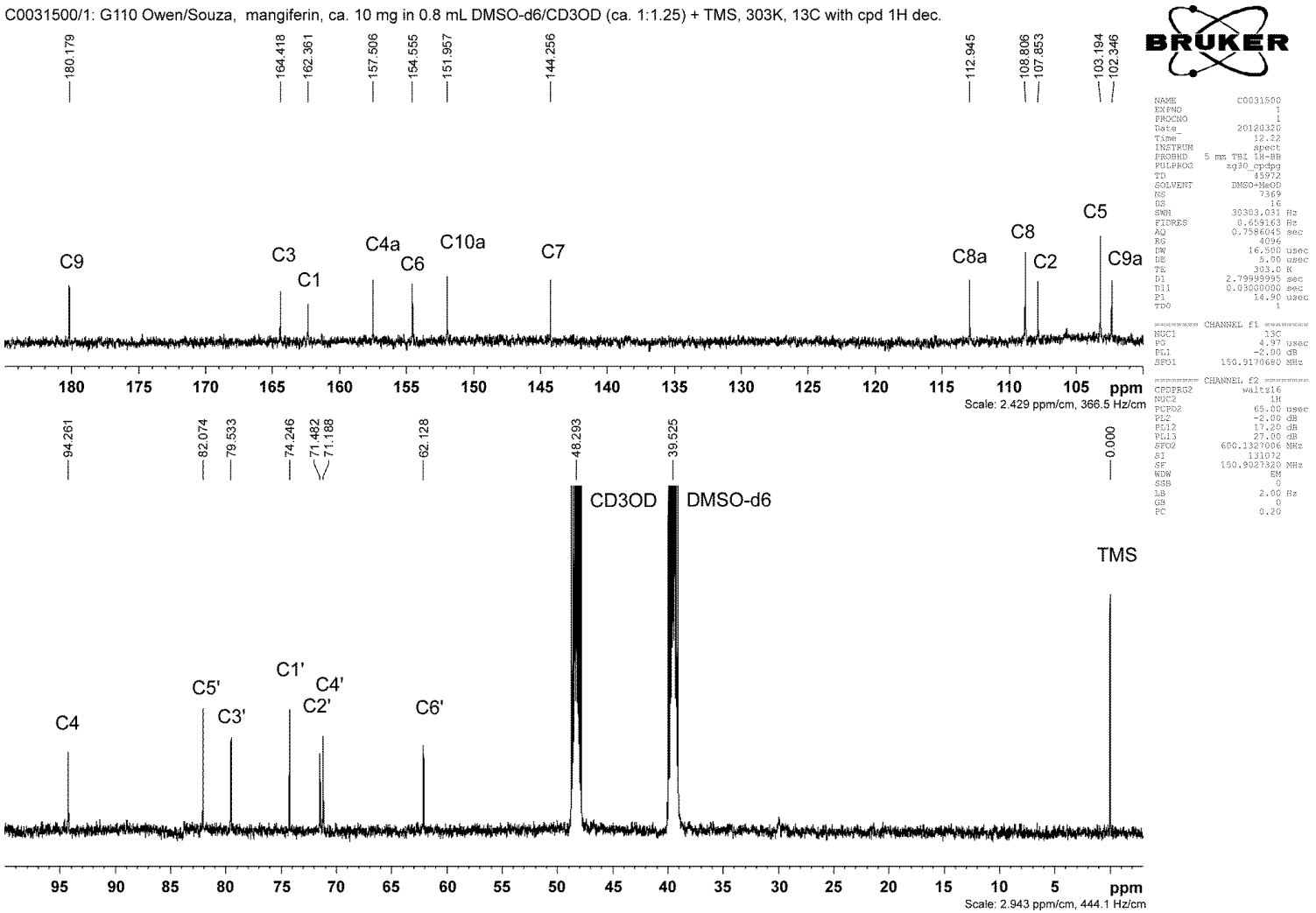

Figure 66 – ^{13}C RMN spectrum (600 MHz) for mangiferin in CD_3OD.

Appendix 11 – Figure 68

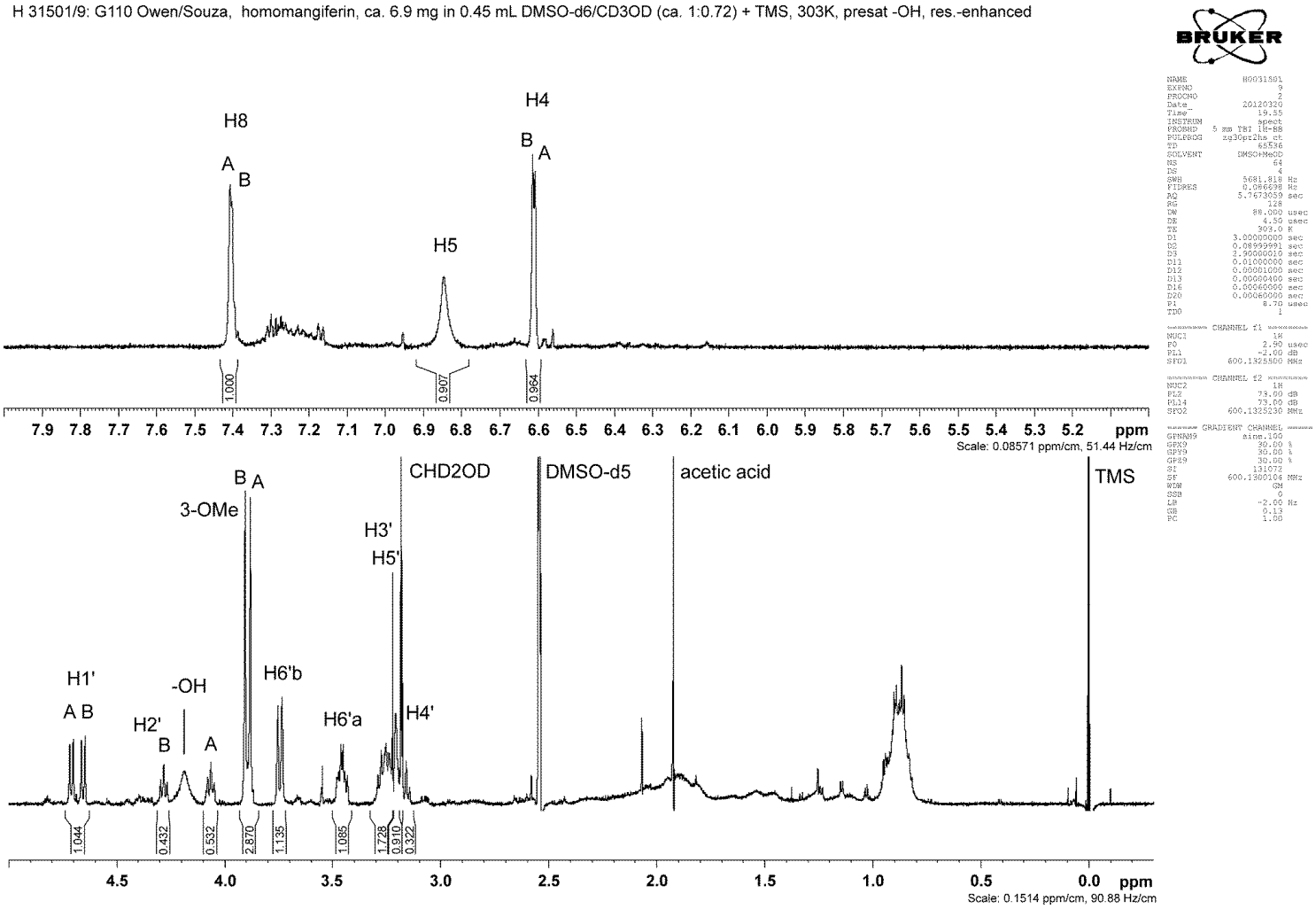

Figure 68 - ^{1}H RMN spectrum (600 MHz) for homomangiferin in CD_3OD.

Appendix 12 – Figure 69

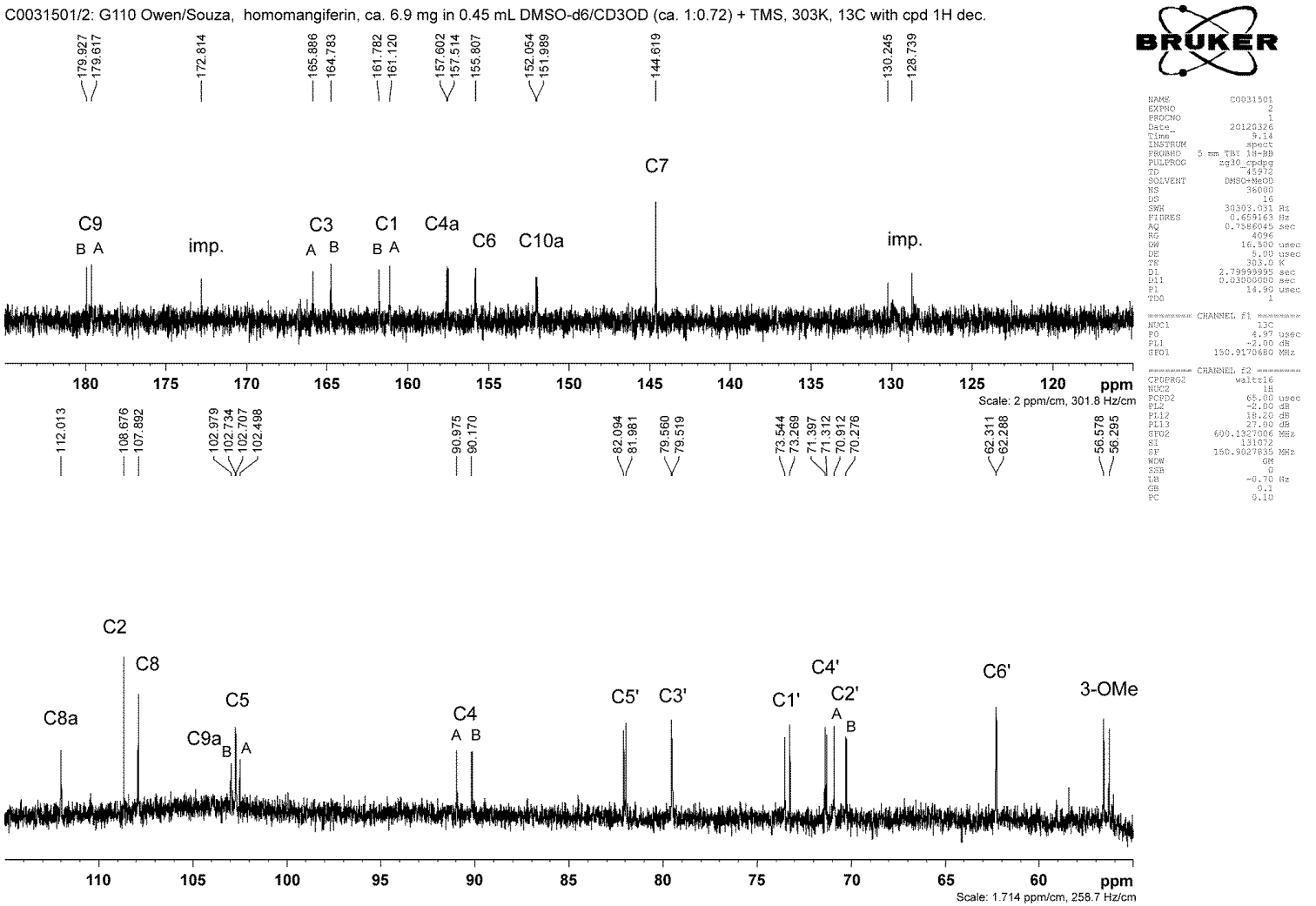

Figure 69 – ^{13}C RMN spectrum (600 MHz) for homomangiferin in CD_3OD.

DEUTSCHES KREBSFORSCHUNGSZENTRUM
IN DER HELMHOLTZ-GEMEINSCHAFT

Genomics and Proteomics Core Facilities
- Contamination Control

Head
Dr. Michael Pawlita

Project Manager
Dr. Markus Schmitt

Im Neuenheimer Feld 242
D-69120 Heidelberg
Phone +49.6221.42 46 06
Fax +49.6221.42 49 32
http://www.dkfz.de/gpcf/contamination_control.html

Multiplex cell Contamination Test, Order ID 10897

Heidelberg 11.11.2011

Dear Madam or Sir,

Many thanks for your order. The multiplex cell contamination test (McCT *v.2*) was conducted as described on the GPCF homepage for the following contaminations: Squirrel Monkey Retrovirus (SMRV), Mycoplasma, Human-, Primate-, Mouse-, Rat-, Chinese hamster-, Syrian hamster-, Feline-, Canine-, Rabbit-, Guinea pig-, and Drosophila cells. DNA Quality was determined by an internal DNA quality control. Positive and negative controls were included to monitor PCR performance.

For documentation of biological safety, please forward this result to the head of your department.

Empty "Result" cells indicate the absence of contaminations tested for. Specifications are given below. Cell lines highlighted in red show considerable contaminations.

Sample ID	Cell line	Species	DNA Quality	Species control		SMRV	Mycoplasma
3829	A240286S,P26	Human	positive	human DNA,			

When citing this service, please use the below mentioned reference and indicate the time that passed between the experiments described in your manuscript and the McCT service.

Best regards,

Dr. Markus Schmitt
(project manager)

Appendix 13 - Multiplex cell Contamination Test for A240286S Cells.

Reference: High-throughput detection and multiplex identification of cell contaminations. Markus Schmitt; Michael Pawlita. Nucleic Acids Research 2009; doi: 10.1093/nar/gkp581.

Result specifications:

SMRV:	Env and gag DNA sequences detected. Cell line should be used in S2/L2 only. SMRV positive cell lines need to be reported to the ZKBS.
"species" cont.:	no DNA of the McCT-user indicated species was detected. However, only DNA from another "species" was detected.
+"species" DNA	original cell does also contain "species" DNA indicating presence of cells of other species
male:	cell line is of male origin or is contaminated by male cells
Mycoplasma (M.):	cell line is contaminated by Mycoplasma. Species is indicated.
* "weak"	weak signal detected, sample will be automatically retested in the next run

DEUTSCHES KREBSFORSCHUNGSZENTRUM
IN DER HELMHOLTZ-GEMEINSCHAFT

Genomics and Proteomics Core Facilities
- Contamination Control

Head
Dr. Michael Pawlita

Project Manager
Dr. Markus Schmitt

Im Neuenheimer Feld 242
D-69120 Heidelberg
Phone +49.6221.42 46 06
Fax +49.6221.42 49 32
http://www.dkfz.de/gpcf/contamination_control.html

Multiplex cell Contamination Test, Order ID 10929

Heidelberg 07.12.2011

Dear Madam or Sir,

Many thanks for your order. The multiplex cell contamination test (McCT *v.2*) was conducted as described on the GPCF homepage for the following contaminations: Squirrel Monkey Retrovirus (SMRV), Mycoplasma, Human-, Primate-, Mouse-, Rat-, Chinese hamster-, Syrian hamster-, Feline-, Canine-, Rabbit-, Guinea pig-, and Drosophila cells. DNA Quality was determined by an internal DNA quality control. Positive and negative controls were included to monitor PCR performance.

For documentation of biological safety, please forward this result to the head of your department.

Empty "Result" cells indicate the absence of contaminations tested for. Specifications are given below. Cell lines highlighted in red show considerable contaminations.

Sample ID	Cell line	Species	DNA Quality	Species control		SMRV	Mycoplasma
4003	Caco-2	Human	positive	human DNA,			

When citing this service, please use the below mentioned reference and indicate the time that passed between the experiments described in your manuscript and the McCT service.

Best regards,

Dr. Markus Schmitt
(project manager)

Appendix 14 - Multiplex cell Contamination Test for Caco-2 Cells.

Reference: High-throughput detection and multiplex identification of cell contaminations. Markus Schmitt; Michael Pawlita. Nucleic Acids Research 2009; doi: 10.1093/nar/gkp581.

Result specifications:

SMRV:	Env and gag DNA sequences detected. Cell line should be used in S2/L2 only. SMRV positive cell lines need to be reported to the ZKBS.
"species" cont.:	no DNA of the McCT-user indicated species was detected. However, only DNA from another "species" was detected.
+"species" DNA	original cell does also contain "species" DNA indicating presence of cells of other species
male:	cell line is of male origin or is contaminated by male cells
Mycoplasma (M.):	cell line is contaminated by Mycoplasma. Species is indicated.
* "weak"	weak signal detected, sample will be automatically retested in the next run